THE UNIVERSITY
of LIVERPOOL

Gold Nanoparticles For Biomolecular Assays

Thesis submitted in accordance with the requirements of the
University of Liverpool for the degree of Doctor of
Philosophy
By

Jenny Louise Aveyard

Acknowledgements

First and foremost I would like to thank my supervisor Dr Robert Wilson not only for giving me the opportunity to carry out this research, but also for his advice, patience, help and support. Without his guidance this would not have been possible. I would also like to thank my co-supervisor Professor Andrew Cossins for his continued support. Many thanks to all of the support staff within the Chemistry Department whom have provided assistance throughout the project. In addition I would also like to express gratitude to the financial sponsors of this project BBInternational.

I am very fortunate to have a fantastic group of friends and I would like to take this opportunity to thank them all for their continued love and support. I would particularly like to thank Ria, Joan, Debbie, Sam, Caroline, Jen and Julie from the Department. I would also like to thank my housemate and long-term buddy Nicky.

I am also eternally grateful to my wonderful boyfriend Graham, who has given love, support and encouragement throughout this PhD especially when times have been tough. I couldn't have done this without you!

Finally I would like to thank my loving and supportive family- my Mum, Dad and my Brother. I dedicate this work to you.

Abstract

The amalgamation of nanotechnology and biology has led to the development of new types of hybrid materials that are expected to produce major advances in areas such as materials science, therapeutics and diagnostics. One of the most promising developments is the use of nanoparticles (NPs) as labels for the detection of analytes in biological assays. The aim of this research project was to prepare gold nanoparticle (GNP) labels for use in such assays. In chapter 1, the optical properties and the use of GNPs in homogeneous and heterogeneous colorimetric assays are reviewed.

In chapter 2 a simple conjugation method is introduced that not only allows almost any biological molecule or hapten to be attached to GNPs but also allows the user to control or vary the mean number of molecules per particle. In this method a high molecular weight aminodextran polymer is functionalized with the molecule of choice and chemical attachment groups that are used to covalently anchor the polymer to the GNPs. This method was used to conjugate biotin and I_{125} functionalized dextrans to GNPs. These functionalized dextrans were then used to investigate the conjugation procedure in more detail. Results from GNP titrations and microbead assays demonstrate that the minimum amount of functionalized dextran required to prevent salt-induced flocculation of the GNPs (equivalence point) is the amount required to coat all of the GNPs and at this point there is no free functionalized dextran in solution.

In chapter 3 the described method was used to conjugate different numbers DNP haptens to GNPs and then these labels were used in non-traditional reagent-limited lateral flow immunoassays. The number of molecules per GNP is varied by simply adjusting the stoichiometry of reagents in the dextran functionalization reaction. Controlling the number of molecules per particle can have important consequences on the sensitivity of a biological assay. Results showed that when the number of DNP molecules per particle decreased, there was an increase in the sensitivity of the assay. Furthermore when the results from these immunoassays were compared to those obtained from traditional reagent-limited lateral flow immunoassays, the non-traditional format proved to be over 50 % more sensitive.

In chapter 4 the conjugation method was used to attach oligonucleotides to GNPs for use in a nucleic acids lateral flow (NALF) device. Although NALF devices are available commercially, detection is usually achieved with the use of antibodies or haptens which can be both problematic and expensive. In addition, many of these devices have issues with sensitivity and are often interfaced with complicated target amplification / purification protocols. In chapter 4 an antibody / hapten independent NALF device is described that can be used to detect the un-purified products from a simple polymerase chain reaction (PCR) amplification protocol. Using the developed NALF device it was possible to detect specific amplification products corresponding to ~1 attomole of template molecules with the unaided eye.

Index

<u>**Appendix I- Publications**</u>

CHAPTER 1

1.1- Introduction

Although gold nanoparticles (GNPs) are considered an invention of modern science, they have in fact been used, perhaps accidentally, in glass and ceramic production for centuries. The incorporation of gold into glass probably dates back to the 4th / 5th century where the addition of gold salts during the glass making process resulted in the formation of GNPs which imparted a ruby red colour to the glass (so-called gold ruby glass). One of the most famous examples is the Lycurgus cup (Figure 1) made by the Romans in 4th century AD that is exhibited at the British Museum. This cup appears green in reflected light such as daylight, but ruby red when light is transmitted through it due to gold-silver alloy nanoparticles approximately 50 - 100 nm in size that are embedded in the cup.[1, 2]

Figure 1: The Lycurgus cup made by the Romans in the 4 th century. In reflected light the cup appears green in colour, but it appears red when light is transmitted through it. Picture from ref 1.

The method for making gold ruby glass was supposedly lost with the fall of Rome and was not re-discovered in Europe until the 17 th century when a German alchemist from a glass-making family Johann Kunckels published the results from his experiments with glass in his famous book *Ars Vitriaria Experimentalis* in 1679.

1

A few years later, Andreas Cassius published his work *De Auro,* in which he described a method of producing a red precipitate from stannic hydroxide and gold, for the colouration of glass which became known as "Purple of Cassius".[3] Despite these early uses of GNPs in glass-making, Michael Faraday was the first to present a scientific paper on their properties and preparation in the 19 th century. In 1857, Faraday reported the formation of deep red solutions of colloidal gold by reduction of an aqueous solution of chloroaurate ($AuCl_4^-$) with white phosphorus in CS_2.[4] Fascinated by the colloids he postulated that the ruby fluid was gold dispersed in liquid in a very finely divided form, so small that it could not be visualised with any microscopes available in his day.[5] Nearly 100 years later Turkevich and colleagues used an electron microscope to reveal that the ruby-coloured colloids made by Faraday's methods had average sizes in the 6 ± 2 nm range.[6] Since Faraday's pioneering work there have been thousands of scientific papers published on the synthesis, functionalisation and properties of GNPs and they have found many applications in electronics, nanodevices and biosensor development. One of the most promising developments is the use of GNPs functionalised with biological molecules as labels for the detection of analytes in biological assays.

The aim of this project was to prepare GNP conjugates for use in biological assays. In this chapter, a brief description of the synthesis and optical properties of GNPs is given, but the main focus is to discuss the use of GNPs as labels in biological assays. Due to the vast amount of research in this area and because the majority of the research carried out for this thesis was performed on lateral flow devices, the discussion will be confined to research concerning visual detection using GNPs.

1.2- Synthesis of GNPs

There are many different methods used to synthesize GNPs, but the most common approach is the simple chemical reduction of tetrachloroauric acid ($HAuCl_4$) solution.[7] In this reaction, $HAuCl_4$ is dissolved and rapidly stirred whilst a reducing agent is added. Before the addition of the reducing agent, 100% gold ions exist in solution. Immediately after the reducing agent is added, gold atoms start to form in the solution, and their concentration rises rapidly until the solution reaches supersaturation. Aggregation of the gold atoms then occurs, in a process called nucleation. Central icosahedral gold cores are formed at nucleation sites. Once this is achieved, the remaining dissolved gold atoms continue to bind to the nucleation sites until all atoms are removed from solution. The number of nuclei formed determines how many particles will finally grow in solution. At a fixed concentration of $HAuCl_4$ in solution, as the concentration of the reducing agent is increased, the number of nuclei that form increases. If the synthesis conditions are optimised, all nucleation sites will be formed simultaneously, resulting in formation of monodisperse gold. To create large colloidal GNPs, with diameters in the range of 15 - 150 nm, $HAuCl_4$ is usually reduced with trisodium citrate in aqueous solution. Medium-sized GNPs between 6 and 15 nm can be formed by reducing $HAuCl_4$ solution with an ascorbate solution. Smaller particles, measuring less than 5 nm in diameter, can be produced by reduction with either white or yellow phosphorus or sodium borohydride.

The GNPs that are commonly used in biological assays are composed of an internal core of gold surrounded by a surface layer of negatively charged ions, such as citrate, which prevents the particles from aggregation. These GNPs are sensitive to

electrolytes because they screen the repulsive electrostatic forces separating the particles. The addition of electrolytes results in aggregation, a colour change and eventual sedimentation of the gold.[8] Most spherical GNPs display a single absorption peak in the visible range. As the particle size increases, the extinction maximum shifts to a longer wavelength, while the width of the absorption spectra relates to the size range.[9]

1.3- Optical properties of GNPs

The optical properties of nanoparticles, both spherical and otherwise, are of great interest to the scientific community. One of the reasons for this is that when nanoparticles are used as a label, very low detection limits are achievable. For example, the extinction coefficient of GNPs is 3 - 4 orders of magnitude higher than those of organic dye molecules.[10] When a solution of noble metal nanoparticles is excited by electromagnetic radiation, the surface conduction electrons of the nanoparticles collectively oscillate resulting in wavelength selective absorption and scattering. This phenomenon is known as localized surface plasmon resonance (LSPR).[11] For most spherical GNPs (> 2 nm), the plasmon band (PB) is usually between 520 – 700 nm of the electromagnetic spectrum which explains the intense colour of colloidal gold solutions. GNPs with diameters between 10 - 20 nm have a PB that is centred around 520 nm but as the particle size increases, the plasmon band shifts to longer wavelengths (Figure 2).
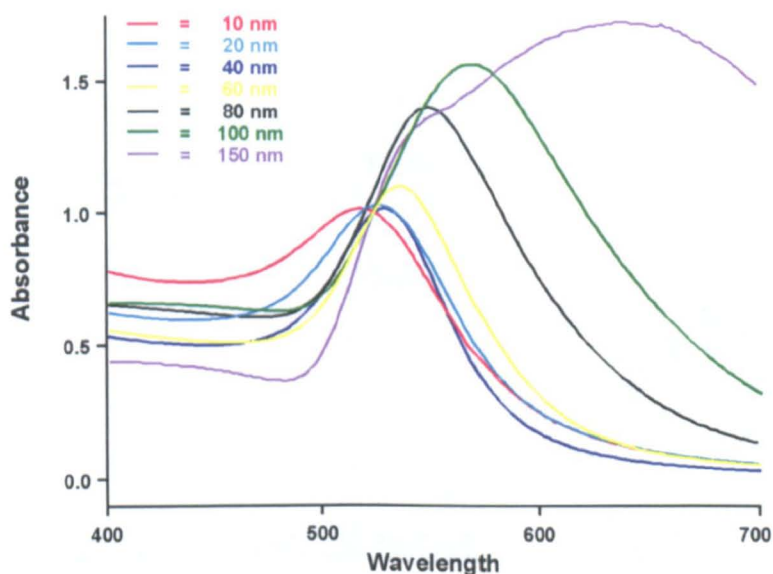
Figure 2: Graph showing UV/vis extinction spectra of different sized GNPs. As the GNP size increases, there is a shift in the plasmon band to longer wavelengths.

The position of the PB is dependent upon a number of parameters including the refractive index of the surrounding medium and the distance between the particles.[12] Underwood and Mulvaney demonstrated the effect of changing the refractive index on the colour of a solution of GNPs.[13] In this approach, GNPs were transferred into solvents with different refractive indices. The GNP solutions changed colour from red (in water) through to purple and this change was accompanied by a red shift in the PB as the refractive index of the solvent increased (Figure 3A and B). Underwood and Mulvaney confirmed that the colour change was due to the change in refractive index by allowing the solvent to evaporate. Upon evaporation, the colour of the solution was restored to red as the refractive index decreased.
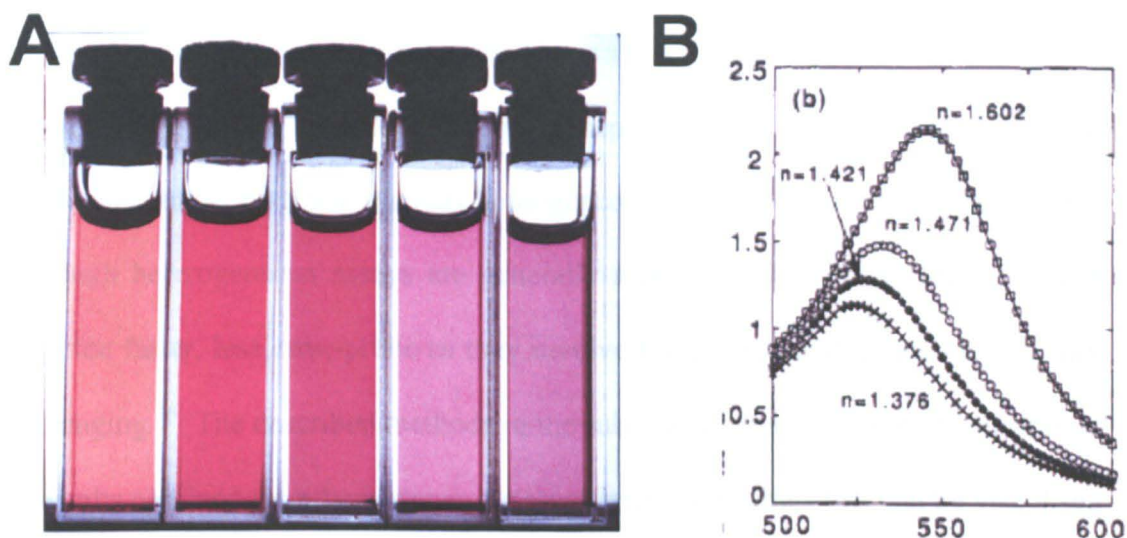
Figure 3: A) Photograph of five solutions of colloidal gold prepared in water and in mixtures of butyl acetate and carbon disulphide. Refractive indices of the solutions at the absorption band maximum are 1.336, 1.407, 1.481, 1.525 and 1.583 respectively. B) Extinction spectra of GNPs in different solvents. The solvents were cyclohexane $n = 1.3761$; dodecane $n = 1.4211$; decalin $n = 1.471$; and CS_2 $n = 1.602$. Photograph and spectra taken from ref 13.

Similar colour changes to those shown in the figures above also occur when GNPs are in close proximity to one another. In a solution of GNPs, if the distance between the individual particles (interparticle distance) is greater than the average particle diameter, the solution will appear red but as the distance between the GNPs decreases to less than the average particle diameter, for example if the particles aggregate, the colour of the solution appears blue. This effect occurs because when many GNPs are located nearby each other, their dipoles overlap and shift the PB to higher wavelengths. The shift of the PB reflects the apparent increase in the diameter of the GNPs as the aggregates form and the size of the shift is dependent on the size of the aggregate. The colourimetric changes that occur to solutions of GNPs upon a change in refractive index or a decrease in interparticle distance have been exploited in many biological assays. This has become possible due to the development of methods that enable the attachment of biological molecules to GNPs.

1.4- Homogeneous colourimetric detection with GNPs

Biological assays can be categorized as heterogeneous or homogeneous.[14] Heterogeneous assays are those that involve separation and washing steps before the target molecule is detected whereas homogeneous assays do not require these steps. Although heterogeneous assays are generally more sensitive, homogeneous assays are often faster, less error-prone as they involve fewer steps and are less technically challenging.[14] The described methods in the subsections below will only concentrate on results obtained from homogeneous assays with GNP labels that can be visualised without the requirement of additional equipment.

1.4.1-Colourimetric detection using antibody functionalised GNPs

In the early 1980's Leuvering and colleagues developed homogeneous immunoassays for several serum and urine analytes (Figure 4) based upon the colour change that occurred when the interparticle distance between GNPs coated with antibodies changed.[15-18] A colour change from red to blue was induced as the GNPs became linked to each other forming aggregates *via* specific reactions with the analyte. The first assay developed was a sandwich immunoassay for the detection of human chorionic gonadotrophin (HCG).[15] In this work, Leuvering functionalised two sets of GNPs with two different antibodies, each specific for a different antibody binding site of the HCG antigen (Figure 4). When the GNPs were mixed with a sample containing HCG, the antibodies on the GNPs sandwiched it forming a network of aggregated GNPs and the colour of the solution changed. At low concentrations of HCG the solution remained red, but as the amount of HCG was increased, the solution changed colour to blue and there was an increase in the PB at longer wavelengths as the size of the aggregates increased. Although novel, this type

of assay was unsuitable for the detection of small monovalent molecules. This is because these molecules have one antibody binding site and are so small that steric hindrance is often a problem.
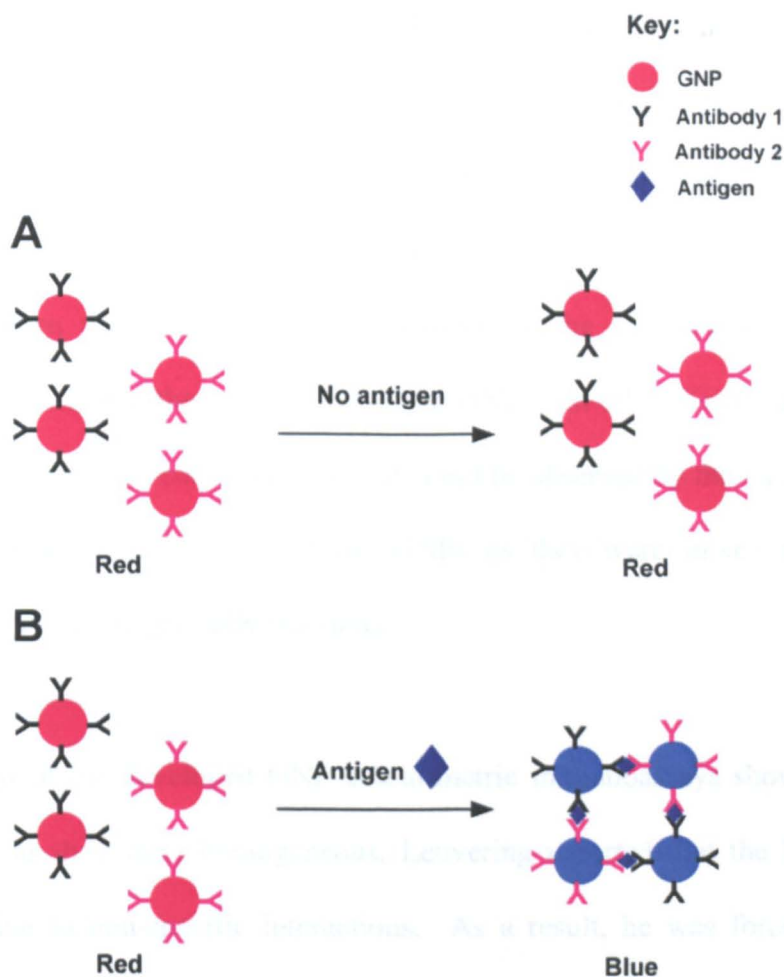
Figure 4: Diagram detailing Leuvering and colleagues sandwich colourimetric immunoassay. Two sets of GNPs that have been functionalised with two different antibodies, each specific for an epitope of the antibody are mixed with a sample. A) Target antigen is not present. The GNP solution remains red. B) Target antigen present. The antibodies immobilised on the GNPs bind to the corresponding epitopes of the target antigen, linking the GNPs together into an aggregated network. The solution changes colour to blue.

To solve this problem Leuvering modified the procedure and developed a competitive assay for small molecules.[16] In this approach, oestrogen was conjugated to a BSA carrier molecule and antibodies specific for oestrogen were conjugated to GNPs. The oestrogen-BSA conjugate and functionalised GNPs were then mixed with a sample containing free oestrogen. The oestrogen in the sample competed with the oestrogen-BSA conjugate for the antibody binding sites on the GNPs. At low concentrations of oestrogen, the conjugate bound to the antibodies and the GNP solution changed colour from red to blue, as a network of aggregated GNPs formed. However, when there was sufficient oestrogen in the solution, it bound to the antibody and inhibited the aggregation of the GNPs. In all of Leuvering's reported assays he attributed the colour change that could be observed by the naked eye to the subsequent change in the size of the GNPs as they were linked together into aggregates by specific antibody reactions.

Although all of the developed GNP colourimetric immunoassays showed promise, particularly as they were homogeneous, Leuvering reported that the PB shift was very sensitive to non-specific interactions. As a result, he was forced to subject crude samples of serum and urine to laborious preparation procedures. Later Englebienne suggested an explanation for the so-called non-specific interactions observed in Leuvering's procedure and found that the aggregation of GNPs was not the only cause of measurable PB shifts.[19-21] During Englebienne's study, measurable changes in the PB wavelength were observed without GNP aggregation when GNPs functionalised with antibodies specific for one antibody binding site of an antigen bound to the antigen. This suggested that the binding reaction between the antigen and the antibody caused a change in the refractive index at the GNP surface which

was responsible for the shift. Englebienne stated that the interference seen in Leuvering's procedure was a consequence of the interaction of serum components with non-specific reactive sites on the antibody. He then went on to develop a high-throughput screening method based on the changes in refractive indexes upon antigen binding and using this technique was able to study the association and dissociation kinetics of the reactions. However, as the shifts in PB were subtle, a colour change could not be observed by eye and an automatic analyzer was employed for detection.

1.4.2-Colourimetric detection of un-amplified nucleic acids with GNPs

The colourimetric changes that occur when the interparticle distance between GNPs decreases have also been employed in the detection of nucleic acids. Mirkin and colleagues designed a DNA detection system based on the colourimetric change imparted by specific aggregation of oligonucleotide functionalised GNPs (Figure 5).[22] In this work two different non-complementary thiolated oligonucleotides were immobilised on two sets of GNPs. Upon mixing the solution remained red due to the non-complementary nature of the sequences. In the next stage, a target oligonucleotide containing a sequence at each end that was complementary to each of the oligonucleotides immobilised on the GNPs was introduced. When added the complementary ends of the target oligonucleotide hybridised to the oligonucleotides immobilised on the GNPs inducing a colour change from red to blue as the GNPs were linked together into an aggregated network. The formation of these aggregates led to a shift in the PB to a longer wavelength (Figure 6). To confirm that aggregation was due to hybridisation, the GNP solution was heated above the melting temperature of the hybridised oligonucleotide complex. When heated, the

colour changed back to red as the oligonucleotides and target "melted" to generate
un-linked GNPs. In a control experiment, a target oligonucleotide sequence with 4
mismatched bases at each end was mixed with the oligonucleotide-GNP conjugates.
This target sequence did not induce aggregation confirming that the effects seen with
the correct target sequence was due to specific hybridisation.

Figure 5: Diagram detailing the DNA colourimetric aggregation-based assay developed by
Mirkin and colleagues.   Two sets of GNPs are functionalised with two different non-
complementary oligonucleotides. A) The situation that occurs when the target is not present.
The GNPs are not aggregated and the solution remains red. B) The situation that occurs when
the target oligonucleotide is present. The target oligonucleotide hybridises to complementary
portions of the sequences immobilised on the GNPs leading to the formation of DNA-linked
GNP aggregates. The solution changes colour to blue.

Figure 6: UV/vis extinction spectra of unlinked and aggregated GNPs. When the oligonucleotide functionalised GNPs are linked via hybridisation of target oligonucleotide, there is a decrease in interparticle distance which results in a red shift in PB. Taken from ref 24.

Later Mirkin and colleagues carried out a more in-depth investigation on the possible applications and detection limits achievable with this colourimetric system.[23-25] The methodology remained similar to the original work except that oligonucleotide-GNP conjugates were subjected to a salt "aging" step to increase the amount of oligonucleotides immobilised on the GNPs. In this work, when the target sequence was added to the oligonucleotide-GNP conjugates, hybridisation and subsequent aggregation did not occur immediately as they had observed in previous work. They attributed the slow reaction to steric hindrance or the high negative charge density on the GNPs caused by extensive loading of oligonucleotides. They discovered that aggregation would occur more rapidly after adding the target sequence if the mixture was heated to 50 °C or frozen in dry ice followed by thawing at room temperature. Although debatable, it was thought that freezing caused the development of high local concentrations of salt, target and oligonucleotide-GNP conjugates within the ice structure which accelerated the hybridisation process. They also investigated the melting temperature profiles of the DNA-linked aggregates in more detail by

monitoring the colour and subsequent changes in the UV/vis spectra of the solutions with the view to developing a system that could detect base mismatches in the target sequence. They found that the DNA-linked aggregates exhibited extremely sharp melting transitions in comparison to fluorophore labelled oligonucleotides indicating that they would be highly specific labels for DNA targets.[24] Target oligonucleotides with base mismatches will hybridize to the oligonucleotide-GNP conjugates, but due to the imperfect complementarity should dissociate at a lower melting temperature than perfectly matched complementary sequences. As the number of base mismatches is increased, there should be a decrease in the melting temperature required to dissociate the sequences. They tested the system with target sequences with between one and six base mismatches and found that when they were heated to a specific temperature, the oligonucleotides melted inducing a colour change from blue to red. However, DNA-linked aggregates formed with the perfectly matched sequences remained blue as this temperature was below the melting temperature required to melt a perfectly matched sequence.[23] Due to the sharp melting transitions of the aggregates, perfectly matched target sequences could be detected even in the presence of the mismatched targets that had a melting temperature one degree below the melting temperature of the perfect target match. The sharp melting transitions are attributed to the high number of oligonucleotides immobilised on each GNP which hybridize to multiple targets to form the aggregates. To observe a colour change in this system, all complexes formed with the target and the oligonucleotide-GNPs are melted simultaneously. Mirkin and colleagues could detect 10 fmol of target oligonucleotide and easily distinguish sequences with only one base mismatch but a disadvantage of this procedure is that it requires precise temperature control and considerable assay optimisation, particularly as they reported that changes in the

hybridisation conditions could lead to variation in the melting temperatures. In addition, the requirement for freeze-thawing and subsequent heating steps to initiate hybridisation could make it very difficult to control the temperature, introduce operator error and lead to false negative or positive results. Murphy and colleagues developed a simple instrument that alleviated these problems (Figure 7).[26] The device was composed of a Peltier device with a calibrated resistor which allowed precise temperature control and an LED and photodiode detector to accurately monitor the changes in colour of the GNP solutions.
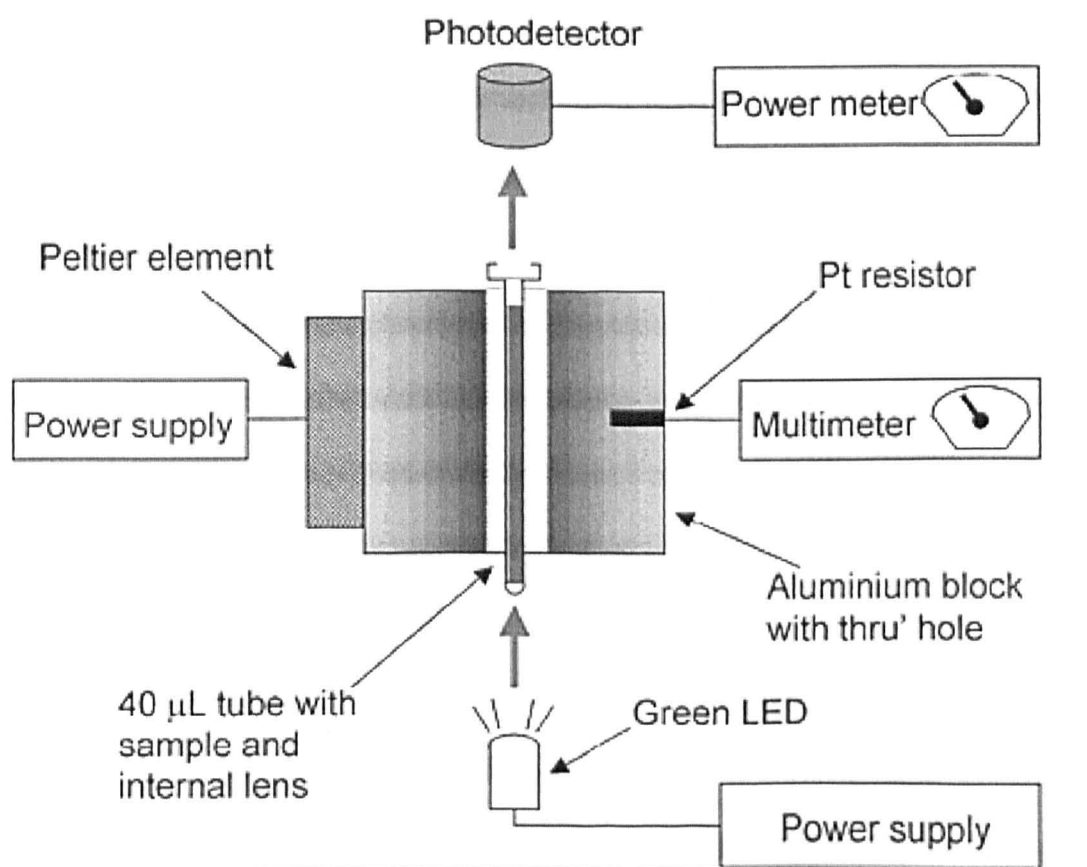
Figure 7: Diagram of the instrument developed by Murphy and colleagues. Taken from ref 26. The Peltier block and resistor allow precise temperature control

Shen and colleagues reported a different approach for their colourimetric aggregation-based assay for detection of single base mismatches in target sequences (Figure 8).[27] Although predominately similar to Mirkin's work, their method included a DNA ligase step to avoid the precise temperature control required in Mirkin's method and the instrumentation used by Murphy. In this work, ssDNA target was mixed with two sets of GNPs that had been functionalised with two different non-complementary oligonucleotides. Upon mixing the target hybridised to the immobilised sequences forming a DNA duplex and an aggregated network of DNA-linked GNPs formed inducing a colour change from red to blue. A high fidelity DNA ligase was then added and when there was a perfect match between the target and the oligonucleotides immobilised on the GNPs, the ligase covalently joined the two GNP oligonucleotide sequences together. However, if there was a mismatch in the target, no covalent linkage was formed. When the solution was heated to 75 °C, the solution containing mismatched sequences changed colour to red as the DNA duplex melted and the aggregate structures disassembled, whereas solutions containing perfectly matched sequences remained blue.
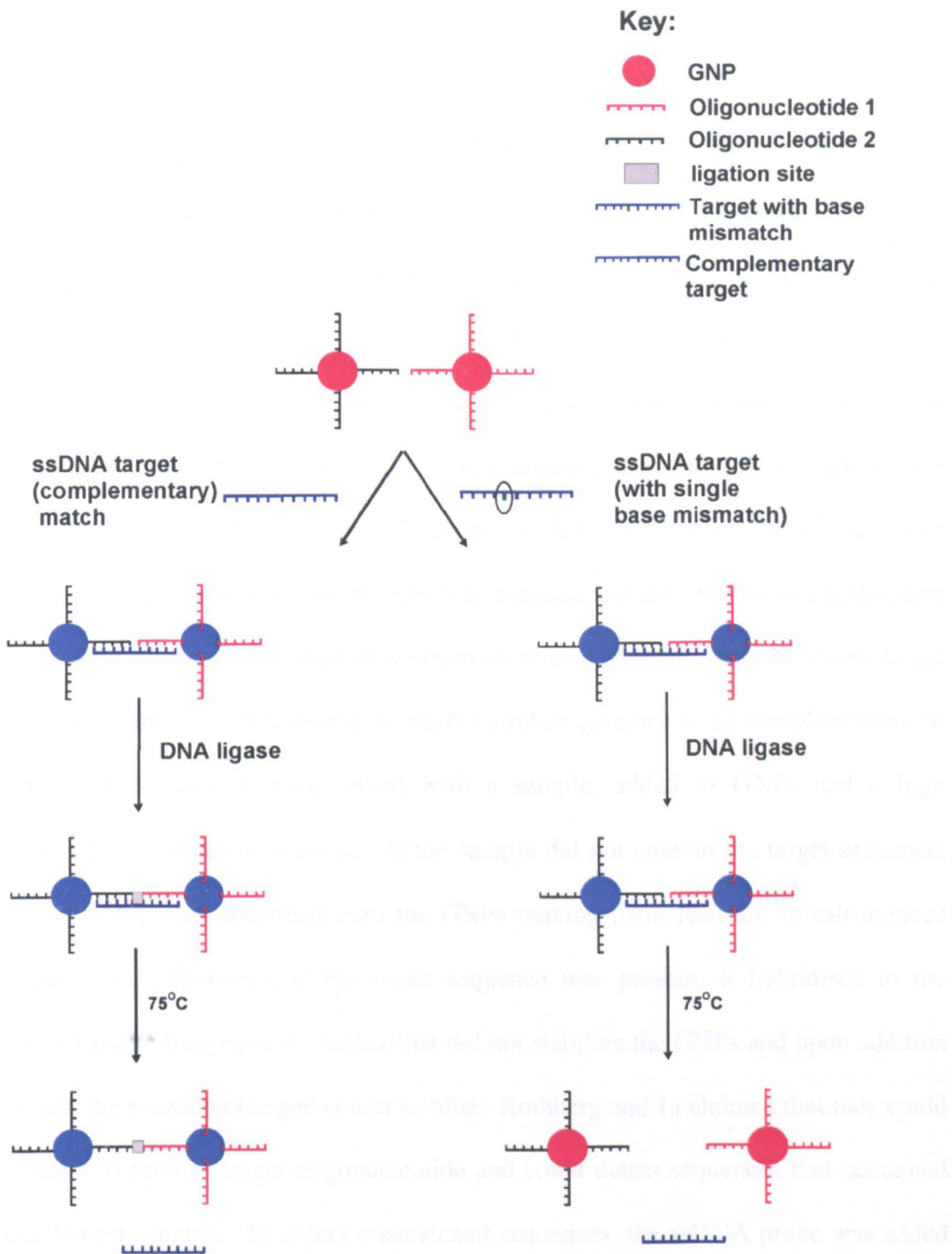
Figure 8: Diagram detailing Shen and colleagues procedure for detecting single base mismatches. Two sets of GNPs functionalised with non-complementary oligonucleotides were mixed with the target or a target with one base mismatch. Upon addition of the target, hybridisation occurred and the solution changed colour from red to blue as DNA-linked aggregates were formed. A DNA ligase was added to the solution and when there was a perfect match between the target sequence and the oligonucleotides immobilised on the GNPs, the ligase covalently joined the two GNP oligonucleotide sequences together and the aggregates remained upon heating to 75 °C. If there was a mismatch in the target sequence, no covalent linkage was formed and upon heating the aggregates dispersed.

The methods discussed so far in this section have all involved the use of GNPs functionalised with nucleic acids, however non-functionalised GNPs have also been used in colourimetric detection methods. Rothberg and Li developed a colourimetric aggregation assay for DNA that did not rely on functionalised GNPs or oligonucleotides (Figure 9).[28] The method was based upon the idea that double (ds) and single (ss) stranded DNA have different electrostatic properties and interact with GNPs in different ways. Rothberg and colleagues found that when ssDNA was mixed with unmodified GNPs and a high concentration of salt was added, the solution remained red, but when dsDNA was added to a solution of GNPs followed by a high concentration of salt, the GNPs aggregated and the solution changed colour from red to blue. They used this observation to devise an assay to detect target oligonucleotides. In this approach, ssDNA probes designed to be complementary to the target of interest were mixed with a sample, added to GNPs and a high concentration of salt was added. If the sample did not contain the target sequence, the ssDNA probes absorbed onto the GNPs making them resistant to salt-induced aggregation. However, if the target sequence was present, it hybridised to the ssDNA probe forming a ds duplex that did not stabilize the GNPs and upon addition of salt, the solution changed colour to blue. Rothberg and Li claimed that they could detect 100 fmol of target oligonucleotide and could detect sequences that contained one base mismatch. To detect mismatched sequences, the ssDNA probe was added to the mismatch sequence and subjected to a brief de-hybridisation step in water before adding the GNPs and salt solution. They observed an obvious colour difference when compared to solutions containing the perfectly matched target sequence. Although simple, there are some problems associated with this method. Other research groups have found that the extent of electrostatic adsorption to GNPs

is dependent on the base composition and length of the ssDNA. For example, Alivisatos and colleagues found that ssDNA containing a high number of guanine and cytosine bases was more likely to adsorb to GNPs.[29]
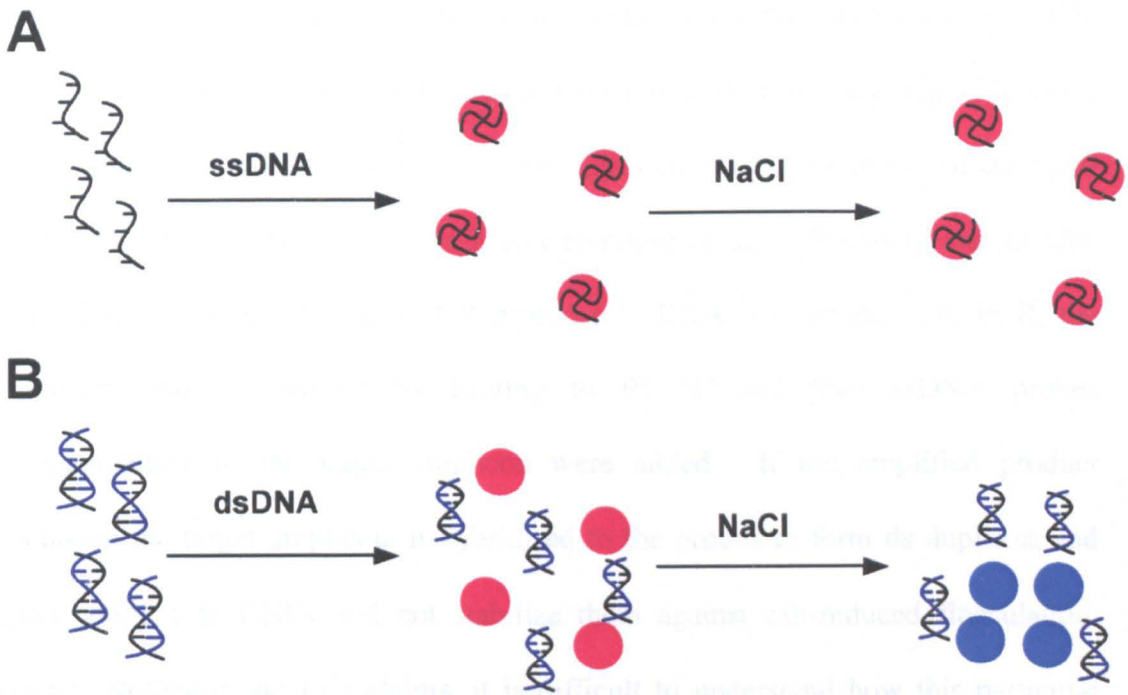
Figure 9: Diagram of Rothberg and Li's colourimetric salt aggregation based assay. A) The situation that occurs if ssDNA is added to GNP. The ssDNA adsorbs onto the GNPs which stabilizes them against salt-induced aggregation. B) The situation that occurs if dsDNA is added to GNPs. If the ssDNA is added to a sample that contains the target of interest, it hybridises forming a dsDNA duplex. When mixed with GNPs the dsDNA does not adsorb to the GNPs and the GNPs aggregate upon addition of salt solution.

1.4.3- Colourimetric detection of amplified nucleic acids using GNPs

All of the colourimetric nucleic acid detection protocols, described in this section so far, have issues with sensitivity. In their current formats they would not be suitable for detection of DNA in most clinical samples. For example, the yield of DNA from a biopsy sample would typically be in the order of 3 x 10^5 copies (0.5 attomoles) of

target sequence, which is well below the detection limit of these colourimetric detection techniques. In order to improve the sensitivity of these assays one possibility is to interface them with an amplification technique such as PCR. Baptista and colleagues interfaced a colourimetric DNA detection assay with a PCR protocol and detected amplified target DNA.[30] In this approach, target DNA was subjected to PCR, then the un-purified amplicons were mixed with oligonucleotide functionalised GNPs. This mixture was subjected to a 95 °C heating step to denature the ds amplicons which were then detected by a change in the colour of the GNP solution upon the addition of a high concentration of salt. Rothberg and Li also interfaced their method with a PCR protocol.[31] DNA was subjected to PCR, the amplicons were denatured by heating to 95 °C and then ssDNA probes complementary to the target amplicon were added. If the amplified product contained the target amplicon, it hybridised to the probes to form ds duplexes and upon addition to GNPs, did not stabilize them against salt-induced flocculation. Despite Rothberg and Li's claims, it is difficult to understand how this particular method could work as they did not include a purification step to remove the ssPCR primers from the reaction mixture. In this paper, Rothberg and Li claim that only 10 ssDNA are required to stabilize each GNP against salt-induced flocculation. If this is the case and the primers are not removed they would adsorb to the GNPs and false negative results could be obtained when the target amplicon is present.

Maeda and colleagues used a more complicated method to detect single base mismatches in PCR amplified products (Figure 10).[32] Whilst this method was not entirely homogeneous as it included a purification step after PCR amplification, it has been included in this section as additional reactions and detection steps were

performed without purification. In this approach, a sample was subjected to PCR and then the amplicons were purified to remove un-extended primers and deoxynucleotide triphosphates (dNTPs). The amplicons were then subjected to a single-base extension reaction with a primer and dideoxy triphosphates (ddNTPs). In regular PCR the primer anneals and the target sequence is extended by dNTPs. Each new nucleotide is added to the 3′-OH group of the last nucleotide added. However, in the single-base extension reaction, the primer anneals to the target and only extends by one base due to the use of the ddNTPs. These nucleotide triphosphates lack a 3'-OH group (Figure 11B) so further extension of the target cannot occur. Following the single-base extension reaction, oligonucleotide functionalised GNPs were then mixed with un-purified extension products. If the product was fully complementary to the sequence attached to the GNPs, hybridisation occurred producing a blunt ended duplex, and the GNPs aggregated upon the addition of salt solution. However, if the extension product contained a mismatched base at the terminal end, hybridisation occurred producing a fork-like structure and the GNPs were resistant to salt-induced aggregation. Maeda and colleagues did not provide an explanation for the increase in stability observed upon hybridisation of mismatched extension products. One possibility is that the presence of a fork-like structure results in an increase in the negative charge density surrounding the GNPs, which leads to greater repulsion between individual GNPs and subsequently higher stability in salt solutions.
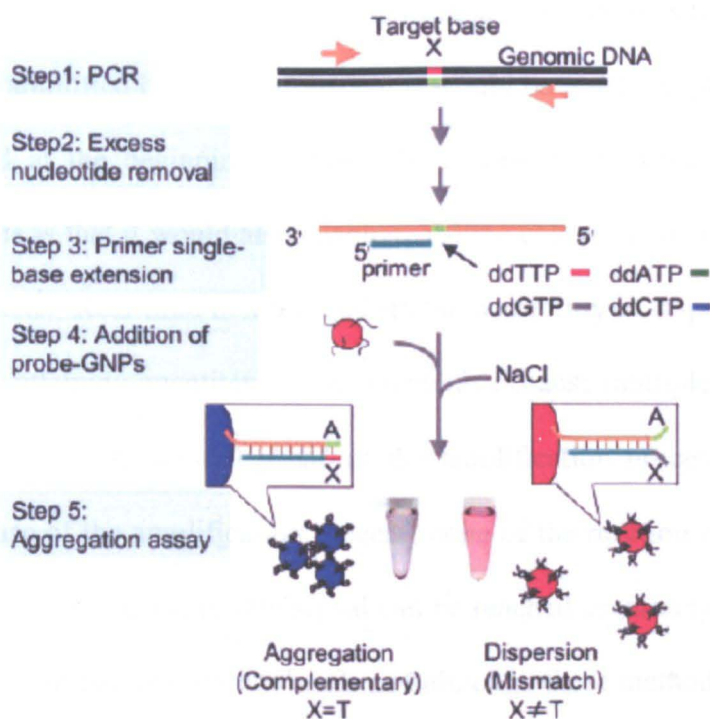
Figure 10: Diagram of Maeda and colleagues' colourimetric detection system. In step 1, target DNA is amplified by a regular PCR protocol. In step 2, the PCR product is purified. In step 3, a single-base primer extension reaction is performed with ddNTP. In step 4 and 5, oligonucleotide functionalised GNPs are mixed with the products of the primer extension reaction and a concentrated salt solution is added. Aggregation is observed if the product of the primer extension reaction is fully complementary to the sequence attached to the GNPs. From ref 32.
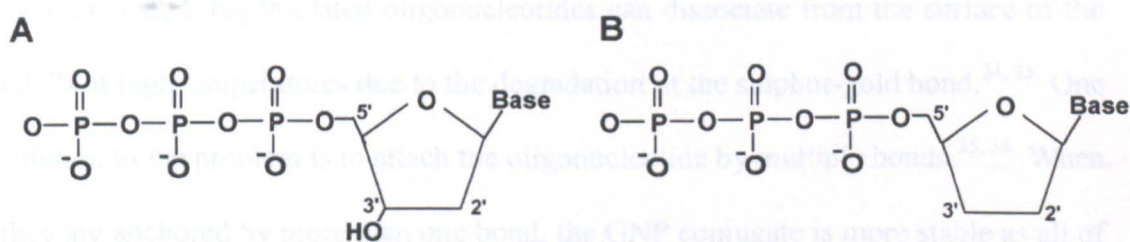
Figure 11: Structures of A) deoxynucleotide triphosphate (dNTP) and B) dideoxy triphosphate (ddNTP). The ddNTP lacks an OH group at the 3-carbon position and as a result, further nucleotides cannot be attached and extension is ceased.

21

The methods mentioned above involve colourimetric detection of nucleic acids after they have been amplified by PCR. However, it would be much simpler if the GNPs could be added at the beginning of the PCR amplification procedure. Another advantage of this is that it would also enable real-time colourimetric detection of the amplified products. Real-time detection offers the possibility of improved precision and accuracy in attaining quantitative measurements because multiple measurements are taken during the exponential phase of the amplification process. During the exponential phase of the amplification process, none of the reaction components are limiting, and therefore the maximum signal can be reached accurately.[33] At present, real-time methods utilize fluorescent labels and although these methods are relatively successful, they are often expensive. If GNP conjugates are to be added before the amplification procedure begins, the conjugates must be stable to PCR conditions such as high temperatures and buffers. They must also be stable in the presence of enzymes and thiol-containing reagents that are often present in enzymatic reactions.[34] Oligonucleotides are most often conjugated to GNPs using thiol chemistry and although the sulphur-gold bond is considered to be relatively strong, various studies have indicated that thiolated oligonucleotides can dissociate from the surface of the GNPs at high temperatures due to the degradation of the sulphur-gold bond.[34, 35] One solution to the problem is to attach the oligonucleotide by multiple bonds.[35, 36] When they are anchored by more than one bond, the GNP conjugate is more stable as all of the bonds have to be broken simultaneously to dissociate the oligonucleotide. Taton and colleagues suggested another alternative as they suspected that dissociation was due to a competitive reaction between thiol groups and the individual bases of the oligonucleotides for the GNP surface. They suggested that increased stability could

be achieved by attaching the oligonucleotides to a shell / outer layer, which would prevent direct contact between the oligonucleotide and the GNP surface.[34]

1.4.4- Colourimetric detection using aptamers

Aptamers are synthetic oligonucleotides that are generated by a selection process known as systemic evolution of ligands by exponential enrichment (SELEX). They bind to non-oligonucleotide targets such as metal ions, organic dyes and drugs, with specificity and an affinity equal to, and often superior to antibodies. Some aptamers can undergo significant structural changes upon binding to the specific ligand and Lu and Liu developed a colourimetric sensor for adenosine based on this concept (Figure 12).[37-39] In this approach, two different thiolated non-complementary oligonucleotides were immobilised on two sets of GNPs then mixed with a linker DNA sequence. The linker sequence contained; 1) a sequence that was fully complementary to the oligonucleotide sequence immobilised on one set of GNPs; 2) five bases that were complementary to the oligonucleotide sequence on the other set of GNPs and 3) an aptamer sequence specific for adenosine. When the oligonucleotide-GNP conjugates were mixed with the linker sequence, hybridisation occurred leading to the formation of DNA-linked aggregates and a change in colour from red to blue. However, in the presence of adenosine, the aptamer specific portion of the linker sequence changed conformation to bind the adenosine, the aggregated GNP structure disassembled and the solution changed colour from blue to red. Lu and Liu also developed colourimetric assays for other analytes based on the same principle simply by replacing the adenosine aptamer sequence with sequences specific for other analytes. A similar aptamer based aggregation assay for adenosine was developed by Li and colleagues.[40] Thiolated oligonucleotide was immobilised

onto GNPs then the oligonucleotide-GNP conjugate was mixed with an aptamer sequence that was complementary to the oligonucleotide sequence immobilised on the GNPs. In the absence of adenosine, upon the addition of highly concentrated salt, the GNP complex was resistant to aggregation and the solution remained red. However, if adenosine was present, the aptamer sequence de-hybridised from the oligonucleotide-GNP and changed conformation to bind to the adenosine. This destabilized the GNPs and upon the addition of a highly concentrated salt, aggregation was induced accompanied by a colour change from red to blue. Li and colleagues claimed that they could detect 10 nmol of adenosine by this method, which is ten times more than Lu and Liu, but further increases in sensitivity could be achieved with assay optimisation.

Wang and colleagues used unmodified GNPs and potassium aptamers in a colourimetric aggregation assay for potassium ions (K^+).[41] The potassium aptamer is a guanine rich single stranded (ss) sequence that folds into a tetraplex structure upon binding to potassium ions. Based on Li and Rothberg's observations of the propensity of unmodified ssDNA to stabilize GNPs against salt-induced aggregation, the ss aptamer sequence was mixed with unmodified GNPs. When a high concentration of salt was added to the solution, the GNP solution remained red due to the stabilization effect of the absorbed single stranded DNA. However, if the ss aptamer was mixed with potassium before addition to the GNPs, it changed conformation to bind the potassium. In this case the GNPs were not stabilized and they aggregated upon addition of salt solution.
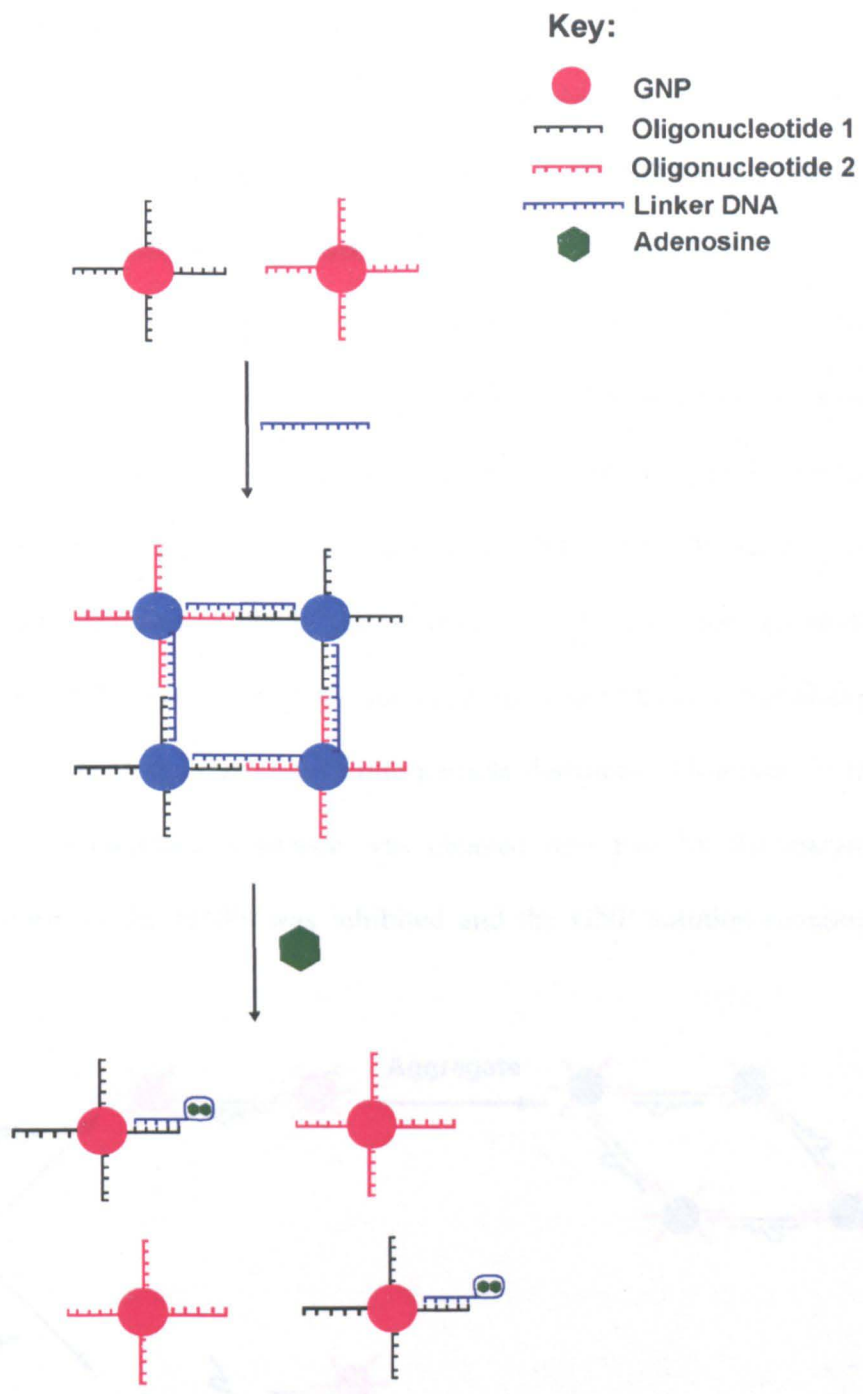
Figure 12: Diagram of Lu and Liu's aptamer based colourimetric assay. Two sets of GNPs functionalised with non-complementary oligonucleotides were linked by hybridisation with the linker DNA sequence. The linker DNA sequence contained a sequence fully complementary to oligonucleotide 1, a partially complementary sequence to oligonucleotide 2 and an aptamer sequence specific for adenosine. When adenosine was added to the solution, the DNA-linked aggregates dispersed and the solution changed colour from blue to red as the aptamer sequence changed conformation to bind the adenosine.

1.4.5-Colourimetric detection of other molecules

Colourimetric assays have also been developed to determine the activity of other molecules such as metal ions and DNA-binding molecules. Lu and Liu developed a colourimetric assay for metal ions that utilized catalytically active DNA molecules called DNAzymes (Figure 13).[42] The DNAzyme was composed of a substrate sequence and an enzyme sequence which recognised Pb^{2+}. The substrate sequence contained a single RNA linkage and a sequence at each end that was complementary to oligonucleotide sequences immobilised on GNPs. When the DNAzyme was mixed with the functionalised GNPs in the absence of Pb^{2+} the oligonucleotides immobilised on the GNPs hybridised to the substrate sequence and a colour change to blue was induced due to the decrease in interparticle distances. However, in the presence of Pb^{2+}, the substrate sequence was cleaved into two by the enzyme sequence, aggregation of the GNPs was inhibited and the GNP solution remained red.
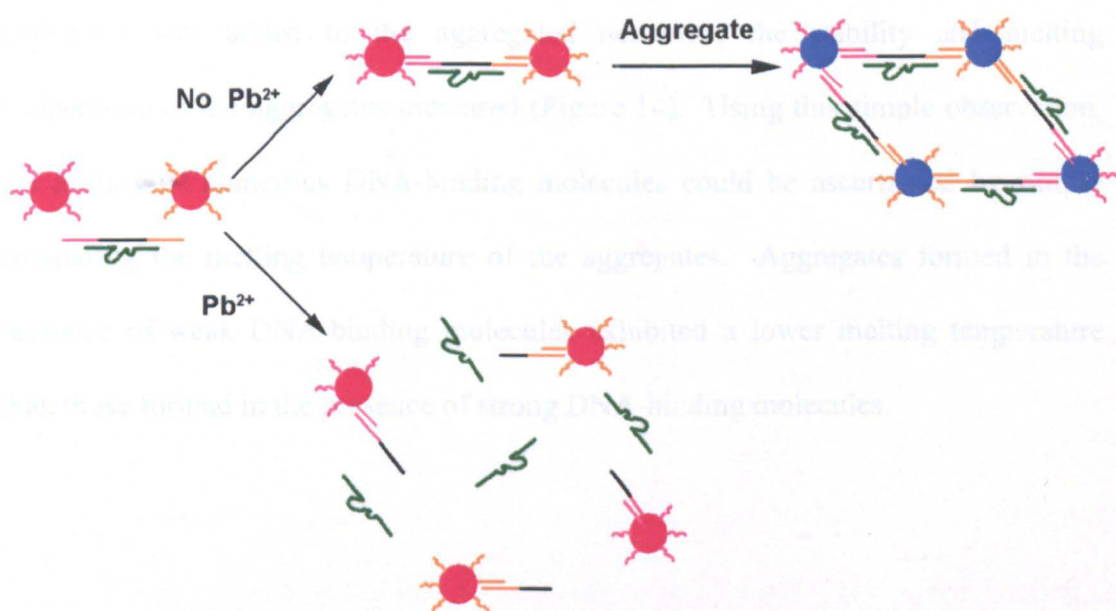
Figure 13: Colourimetric assay based on DNAzymes developed by Lu and Liu. Enzyme strand = green. Substrate strand (black) had extended regions that were complementary to the sequences immobilised on the GNPs (pink and orange). When metal ions were not present, the oligonucleotides immobilised on the GNPs hybridised to the extended regions of the substrate strand. When metal ions were present, the substrate strand was cleaved by the enzyme strand and aggregation was prevented.

Mirkin and colleagues also developed a colourimetric assay for the detection of mercury ions.[43] Two different oligonucleotides, complementary to each other except for one mismatched thymidine base were immobilised onto two sets of GNPs. When mixed, despite the mismatch, the oligonucleotides hybridised together forming DNA-linked aggregates that had a characteristic melting temperature. When mercury ions were present, they bound to the mismatched bases increasing the stability and therefore the melting temperature of the DNA-linked aggregates. A similar system was employed to determine the affinities of DNA-binding molecules such as the anticancer drugs doxorubicine and amsacrine.[44] These particular drugs are known to bind to DNA and the affinity is indicative of the biological activity. In this colourimetric assay, two different oligonucleotides, complementary to each other were immobilised onto two sets of GNPs. Upon mixing the oligonucleotides hybridised together inducing a colour change from red to blue as DNA-linked GNP aggregates formed. Mirkin and colleagues found that if a solution of DNA-binding molecules was added to the aggregated networks, the stability and melting temperature of the aggregates increased (Figure 14). Using this simple observation, the affinity of numerous DNA-binding molecules could be ascertained by simply comparing the melting temperature of the aggregates. Aggregates formed in the presence of weak DNA-binding molecules exhibited a lower melting temperature than those formed in the presence of strong DNA-binding molecules.

Melting Temperature (T_m 1)

Melting Temperature (T_m 2)
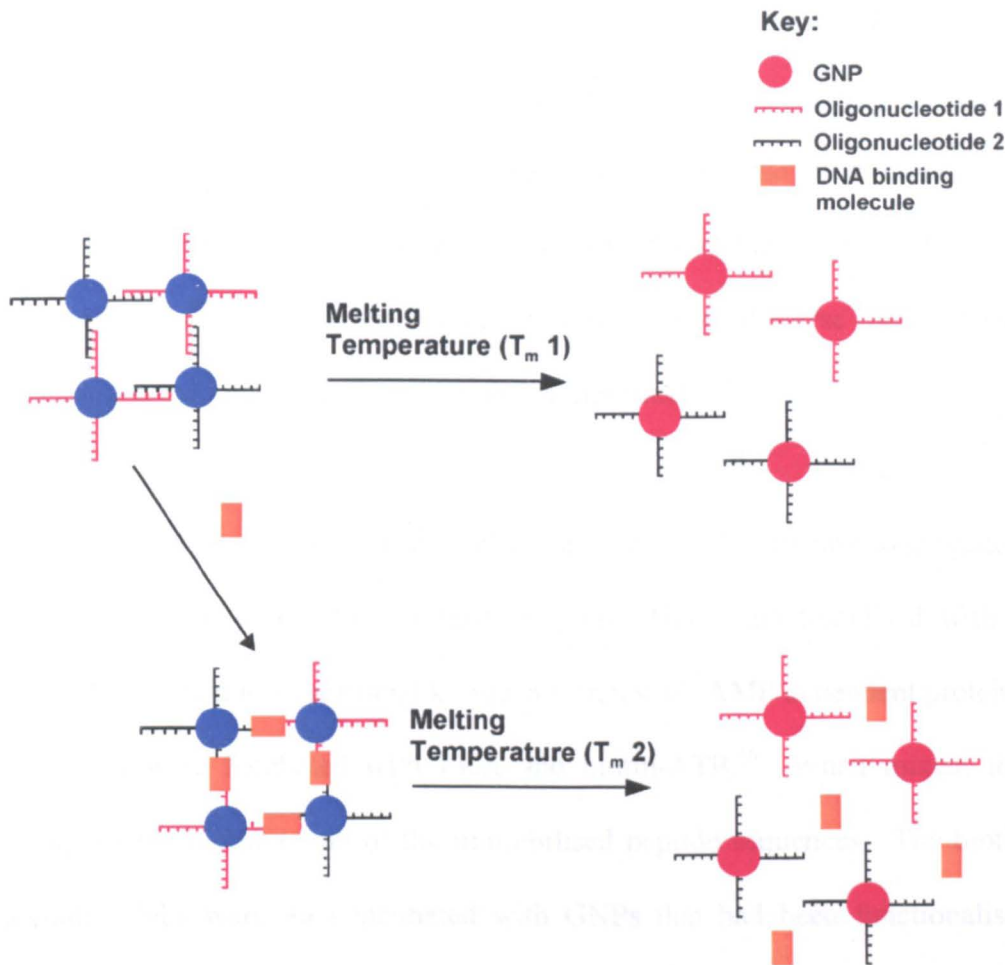
Figure 14: Diagram showing Mirkin and colleagues aggregation based colourimetric assay for the determination of the affinity of DNA-binding molecules. Two sets of GNPs functionalised with complementary oligonucleotides were mixed and formed DNA-linked GNP aggregates. These DNA-linked aggregates could be dispersed by heating the solution above the melting temperature of the DNA duplex. If DNA-binding molecules were added, the melting temperature required to disperse the aggregates increased.

1.4.6- Colourimetric detection of enzymes using GNPs

Mirkin also employed a similar system to determine the activity and inhibition of the enzyme endonuclease.[45] In this approach, two different complementary oligonucleotides were immobilised on two sets of GNPs and when mixed, a network of DNA-linked aggregates formed. These aggregates were then used to determine the enzymatic activity of the endonuclease DNase I, which catalyzes nucleic acid hydrolysis. Adding this enzyme to DNA-linked aggregates leads to the degradation

of the DNA duplex and induces a colour change from blue to red as the GNPs are re-dispersed. If the concentration of endonuclease was increased, the time taken for the aggregates to disperse increased. This method was also used to determine the efficiency of compounds that bind to DNA and inhibit the enzyme activity. As the efficiency of the inhibitor increased, the time taken to disperse the aggregates and observe the colour change from blue to red increased.

Wang and colleagues developed a different type of colourimetric aggregation assay to screen for inhibitors for a kinase enzyme. GNPs functionalised with peptide sequences known to be artificial kinase substrates of cAMP dependent protein kinase A (PKA) were incubated with PKA and biotin-ATP.[46] When mixed, the PKA catalyzed the biotinylation of the immobilised peptide sequences. The biotinylated peptide GNPs were then incubated with GNPs that had been functionalised with avidin. Over time, the solution of mixed GNPs changed colour from red to blue as the biotinylated peptides bound to the avidin subsequently forming a network of aggregated GNPs. In order to screen for inhibitors, peptide functionalised GNPs were mixed with PKA, biotin-ATP and the potential inhibitor. In the presence of an effective inhibitor, PKA did not catalyze the biotinylation of the peptide and when the GNPs were mixed with the avidin functionalised GNPs, aggregation did not occur. Wang and colleagues suggested that this method would be useful for the identification of kinases, substrates and potential inhibitors which are of great importance in drug discovery. In order to do this however, the method would require some minor alterations to enable a more high-throughput approach that would be necessary for the screening of many compounds.

In another example, Shen and colleagues used unmodified GNPs in a colourimetric aggregation based assay for hydrogen peroxide.[47] Horseradish peroxidase (HRP) and the substrate o-phenylenediamine (OPD) were mixed with unmodified GNPs. If hydrogen peroxide was present, HRP catalyzed the oxidation of the OPD resulting in the production of azoaniline. This product cross-linked the GNPs inducing a colour change from red to blue. One of the major problems associated with Shen's method was that GNP aggregation was induced in the absence of hydrogen peroxide if there was a high concentration of OPD or HRP in the reaction mixture, so the concentrations of both had to be carefully monitored. In addition, they also found that certain compounds could affect the oxidation of OPD and interfere with the results of the colourimetric assay.

1.4.7- Non-aggregation based homogeneous colourimetric detection with GNPs

The colourimetric assays mentioned in this chapter so far rely on a colour change imparted by the aggregation or disassembly of GNPs induced by specific binding events or high concentrations of salt. However, as mentioned in an earlier section of this chapter, the colourimetric properties of GNPs can be affected by other parameters. Willner and colleagues developed a colourimetric assay that did not rely on aggregation but on the catalytic growth of individual GNPs which imparted a colourimetric change in the solution.[48] They mixed gold salts with seed particles and surfactant (growth solution) and measured the change in absorbance of the solution upon the addition of different concentrations of nicotinamide adenine dinucleotide (NADH). In the absence of NADH, the solution was orange in colour and had a characteristic absorbance band at 393 nm due to the presence of $AuCl_4^-$. However, as the concentration of NADH increased the absorbance band at 392 nm decreased,

and the absorbance increased at 524 nm indicating the growth of the seed particles. The reactions are outlined below in equations 1 and 2. In the first stage of this reaction, the $AuCl_4^-$ is reduced to Au^I by NADH. In the second stage of the reaction, the Au^I species is reduced, catalyzed by the GNPs, which act as seeds to form larger GNPs.

$$AuCl_4^- + NADH \longrightarrow Au^I + 4\,Cl^- + NAD^+ + H^+ \qquad (1)$$

$$2Au^{I} + NADH \xrightarrow{\text{GNPs}} 2Au^0 + NAD^+ + H^+ \qquad (2)$$
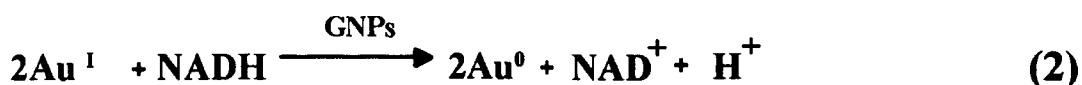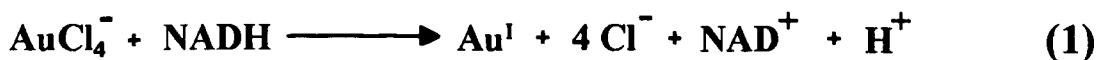
Willner and colleagues used the catalytic growth assay to monitor enzymatic transformations. The enzyme NAD^+ dependent lactate dehydrogenase (LDH) was mixed with different concentrations of lactate and then mixed with the growth solution. LDH catalyzes the conversion of lactate to pyruvate (Figure 15). In this reaction lactate is oxidized and converted to pyruvate and NAD^+ is reduced and is converted to NADH. As the concentration of lactate is increased, the concentration of NADH produced increases leading to the growth of the GNP seeds. Willner and colleagues have since used similar GNP growth methods to detect glucose in the presence of glucose oxidase [49] and have also enlarged GNPs by the biocatalyzed deposition of copper.[50]
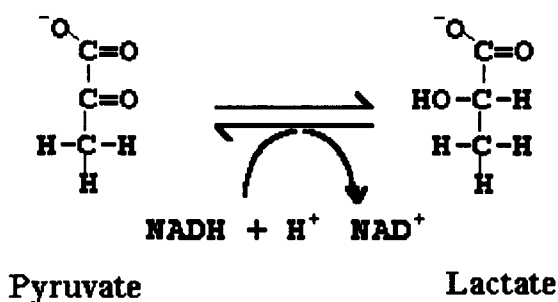
Pyruvate   Lactate

Figure 15: The catalytic conversion of lactate to pyruvate by LDH. Lactate is oxidized and is converted to pyruvate. NAD^+ is reduced and is converted to NADH.

1.5- Heterogeneous colourimetric detection using GNPs

The assays described so far in this chapter have involved the solution phase detection of various analytes but many colourimetric assays have also been performed using solid supports such as microbeads, membranes or glass. These methods can be described as heterogeneous as they require washing and separation steps to separate free from bound label. Although some homogeneous methods such as those described earlier may be faster and less technically challenging, heterogeneous assays are often more sensitive because the washing steps can remove interferents and reduce non-specific binding which improves the detection limit of the assay.[14] Again as in the previous sections the described methods in this section will only concentrate on results obtained with GNP labels that can be visualised without the requirement of additional equipment.

1.5.1- Microbead assays

As mentioned in the earlier sections of this chapter, a great deal of research on colourimetric detection methods, particularly in the solution phase was carried out by Mirkin and colleagues. They went on to apply some of the same techniques in solid

phase detection methods and developed a heterogeneous microbead assay for the detection of target oligonucleotides (Figure 16).[51] In this approach, one oligonucleotide sequence was immobilised onto GNPs (detector probe) and a different sequence was immobilised onto white microspheres (capture probe). Both sequences had regions that were complementary to the target of interest. The sample was mixed with the capture probe and the detector probe was added. If the sample contained the target sequence, it hybridised to the capture probe and the detector probe and the GNPs were bound to the microspheres. The solution was then passed through a filter membrane and the presence of the target was indicated by the formation of a red dot when the microspheres were retained on the membrane.
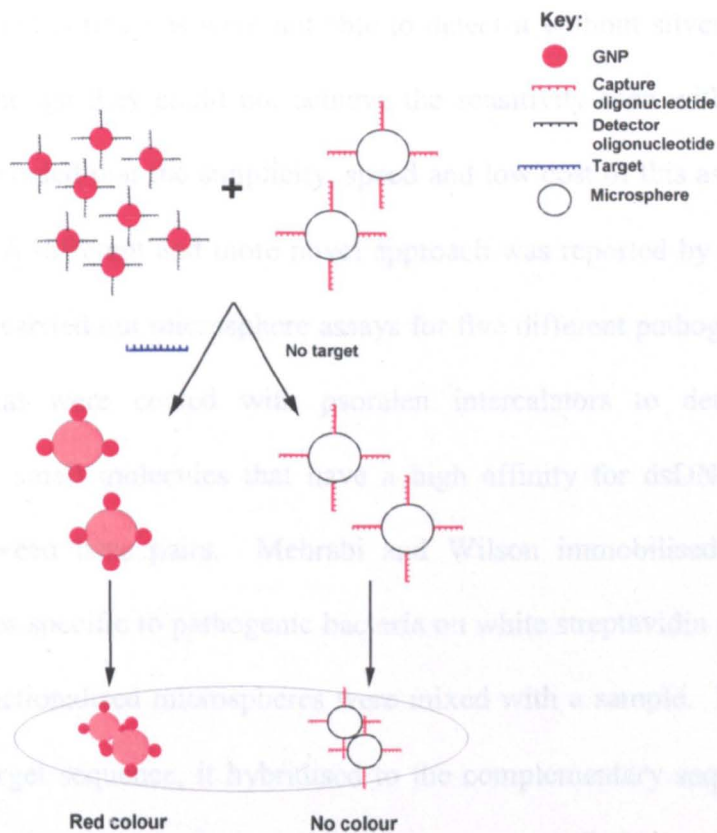
Figure 16: Mirkin and colleagues GNP microsphere colourimetric assay. GNPs functionalised with detector oligonucleotide are mixed with white microspheres functionalised with capture oligonucleotides and the sample. If the sample contains the target oligonucleotide it is sandwiched between the capture and detector oligonucleotides. The microspheres are applied to a membrane, excess GNPs are washed away and the presence of target oligonucleotide is indicated by the development of a red colour on the membrane as the microspheres are retained. If the target oligonucleotide is not present, the membrane remains white.

In another example, Upadhyay and colleagues developed a microbead assay to detect target DNA from *Mycobacterium tuberculosis*.[52] In this work, capture oligonucleotides were attached to microbeads and detector oligonucleotides were conjugated to GNPs. Both oligonucleotide sequences had regions complementary to the target of interest. Small amounts of target DNA, equivalent to amounts usually subjected to PCR amplification were extracted from samples, heated to 95 °C to denature and then plunged into ice and salt mixture to prevent re-annealing. The target was then mixed with the oligonucleotide functionalised microbeads and GNPs for hybridisation. Following hybridisation the mixture was applied to a filter and the filter was washed to remove un-reacted GNPs. As the amount of target DNA was low, Upadhyay and colleagues were not able to detect it without silver staining the membrane. Although they could not achieve the sensitivity seen with PCR based assays, they concluded that the simplicity, speed and low cost of this assay were the major benefits. A different and more novel approach was reported by Mehrabi and Wilson.[53] They carried out microsphere assays for five different pathogenic bacteria using GNPs that were coated with psoralen intercalators to detect dsDNA. Intercalators are small molecules that have a high affinity for dsDNA and insert specifically between base pairs. Mehrabi and Wilson immobilised biotinylated capture sequences specific to pathogenic bacteria on white streptavidin microspheres and then the functionalised microspheres were mixed with a sample. If the sample contained the target sequence, it hybridised to the complementary sequence on the microspheres to form a ds duplex. The hybridised target could then be detected colourimetrically by the addition of psoralen functionalised GNPs. The psoralen coated GNPs intercalated into the ds duplex and the microspheres became pink. As the amount of target sequence was increased, the colour of the beads also increased.

Mehrabi and Wilson could detect as little as 25 pmols of target sequence using the microbead assay and were also able to increase the detection limit further by performing a PCR amplification step before detection in a membrane-based assay, which will be discussed in section 1.5.3.

1.5.2- Western Blot

One of the first membrane based techniques was developed by Ed Southern in the 1970's. Termed Southern blotting, this method was developed for the analysis of DNA fragments that had been separated on agarose gels. Separated DNA is capillary transferred onto a nitrocellulose membrane where it is then probed by RNA or cDNA.[54] This particular concept was adapted for the detection of proteins by Towbin and colleagues. The western blot or immunoblot method is based upon the transfer of separated proteins from gels to membranes, where they are detected with labelled probes.[55] Like Southern blotting, western blotting uses electrophoresis to separate proteins by size. The proteins are then transferred to a membrane where they are identified using labelled antibodies specific to the target protein. A great deal of research in this area has involved the use of radiolabelled or enzyme labelled probes, however, GNP labels have become increasingly popular since the development of GNP conjugation methods. GNP labelled probes are easier to use than enzymatic labels that often require multiple washing and reaction steps, and their use also avoids the safety issues involved with radiolabels. Although they are still extensively used western blots do have some drawbacks. They are often lengthy and quite complicated procedures that require trained personnel.

1.5.3- Dot-blots and arrays

Another category of membrane-based assay is the dot-blot. Dot-blots can be used to detect multiple proteins, are relatively inexpensive, simple to perform and also offer high specificity and relatively high sensitivity. In this approach complex protein samples are applied directly to a membrane as spots. The membrane is then washed and blocked before the protein is detected. Detection is achieved with the use of a labelled probe either directly in one simple step or indirectly. Matsuzawa and colleagues developed a dot-blot assay with a direct detection step to identify blood from different species of animals.[56] Blood samples were spotted onto a membrane and allowed to dry. Following blocking, GNPs conjugated with antiserum to human IgG were applied and drawn through the membrane by vacuum. The GNP labelled antiserum bound to blood extracts taken from humans or monkeys producing a red spot on the membrane, but did not bind to extracts from other species of animals. Although much of the research was performed in the early 80's and 90's, dot-blots are still widely used today.[57] In recent years they have also been adapted for the detection of DNA, but much of this work utilizes enzyme or radiolabel detection methods.

Arrays are solid supports, usually glass microscope slides, silicon chips or membranes onto which probe molecules such as antibodies, antigens, peptides or DNA are spotted at fixed locations to enable the high-throughput analysis of target molecules. The sample is applied to the array of molecules and after washing, detection of the bound target is achieved with a labelled detector reagent. Moeremans and colleagues used a membrane array for the detection of antigenic proteins.[58] A primary antibody specific for the protein was first applied to the

36

membrane. After washing, the antibody-antigen binding reaction was visualised by the addition of a GNP labelled secondary antibody. Hsu used exactly the same approach for the detection of viral proteins.[59] Brada and Roth reported a slightly different detection strategy.[60] The immobilised antigens were first reacted with a primary antibody and then the reaction was visualised by the addition of a GNP labelled protein A. A slightly more complicated method was applied by Vera-Cabrera and colleagues for the detection of antibodies in tuberculosis patients.[61] In this work, antigen was attached to the membrane and a sample was applied. If the sample contained the antibody, this bound to the immobilised antigen on the membrane. Although this antibody-antigen complex could have then been detected using GNP labelled protein A, Vera-Cabrera and colleagues found that they could improve the sensitivity of the assay if they first added a rabbit anti-human serum that specifically bound to the antibody before detection with GNP labelled protein A.

An elegant membrane based array that used GNP labels for the detection of DNA from different pathogenic bacteria which could also be interfaced with a PCR protocol was described by Mehrabi and Wilson.[53] Capture oligonucleotides specific to five pathogenic bacteria were covalently attached to a membrane and then the membrane was incubated with the products of an asymmetric PCR protocol. GNPs that had been coated with intercalating molecules were then applied to the membrane. If any of the target sequences were present in the PCR products, they hybridised to the specific capture oligonucleotides forming a double-stranded duplex on the membrane. The intercalating GNPs then inserted into the duplex and a red spot was observed on the membrane. Mehrabi and Wilson were able to detect

amplified products corresponding to 1 attomole of template molecules with the unaided eye using this membrane-based assay.

Sun and colleagues used 250 nm sized positively charged GNPs to detect the hybridisation of target oligonucleotides to probe oligonucleotides immobilised on glass microscope slides.[62] The detection was based on an electrostatic interaction between positively charged GNPs and the negatively charged hybridised target molecules. The quantity of deposited GNPs was proportional to the amount of negative charge on the spot. As a result, spots on the array that had hybridised target and probe showed more gold binding than non-hybridised spots due to the increased negative charges. With exception to the work by Sun and colleagues, visual detection of specifically bound GNPs on glass microarrays is usually only achieved with silver enhancement. This is because in many cases the surface density of GNPs bound to the array is too low for visual detection. In silver enhancement, silver salts ($AgNO_3$) are mixed with a reducing agent such as hydroquinone. In the presence of GNPs, silver ions are reduced into metallic silver which is then deposited on the particles. The silver shell around the GNP then autocatalyzes further silver depositions leading to an increase in the size of the particle. Taton and colleagues used silver enhancement to detect hybridised target oligonucleotides in a DNA microarray. GNPs functionalised with an oligonucleotide sequence complementary to a target oligonucleotide were used to detect target oligonucleotides that had hybridised to probe oligonucleotides attached to functionalised glass microscope slides. Bound GNPs were then visualised after the addition of silver enhancement solution.[63] In another example, Alexandre and colleagues used streptavidin functionalised GNPs and silver enhancement to visualise the hybridisation of

biotinylated target oligonucleotides to probe oligonucleotides attached to functionalised glass microscope slides.[64]

1.5.4- Flow-through devices

Flow-through devices are simple membrane-based colourimetric tests usually comprising of a membrane containing an immobilised capture reagent such as an antibody and an absorbent pad (Figure 17).[14] When a sample containing the target analyte is applied it flows through the membrane and binds to the capture reagent. Detection reagents, such as labelled antibodies, wash solutions and other reagents required for the assay are then sequentially applied. The presence or absence of the analyte is generally indicated by a visible coloured response on the membrane which is usually proportional to the amount in the sample. There are many different flow-through devices available commercially for the detection of a large variety of analytes. One such device, the Reveal Rapid HIV-1 test, has been developed by MedMira for the detection of Human Immunodeficiency Virus (HIV) antibodies in HIV infected patients. The sample is applied to a nitrocellulose membrane that contains immobilised HIV antigens. If anti-HIV antibodies are present, they bind to the antigens on the membrane. Following washing, the bound antibodies are visualised by the addition of a GNP labelled protein A detection reagent. Although flow-through devices offer fast, visible results and are relatively inexpensive to produce, there are drawbacks associated with this type of test. Many of the devices require sequential addition of reagents, some of which must be applied within and for a specific time period. In most cases, they also require washing steps in-between the additions of the various reagents. Insufficient incubation times or washing of the membrane could lead to false positive or negative results. For example, when using

the MedMira HIV test, both sample application time and colour development time must be carefully monitored. If allowed to proceed for too long, the test results are considered invalid. As a result, flow-through assays should only be carried out in the laboratory by trained personnel to avoid ambiguous results.
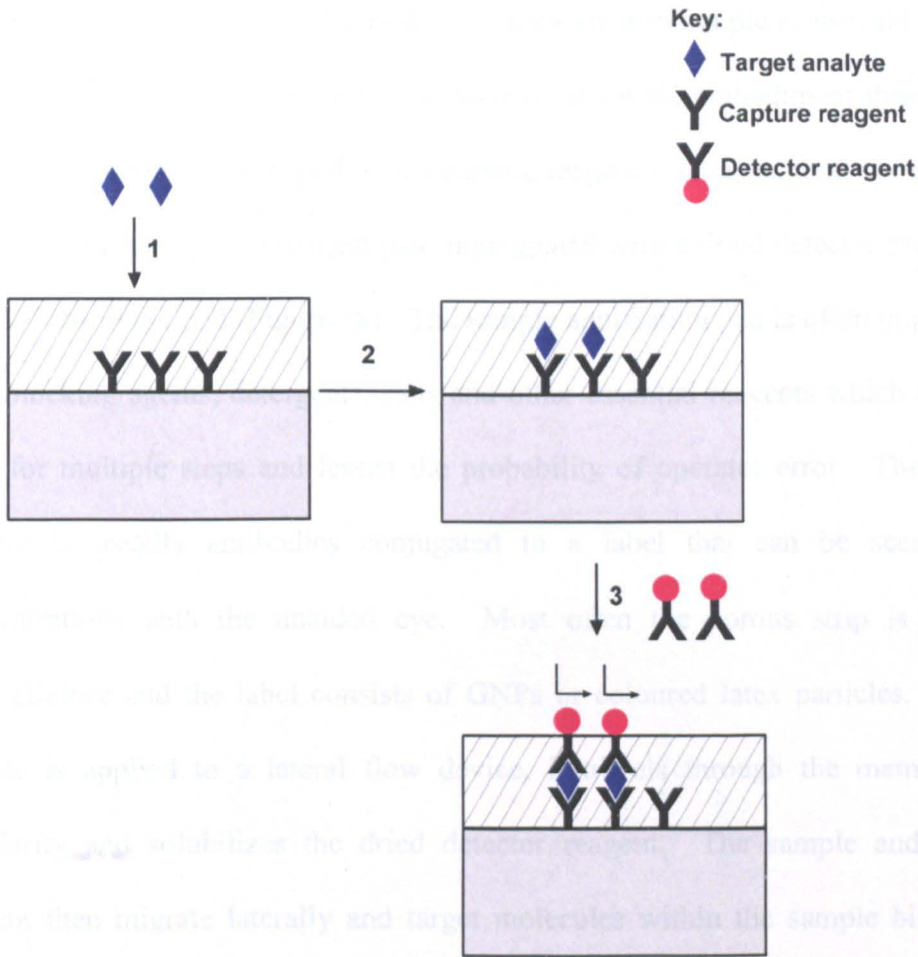
Figure 17: Schematic diagram of a sandwich format flow-through device. In step 1, a sample is applied to membrane (hatched). In step 2, the target analyte binds to the immobilised capture reagent. In step 3, detector reagent is applied to the membrane, binds to the analyte and a colourimetric signal is produced.

1.5.5- Immunochromatographic devices

Immunochromatographic or lateral flow devices are one of the most common forms of membrane-based colourimetric test. Although these devices are very similar to

flow-through devices, the main advantage of this format is that the detection of an analyte is potentially achieved in one step as the detector and capture reagents are contained within the strip. These tests have become familiar through their use in clinics, at hospital bed sides, field locations, as well as in over-the-counter tests. They are inexpensive, mass producible, non-instrumental, reliable and usually provide results in minutes.[65] In most cases they are also simple to use and interpret, even by non-specialized personnel. In their most simple embodiment these devices consist of a porous strip striped with a capture reagent such as antibody or antigen, a sample application pad, a reagent pad impregnated with a dried detector reagent and a wick / absorbent pad (Figure 18). The sample application pad is often impregnated with blocking agents, detergents, salts and other essential reagents which avoid the need for multiple steps and lessen the probability of operator error. The detector reagent is usually antibodies conjugated to a label that can be seen at low concentrations with the unaided eye. Most often the porous strip is made of nitrocellulose and the label consists of GNPs or coloured latex particles. When a sample is applied to a lateral flow device, it travels through the membrane by capillarity and solubilizes the dried detector reagent. The sample and detector reagent then migrate laterally and target molecules within the sample bind to the capture reagent immobilised on the test-line. Excess reagents are then absorbed by the wick.

SP   RP   NC   TL   AP

Direction of flow
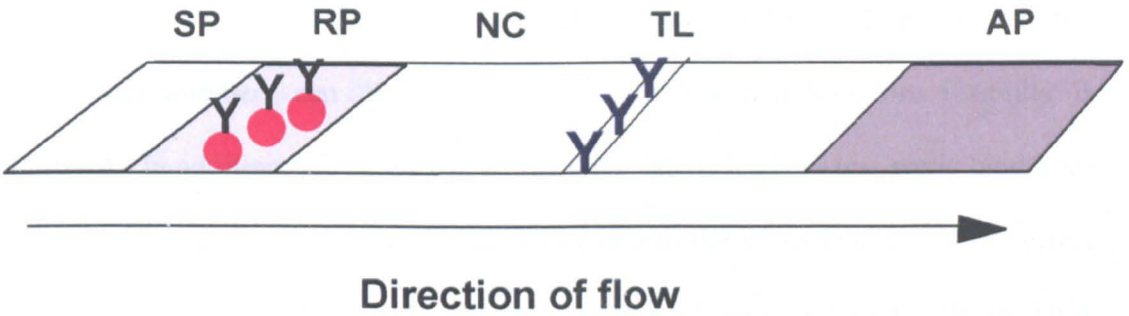
Figure 18: Schematic diagram of a lateral flow device. SP= sample application pad; RP= reagent pad; NC= nitrocellulose strip; TL= test-line and AP= absorbent pad / wick.

Key:

● GNP

● Coloured latex particle

Y Capture antibody

Y Detector antibody

♦ Analyte

A

B
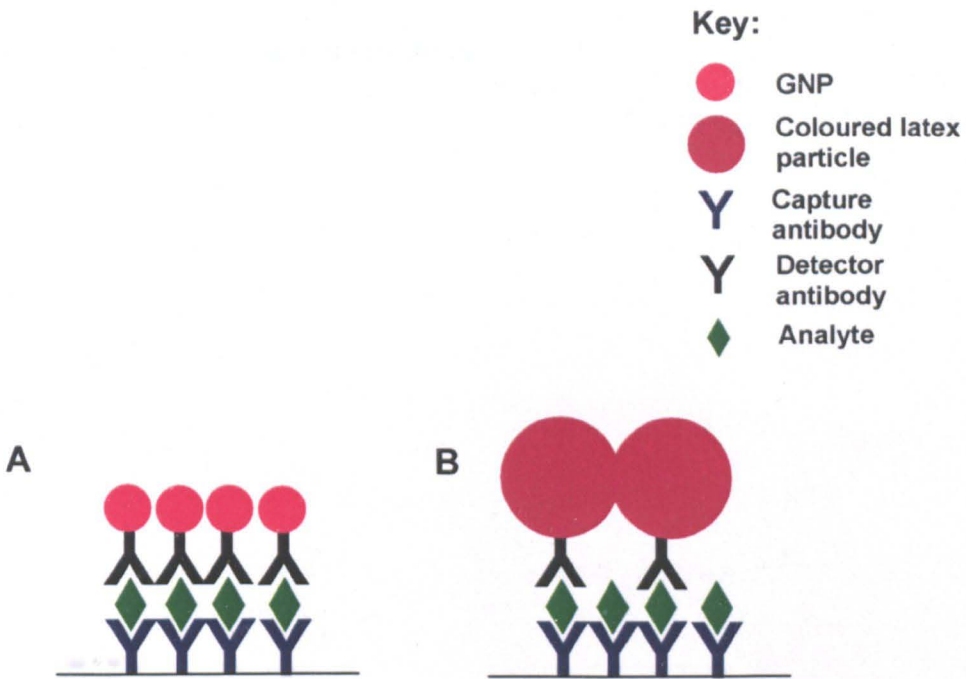
Figure 19: The situation that occurs at the test-line when lateral flow assays are performed with A) GNP labelled antibodies. As the GNPs are smaller, more GNPs can pack in at the test-line and less steric hindrance occurs. All of the bound analyte is detected. B) Large latex particle labelled antibodies. As the latex particles are larger, fewer particles can bind to the captured analyte.

GNPs are often the label of choice in lateral flow devices due to their high extinction coefficients and stability. To observe comparable sensitivity in dyed latex particle assays it is often necessary to use much larger particles (~ 150 – 450 nm).[65, 66] Due

42

to the high extinction coefficients of GNP labels, small GNPs (~ 40 nm) can be used and greater numbers can "pack" at the capture line and therefore visibility is improved. In addition, the small size of the GNP labels leads to less steric hindrance at the test-line as the particles are more accessible to the target analyte.[65] The effect at the test line in a reagent-excess or "sandwich" assay using GNPs or latex microspheres is illustrated in Figure 19. Much of the research carried out for this thesis involved the use of lateral flow assays. As a result, a more comprehensive discussion on these devices, the different types available and research in this area is contained in chapters 3 and 4 of this thesis.

1.6-References

1. Freestone, I., Meeks, N., Sax, M., Higgitt, C., *Gold Bull.*, (2007), **40**, 270-277.

2. Wagner, F.E., Haslbeck, S., Stievano, L., Calogero, S., Pankhurst, Q.A., Martinek, K.P., *Nature*, (2000), **407**, 691-692.

3. Hunt, L.B., *Gold Bull.*, (1976), **9**, 134-139.

4. Faraday, M., *Philos. Trans. R. Society. London*, (1857), **147**, 145-

5. Thompson, D., *Gold Bull.*, (2007), **40**, 267-269.

6. Turkevich, J., *Gold Bull.*, (1985), **18**, 86-91.

7. Turkevich, J., Stevenson, P.C., Hillier, J., *Discuss. Faraday Soc.*, (1951), **11**, 55-75.

8. Chandler, J., Gurmin, T., Robinson, N., *IVDTechnology magazine*, (2000), March issue.

9. Carney, J., Braven, H., Seal, J., Whitworth, E., *IVDTechnology Magazine* (2006), March issue.

10. Fritzsche, W., Taton, T.A., *Nanotechnology*, (2003), **14**, R63-R73.

11.. Englebienne, P., Van Hoonaker, A., Verhas, M., *Spectroscopy*, (2003), **17**, 255-273.

12. Moores, A., Goettmann, F., *New. J. Chem.*, (2006), **30**, 1121-1132.

13. Underwood, S., Mulvaney, P., *Langmuir*, (1994), **10**, 3427-3430.

14. Price, C.P., Newman, D.J. *Principle and Practice of Immunoassay* (1997), Macmillan Publishers, London.

15 Leuvering, J.H.W., Thal, P.J.H.M., van der Waart, M., Schuurs, A.H.W.M., *J. Immunol. Methods*, (1981), **45**, 183-194.

16. Leuvering, J.H.W., Thal, P.J.H.M., White, D.D., Schuurs, A.H.W.M., *J. Immunol. Methods*, (1983), **62**, 163-174.

17. Leuvering, J.H.W., Goverde, B.C., Thal, P.J.H.M., Schuurs, A.H.W.M., *J. Immunol. Methods*, (1983), **60**, 9-23.

18. Gribnau, T.J.C., Leuvering, J.H.W., *J. Chromatogra.*, (1986), **376**, 175-189.

19. Englebienne, P., *Analyst*, (1998), **123**, 1599-1603.

20. Englebienne, P., Van Hoonacker, A., Verhas, M., *Analyst*, (2001), **126**, 1645-1651.

21. Englebienne, P., *J. Mater. Chem.*, (1999), **9**, 1043-1054.

22. Mirkin, C.A., Letsinger, R.L., Mucic, R.C., Storhoff, J.J., *Nature*, (1996), **382**, 607-609.

23. Elghanian, R., Storhoff, J.J., Mucic, R.C., Letsinger, R.L., Mirkin, C.A., *Science*, (1997), **277**, 1078-1081.

24. Storhoff, J.J., Elghanian, R., Mucic, R.C., Mirkin, C.A., Letsinger, R.L., *J. Am. Chem. Soc.*, (1998), **120**, 1959-1964.

25. Reynolds, R.A., Mirkin, C.A., Letsinger, R.L., *J. Am. Chem. Soc.*, (2000), **122**, 3795-3796.

26. Murphy, D., O'Brien, P., Redmond, G., *Analyst*, (2004), **129**, 970-974.

27. Li, J., Chu, X., Liu, Y., Jiang, JH., He, Z., Zhang, Z., Shen, G., Yu, RQ., *Nucl. Acids Res.*, (2005), **33**, e168.

28. Li, H., Rothberg, L., *P. Natl. Acad. Sci. USA.*, (2004), **101**, 14036-14039.

29. Parak, W.J., Pellegrino, T., Micheel, C.M., Gerion, D., Williams, S.C., Alivisatos, A.P. *Nano Lett.*, (2003), **3**, 33-36.

30. Baptista, P.V, Koziol-Montewka, M., Paluch-Oles, J., Doria, G., Franco, R., *Clin .Chem.*, (2006), **52**, 1433-1434.

31. Li, H., Rothberg, L.J., *J. Am. Chem. Soc.*, (2004), **126**, 10958-10961.

32. Sato, K., Hosokawa, K., Maeda, M., *Nucl. Acids Res.*, (2005), **33**, e4.

33. Storhoff, J.J., Fritz, B.M., Herrmann, M., (2003) PCT Int. Appl. 2003048769.

34. Herdt, A.R., Drawz, S.M., Kang, Y., Taton, T.A., *Colloid Surface B*, (2006), **51**, 130-139.

35. Letsinger, R.L., Elghanian, R., Viswanadham, G., Mirkin, C.A., *Bioconjugate Chem.*, (2000), **11**, 289-291.

36. Li, Z., Jin, R., Mirkin, C.A., Letsinger, R.L., *Nucl. Acids Res.*, (2002), **30**, 1558-1562.

37. Liu, J., Lu., Y., *Angew. Chem. Int. Ed.*, (2006), **45**, 90-94.

38. Liu, J., Lu, Y., *Nature Protocols*, (2006), **1**, 246-252.

39. Liu, J., Lu, Y., *J. Am. Chem. Soc.*, (2007), **129**, 8634-8643.

40. Zhao, W., Chiuman, W., Brook, M.A., Li, Y., *ChemBioChem.*, (2007), **8**, 727-731.

41. Wang, L., Liu, X., Hu, X., Song, S., Fan, C., *Chem. Commun.*, (2006), 3780-3782.

42. Liu, J., Lu, Y., *J. Am. Chem. Soc.*, (2004), **126**, 12298-12305.

43. Lee, JS., Han, MS., Mirkin, C.A., *Angew. Chem. Int. Ed.*, (2007), **46**, 4093-4096.

44. Han, MS., Lytton-Jean, A.K.R., Oh, BK., Heo, J., Mirkin, C.A., *Angew. Chem. Int. Ed.*, (2006), **45**, 1807-1810.

45. Xu, X., Han, MS., Mirkin, C.A., *Angew. Chem. Int. Ed.*, (2007), **46**, 3468-3470.

46. Wang, Z., Levy, R., Fernig, D.G., Brust, M., *J. Am. Chem. Soc.*, (2006), **128**, 2214-2215.

47. Wu, Z.S., Zhang, S.B., Guo, M.M., Chen, C.R., Shen, G.L., Yu, R.Q., *Anal. Chim. Acta.*, (2007), **584**, 122-128.

48. Xiao, Y., Pavlov, V., Levine, S., Niazov, T., Markovitch, G., Willner, I., *Angew. Chem. Int. Ed.*, (2004), **43**, 4519-4522.

49. Zayats, M., Baron, R., Popov, I., Willner, I., *Nano Lett.*, (2005), **5**, 21-25.

50. Shlyahovsky, B., Katz, E., Xiao, Y., Pavlov, V., Willner, I., *Small*, (2005), **2**, 213-216.

51. Reynolds, R.A., Mirkin, C.A., Letsinger, R.L., *Pure Appl. Chem.*, (2000), **72**, 229-235.

52. Upadhyay, P., Hanif, M., Bhaskar, S., *Clin Microbiol Infect.*, (2006), **12**, 1118-1122.

53. Mehrabi, M., Wilson, R., *Small*, (2007), **9**, 1491-1495.

54. Southern, E.M., *J. Mol. Biol.*, (1975), **98**, 503-517.

55. Towbin, H., Staehelin, T., Gordon, J., *Proc. Natl. Acad. Sci. USA*, (1979), **76**, 4350-4350.

56. Matsuzawa, S., Kimura, H., Itoh, Y., Wang, H., Nakagawa, T., *J Forensic Sci.*, (1993), **38**, 448-454.

57. Hou, S.Y., Chen, H.K., Cheng, H.C., Huang, C.Y., *Anal. Chem.*, (2007), **79**, 980-985.

58. Moeremans, M., Daneels, G., Van Dijck, A., Langanger, G., De Mey, J., *J Immunol. Methods.* (1984), **74**, 353-360.

59. Hsu, Y.H., *Anal. Biochem.*, (1984), **142**, 221-225.

60. Brada, D., Roth, J., *Anal. Biochem.*, (1984), **142**, 79-83.

61. Vera-Cabrera, L., Rendon, A., Diaz-Rodriguez, M., Handzel, V., Laslo, A., *Clin. Diagn. Lab. Immun.*, (1999), **6**, 686-689.

62. Sun, Y., Fan, W.H., McCann, M.P., Golovlev, V., *Anal. Biochem.*, (2005), **345**, 312-319.

63. Taton, T.A., Mirkin, C.A., Letsinger, R.L., *Science*, (2000), **289**, 1757-1760.

64. Alexandre, I., Hamels, S., Dufour, S., Collet, J., Zammatteo, N., DeLongueville, F., *Anal. Biochem.*, (2001), **295**, 1-8.

65. Weiss, A., *IVDTechnology Magazine*, (1999), Nov issue.

66. Jones, K.D., Schultz, D.A., *IVDTechnology Magazine*, (2004), April issue.

CHAPTER 2

2.1- Introduction

In the last two decades, researchers have developed the ability to manipulate matter at the level of single atoms and small groups of atoms-the so-called "nanoscale", and to characterize the properties of materials and systems at this scale. This ability has lead to the discovery that these materials have unique optical, electronic, conductive and catalytic properties that are completely different from the properties of the same material in the bulk scale.[1] Nanoscale science is a multi-disciplinary field requiring chemists, biologists, engineers and physicists to investigate and manipulate these unique properties at the nanoscale in order to develop new products with potential applications in catalysis, optoelectronics, medicine and biosensing. Simple nanomaterials are already in use to a great extent in everyday products such as cosmetics, sunscreens, pharmaceuticals and paints, but more recently, more sophisticated uses for these materials have been realized. The use of more complex nanomaterials in medicine, computing, communications and electronics has lead to the development of smaller, faster, cheaper and more powerful products. For example, IBM have developed a nano-magnetic resonance (nano-MRI) imaging microscope that is capable of visualizing structures at resolutions 60,000 x better than current MRI instruments. This equipment has the capability to visualise individual atoms in three dimensions and with further development has possible applications understanding how proteins interact with drugs at the atomic scale.[3] In another example, researchers at the Lawrence Berkeley laboratory at the University of California have developed the first fully functional nanoradio from a carbon nanotube which is 10,000 x smaller than a human hair.[4]

In the development of novel nanodevices the biggest challenge is in organizing the nanomaterials and assembling them into structures without affecting their unique properties.[4] Two main approaches are commonly used to construct nanostructures; the "top-down" approach and the "bottom-up" approach. The top-down approach is commonly used in the microelectronics industry and involves the break down of large bulk materials with chemical or mechanical energy without atomic-level control to generate nanostructures.[5] A key advantage of this approach is that the parts are both patterned and built in place, so that no assembly step is needed. The construction of nanostructures by the top-down approach is most often achieved using some form of lithography, an age-old printing method invented by Alois Senefelder in 1798. In the early days of lithography, text, a pattern or an image was chemically etched onto a smooth piece of stone (hence the name "lithography"— which literally means writing on stone). The pattern could then be transferred to paper or fabric by applying an ink to the stone and pressing onto the desired material.[6] In the context of nanotechnology, lithography is widely employed by the semiconductor industry to pattern the surface of silicon wafers (the stone) from which computer chips are made. There are several types of lithography used in top-down nanostructure fabrication. Dip pen nanolithography (DPN), developed at Northwestern University, is based upon the dip pens (quills) used in the 19 th century.[7] The method utilizes atomic force microscopy (AFM) tips where the cantilever acts as a pen, which is coated with atoms or molecules acting as the ink and then manipulated across a substrate, the paper to draw lines or patterns. The ink can be anything that will chemically interact with the substrate. This particular form of lithography has been used to construct metal nanowires which can be used as electrical connections between carbon nanotubes. Whilst this procedure is relatively

simple to perform, it is very time-consuming, often expensive and the range and complexity of structures that can be created is limited.[8] The most widely used form of lithography is photolithography. In this procedure, the substrate is coated with a light-sensitive photoresist and a mask is used which enables the user to selectively expose areas of the photoresist to light. Areas of the photoresist not covered by the mask harden on exposure to the light, whilst the remainder of the photoresist is soft and can be chemically etched away. This procedure is widely used in the production of computer chips and can be used to create features of ~100 nm and above. It cannot be used to create smaller features as the technique is limited by the wavelength of the light.[9] However, other lithographic techniques, that work in a similar way such as x-ray or electron beam lithography can be employed when features <100 nm are required.[10] In electron beam lithography, the resist is exposed to a computer controlled electron beam. Although this enables greater control over the structures created this technique is both costly and labor intensive.

In contrast to the top-down approach, the bottom-up or self-assembly approach involves the fabrication of nanostructures from single atoms and molecules which assemble themselves chemically by principles of molecular recognition.[5] The bottom-up approach is more versatile and provides almost infinite opportunities. First described by Richard Feynman whom entitled his world famous nanotechnology lecture "There's plenty of room at the bottom," the "bottom-up" approach aims to replicate nature's ability to produce clusters of specific atoms, which can then self-assemble into more elaborate structures. When using the bottom-up approach for nanostructure development, two important aspects must be addressed: the first is the synthesis of the individual nano-building blocks and the

second is the assembly of these building blocks to create a nanostructure with the desired structural properties and functions. The properties of many nanostructures are not only related to the individual nano-building blocks, but are also determined by the distance and interactions between the individual blocks. In recent years, a large variety of nano-building blocks with a regular shape and size such as nanotubes, nanorods and nanoparticles have been successfully synthesised using chemical or physical methods, however, the organization of these nano-building blocks into more complex structures is proving to be more difficult. To date this has mainly been achieved using supramolecular chemistry approaches. This is the area of chemistry that focuses on the non-covalent interactions that occur between molecules such as electrostatic binding, hydrogen bonding and van der Waals forces.[11] The formation of nanostructures can be achieved by introducing functional groups on the surface of the nano-building block by chemical modification so that the nano-building blocks then assemble into a network through non-covalent interactions with other molecules. By selective design of the functional groups, different structures such as one dimensional nanowires, two dimensional nanoarrays and three dimensional crystals can be obtained. However this method of self-assembly is not without its problems. In order to build nanostructures using this approach, the functionality of the nano-building blocks must be carefully controlled so that they assemble in the desired way. If they are not the assembly of the nano-building blocks can be irreproducible, un-predictable and the complexity of structures obtained is limited.

In recent years many researchers have investigated the possibility of using biomolecules as templates to guide the assembly and enable the construction of more

complex nanostructures. One of the reasons for this is that molecular recognition is already built into the biomolecule enabling selective self-assembly. In nature, self-assembly is the basic building principle for generating large complex structures of biomolecules that have well-defined geometrical shapes and unique properties. In the biological world, the self-assembly of biomolecules begins with the construction of monomer molecules such as nucleotides, amino acids and lipids, which form polymers such as DNA, proteins, and polysaccharides. These polymers are the basis for larger assemblies such as cell membranes and organelles. After further assembly, these polymers form cells, organs, and organisms. This ability to undergo highly controlled assembly makes biomolecules ideal for applications in nanotechnology.[12] One of the most widely used biomolecules for this purpose is DNA due to the highly specific Watson-Crick interactions that occur between the bases. Furthermore, advances in synthetic DNA production, the ability to introduce chemical functionalities and the existence of branched DNA molecules that permit complex shapes to be formed [13, 14] have contributed to its extensive use. There are many examples of DNA templated assembly, it has been selectively folded into complex shapes and patterns to create templates onto which nanowires, carbon nanotubes (CNTs) or nanoparticles can be chemically synthesised *in situ* or attached to in order to create electronic circuits.[15] A DNA template has also been used to position transition metals with luminescent or redox activity into an ordered array.[16] Although there are advantages to using biological molecules to construct complex nanostructures, these methods are not without their problems. Firstly, when using DNA, a large number of different DNA strands are required. This makes the construction process highly sensitive to the ratio of the strands and it often entails

multiple reaction and purification steps. In addition, templates made purely of DNA can be difficult to characterize.[17]

An alternative approach which could alleviate some of the problems with self-assembly would be to use covalent bond chemistry. If the nano-building blocks possessed a controlled chemical functionality, then covalent chemical reactions could be used to create nanostructures in an ordered and precise manner.[18] This is because a higher level of control can be asserted on a chemical reaction than on a self-assembly approach. Covalent approaches have been applied to construct nanostructures from carbon nanotubes (CNTs). The covalent approach is often favoured as it is difficult to self-assemble CNTs into nanostructures due to their propensity to form aggregates due to strong van der Waals forces between the tubes.[19] Introducing chemical functionalities that can form covalent bonds, such as carboxylic acid or amine groups to these CNTs, has enabled novel two and three dimensional nano-architectures with unique electronic and mechanical properties to be assembled. Furthermore, using the covalent approach, the distance between the individual CNTs and their orientation can be varied by varying the length or position of the covalent linker group. Strong covalent linkages can also provide high stability and rigidity for the nanostructure.[20] In order to use covalent bond chemistry to control the formation of nanostructures in a precise way; it is first necessary to control the chemical functionality of the individual nano-building blocks. The problem with this is that it is often difficult to control the number of functional groups due to the presence of multiple reactive sites on the nano-building blocks surface. For example, GNPs with a diameter of 2 nm will have a total of 100 surface gold atoms available for functionalisation. Attempting to functionalise a solution of

these GNPs with thiol groups for example, could lead to a mixture of GNPs with either no functional groups or with multiple functional groups, which when assembled, could form irreproducible nanostructures. In order to overcome this problem, and use a covalent approach a method is needed that can be used to functionalise nano-building blocks in a controllable manner.

In this chapter, a simple and novel method for functionalising nano-building blocks, GNPs in particular, is reported. This method is based upon high molecular weight polymers that can be functionalised with the desired molecules. The polymer is characterized after functionalisation which enables the user to know the mean number of molecules per polymer. A known amount of the characterized polymer is then mixed with a fixed amount of GNPs and is conjugated to the particles *via* a plurality of dative covalent bonds. The result is a GNP conjugate that is coated with a known mean number of molecules. In addition, this method can also be used to control or vary the number of molecules per particle simply by changing the stoichiometry of reagents used in the polymer functionalisation reaction. The chemistry is very simple and the method can be used to attach many different types of molecules including haptens, antibodies and oligonucleotides to nanoparticles. It could also be used to introduce a controlled number of chemical functionalities to the GNPs which would enable the construction of covalently linked nanostructures.

2.2- Materials

Aminodextran (MW 70 kDa, 16 primary amines per molecule) was from Molecular Probes, Eugene, OR. Glycine, 2-mercaptoethanol, 3-(2-pyridyldithio)propionic acid N-hydroxysuccinimide ester (SPDP), biotinamidohexanoic acid N-hydroxysuccinimide ester (biotin-NHS), avidin, biotin, 2-(4-hydroxyphenylazo)benzoic acid (HABA), bovine serum albumin (BSA), dithiothreitol (DTT) and dialysis tubing (molecular weight cut-off 12000) were from Sigma. o-Phthalicdicarboxaldehyde was from Lancaster Synthesis. Streptavidin coated microspheres (0.49μm) were from Bangs Laboratories, IN. Solution A: 0.1 M sodium borate, pH 10 with 0.05 % 2-mercaptoethanol. Solution B: 20 % aqueous ethanol with 0.4 mg ml^{-1} o-phthalicdicarboxaldehyde. 3 x PBS: 45 mM sodium phosphate, 0.45 M NaCl, pH 7.4. Bicarbonate solution: 0.1 M sodium bicarbonate, pH 8.3. Acetate buffer: 0.1 M sodium acetate, pH 4.5. Wash solution I: 1 × PBS, 0.5% Tween-20, pH 7·4. Wash solution II: 1 × PBS, 0.5% Tween-20, 33mgml^{-1} BSA pH 7·4. HABA assay buffer: 0.05 M sodium phosphate, 0.15 M NaCl, pH 6. All GNPs were prepared by BBInternational, Cardiff, UK. The diameter of the GNPs was determined using a ZetaPlus analyser (Brookhaven Instruments, Worcestershire, UK) and transmission electron microscopy (TEM) using a Phillips 410 operating at 80 kV or a Phillips CM12 operating at 100 kV. TEM samples were prepared by placing a drop of GNP solution on a 200 mesh nickel grid (Agar Scientific) and allowing it to dry in air. UV/vis spectra were recorded on a Hewlett Packard 8452A Diode Array Spectrophotometer.

2.3- Methods

2.3.1- Determination of amine content in aminodextran

An o-phthalicdicarboxaldehyde (OPA) assay was carried out to verify the number of amines available for functionalisation in commercially prepared aminodextran. A series of standard solutions containing 0, 1 mM, 2 mM, 3 mM and 4 mM of glycine were prepared in distilled water. To generate a standard curve, 0.25 ml of glycine solution was mixed with 0.75 ml of de-ionized water, 1.5 ml of solution A and 0.5 ml of solution B. The solution was allowed to stand at room temperature for 10 minutes before reading the absorbance at 334 nm. To determine the concentration of available amines, glycine solution was substituted for 0.25 ml of solution containing 5 mg ml^{-1} of aminodextran.

2.3.2- Synthesis of protected disulphide (PDP)-functionalised dextran

PDP moieties were introduced in to aminodextran by adding 300 μl of 60 mM N-succinimidyl 3-(2-pyridyldithio)propionate (SPDP) in dry DMF dropwise with stirring to 15 mg of aminodextran in 3 ml of PBS over a period of 5 hours. After stirring overnight, un-reacted SPDP was removed by dialysis against 4 x 1 L of deionised water for a total of 48 hours. The concentration of dextran in the dialysed solution was calculated by correcting for the increase in volume of the solution.

2.3.3- Determination of the PDP content of functionalised dextran

The concentration of PDP in the functionalised dextran was determined by treating the dextran with the low molecular weight thiol compound dithiothreitol (DTT). 100 μl of functionalised dextran was added to 0.9 ml of bicarbonate solution. To this,

100 µl of 5 mM DTT also in bicarbonate solution was added and the absorbance increase at 343 nm (ϵ_{343} = 8.08 x 10^3 M^{-1} cm^{-1}) was recorded.

2.3.4-Titration of PDP functionalised dextran against GNPs

The minimum amount of PDP functionalised dextran required to prevent salt-induced flocculation of fixed amounts of 10 nm GNPs (5.7 x 10^{12} particles per ml) was determined by titration. Increasing amounts of a 1:200 dilution of PDP functionalised dextran (in de-ionized H_2O) were added to 0.66 ml aliquots of GNPs. After vortexing, 0.33 ml of 3 x PBS was added to each aliquot and aggregated GNPs were removed by passing each solution through a 0.2 µm syringe filter. The absorbance of each solution at 520 nm was then determined by UV/vis spectroscopy.

2.3.5- Time-course titrations of PDP functionalised dextran

The minimum amount of PDP functionalised dextran required to prevent salt-induced flocculation of fixed amounts of 10 nm GNPs was determined by titration. Increasing amounts of a 1:100 dilution of PDP functionalised dextran were added to 4 ml aliquots of 10 nm GNPs using a syringe controlled by a stepper motor that allowed the volume of PDP functionalised dextran added to be controlled accurately. After dextran addition, 0.66 ml aliquots were removed and 0.33 ml of 3 x PBS was added to the GNPs; 1) immediately, 2) after 10 minutes of stirring, 3) after 1 week of stirring, 4) after 3 weeks of stirring and 5) after 7 months of stirring. Following addition of PBS, aggregated GNPs were removed by passing the solutions through a 0.2 µm syringe filter and the absorbance of each solution at 520 nm was measured.

2.3.6- The effect of pH on the titration of PDP functionalised dextran

PDP functionalised dextran was diluted 1:200 with acetate buffer or bicarbonate buffer and the minimum amount of functionalised dextran required to prevent salt-induced flocculation of a fixed amount of GNPs was determined by titration as in section 2.3.4.

2.3.7- The relationship between particle size and the equivalence point of functionalised dextran

3 ml aliquots of 5, 10, 20, 40, 60, 80 and 100 nm GNPs obtained from BBInternational were pipetted into clean, dust-free cuvettes and the diameters of the particles were confirmed by dynamic light scattering. Size distribution measurements of each aliquot of GNPs were obtained over a period of 5 minutes. The minimum amount of functionalised dextran required to prevent salt-induced flocculation of each different size was then determined by titration as in section 2.3.4.

2.3.8- Synthesis of biotin functionalised dextrans

Five dextrans functionalised with different amounts of biotin were synthesised as follows: 200 μl of biotin-NHS solution, in dry DMF was added dropwise with stirring, over a period of 5 hours to 2 ml aliquots of PBS containing 10 mg of aminodextran; the concentrations of biotin-NHS in the DMF solutions were; 1) 0.7 mM, 2) 1.75 mM, 3) 3.5 mM, 4) 5 mM or 5) 7 mM. At the end of this time, 200 μl of 60 mM SPDP in dry DMF was added in the same way. After stirring for a further 5 hours, un-reacted biotin and SPDP were removed by dialysis against 4 x 1 L of deionised water for a total of 48 hours.

2.3.9- 4′-Hydroxyazobenzene-2-carboxylic acid (HABA) dye assay for biotin

To generate a standard curve, 75 μl of 10 mM HABA dye (in 1 M NaOH) was added to 1.5 mg of avidin in 3 ml of HABA assay buffer. After recording the absorbance at 500 nm, 2 μl amounts of a 0.5 mM biotin standard solution in HABA assay buffer were added to the cuvette and the decrease in the absorbance at 500 nm was recorded after each addition. The concentration of biotin in functionalised dextrans was determined in the same way except that the biotin standard solution was substituted with 100 μl of biotin functionalised dextran.

2.3.10- Titration of biotin functionalised dextran against GNPs

The minimum amount of biotin functionalised dextran required to prevent flocculation of 10 nm GNPs in PBS was determined by titrating variable amounts of a 1:100 dilution of each biotin functionalised dextran solution against a fixed volume of 10 nm GNPs as in section 2.3.4. Biotin-GNP conjugates were prepared by adding this minimum amount of biotin functionalised dextran to 10 nm gold followed by a 2:3 dilution with 3 x PBS containing 90 mg ml $^{-1}$ bovine serum albumin (BSA), and 1.5 % Tween-20.

2.3.11- Determining the concentration of biotin-GNP conjugate required for streptavidin bead assays

Aliquots of streptavidin microspheres were washed 3 x by centrifugal precipitation at 13000 g with 1 ml of wash solution I. GNPs coated with the equivalence point of biotin functionalised dextran were diluted to different concentrations with wash buffer II, 10μL aliquots of washed streptavidin microspheres were added to each, and tubes were slow-tilt rotated at room temperature for 30 minutes. At the end of this

time, un-bound biotin-GNPs were removed by centrifugally precipitating the beads at 300 g for 10 minutes. The beads were vortexed to re-suspend and centrifugally precipitated 3 x in wash buffer II at 1200 g for 10 minutes. After removal of the supernatant, the beads were re-suspended in 0.9 ml of de-ionised water and the beads were centrifugally precipitated at 13000 g for 10 minutes. At the end of this time the supernatant was removed and the beads were dried by vacuum centrifugation for 40 minutes. The dried beads were then re-suspended by sonication in 21μL of de-ionised water and transferred to a microwell plate. Images of the beads were acquired with an office document scanner and then imported into iGrafx Image 1.0 (Bournemouth, UK) and converted to greyscale. The depth of colour was determined on a scale of 0 – 255 by activating the "view → information" option and pointing the mouse cursor at the area to be interrogated.

2.3.12- Streptavidin bead assays with centrifugally washed and un-washed biotin-GNP conjugates

Filtered biotin-GNP conjugate solutions from selected points on the titration curve were washed 3 x by centrifugal precipitation at 17500 g in 1 x PBS buffer. After the final wash, each aliquot of washed biotin-GNPs was re-suspended and diluted to contain the required number of GNPs per ml with 1 x PBS containing 0.5% Tween and 30 mg ml^{-1} BSA. Aliquots of un-washed biotin-GNP conjugates from the same points on the titration curve were also diluted to contain the same number of GNP per ml with the same buffer. 10 μl aliquots of washed streptavidin beads were added to both washed and un-washed biotin-GNP conjugates and the beads were slow-tilt rotated at room temperature for 30 minutes. At the end of this time, un-bound biotin-

GNPs were removed by centrifugal precipitation and the beads were dried and imaged as detailed in section 2.3.11.

2.3.13- Streptavidin bead assays

Biotin-GNP conjugates coated with the equivalence point of biotin functionalised dextran were prepared as above (section 2.3.10). Biotin-GNP conjugate was then diluted to contain the required number of GNPs per ml with 1 x PBS containing 0.5% Tween and 30 mg ml^{-1} BSA. A series of biotin solutions ranging from 0.5 mM to 275 pM were prepared by serially diluting a 0.5 mM stock solution of biotin with 1 x PBS. 25μL of each biotin solution was then added to each aliquot of biotin coated GNPs. After mixing, 10μL aliquots of washed streptavidin beads were added to each and the beads were slow-tilt rotated at room temperature for 30 minutes. At the end of this time, un-bound biotin-GNP and biotin were removed by centrifugal precipitation and the beads were dried and imaged as described in section 2.3.11.

2.4- Results

2.4.1- Determination of amine content in aminodextran

When commercial aminodextrans are purchased they are supplied with an information sheet which provides an estimation of the number of amines per dextran molecule. In order to confirm the exact number of amines that were available for functionalisation an o-phthalicdicarboxaldehyde (OPA) assay was carried out. At pH 10, OPA, in the presence of a thiol compound such as mercaptoethanol, reacts with primary amines to form coloured product which shows an absorption band at 335 nm (Figure 1).[21] In this work, a standard curve was first generated with glycine standard solutions containing a known concentration of amines (Figure 2; black squares). The glycine solution was then substituted for aminodextran and the concentration of amines in the dextran was then determined by comparison with the standard curve. According to the manufacturer, the aminodextran was estimated to contain 20 amines per molecule of dextran. A 5 mg ml^{-1} solution of aminodextran was prepared which when diluted with the assay solutions should yield an amine concentration of ~120 μM. The results show that aminodextran contained ~117 μM of amines (Figure 2; red dot) and confirm that the information provided by the manufacturer was correct.
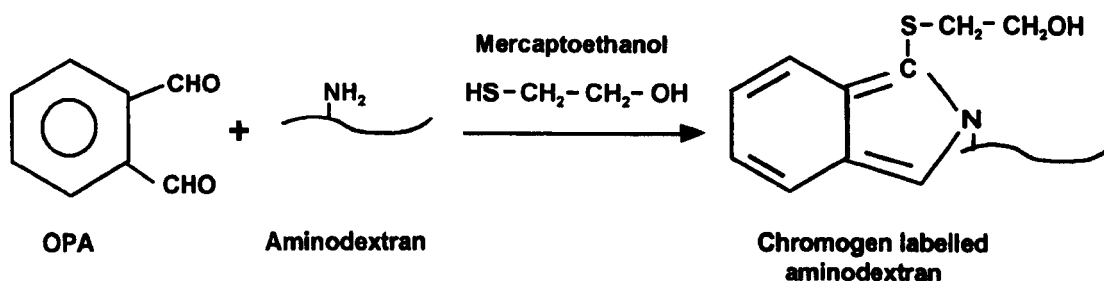
Figure 1: OPA assay for amines. OPA reacts with the primary amines in the dextran at pH 10 in the presence of mercaptoethanol to form a coloured product which has a characteristic absorbance at 335 nm.
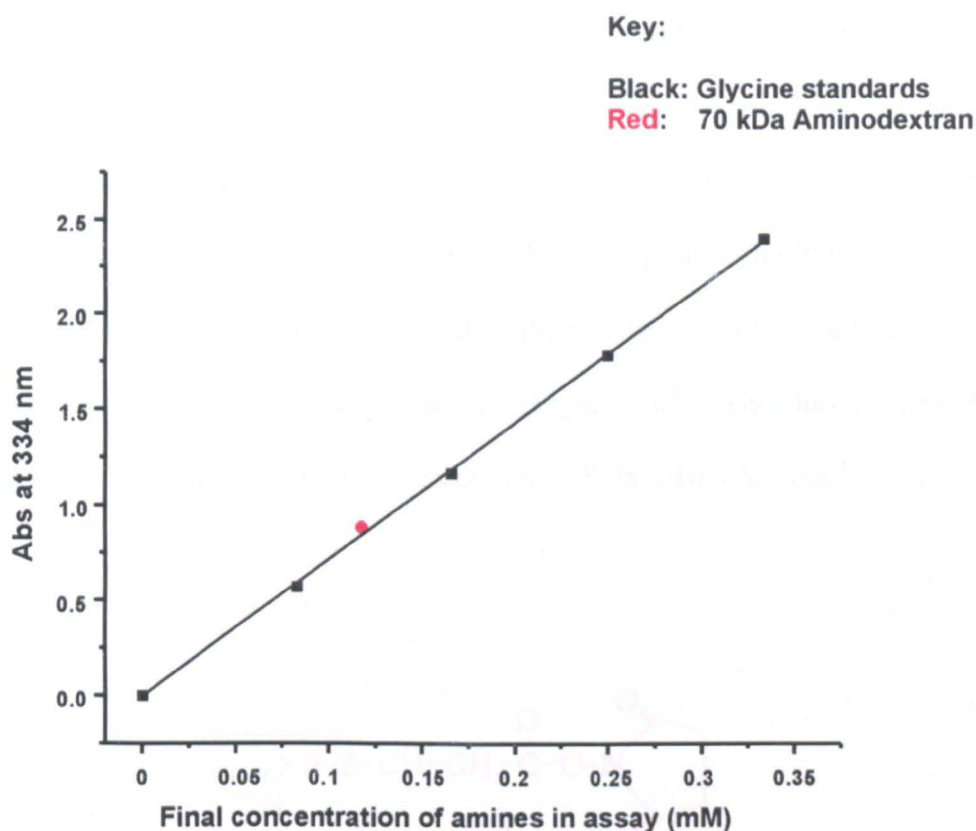
Figure 2: Standard curve obtained from OPA assay. Black squares represent glycine standard solutions containing a known concentration of amines. To determine the concentration of available amines in aminodextran, glycine solution was substituted for an aminodextran solution. The graph shows that the concentration of amines in the assay solution was ~117 μM (red dot).

2.4.2- Synthesis of PDP functionalised dextran

Heterobifunctional reagents are a class of reagents that contain two different reactive groups that can couple to two different functional targets on proteins and other macromolecules. The most popular heterobifunctional reagents are those that contain amine and thiol reactive groups. In this work, the heterobifunctional reagent *N*-succinimidyl 3-(2-pyridyldithio)propionate (SPDP) formulated by Carlsson and Drevin shown in Figure 3 was used to modify aminodextran.[22] This reagent contains an NHS ester, which reacts with the primary amines in the aminodextran to form stable amide bonds at one end, and a 2-pyridyl disulphide (PDP) group at the other end. Following modification with SPDP and purification by dialysis, the product is a

dextran polymer that is functionalised with a plurality of PDP groups (Figure 4). The number of PDP groups incorporated into the dextran can be quantified by treating the functionalised dextran with a low molecular weight thiol compound such as dithiothreitol (DTT). Upon addition of the thiol compound, the PDP groups within the dextran are reduced to thiol functionalities *via* a thiol-disulphide exchange reaction and pyridine-2-thione is released (Figure 5).[22] This has an absorbance maximum at 343 nm with a molar absorptivity of 8.08×10^{3} M^{-1} cm^{-1}.
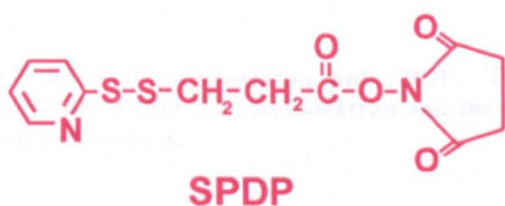
Figure 3: The heterobifunctional reagent SPDP. This reagent contains an NHS ester which reacts with primary amines to form stable amide bonds at one end, and a 2-pyridyl disulphide (PDP) group which reacts with thiol (-SH) containing molecules at the other end.

Figure 4: The functionalisation of aminodextran with SPDP. The NHS ester of the reagent reacts with the primary amines within the aminodextran and the product is a dextran polymer that is functionalised with PDP groups.
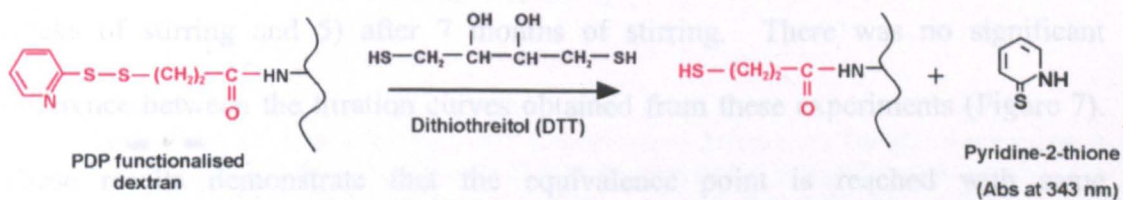
Figure 5: Diagram showing the quantification of PDP groups within PDP functionalised dextran by reduction with the low molecular weight thiol compound DTT. When DTT is added to PDP functionalised dextran, the disulphide bonds break and pyridine-2-thione is released. This compound has a characteristic absorbance at 343 nm.

2.4.3- Titration of PDP functionalised dextran against GNPs

To investigate how GNPs interact with high molecular weight polymers, aminodextrans functionalised with PDP groups were added to fixed numbers of 10

nm particles and a buffer containing a high concentration of NaCl was added. In the absence of PDP functionalised dextran, all of the GNPs flocculate, forming a dark blue suspension that eventually precipitates; these flocculated particles can be removed by passing the solution through a 0.2 μm filter. As the amount of dextran is increased, more particles are stabilized, until eventually a point is reached beyond which, none of the particles flocculate when NaCl is added. The minimum amount of functionalised dextran required to prevent the GNP flocculating in the presence of NaCl is termed the equivalence point. Images of GNPs titrated with PDP functionalised dextran before and after filtering are shown in Figure 6A, and a plot of absorbance at 520 nm against the volume of dextran solution added is shown in Figure 6B. To investigate in more detail whether PDP functionalised dextrans were attached immediately upon contact with the GNPs, a series of time course titrations were carried out. In this work, PDP functionalised dextran was added to the GNPs and buffer with a high concentration of NaCl was added to the GNPs; 1) immediately, 2) after 10 minutes of stirring, 3) after 1 week of stirring, 4) after 3 weeks of stirring and 5) after 7 months of stirring. There was no significant difference between the titration curves obtained from these experiments (Figure 7). These results demonstrate that the equivalence point is reached with same concentration of functionalised dextran, even when the GNPs and the dextran are stirred for 7 months. If it was necessary to stir the GNPs and functionalised dextran for prolonged periods to ensure efficient and homogeneous coating of the GNPs, the concentration of dextran required to reach the equivalence point would decrease as the stirring time increased and the titration curves would shift to the left. This is an important result as it confirms that GNP conjugates can be prepared reproducibly by this method in minutes.

A
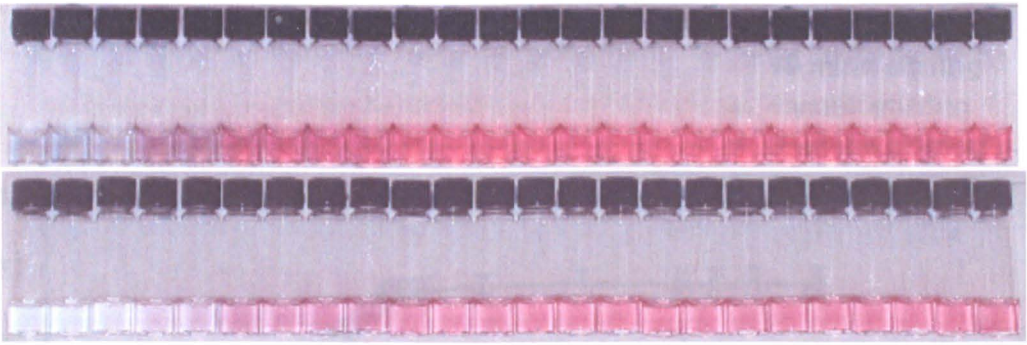
B
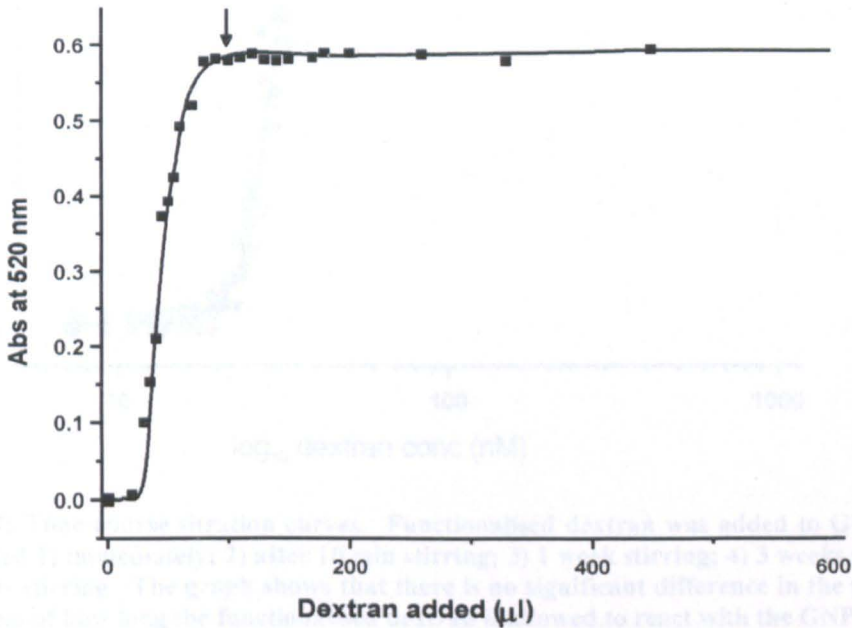
Figure 6: Images of GNP titration with PDP functionalised dextran. A) The top image shows the GNPs before filtration. When the amount of PDP dextran added is insufficient to coat all of the GNPs in solution, the GNPs flocculate upon addition of NaCl forming a blue solution. As the amount of dextran is increased, an increasing number of GNPs are coated until a point is reached where none of the GNPs flocculate upon addition of NaCl. At this point all of the GNPs are coated and the solution remains pink. The bottom image shows the GNPs after filtration. Flocculated GNPs are removed by passing the solution through a filter. B) Corresponding titration curve after filtration. Flocculated GNPs are removed by filtration. As the amount of PDP functionalised dextran is increased, an increasing number of GNPs are stabilized, the solution is pink and there is an increase in absorbance at 520 nm. After the equivalence point is reached, there is no further increase in absorbance at 520 nm.

Key:
- ■ Immediate
- ● 10 mins stirring
- ▲ 1 week stirring
- ▼ 3 weeks stirring
- ◆ 7 months stirring
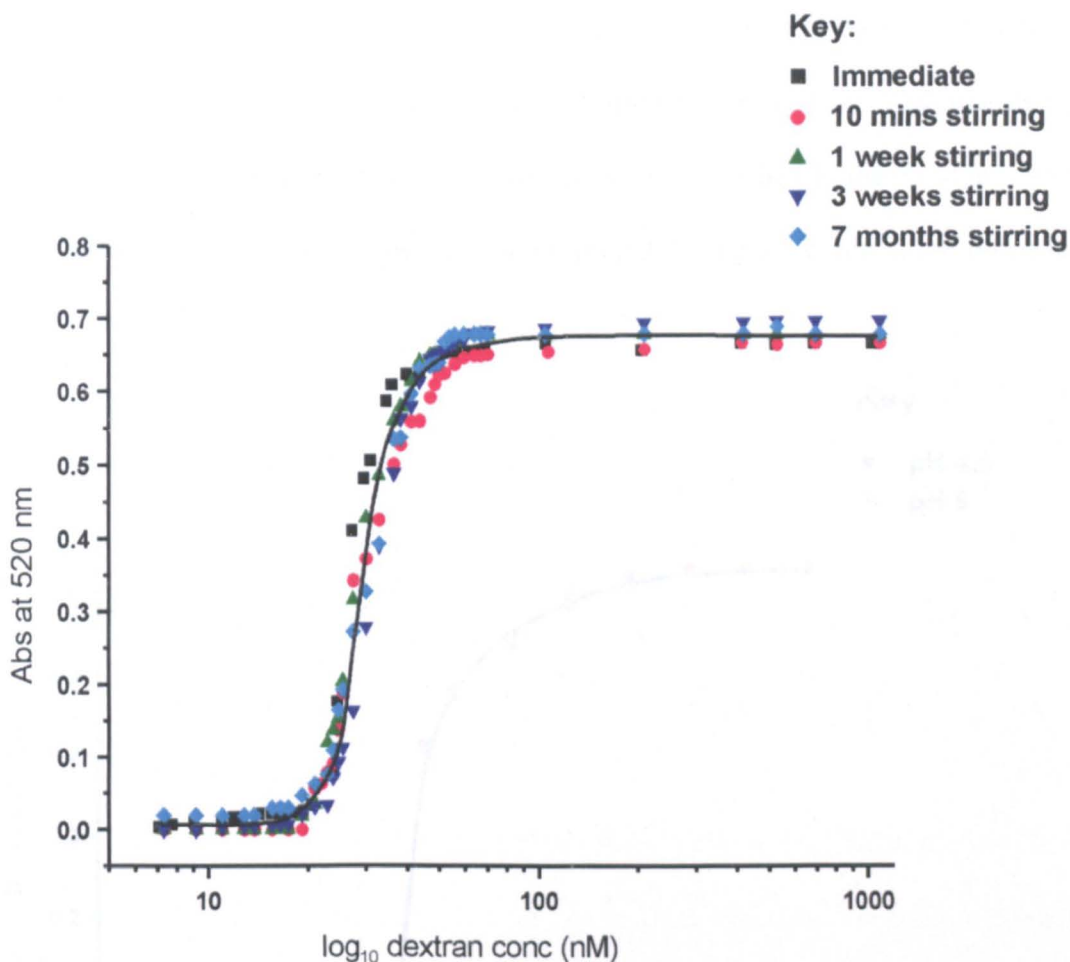
Figure 7: Time course titration curves. Functionalised dextran was added to GNPs and NaCl was added 1) immediately; 2) after 10 min stirring; 3) 1 week stirring; 4) 3 weeks stirring and 5) 7 months stirring. The graph shows that there is no significant difference in the titration curve regardless of how long the functionalised dextran is allowed to react with the GNPs.

2.4.4- The effect of pH on the titration of PDP-functionalised dextran

For biomolecules such as enzymes and antibodies to retain their structure and function their environment must be maintained at their optimum pH. If these molecules were attached to aminodextran it would be necessary to maintain this optimum pH in order to retain the biomolecules function when conjugated to GNPs. As a result it was necessary to investigate the effects of pH on the titration of aminodextran with GNPs. In order to do this, both the pH of the PDP-functionalised dextran and the GNPs were adjusted using an acidic or basic buffer and then the

dextran was titrated against GNPs in the usual way. Results from these experiments can be seen in Figure 8. Both titration curves obtained from these experiments were exactly the same indicating that if biomolecules were attached to the dextran it would be possible to maintain the molecules optimum pH during the conjugation procedure.
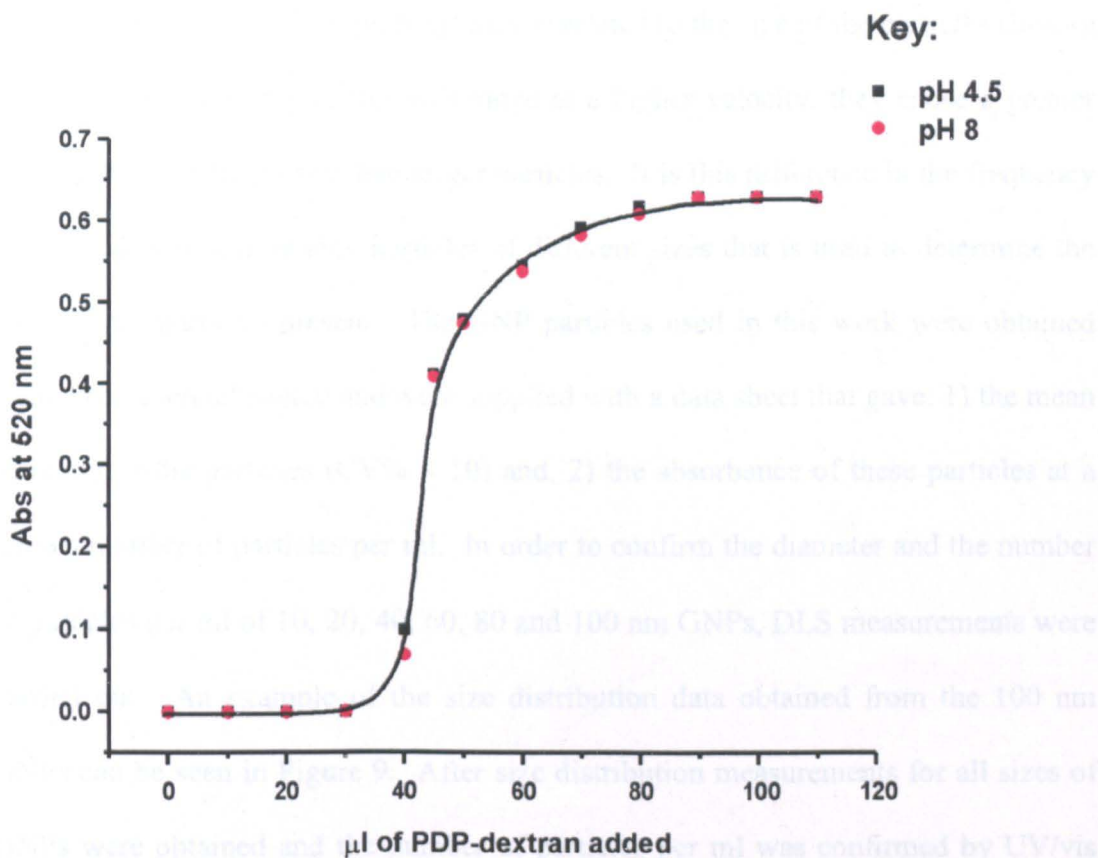
Figure 8: Results obtained when functionalised dextran was titrated against GNPs at alkaline and acidic pH. There is no significant difference in the titration curves indicating that functionalised dextrans can be attached to GNPs regardless of the pH.

2.4.5- The relationship between GNP size and the equivalence point of functionalised dextran

Dynamic light scattering (DLS) is a technique which can be used to determine the size distribution profile of small particles in solution.[23] Particles suspended in solution are subject to Brownian motion. This is the motion induced when the

particles are bombarded by solvent molecules that are moving due to their thermal energy. By bombardment, molecules that are much smaller than the particles, for example water molecules, can impart a change to the direction of the particle and its velocity. If a known frequency of light is directed at the moving particles, the light is scattered from the particles at a different frequency. For the purposes of particle measurement, the shift in light frequency is related to the size of the particles causing the shift. As smaller particles will move at a higher velocity, they cause a greater shift in the light frequency than larger particles. It is this difference in the frequency of the scattered light among particles of different sizes that is used to determine the sizes of the particles present. The GNP particles used in this work were obtained from a commercial source and were supplied with a data sheet that gave: 1) the mean diameter of the particles (CV% < 10) and, 2) the absorbance of these particles at a known number of particles per ml. In order to confirm the diameter and the number of particles per ml of 10, 20, 40, 60, 80 and 100 nm GNPs, DLS measurements were carried out. An example of the size distribution data obtained from the 100 nm GNPs can be seen in Figure 9. After size distribution measurements for all sizes of GNPs were obtained and the number of particles per ml was confirmed by UV/vis spectroscopy, titrations of all sizes were carried out. These titrations were carried out to determine if there was a relationship between the minimum amount (equivalence point) of functionalised dextran required to prevent salt-induced flocculation and the particle diameter. A graph showing these results can be seen in Figure 10. There is a linear relationship between the concentration of functionalised dextran added at the equivalence point and the square of the GNP diameter, the latter is proportional to the surface area of the particles.

jenny2new100nmgnp (Combined)	
Effective Diameter:	104.9 nm
Polydispersity:	0.127
Avg. Count Rate:	267.6 kcps
Sample Quality:	9.6
Elapsed Time:	00:05:00

Run	Eff. Diam. (nm)	Half Width (nm)
1	98.2	34.8
2	101.1	42.6
3	105.8	39.4
4	106.6	39.0
5	108.8	42.5
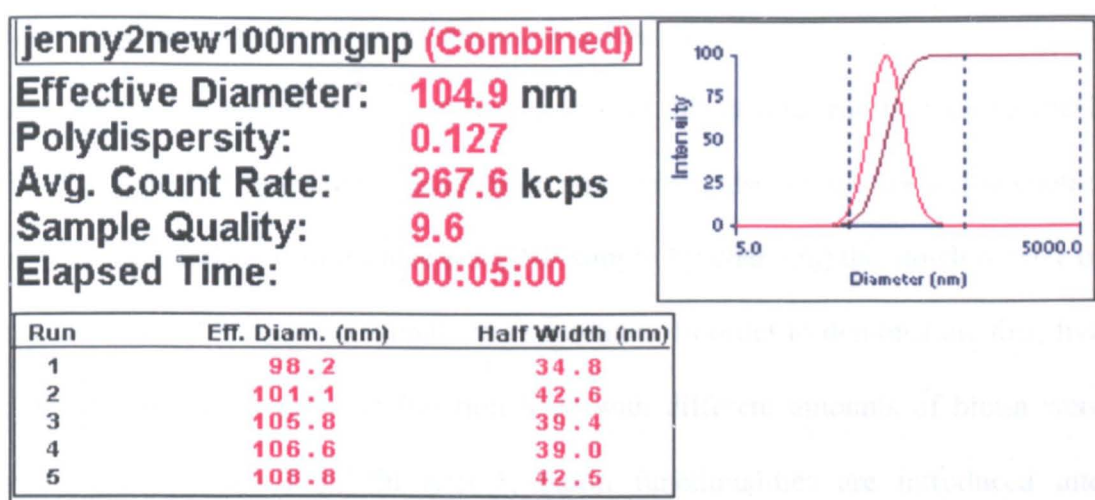
Figure 9: Example of the data obtained from the DLS experiments. This data was obtained with commercially prepared 100 nm GNPs and demonstrates that the average diameter was 104.9 nm.
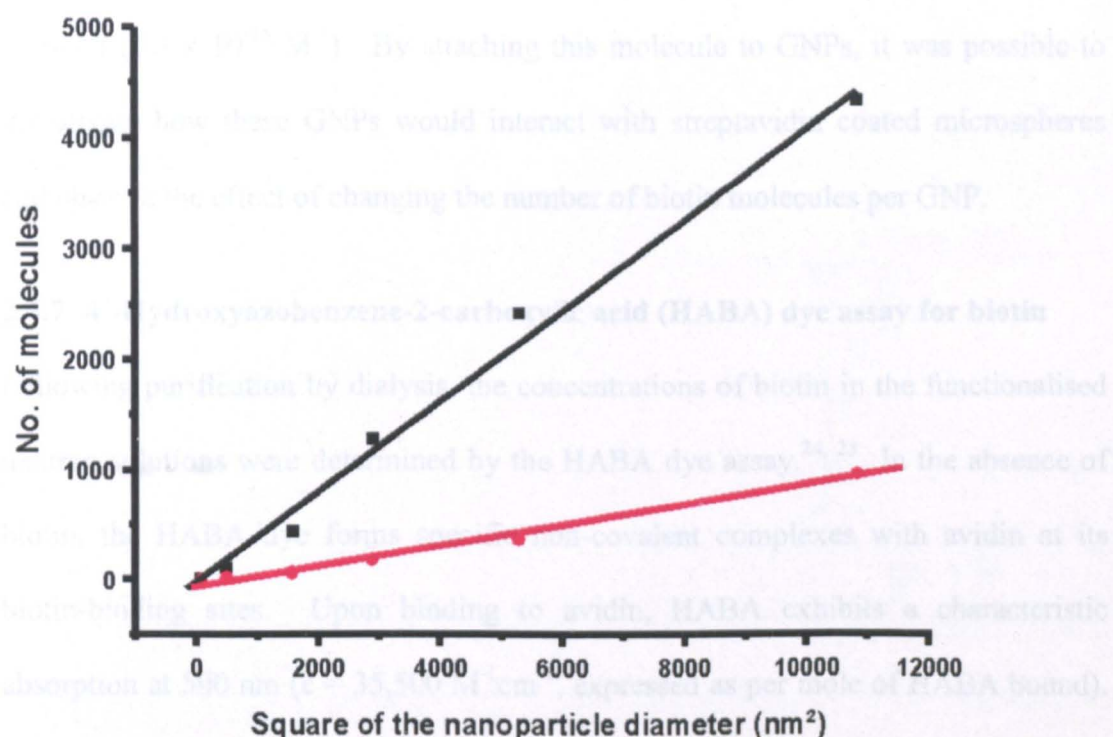
Figure 10: Graph showing the relationship between the number of molecules per particle as determined from the equivalence point of the titrations, and the square of the GNP diameter, as determined from the DLS experiments. The values for the red line were obtained using a dextran functionalised with a low number of molecules. The values for the black line were obtained from a dextran functionalised with high numbers of molecules. The equivalence amount of dextran is dependent on the molecular weight of the dextran and the square of the GNP diameter, the latter is proportional to the surface area of the particles.

2.4.6- Synthesis of biotin functionalised dextran

The dextran functionalisation reaction reported in this chapter can be used to attach almost any molecule to GNPs. In addition, the method also allows the user to control or vary the number of molecules per GNP simply by changing the stoichiometry of reactants in the dextran functionalisation reaction. In order to demonstrate this, five PDP-dextrans that were also functionalised with different amounts of biotin were synthesised (Figure 11). In step 1, biotin functionalities are introduced into aminodextran using biotin-NHS. The NHS ester end of the reagent reacts with the primary amines in the dextran to form stable amide bonds. In step 2, PDP groups are introduced into biotin functionalised dextran using SPDP. Biotin is a low molecular weight molecule that binds to avidin or streptavidin with a very high association constant (1.3×10^{-15} M^{-1}). By attaching this molecule to GNPs, it was possible to investigate how these GNPs would interact with streptavidin coated microspheres and observe the effect of changing the number of biotin molecules per GNP.

2.4.7- 4′-Hydroxyazobenzene-2-carboxylic acid (HABA) dye assay for biotin

Following purification by dialysis, the concentrations of biotin in the functionalised dextran solutions were determined by the HABA dye assay.[24, 25] In the absence of biotin, the HABA dye forms specific non-covalent complexes with avidin at its biotin-binding sites. Upon binding to avidin, HABA exhibits a characteristic absorption at 500 nm ($e = 35,500$ $M^{-1}cm^{-1}$, expressed as per mole of HABA bound). The addition of a biotin solution to this complex results in the displacement of the HABA dye from the avidin binding sites. This occurs because the association constant of the avidin-biotin interaction (1.3×10^{-15} M^{-1}) is much greater than that for avidin-HABA interaction (6×10^{-6} M^{-1}). As HABA is displaced, the absorbance of the complex decreases proportionately. Therefore, the amount of biotin present in

the solution can be determined by plotting the absorbance of the avidin-HABA complex at 500 nm versus the absorbance with increasing concentrations of added biotin. Comparing an unknown biotin containing sample to this standard curve (Figure 12) allows determination of the biotin concentration in the sample.
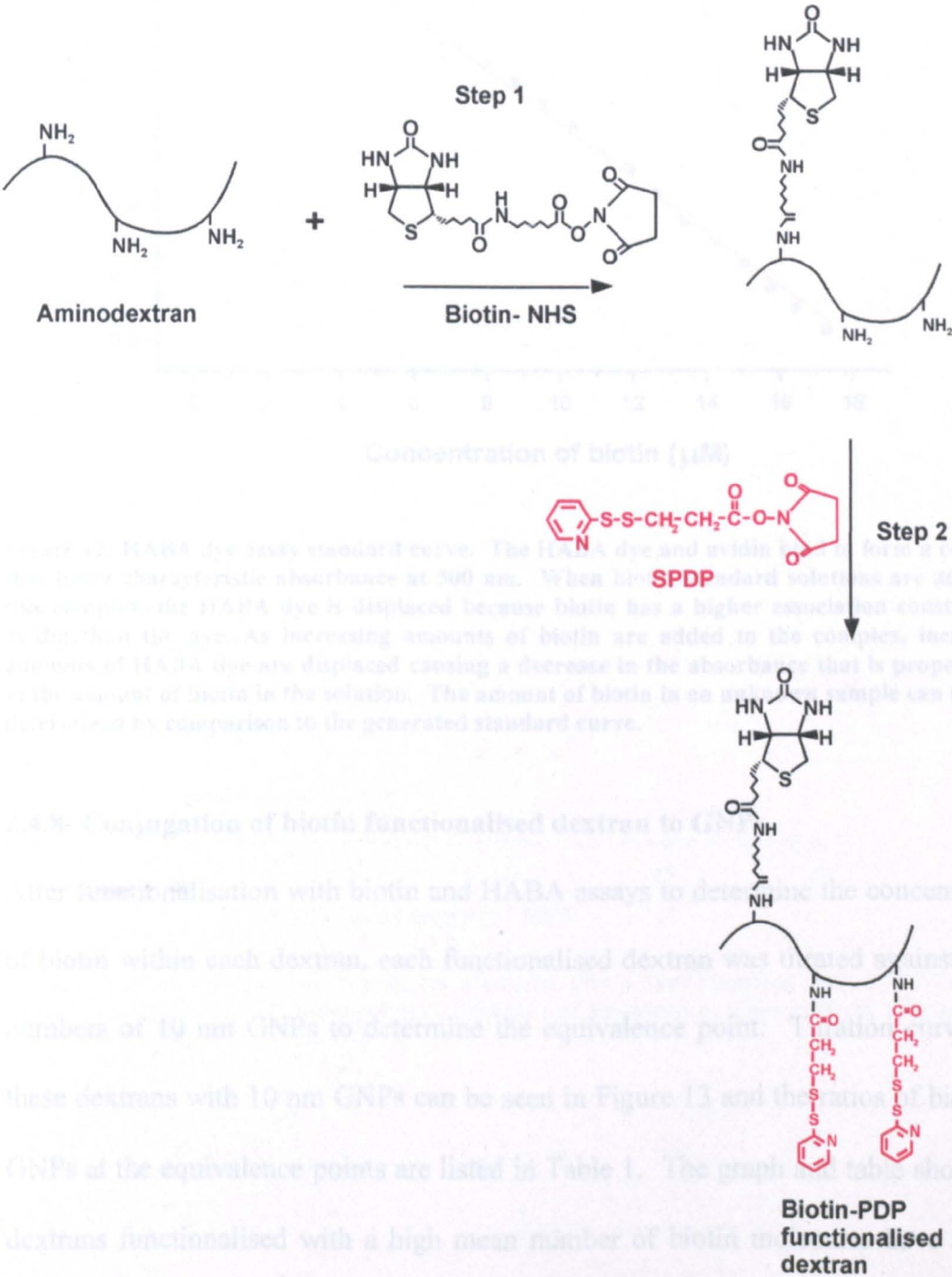
Figure 11: Synthesis of biotin functionalised dextran. In step 1 biotin functionalities are introduced into aminodextran using biotin-NHS. The NHS ester of the reagent reacts with primary amines in the dextran to form stable amide bonds. In step 2, PDP groups are introduced into the biotin functionalised dextran using SPDP.
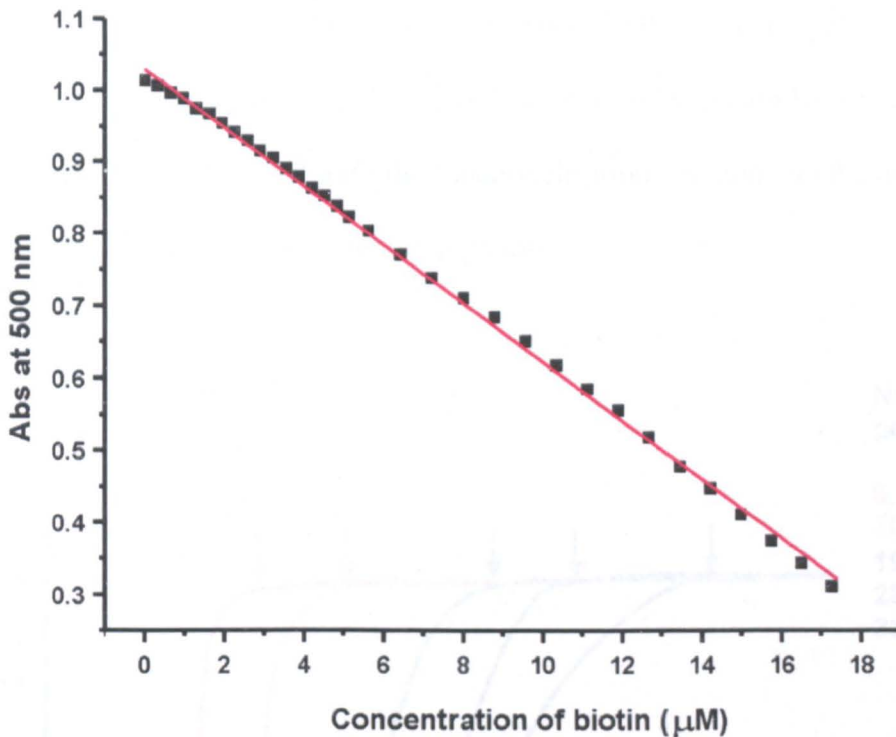
Figure 12: HABA dye assay standard curve. The HABA dye and avidin bind to form a complex that has a characteristic absorbance at 500 nm. When biotin standard solutions are added to this complex, the HABA dye is displaced because biotin has a higher association constant for avidin than the dye. As increasing amounts of biotin are added to the complex, increasing amounts of HABA dye are displaced causing a decrease in the absorbance that is proportional to the amount of biotin in the solution. The amount of biotin in an unknown sample can then be determined by comparison to the generated standard curve.

2.4.8- Conjugation of biotin functionalised dextran to GNPs

After functionalisation with biotin and HABA assays to determine the concentration of biotin within each dextran, each functionalised dextran was titrated against fixed numbers of 10 nm GNPs to determine the equivalence point. Titration curves for these dextrans with 10 nm GNPs can be seen in Figure 13 and the ratios of biotin to GNPs at the equivalence points are listed in Table 1. The graph and table show that dextrans functionalised with a high mean number of biotin molecules have a high number of biotins per GNP after conjugation. The mean number of biotin molecules per dextran can be varied by adjusting the stoichiometry of biotin-NHS reagent to aminodextran in the functionalisation reaction. A graph showing the relationship

between the amount of biotin-NHS ester added during the dextran functionalisation reaction and the number of biotin molecules per GNP after conjugation can be seen in Figure 14. The graph shows that there is a linear relationship between the amount of biotin-NHS ester added during the functionalisation reaction and the mean number of biotin molecules per GNP after conjugation.
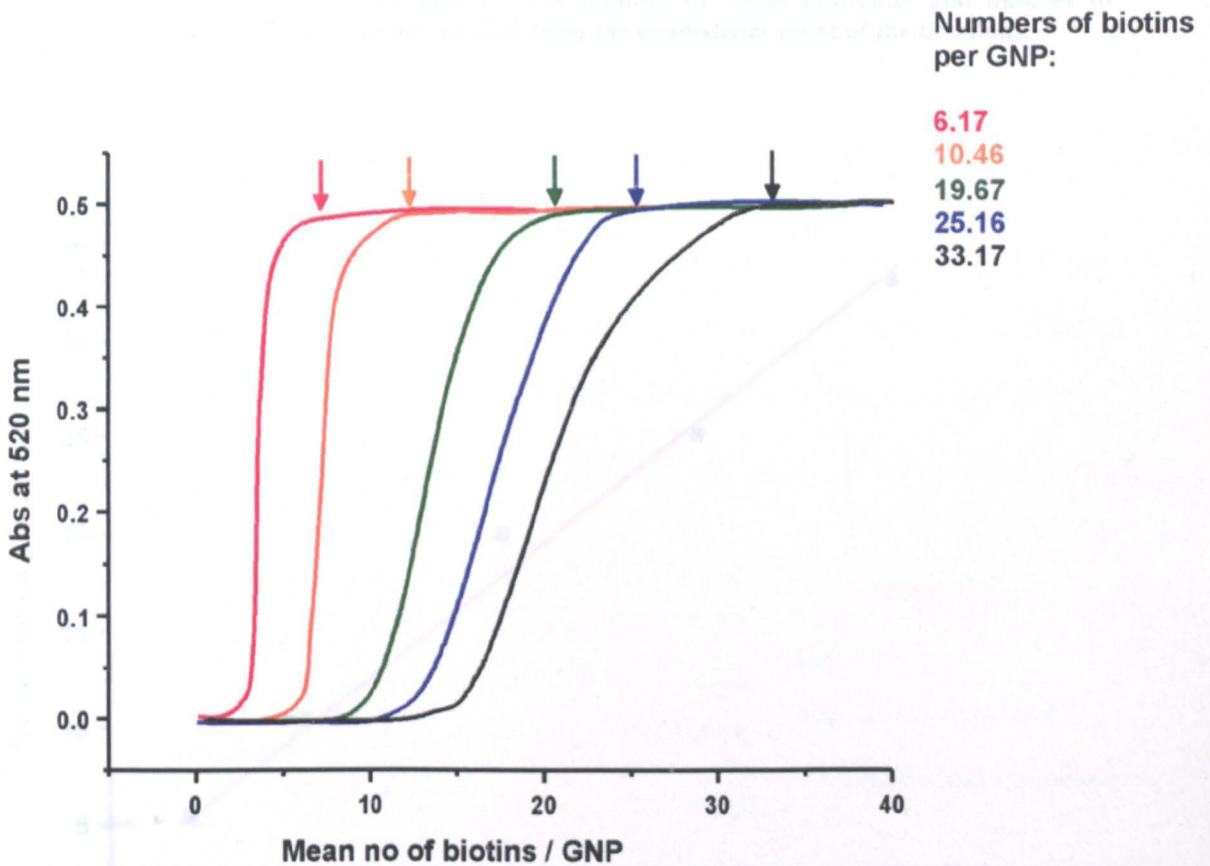
Figure 13: Overlaid titration curves for prepared biotin functionalised dextrans. Coloured arrows denote equivalence point for each dextran and the mean number of biotin molecules per GNP at this point.

Haptens / Dextran	Haptens / GNP	Dextran / GNP
1.1	6.17	5.6
1.93	10.46	5.41
3.3	19.67	5.96
4.37	25.16	5.75
6.1	33.17	5.43

Table 1: Table denoting the values obtained from the biotin functionalisation and titration experiments. The concentration of dextran in the dialysed solutions was calculated by correcting for the increase in volume of the solution, and the concentration of biotin haptens was determined from the HABA assays. The number of biotin molecules and number of dextran molecules per GNP were determined from the equivalence point of the titrations.
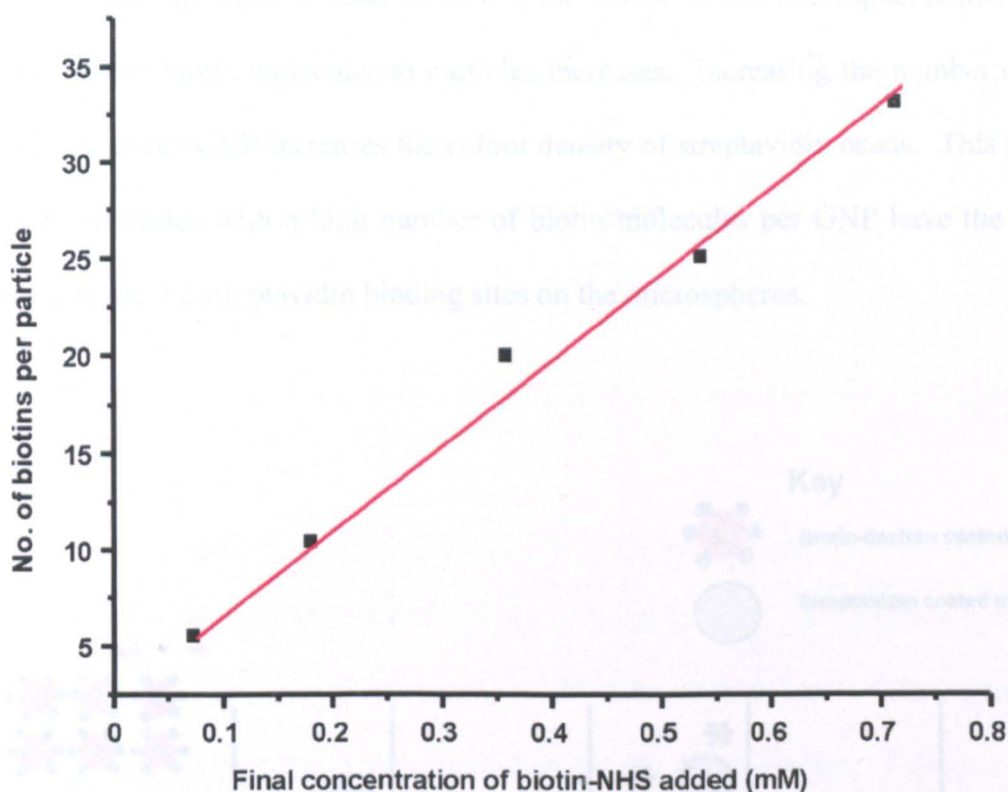
Figure 14: Graph showing the relationship between the amount of biotin-NHS ester added during the dextran functionalisation reaction and the number of biotins per particle as determined from the equivalence point of the titration. The graph shows that the number of biotin molecules per GNP after conjugation is proportional to the amount of biotin NHS ester added to the aminodextran during the functionalisation reaction.

2.4.9- Streptavidin bead assays

The properties of GNPs coated with biotin functionalised dextran were investigated by mixing them with white polystyrene microspheres coated with streptavidin as shown in Figure 15. GNPs with high mean numbers of probe molecules, such as biotin, will have the greatest affinity for the complementary binding molecule. To investigate this, biotin-GNP conjugates containing different mean numbers of biotin molecules per particle were prepared and used in a streptavidin microsphere assay. Figure 16 shows that when fixed amount of streptavidin-coated microspheres were mixed with the same number of GNPs, the colour of the microspheres increases as the ratio of biotin molecules to particles increases. Increasing the number of biotin molecules per GNP increases the colour density of streptavidin beads. This suggests that conjugates with a high number of biotin molecules per GNP have the greatest affinity for the streptavidin binding sites on the microspheres.

Key

Biotin-dextran coated GNP

Streptavidin coated microsphere
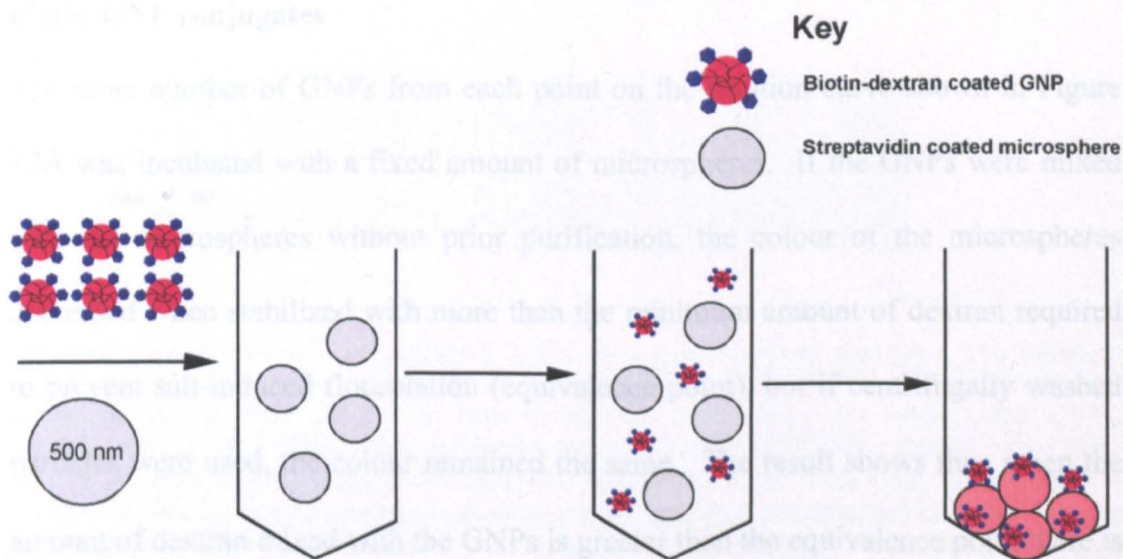
Figure 15: Streptavidin microsphere assay. Biotin dextran coated GNPs are mixed with white streptavidin coated microspheres. The biotin on the coated GNPs binds to streptavidin and the microspheres become pink.
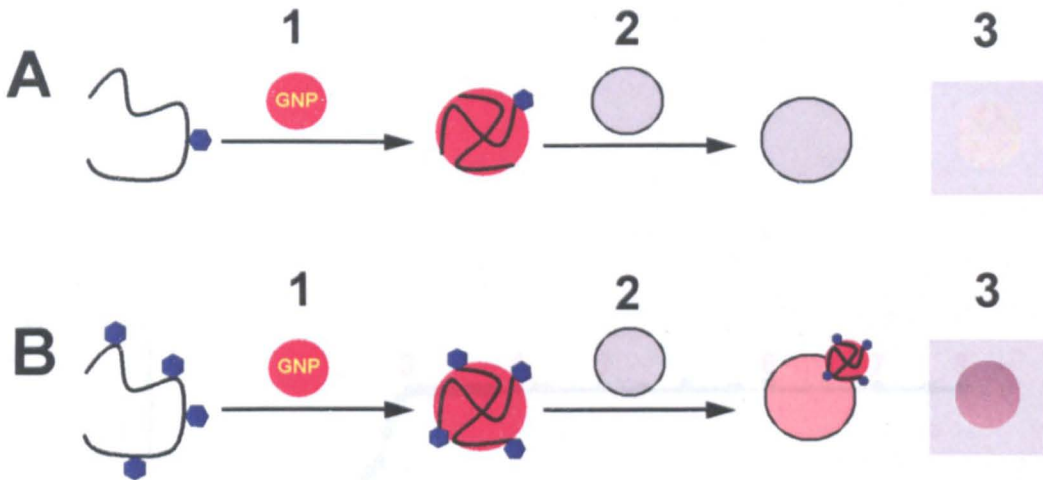
Figure 16: In step 1, biotin functionalised dextran is added to GNPs and becomes attached via a plurality of disulphide bonds. In step 2, biotin coated GNPs are mixed with white streptavidin coated microspheres. In step 3, after washing to remove un-bound biotin coated GNP, streptavidin microspheres are imaged. A) dextran polymer A has a low number of biotin molecules attached and so after conjugation, the GNP has a low affinity for the streptavidin beads. B) As dextran polymer B has a higher number of biotin molecules attached, after conjugation, the GNP has a higher affinity for the streptavidin beads.

2.4.10- Streptavidin bead assays with centrifugally washed and un-washed biotin-GNP conjugates

The same number of GNPs from each point on the titration curve shown in Figure 17A was incubated with a fixed amount of microspheres. If the GNPs were mixed with the microspheres without prior purification, the colour of the microspheres decreased when stabilized with more than the minimum amount of dextran required to prevent salt-induced flocculation (equivalence point), but if centrifugally washed particles were used, the colour remained the same. The result shows than when the amount of dextran mixed with the GNPs is greater than the equivalence point there is free biotinylated dextran in the solution that competes with the GNPs for the streptavidin binding sites on the microspheres. This competing dextran can be removed by washing the GNPs with a centrifuge. This is an important result as it

indicates that all of the dextran added at the equivalence point is conjugated to the

GNPs.
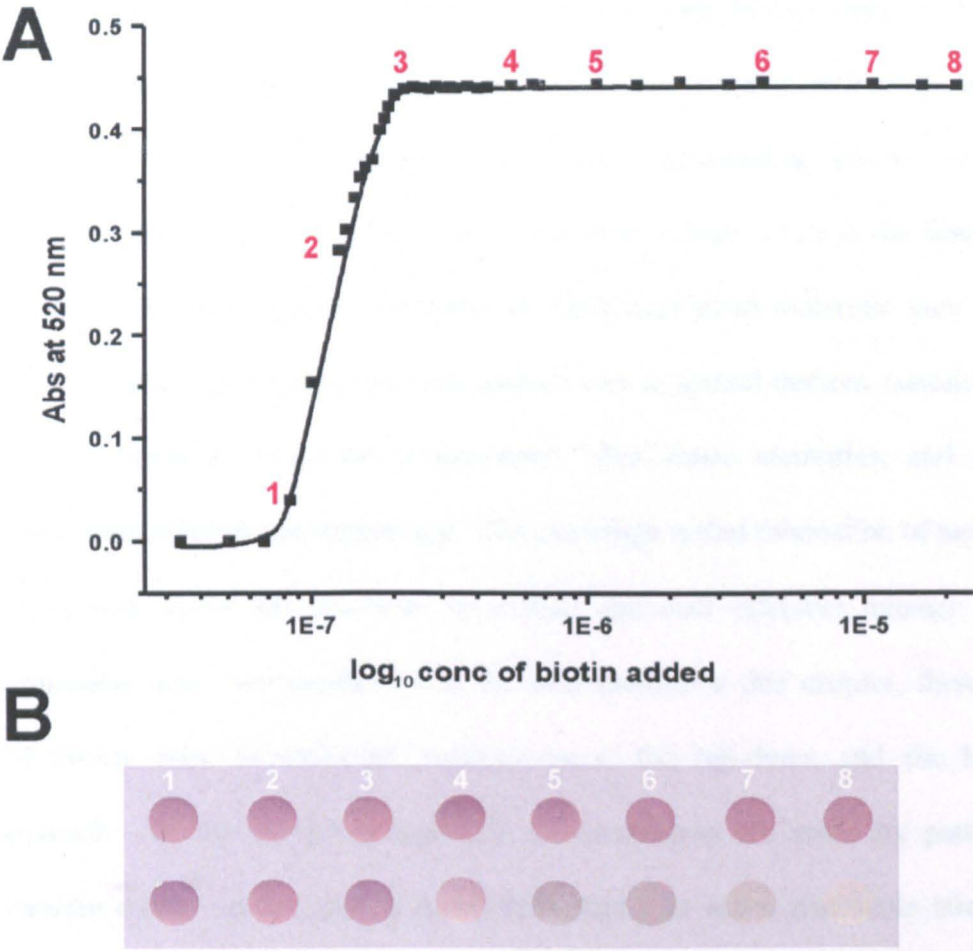
Figure 17: A) Titration curve obtained with biotin functionalised dextran. The numbers correspond to the bead assay images shown below the graph. Point 3 on the graph corresponds to the equivalence point. B) Results from streptavidin bead assays with biotin coated GNPs. Top row = assay carried out with centrifugally washed biotin coated GNPs. Bottom row = assay carried out with un-washed biotin coated GNPs. Results show that if the GNPs are coated with more than the equivalence point amount of biotin functionalised dextran and the GNPs are not centrifugally washed (B: bottom row wells 4-8) there is free biotin functionalised dextran in solution. This free dextran competes with the dextran on the GNPs for binding sites on the streptavidin beads and leads to a reduction in the colour density of the beads. If the biotin coated GNPs are centrifugally washed before the bead assay, any free biotin functionalised dextran is removed from the solution and there is no reduction in colour during the bead assay.

2.5- Discussion

The unique optical, electronic and catalytic properties exhibited by materials at the nano-scale have lead to many potential applications in electronics, nanodevices and biosensor development.[26] Whilst a great deal of work has been devoted to the synthesis of nano-building blocks such as nanoparticles, nanotubes and nanowires, the precise organisation of these individual building blocks into more complex nanostructures that will allow the properties of these materials to be exploited is still a major problem. The ability to assemble nano-building blocks into arrays, networks, and circuits in a precise and controlled manner is key to the fabrication of a variety of nanodevices. Networks of nanometer-sized materials may exhibit a variety of quantum phenomena, with applications in optical devices, nanometer-sized sensors, advanced computer architectures, ultra dense memories, and quantum-information science and technology. The challenge is that fabrication of nanoparticle arrays with nanoscale precision in a time and cost effective manner is still a formidable task. As mentioned in the introduction to this chapter, there are two approaches used to construct nanostructures, the top-down and the bottom-up approach. In the top-down approach, nanostructures are made by patterning or "carving down" larger objects using lithography to make nanoscale structures in precise patterns. Whilst this approach has enabled the miniaturization of electronic devices to a certain point, the size and complexity of the nanostructures that can be constructed by this approach is still limited.[27] In addition, many of the techniques used in top-down approaches are complicated, time-consuming and expensive.

The bottom-up approach involves the assembly of individual atoms and molecules into larger structures by chemical or physical forces operating at the nanoscale. Most

of the research conducted in this area has involved the use of supramolecular chemistry approaches, in which the structures are assembled and held together by non-covalent interactions. For example, Shenhar and Rotello used this approach to construct nanoparticle assemblies for catalytic applications.[28] They used silica and GNPs both functionalised with carboxylic acid groups and a flexible amine functionalised polymer to assemble the nanoparticles into binary aggregates. In this approach, the silica nanoparticles served as a scaffold which the amine polymer surrounded, separated only by repulsive Coulombic interactions between the charged particle and polymer. The GNPs then assembled around the polymer in the same way. The size of the aggregates could be controlled by changing the stoichiometry or the order of component addition during the assembly process. In another example, Liu and colleagues prepared two dimensional arrays of GNPs on silica substrates.[29] This was achieved by silanizing a silica substrate to introduce amine functionalities, then adsorbing GNPs to the functionalised substrate to create a monolayer. The GNPs were attached to the substrate via electrostatic interactions between the positively charged amino groups on the substrate and the negatively charged GNPs. There are still some limitations associated with the construction of nanostructures using supramolecular chemistry approaches. A major disadvantage is that the complexity of structures created is limited and in addition, the assembled structures are often irreproducible. But perhaps more importantly, the assembled structures are often unpredictable and cannot be controlled in a precise manner.

Interest in the concept of self-assembled nanostructures and problems with their construction led to the idea of using DNA as a template for the programmed assembly of nanoscale arrays. The unique recognition properties of DNA, advances

in the synthesis of oligonucleotides and the ability to modify DNA with functional groups at predetermined sites have made this an attractive material. Many different types of nanoparticles including gold,[30, 31, 32,] silver,[33] palladium[34] and cadmium selenide[35] have been organized using this technique. For example, Warner and colleagues prepared linear, ribbon and branched GNP assemblies with consistent interparticle spacings for applications in nanoelectronics using DNA as a template.[36] In this approach, GNPs with cationic groups on the surface were synthesised and assembled along the negatively charged phosphate backbone of DNA. In another example, Braun and colleagues used DNA stretched between two gold electrodes to grow silver nanowires.[33] In this approach, two gold electrodes were functionalised with non-complementary thiolated oligonucleotides and a 16 μm piece of DNA with ends complementary to each oligonucleotide was introduced to form a bridge between the electrodes. Silver ions were then deposited and complexed with the amino groups present along the DNA bridge. The silver ions were then chemically reduced to silver nanoparticles.

2.5.1- Introducing controlled functionality

Despite the success of supramolecular self-assembly and biomolecule templated assembly methods for the development of nanostructures, the level of control on the resulting nanostructures and of the properties of these structures is still limited. An alternative approach which could help alleviate these problems is to use covalent bond chemistry. [18, 20, 37] In using a covalent approach, the strength of the covalent bond yields nanostructures that are more robust and have increased stability. It also allows more precise control over the properties of the nanostructure, which can be tuned freely and reversibly by controlling the length or position of the molecules

between the particles and attachment group. In order to use a covalent approach, the chemical functionality of the individual nano-building blocks must be controlled. Without control it is likely that the nanostructures obtained will be irreproducible, but, at present there are very few methods available that will allow this level of control. Hainfield and Powell developed a nanogold product with a single functional group attached to the particle surface.[38] In this work, a mixture of non-functionalised and functionalised triphenyl phosphine ligands were used to control the number of functional groups attached to a nanocluster. In the case of a gold nanocluster with a diameter of 0.8 nm, there were a total of 7 ligands on the surface. If a ratio of 6:1 of non-functionalised and functionalised ligand is used during the synthesis reaction, the product would contain on average six non-functionalised ligands and one functionalised ligand. Using this protocol, a mixture of nanocluster products were obtained including mono-functionalised, non-functionalised and multi-functionalised particles, however, these could be separated using ion exchange chromatography. This method was also used to functionalise larger nanoclusters but it was more difficult to introduce a controlled number of functional groups and separate them due to the complicated product mixture. This occurred because these clusters contained many surface reactive sites and despite careful control of the ratio of functionalised or non-functionalised ligands the formation of multi-functionalised particles each with different numbers of ligands attached could not be prevented. Other approaches that have been proposed for the controlled chemical functionalisation of nanoparticles but the majority of these are also based upon the ratio of reactants in a similar manner to the Hainfield method and are therefore subject to the same problems. The other disadvantage of this approach is the way in which the ligands are attached to the particle surface. The triphenylphosphine ligands are immobilised

to the particle *via* electrostatic interactions. There have been reports that these ligands can dissociate at high temperatures and when in the presence of solutions of high ionic strength, which significantly limits the applications of these gold nanoclusters.[39] Worden and colleagues described a different approach for the controlled chemical functionalisation of GNPs.[37, 40] In this work, a solid phase synthesis "catch and release" technique was described whereby a controlled density of thiol ligands was immobilised onto a polymer resin support using a bifunctional linker that also contained a carboxyl group. In this approach, GNPs protected with alkanethiolate ligands were attached to the support *via* an exchange reaction between the thiol ligands on the support and those on the nanoparticles. Worden and colleagues claimed that if the density of thiol ligands on the support was low enough, each nanoparticle would react with only one thiol ligand on the support. The attached particles could then be cleaved using solvent to yield single nanoparticles functionalised with one carboxyl group. To confirm that the particles contained only one carboxyl group, the released particles were coupled together by addition of a diamine solution such as ethylenediamine and then analysed by transmission electron microscopy (TEM). If the nanoparticles contained one carboxyl group, the diamine would link two nanoparticles together into a nanoparticle dimer, the presence of more than one carboxyl group would result in the formation of nanoparticle clusters. From these experiments, Worden and colleagues observed that a high percentage of the nanoparticles obtained from the solid synthesis approach were functionalised with just one carboxyl ligand. Although this method appears to produce higher yields of mono-functional GNPs than the solution phase approach reported by Hainfield, there are also some limitations. The yield of mono-functional particles obtained is highly dependent on the rigidity of the solid phase support. If the

polymer support is not sufficiently cross-linked multiple bifunctional thiol ligands are attached to the same particle and the functionalisation cannot be controlled. In addition, although the development of a method to produce particles with a single functional group is important, for the construction of some nanostructures it may be necessary to introduce more than one to the same nanoparticle in a controlled manner. A great deal of experimental work on the rigidity and functionalisation of the polymer support and the solvents used would be necessary to adapt Worden and colleagues procedure to produce a high yield of particles with more than one functionality and they accept that a more detailed investigation is needed to explore the potential of this approach.

2.5.2- An alternative method for covalently attaching known numbers of functionalities to GNPs

In this chapter a conjugation method based on high molecular weight polymers was described that not only allows the user to attach almost any molecule or functional group to nanoparticles but also allows the user to control or vary the number of molecules per particle.[41-45] The method involves synthesizing the entire polymer surface layer prior to conjugation to the particle. This allows the surface layer to be purified and characterized before conjugation to the particles. As a result, the mean number of functionalities per polymer can be determined without interference from the particles. In this method, an aminodextran polymer is first characterized to determine the exact number of amines available for functionalisation. Once this number has been determined, the desired functionality and PDP groups are introduced into a known amount of aminodextran using amine reactive heterobifunctional reagents. The functionalised dextran is then purified to remove

un-reacted reagents and characterized to determine the mean number of functionalities per dextran. In order to attach known numbers of molecules to GNPs using this method, it is essential to also know the number of GNPs per ml. The GNPs used in this work were supplied from a commercial source and contained a data sheet that stated the mean diameter of the particles, the absorbance at 520 nm and the corresponding number of particles per ml. To confirm that this data was correct, DLS measurements and UV/vis spectra of all GNPs were obtained. Data obtained from these experiments corresponded with that supplied by the manufacturer. To conjugate known numbers of molecules to GNPs the minimum amount of functionalised dextran required to prevent salt-induced flocculation of GNPs is determined by titration. Different amounts of functionalised dextran solution are added to known numbers of GNPs followed by concentrated NaCl solution. In the absence of any added dextran the solution turns blue due to flocculation of the particles, but as the amount of dextran is increased an increasing fraction of the particles remain pink as shown in section 2.4.3, Figure 6A. When this colour change is plotted against the amount of dextran added, titration curves similar to that shown in section 2.4.3, Figure 6B are obtained. The arrow on the plot indicates the equivalence point at which just enough dextran has been added to prevent any flocculation of the particles. As the number of GNPs is known from the DLS and UV/vis measurements, the mean number of functionalities per aminodextran molecule is known from characterization and the mean number of aminodextrans per particle is known from the titrations, the mean number of functionalities per particle is also known. Using this method, the number of molecules per GNP can also be varied simply by changing the stoichiometry of reactants in the dextran functionalisation reaction. In order to investigate the

conjugation procedure and the effect of changing the number of molecules per GNP, different numbers of biotin molecules were attached to high molecular weight aminodextran polymers and then these functionalised dextrans were conjugated to GNPs. The process by which these dextrans were functionalised and conjugated is shown schematically in Figure 18. In step 1 biotin is covalently attached to a known amount of aminodextran that was also functionalised with PDP groups; the amount of biotin was varied by reacting different amounts of the corresponding N-hydroxysuccinimide ester with a fixed amount of dextran. In step 2 the solutions were dialysed to remove molecules that were not covalently attached to dextran and then the biotin concentration of each dialysed solution was determined by the HABA assay.[24, 25] In step 3 the dextrans were conjugated to GNPs by the dative covalent bonds that formed when disulphide bonds in PDP ruptured on contact with the gold. As shown in section 2.4.8, Table 1, the number of dextran molecules required to stabilize the same number of GNPs is constant. This confirms that the only way to change the number of biotin molecules per GNP is to change the number of biotin molecules per dextran.

To determine the relationship between the amount of dextran added at the equivalence point and the diameter of the GNPs, functionalised dextrans were titrated against GNPs of different diameters. The results show that for a given molecular weight of dextran, there is a linear relationship between the minimum amount of functionalised dextran required to prevent salt-induced flocculation of the particles and the square of the nanoparticle diameter, the latter being proportional to the surface area of the GNPs. To confirm that the amount of functionalised dextran added at the equivalence point was conjugated to the GNPs, streptavidin bead assays

were carried out with centrifugally washed and un-washed biotin coated GNPs. When the amount of biotin functionalised dextran added to the GNPs exceeded the equivalence amount, and the GNPs were not centrifugally washed, the colour of the microspheres decreased as shown in the image in Section 2.4.10, Figure 17B (bottom row, wells 4-8). These results suggest that when GNPs are mixed with the minimum amount of PDP-dextran that prevents salt-induced flocculation, all of the added dextran is attached to the particles. If the dextran is also functionalised with another molecule such as biotin, this will also be attached to the particles. It also suggests that if the number of molecules attached to the dextran is changed then the mean number of molecules per particle will also be changed.
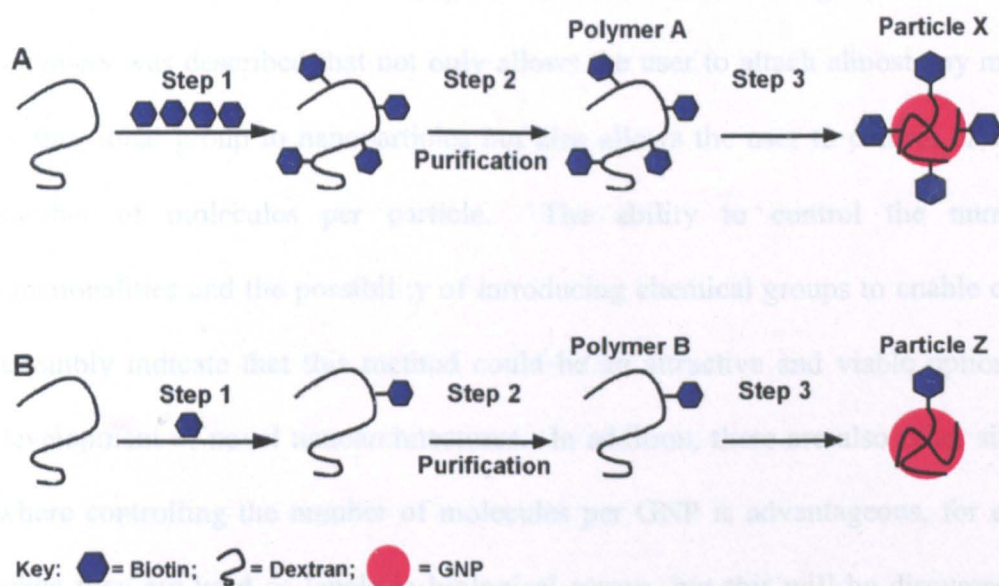
Figure 18: Schematic diagram showing functionalisation and conjugation of dextran to GNPs. In step 1, biotin is covalently attached to an aminodextran polymer that was also functionalised with PDP groups. In step 2, the functionalised dextran is purified to remove un-reacted reagents and then characterized to determine the mean number of functionalities per dextran molecule. In step 3, the characterized dextran is conjugated to GNPs. The number of functionalities per dextran molecule can be controlled by adjusting the stoichiometry of biotin-NHS ester in the functionalisation reaction. As polymer A is functionalised with more biotin molecules than polymer B, there will be more biotin molecules attached to particle X than particle Z after conjugation.

2.6- Summary

The unique optical, electronic, conductive and catalytic properties exhibited by materials at the nanoscale have led to their extensive use in the development of new products with potential applications in catalysis, optoelectronics, medicine and biosensing. Although there are now numerous different methods that enable the synthesis of different types of nano-building blocks such as nanoparticles, nanotubes and nanorods with controlled shapes and sizes, the organization of these building blocks into more complex structures with the desired properties in a controllable and reproducible manner is still a formidable challenge. In order to control the assembly of nano-building blocks, it is essential to control the number of functionalities on the individual blocks. To date, there are very few methods that enable this level of control. In this chapter a conjugation method based on high molecular weight polymers was described that not only allows the user to attach almost any molecule or functional group to nanoparticles but also allows the user to control or vary the number of molecules per particle. The ability to control the number of functionalities and the possibility of introducing chemical groups to enable covalent assembly indicate that this method could be an attractive and viable option in the development of novel nanoarchitectures. In addition, there are also other situations where controlling the number of molecules per GNP is advantageous, for example when they are used as labels in biological assays, but this will be discussed in the next chapter.

2.7- References

1. Katz, E., Willner, I., *Angew. Chem. Int. Ed.*, (2004), **43**, 6042-6108.

2. Jensen, K., Weldon, J., Garcia, H., Zettl, A. *Nano Lett.*, (2007),

3. http://www03.ibm.com/industries/healthcare/doc/content/news/pressrelease/24441 15105.html?g_type=rssfeed_leaf

4. Shenhar, R., Norsten, T.B., Rotello, V.M., *Adv Mater.*, (2005), **17**, 657-669.

5. Ratner, M., Ratner, D., *Nanotechnology: A gentle introduction to the next big idea* (2003), Prentice Hall, New Jersey.

6. Twyman, M. *Lithography- Techniques of drawing on stone and their applications in topography* (1970), Oxford University Press, London.

7. Pinar, R.D., Zhu, J., Xu, F., Hong, S., Mirkin, C.A. *Science*, (1999), **283**, 661-663.

8. Gould, P. *MaterialsToday*, (2003), May issue, 34-39.

9. Cheng, X., Li, D., Guo, L.J., *Nanotechnology*, (2006), **17**, 927-932.

10. Craighead, H.G. *Science*, (2000), **290**, 1532-1535.

11. Lehn, J.M. *Science*, (1993), **260**, 1762-1763.

12. Tang, Z., Kotov, N.A., *Adv. Mater.*, (2005), **17**, 951-962.

13. Holliday, R. *Genet. Res.*, (1964), **5**, 282-304.

14. Seeman, N.C. *Acc. Chem. Res.*, (1997), **30**, 357-363.

15. Rothemund, P.W.K. *Nature*, (2006), **440**, 297-302.

16. Mitra, D., Di Cesare, N., Sleiman, H.F. *Angew. Chem. Int. Ed.*, (2004), **43**, 5804-5808.

17. Storhoff, J.J., Mirkin, C.A. *Chem. Rev.*, (1999), **99**, 1849-1862.

18. Grill, L., Dyer, M., Lafferentz, L., Persson, M., Peters, M.V., Hecht, S. *Nature Nanotech.*, (2007), **2**, 687-691.

19. Guldi, D.M., Aminur Rahman, G.M., Sgobba, V., Ehli, C. *Chem. Soc. Rev.*, (2006), **35**, 471-487.

20. Romo-Herrera, J.M., Terrones, M., Terrones, H., Dag, S., Meunier, V. *Nano Lett.*, (2007), **7**, 570-576.

21. Medina Hernandez, M.J., Villanueva Camanas, R.M., Cuenca, E.M., Alverez-Coque, M.C.G. *Analyst*, (1990), **115**, 1125-1128.

22. Carlsson, J., Drevin, H., Axen, R. *Biochem. J.*, (1978), **173**, 723-737.

23. Nalwa, H.S., *Encyclopedia of nanoscience and nanotechnology*, (2004), American scientific publishers, California.

24. Green, N.M. *Biochem. J.*, (1965), **94**, 23c-24c

25. Livnah, O., Bayer, E.A., Wilchek, M., Sussman, J.L., *Febs letts.*, (1993), **328**, 165-168.

26. Shipway, A.N., Katz, E., Willner, I., *CHEMPHYSCHEM.*, (2000), **1**, 18-52.

27. Niemeyer, C.M., *Angew. Chem. Int. Ed.*, (2001), **40**, 4128-4158.

28. Shenhar, R., Rotello, V.M., *Acc. Chem. Res.*, (2003), **36**, 549-561.

29. Zheng, J., Zhu, Z., Chen, H., Liu, Z., *Langmuir*, (2000), **16**, 4409-4412.

30. Alivisatos, A.P., Johnsson, K.P., Peng, X., Wilson, T.E., Loweth, C.J., Bruchez Jr, M.P., Schultz, P.G., *Nature*, (1996), **382**, 609-611.

31. Mirkin, C.A., Letsinger, R.L., Mucic, R.C., Storhoff, J.J., *Nature*, (1996), **382**, 607-609.

32. Kumar, A., Pattarkine, M., Bhadbhade, M., Mandale, A.B., Ganesh, K.N., Datar, S.S., Dharmadhikari, C.V., Sastry, M., *Adv. Mater.*, (2001), **13**, 341-344.

33. Braun, E., Eichen, Y., Sivan, U., Yoseph, G.B., *Nature*, (1998), **391**, 775-778.

34. Richter, J., Seidel, R., Kirsch, R., Mertig, M., Pompe, W., Plaschke, J., Schackert, H.K., *Adv. Mater.*, (2000), **12**, 507- 510.

35. Alivisatos, A.P., *Nat. Biotechnol.*, (2004), **22**, 47-52.

36. Warner, M.G., Hutchison, J.E., *Nat. Mater.*, (2003), **2**, 272-277.

37. Shaffer, A.W., Worden, J.G., Huo, Q., Langmuir, (2004), 20, 8343-8351.

38. Hainfield, J.F., Powell, R.D., *J. Histochem. Cytochem.*, (2000), **48**, 471-480.

39. Brown, L.O., Hutchison, J.E., *J. Am. Chem. Soc.*, (1997), **119**, 12384-12385.

40. Worden, J.G., Shaffer, A.W., Huo, Q., *Chem. Commun.*, (2004), 518-519.

41. Wilson, R. *Chem. Commun.*, (2003), 108-109.

42. Wilson, R., Chen, Y., Aveyard, J., *Chem. Commun.*, (2004), 1156-1157.

43. Chen, Y., Aveyard, J., Wilson, R., *Chem.Commun.*, (2004), 2804-2805.

44. Mehrabi, M. & Wilson, R. *Small*, (2007), **9**, 1491-1495.

45. Aveyard, J., Mehrabi, M., Cossins, A., Braven, H., Wilson, R. *Chem. Commun.*, (2007), **41**, 4251-4253.

CHAPTER 3

3.1- Introduction

Lateral flow devices, also known as immunochromatographic assays, are disposable membrane based tests that provide visible evidence of the presence or absence of an analyte or analytes in liquid samples. First introduced in the 1980's, they have subsequently become one of the most important products of the diagnostics industry;[1] the most successful and well known device being the home pregnancy test. Since their introduction they have become well established in a variety of point-of-care (POC) and field-use applications, including medical diagnostics, forensics, environmental monitoring and food safety because they offer many advantages over traditional laboratory-based assays, which are often time-consuming, labour intensive and complicated. These devices are inexpensive, easy to manufacture and versatile, as one style of device can be easily adapted for the detection of another analyte. No instrumentation is required to perform the tests which enables their use in clinics, at the hospital bed side, at home or in the field. In addition, they are simple, robust and very user-friendly which allows the user to test samples and interpret results with little or no basic training. The devices only require small volumes of liquid sample and a qualitative result can be seen with the unaided eye in minutes.

Lateral flow devices consist of a porous membrane, usually nitrocellulose, onto which a line of a specific capture reagent is immobilised, usually antibodies or antigens. A glass fibre absorbent pad is attached to the distal end of the nitrocellulose strip and a conjugate pad containing dried detector reagent is fixed to the proximal end of the strip. The detector reagent is a label coated with antibodies

or antigens specific to the analyte that is to be detected; most often this label is GNPs, although other labels such as dyed microspheres can be used. When the lateral flow device is immersed in a sample, the dried detector reagent is solubilised and the solution migrates through the pores of the membrane by capillarity toward the immobilised capture reagent. The detector reagent and / or sample then bind to the immobilised capture reagent and a visual signal is produced.[2] Like other immunoassays, lateral flow immunoassays can be divided into two categories: reagent-excess and reagent-limited.[3] In reagent-excess immunoassays the number of binding sites that are occupied by an analyte are measured. The analyte is added to an excess of antibody and the amount of bound analyte can be determined with the use of a second labelled antibody. In reagent-limited immunoassays, the number of un-occupied binding sites is measured. In this type of assay, the analyte and a known amount of labelled analyte compete for a limited amount of antibody. The amount of analyte can be determined from the proportion of labelled analyte that is bound to the antibody. A diagram depicting a reagent-excess lateral flow immunoassay can be seen in Figure 1. The situation that obtains when a negative sample is applied to the membrane is depicted in Figure 1A. In step 1, the sample is applied to the membrane and the antibody labelled GNP detector reagent is solubilised. In step 2, the antibody labelled detector reagent moves through the pores of the membrane towards the immobilised antibody capture reagent by capillarity. In step 3, the antibody labelled detector reagent passes through the immobilised antibody capture reagent, does not produce a signal and is adsorbed by the absorbent pad. The situation that obtains when a positive sample is applied to the membrane is depicted in Figure 1B. In step 1, the sample is applied to the membrane and the detector reagent is solubilised. In step 2, the analyte in the sample binds to the antibody labelled detector reagent and it

moves through the pores of the membrane towards the immobilised antibody capture reagent by capillarity. In step 3, the labelled antibody-analyte binds to the immobilised capture reagent and a red signal is produced. In the reagent-excess format of lateral flow immunoassay, the amount of colour developed at the test line of the membrane is proportional to the amount of analyte in the sample.
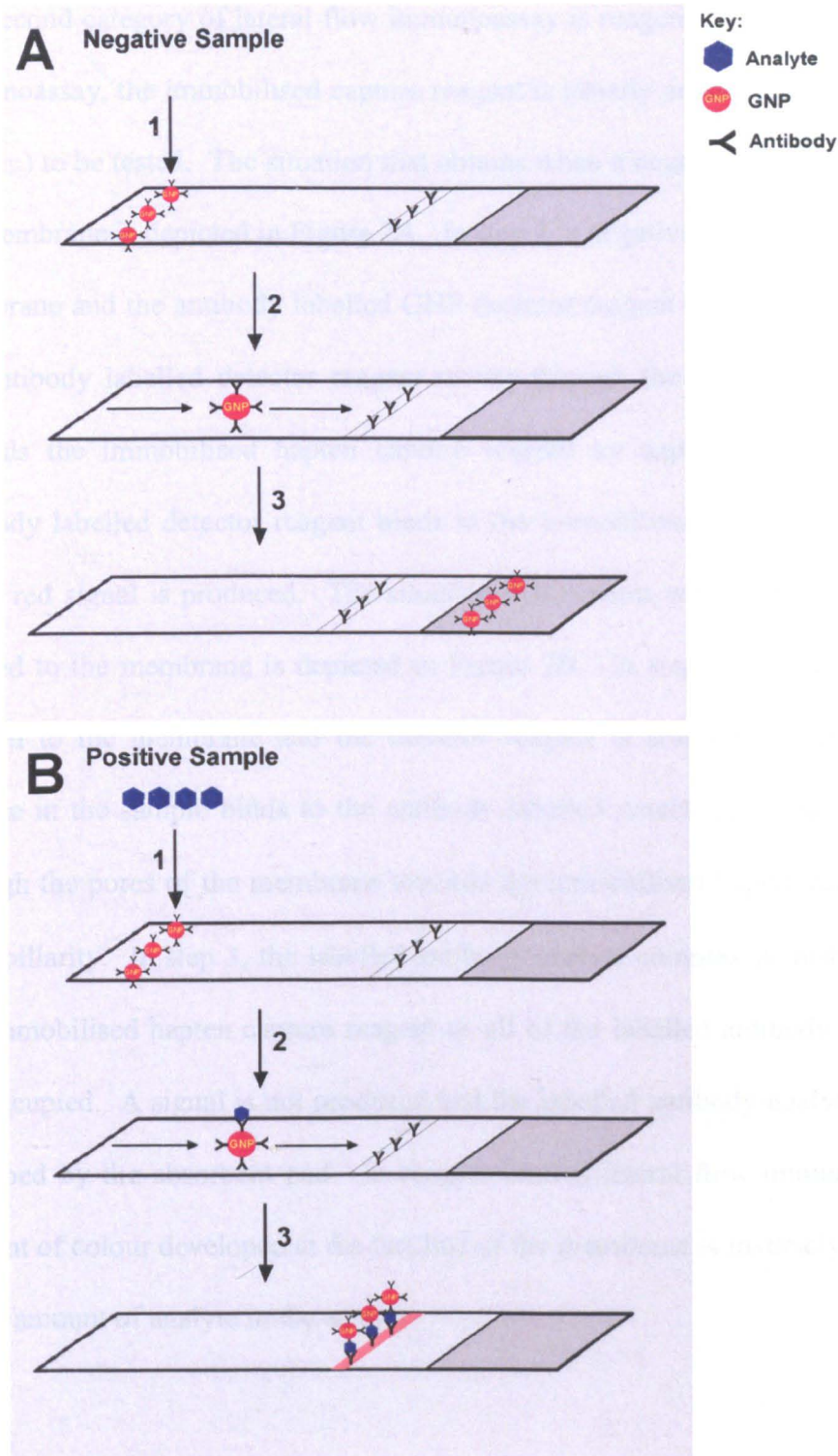
Figure 1: Diagram of a reagent-excess lateral flow device. A) The situation that obtains when a negative sample is applied to the membrane. In step 1 a negative sample (without analyte) is applied to the membrane and the labelled antibodies are solubilised. In step 2, the labelled antibodies move through the membrane by capillarity. In step 3 the labelled antibody passes through the test line and is absorbed by the absorbent pad. B) The situation that obtains when a positive sample is applied to the membrane. In step 1, a positive sample is applied to the membrane. In step 2, the labelled antibody binds to the analyte in the sample, and the labelled antibody-analyte complex moves through the membrane by capillarity. In step 3, the complex is captured by a secondary antibody immobilised on the test line of the membrane forming a "sandwich". The amount of colour developed at the test line is proportional to the amount of analyte in the sample.

The second category of lateral flow immunoassay is reagent-limited. In this type of immunoassay, the immobilised capture reagent is usually an analogue of the analyte (hapten) to be tested. The situation that obtains when a negative sample is applied to the membrane is depicted in Figure 2A. In step 1, a negative sample is applied to the membrane and the antibody labelled GNP detector reagent is solubilised. In step 2, the antibody labelled detector reagent moves through the pores of the membrane towards the immobilised hapten capture reagent by capillarity. In step 3, the antibody labelled detector reagent binds to the immobilised hapten capture reagent and a red signal is produced. The situation that obtains when a positive sample is applied to the membrane is depicted in Figure 2B. In step 1, a positive sample is applied to the membrane and the detector reagent is solubilised. In step 2, the analyte in the sample binds to the antibody labelled detector reagent and it moves through the pores of the membrane towards the immobilised hapten capture reagent by capillarity. In step 3, the labelled antibody-analyte complex is unable to bind to the immobilised hapten capture reagent as all of the labelled antibody binding sites are occupied. A signal is not produced and the labelled antibody-analyte complex is adsorbed by the absorbent pad. In reagent-limited lateral flow immunoassays, the amount of colour developed at the test line of the membrane is inversely proportional to the amount of analyte in the sample.
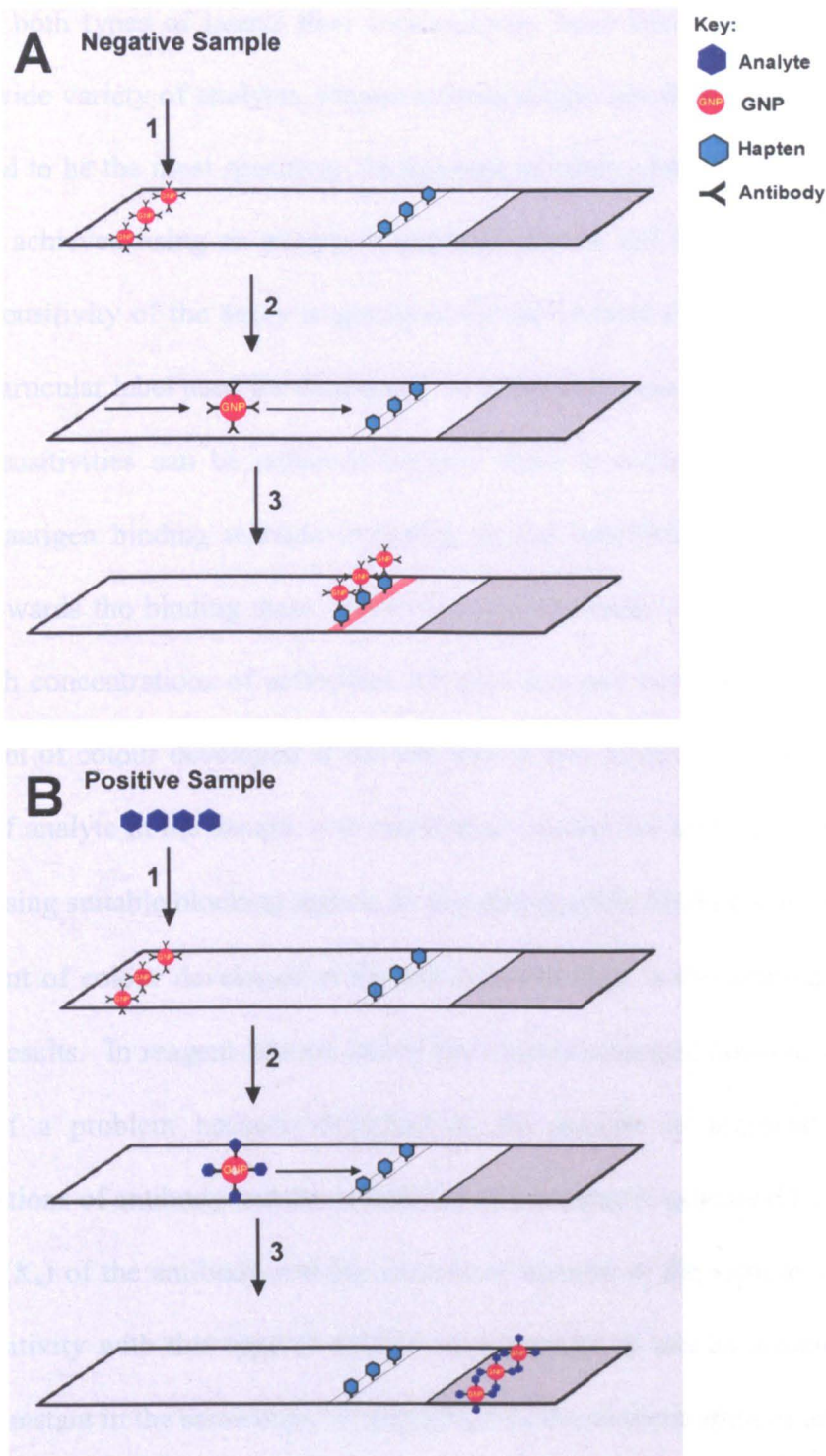
Figure 2: Diagram of reagent-limited lateral flow device with GNP labelled antibodies. A) The situation that obtains when a negative sample (without analyte) is applied to the device. In step 1, a negative sample is applied to the membrane and the labelled antibodies are solubilised. In step 2 the labelled antibodies move through the membrane by capillarity. In step 3 labelled antibodies bind to analogues of the analyte (hapten) that are immobilised on the test line producing a red line. B) The situation that obtains when a positive sample (containing antigen) is applied to the device. In step 1, a positive sample is applied and the labelled antibodies are solubilised. In step 2 the antigens in the sample bind to the labelled antibodies and move through the membrane by capillarity. In step 3, as the antigen in the sample has filled all of the labelled antibody binding sites, the antibody is unable to bind to the immobilised hapten so it passes through the test line and there is no colour development.

Although both types of lateral flow immunoassay have been used successfully to detect a wide variety of analytes, reagent-excess assays are often chosen as they are considered to be the most sensitive. In this type of assay, detection of an analyte is generally achieved using an excess of antibody (hence the term "reagent-excess") and the sensitivity of the assay is governed by the amount of non-specific binding and the particular label used for detection.[4] In using high concentrations of antibody, greater sensitivities can be achieved because there is a higher probability of an antibody-antigen binding reaction occurring as the equilibrium of the reaction is shifted towards the binding state. However, the downside of this approach is that using high concentrations of antibodies can also increase non-specific binding. As the amount of colour developed at the test line in this format is proportional to the amount of analyte in the sample it is essential to control the amount of non-specific binding using suitable blocking agents, as any non-specific binding will contribute to the amount of colour developed at the test line resulting in the attainment of false positive results. In reagent-limited lateral flow immunoassays, non-specific binding is less of a problem because detection of the analyte is achieved using low concentrations of antibody and the sensitivity of the assay is governed by the affinity constant (K_a) of the antibody and the amount of analyte in the sample. To achieve high sensitivity with this type of assay it is important to use an antibody with an affinity constant in the same order of magnitude as the concentration of analyte in the sample.[4] This is because when the affinity of the antibody is low, the binding sites will remain un-occupied when low concentrations of analyte are present and as a result there is a reduction in sensitivity. Accuracy during the attainment of results is also an important factor that contributes to the overall sensitivity of the lateral flow immunoassay. At zero concentration of analyte in reagent-excess immunoassays,

there is no colour development at the test-line, however, in the reagent-limited assays this situation is reversed with the colour of the test line at a maximum at zero concentration of analyte. More specific results can be obtained with the reagent-excess format as it is much easier and less error-prone for the user to observe the colour developed at a test line than to determine the decrease in colour from a maximum value. In addition to increased sensitivity, reagent-excess immunoassays are often chosen because they also offer specificity. This is because unlike reagent-limited assays, detection of the analyte is reliant on the specific interaction of two different antibody binding sites with two different epitopes of the target analyte. However, despite the increased sensitivity and specificity the reagent-excess immunoassays offer, there are certain cases when this type of assay cannot be applied. For example, the reagent-excess format cannot be used to detect small target analytes such as pesticides, explosives and drugs. This is because these analytes either have one epitope for antibody binding or are so small that steric hindrance prevents two large antibodies from binding to the analyte simultaneously.[4,5] Reagent-limited immunoassays are also chosen when the concentration of analyte to be detected is high. This is because in situations of analyte excess, the "hook effect" occurs in reagent-excess assays. The "hook effect" is a term commonly used to describe the decrease in signal that can occur when the concentration of target analyte exceeds the capacity of the capture reagent.[4,6] Therefore at very high analyte concentrations there is a reduction in colour development at the test line which leads to an underestimation of the amount of analyte in the sample.

Although both reagent-excess and reagent-limited lateral flow devices are relatively sensitive given their simplicity they are often not as sensitive as conventional immunoassays. Improving the sensitivity without losing any of the advantages of lateral flow detection is a major hurdle and as a result many researchers have sought to increase the sensitivity by incorporating enzymatic or fluorescent labels to amplify the signal. However, these methods are often more complicated, error-prone and can require expensive detection equipment which in turn relinquishes the key advantages of lateral flow detection. One possibility that could improve sensitivity of these devices, but has not been investigated, is to vary the number of probe molecules attached to individual particle labels. The reason for this is that existing lateral flow devices are mostly based on antibodies conjugated to labels by a method that does not allow the number of antibodies per particle to be varied. Changing the number of probe molecules changes the affinity of the particle and those with high numbers will have a higher probability of binding to a target molecule than those with a low number. In chapter 2 a simple conjugation method based on high molecular weight polymers was described. An advantage of this method is that it allows almost any molecule to be attached to GNPs .[7-10] In addition this method also allows the mean number of molecules per particle to be varied by simply changing the mean number of probe molecules per polymer. Another advantage of this method is that it also allows the mean number of probe molecules attached to the particles to be known without resorting to complicated and indirect methods to find this out. In this chapter, this method was used to prepare GNP-dinitrophenol (DNP) conjugates for use in a different type of reagent-limited lateral flow device (non-traditional). A diagram of the device can be seen in Figure 3A and B. This device is the reverse of the reagent-limited device depicted in Figure 2A and B (traditional), the detector

reagent was haptens conjugated to GNPs instead of antibodies, and the immobilised capture reagent was antibodies instead of the analogue of the analyte. The situation that obtains when a negative sample is applied to the device is depicted in Figure 3A. In step 1, a negative sample is applied and the GNP labelled hapten detector reagent is solubilised. In step 2, the labelled hapten detector reagent moves through the pores of the membrane towards the immobilised antibody capture reagent by capillarity. In step 3, the hapten labelled detector reagent binds to the immobilised antibody capture reagent and a red signal is produced. The situation that obtains when a positive sample is applied to the membrane is depicted in Figure 3B. In step 1, a positive sample is applied to the membrane and the detector reagent is solubilised. In step 2, the analyte in the sample and the labelled hapten detector reagent moves through the pores of the membrane towards the immobilised antibody capture reagent by capillarity. In step 3, the labelled hapten detector reagent is unable to bind to the immobilised antibody capture reagent as the analyte in the sample has occupied all of the antibody binding sites. A signal is not produced and the labelled hapten detector reagent is absorbed by the absorbent pad. Like the reagent-limited device depicted in Figures 2A and B, the amount of colour developed at the test line of the membrane is inversely proportional to the amount of analyte in the sample.
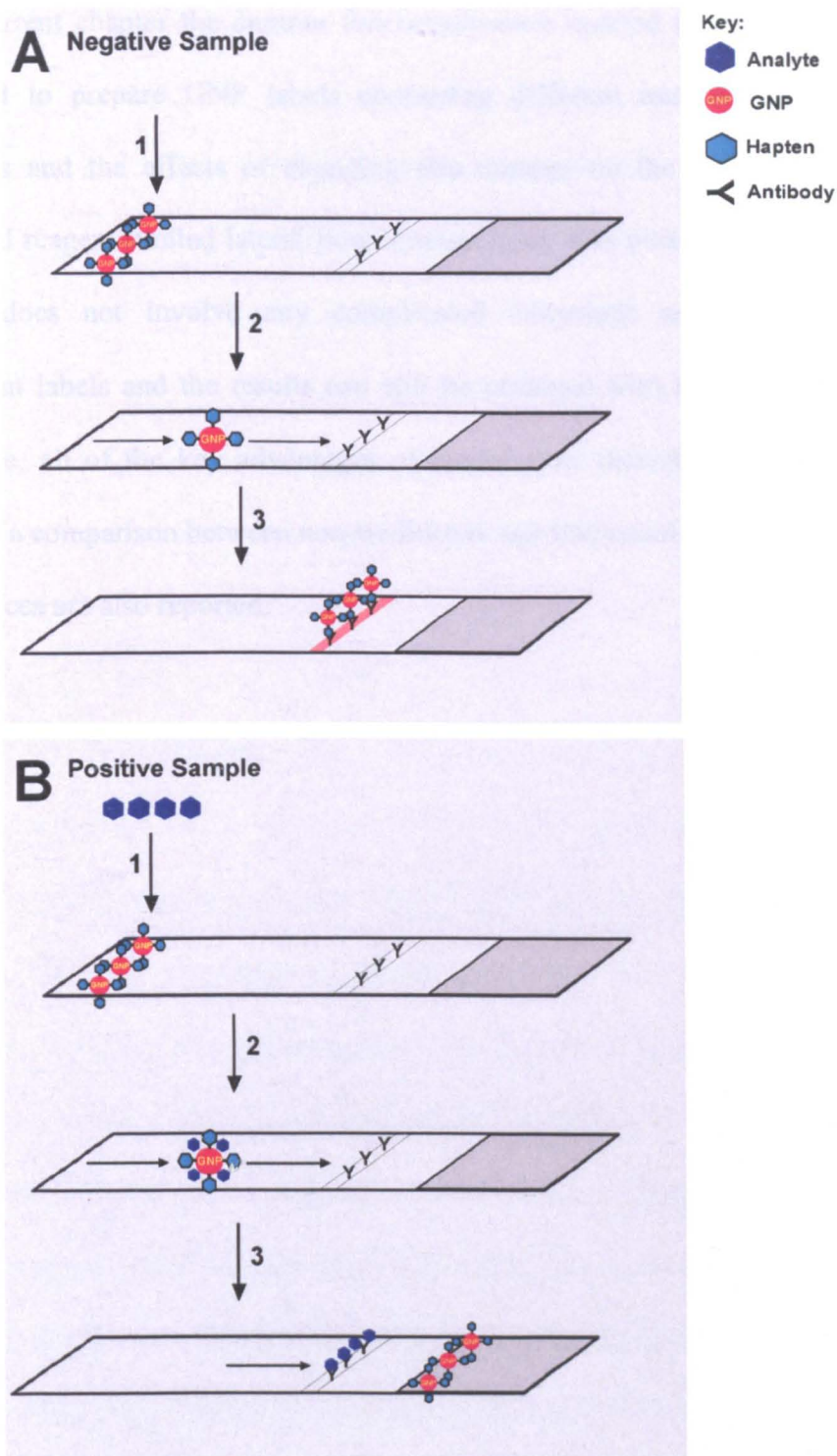
Figure 3: Diagram of a different type of reagent-limited lateral flow device based on labelled haptens. A) The situation that obtains when a negative sample (without analyte) is applied to the device. In step 1, a negative sample is applied to the membrane and the labelled haptens are solubilised. In step 2 the labelled haptens move through the membrane by capillarity. In step 3 labelled haptens bind to antibodies that are immobilised on the test line producing a vivid red line. B) The situation that obtains when a positive sample (containing antigen) is applied to the device. In step 1, a positive sample is applied and the labelled haptens are solubilised. In step two the antigens in the sample and the labelled haptens move through the membrane by capillarity. In step 3, the analyte in the sample binds to the antibodies immobilised on the test line and the labelled hapten passes through and there is no colour development.

In the current chapter the dextran functionalisation method described in chapter 2 was used to prepare GNP labels containing different numbers of DNP probe molecules and the effects of changing this number on the sensitivity of a non-traditional reagent-limited lateral flow immunoassay was investigated. Because this method does not involve any complicated enzymatic amplification steps or fluorescent labels and the results can still be obtained with speed and read by the naked eye, all of the key advantages of lateral flow detection are retained. The results of a comparison between non-traditional and traditional reagent-limited lateral flow devices are also reported.

3.2- Materials

Aminodextran (MW 70 kDa, 16 primary amines per molecule) was from Molecular Probes, Eugene, OR. Dinitrophenol N-hydroxysuccinimide ester (DNP-NHS) was synthesised in-house.[11, 12] N-succinimidyl 3-(4- hydroxy, 5-[^{125}I]iodophenyl)-propionate (^{125}I-NHS) and PD10 columns were from Amersham Biosciences. 3-(2-pyridyldithio)propionic acid N-hydroxysuccinimide ester (SPDP), bovine serum albumin (BSA), dithiothreitol (DTT), dinitrophenol (DNP), Sepharose 2B and dialysis tubing (molecular weight cut-off 12000) were from Sigma. 3 x PBS: 45 mM sodium phosphate, 0.45 M NaCl, pH 7.4. GNP (40 nm) and Lateral flow strips were prepared by BBInternational, Cardiff, UK. HiFlow plus (HF135) nitrocellulose membrane was from Millipore, UK. The adhesive coated backing sheet was from G&L Precision Die Cutting Inc, San Jose, CA. The reagent dispensing module for lateral flow strips was a Kinematic Matrix 1600 and the automatic cutter was a Kinematic Matrix 2360 (Kinematic Automation, CA). The diameter of the GNPs was determined using a ZetaPlus analyser (Brookhaven Instruments, Worcestershire, UK) and transmission electron microscopy (TEM) using a Phillips 410 operating at 80 kV or a Phillips CM12 operating at 100 kV. TEM samples were prepared by placing a drop of GNP solution on a 200 mesh nickel grid (Agar Scientific) and allowing it to dry in air. UV/vis spectra were recorded on a Hewlett Packard 8452A Diode Array Spectrophotometer. Gamma emission from ^{125}I was detected with an n-type hyperpure germanium GMX model detector (Ortec, Oak Ridge, TN). The data from the detector was collected with a NIM spectroscopy amplifier and TRUM data acquisition card interfaced with Maestro 32 software (all from Ortec).

3.3-Methods

3.3.1- Characterization of GNPs

The GNPs used in this work were obtained from a commercial source. Each batch is prepared from a known mass of gold (in gold (III) chloride) and characterized by dynamic light scattering and TEM. If the amount of gold used to prepare the particles and the mean diameter are known, the number of particles in a given volume of can be calculated using a value of 1.7×10^{-2} cubic nanometers for the volume occupied by one atom of gold. The particles used in this work were supplied with a data sheet that gave: 1) the mean diameter of the particles (CV% < 10) and, 2) the absorbance of these particles at a known number of particles per ml (for example, the 40 nm particles had 9×10^{10} particles per ml and an absorbance of 1 at 520 nm). The concentration of GNPs was determined by multiplying the number of particles per ml by 1000 and then dividing by Avogadro's number (6.02×10^{23}).

3.3.2- Synthesis of ^{125}I -functionalised dextran

To 5 mg of aminodextran in 1 ml of PBS, 100 μl of N-succinimidyl 3-(4- hydroxy, 5-[^{125}I]iodophenyl)-propionate (18.2 MBq) in dry DMF was added dropwise over a period of 2 hours of stirring. At the end of this time, 100 μl of 60 mM SPDP in dry DMF was added in the same way. After stirring overnight, the ^{125}I -functionalised dextran was diluted 1:2 with PBS and un-reacted ^{125}I and SPDP were removed by gel exclusion chromatography on a PD10 column.

3.3.3- Titration of ^{125}I - functionalised dextran against GNPs

The minimum amount of ^{125}I -functionalised dextran required to prevent salt-induced flocculation of 40 nm gold nanoparticles was determined by titrating variable amounts of ^{125}I -functionalised dextran against fixed volumes of 40 nm GNPs (9×10^{10} particles per ml). Increasing amounts of ^{125}I -functionalised dextran were added to 0.66 ml aliquots of GNPs and a gamma counter was used to measure the average counts/sec in each solution. 0.33 ml of 0.45M NaCl was added to each solution and each was passed through a 0.2 μm syringe filter. After filtration the average counts/sec in each solution were recorded and the absorbance of each was obtained by UV/vis spectroscopy. At the end of this time, each solution was centrifuged at 700g for 10 minutes. The supernatants were removed and counted before re-suspending the radiolabelled GNP pellet in fresh solution and re-counting.

3.3.4- Synthesis of DNP functionalised dextrans

Six dextrans functionalised with different amounts of DNP haptens were synthesised as follows: 100 μl of DNP-NHS solution, in dry DMF was added dropwise with stirring, over a period of 5 hours to 1 ml aliquots of PBS containing 5 mg of aminodextran; the concentrations of DNP-NHS in the DMF solutions were; 1) 0.5 mM, 2) 0.85 mM, 3) 2 mM, 4) 3 mM, 5) 7 mM or 28 mM. At the end of this time, 100 μl of 60 mM SPDP in dry DMF was added in the same way. After stirring for a further 5 hours, un-reacted DNP and SPDP were removed by dialysis against 4 x 1 L of deionised water for a total of 48 hours. The concentration of dextran in the dialysed solutions was calculated by correcting for the increase in volume of the solution, and the concentration of DNP haptens was determined by UV/vis spectrophotometry ($\epsilon_{360} = 1.7 \times 10^4$ M^{-1} cm^{-1}). The concentration of PDP was

determined by measuring the absorbance increase at 343 nm following reduction with DTT (ϵ_{343} = 8.08 x 10^3 M^{-1} cm^{-1}).

3.3.5-Preparation of DNP-GNP conjugates

The minimum amount of DNP functionalised dextran required to prevent flocculation of 40 nm gold nanoparticles in PBS was determined by titrating variable amounts of each DNP functionalised dextran solution against a fixed volume of 40 nm GNPs (9 x 10^{10} particles per ml) as described in chapter 2. DNP-GNP conjugates were prepared by adding this minimum amount of DNP functionalised dextran to 40 nm gold followed by a 2:3 dilution with 3 x PBS containing 3 mg ml $^{-1}$ bovine serum albumin (BSA), 3 mg ml $^{-1}$ glucose and 1.5 % Tween-20.

3.3.6- Gel exclusion chromatography of DNP-GNP conjugate and lateral flow assay

2 x 1 ml aliquots of 40 nm GNP coated with the minimum amount of DNP dextran required to prevent salt induced flocculation were prepared. 1 ml was applied to a gel exclusion column (1 x 60 cm length; 10 ml void volume) containing Sepharose 2B. The elution fraction containing the DNP-GNP conjugate was collected and the number of GNP per ml was determined by UV/vis spectroscopy. The un-purified aliquot was diluted to contain the same number of particles per ml as the purified conjugate and lateral flow devices striped with anti-DNP were inserted into both conjugates. After colour development, images of the lateral flow strips were acquired with an office document scanner and then imported into iGrafx Image 1.0 (Bournemouth, UK) and converted to greyscale. The depth of colour was

determined on a scale of 0 – 255 by activating the "view → information" option and pointing the mouse cursor at the area to be interrogated.

3.3.7-Preparation of DNP solution for reagent-limited lateral flow immunoassays

A stock solution of DNP was prepared by dissolving 25 mg of DNP in 0.5 ml of acetonitrile. A series of DNP solutions (from 2 to 2×10^6 ppb) were prepared by serially diluting stock with PBS buffer containing 1 mg ml $^{-1}$ BSA, 1 mg ml $^{-1}$ glucose and 0.5 % Tween-20 into 10 ml volumetric flasks.

3.3.8- Reagent-limited lateral flow assays

Lateral flow devices were prepared by BBInternational. For preparation of the lateral flow strips, a HiFlow plus nitrocellulose membrane (HF 135) and an absorbent pad were mounted on an adhesive coated backing sheet. The capture antibody, anti-DNP, was applied in a line using the reagent dispensing module and the assembled membrane was cut into 40 mm x 3 mm strips using the automatic cutter. The immunoassay solutions were prepared by mixing 100 μl of each DNP-GNP conjugate (0.2 OD) with 100 μl of each DNP solution. For reagent-limited immunoassays, the lateral flow devices were inserted into 150 μl of freshly prepared immunoassay solution and developed for 20 minutes. Images of all lateral flow strips were acquired and analysed as in section 3.3.6.

3.4- Results

3.4.1-Synthesis of ^{125}I functionalised dextran

To investigate the titration and conjugation of functionalised dextrans to GNPs a radiolabelled dextran was synthesised. When titrations of functionalised dextrans are carried out, the minimum amount of dextran required to prevent salt induced flocculation of the particles was determined. Different amounts of functionalised dextran are added to known numbers of GNPs followed by a concentrated NaCl solution. In the absence of any dextran the solution turns blue due to flocculation of the particles, but as the amount of dextran increases, an increasing fraction of particles remain red. Titration curves are then obtained by plotting the colour change against the amount of dextran added. The point at which enough dextran has been added to prevent flocculation is termed the equivalence point. At the equivalence point it is assumed that all of the functionalised dextran is conjugated to the particles and there is no free dextran remaining in the GNP solution. Even the presence of very low amounts of free functionalised dextran would have a detrimental effect on sensitivity when the GNP conjugate is used in a biological assay. In order to investigate in more detail whether all of the dextran added at the equivalence point was conjugated to the GNPs, and to enable sensitive detection of very low amounts of free functionalised dextran, a radiolabel dextran was synthesised. Aminodextran was functionalised with iodine (^{125}I) and a plurality of protected disulphide (PDP) groups using NHS ester chemistry. In the first stage of the synthesis, ^{125}I was introduced into the aminodextran using *N*-succinimidyl 3-(4- hydroxy, 5-[^{125}I]iodophenyl)-propionate (Bolton and Hunter Reagent). When mixed with aminodextran, the NHS ester of the reagent reacts with the primary amines in the dextran to form stable amide bonds. In the second stage of the synthesis, PDP

groups were introduced into the ^{125}I functionalised dextran using SPDP. As mentioned in chapter 2, SPDP is a heterobifunctional reagent that contains an NHS ester and a PDP functionality.[13] Following functionalisation of the dextran, unreacted Bolton and Hunter reagent and SPDP were removed by gel exclusion chromatography.

3.4.2-Titration of ^{125}I functionalised dextran against GNPs

[125]I is a radioisotope of iodine which is used in biological assays and in radiation therapy.[14] It has a half-life of 60 days and it emits gamma-rays with maximum energies of 35 keV, some of which are internally converted to x-rays. Gamma rays are high energy photons that have no charge or mass.[15] As ^{125}I is a gamma emitter, it is much easier and less problematic to detect than β particle emitting radioisotopes that require a mixture of scintillation cocktails for detection. In this work, a gamma spectrometer was used to determine the energy and the count rate of gamma rays emitted by radioactively labelled GNPs. The gamma spectrometer included a high purity germanium detector, a multi-channel analyzer, an amplifier and data readout device. Gamma rays interacted with the detector and the voltage pulse produced by the detector was shaped by a multi-channel analyzer. The multi-channel analyzer takes the small voltage signal produced by the detector, reshapes it into a Gaussian or trapezoidal shape, and then converted it into a digital signal. In this work, dextran was functionalised with ^{125}I and then titrated against known numbers of GNPs. In order to investigate whether all of the dextran added at the equivalence point was conjugated to the GNPs, the particles were centrifugally washed, re-suspended in fresh solution and then the radioactivity counts in both the GNP solution and the supernatant were measured. The results shown in Figure 4 demonstrate that there

was no radioactivity in the supernatant indicating that all of the added dextran at the equivalence point was attached to the particles. However, if GNPs were mixed with more than the equivalence amount of dextran, radioactivity was detected in the supernatant.
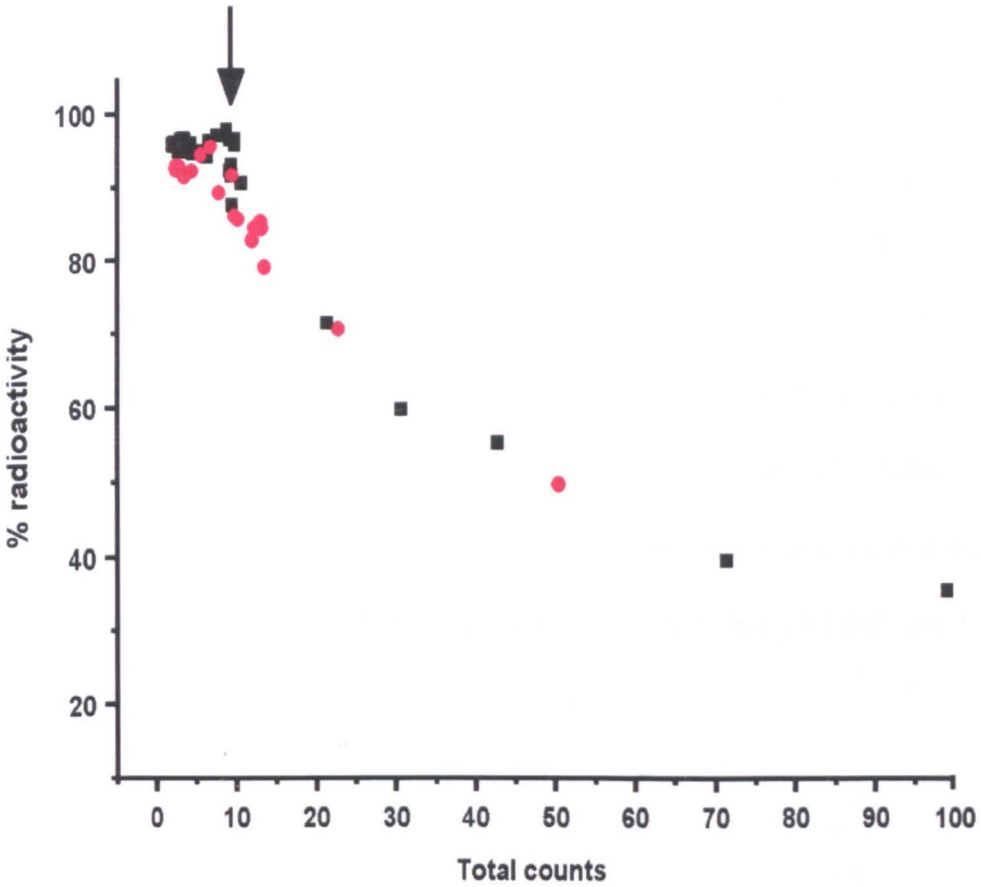
Figure 4: Graph showing the % of total counts added that is attached to the GNPs. At points below and up to the equivalence point (indicated by the arrow on the graph), ~100 % of radiolabelled dextran added is attached to the GNPs. When the amount of radiolabelled dextran added exceeds the equivalence amount, radiolabelled dextran is detected in the supernatant.

3.4.3-Synthesis of DNP functionalised dextrans

In order to investigate the effects of changing the number of probe molecules per GNP on the sensitivity of a non-traditional reagent-limited lateral flow device, a series of dextrans, each functionalised with different amounts of DNP hapten molecules were synthesised. Aminodextran was functionalised with DNP hapten molecules and a plurality of PDP groups using NHS ester chemistry. The reaction scheme can be seen in Figure 5. In step 1, the NHS ester of the DNP-NHS reacts with primary amines in the dextran to form stable amide bonds. In step 2, PDP groups were introduced into the aminodextran using SPDP. After functionalisation the conjugates were dialysed to remove un-reacted SPDP and DNP and the functionalised dextrans were characterised by UV/vis spectroscopy to determine the mean number of DNP molecules. The mean number of DNP hapten molecules per dextran can be varied by changing the stoichiometry of DNP-NHS reagent to aminodextran in the functionalisation reaction. Dextrans functionalised with a high mean number of DNP haptens will have a high number of DNP per GNP after conjugation.
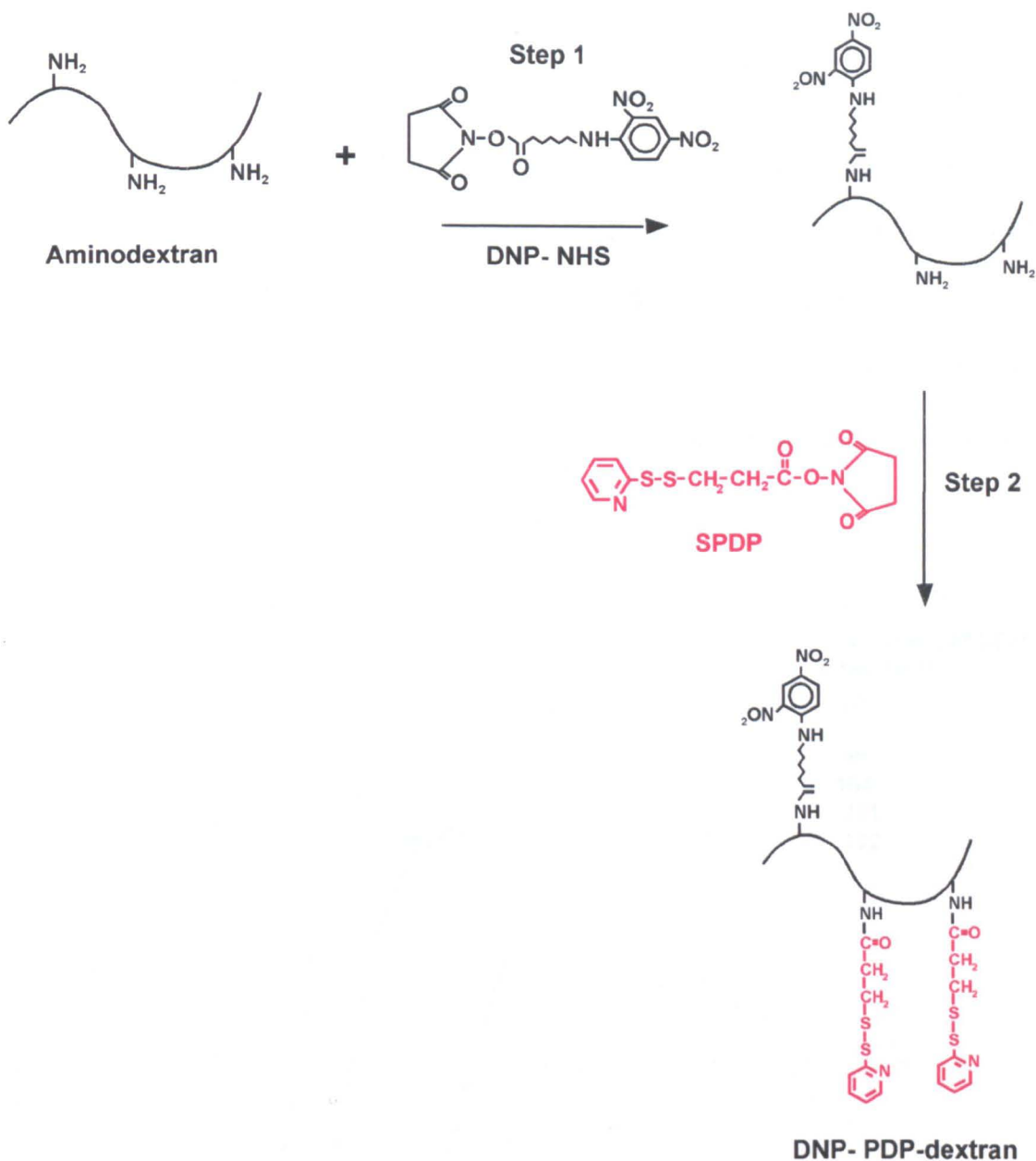
Figure 5: DNP functionalised dextran was synthesised by functionalising 70 kDa aminodextran with DNP and disulphide bonds using NHS ester chemistry. In step 1, the NHS ester of the DNP-NHS ester reacts with the amines within the aminodextran. In step 2, the remaining amines are then functionalised with SPDP to introduce disulphide moieties into the dextran.

3.4.4-Conjugation of DNP functionalised dextran to GNPs

Dextrans functionalised with different numbers of DNP molecules were used to prepare DNP-GNP conjugates. Variable amounts of each DNP functionalised

dextran were titrated against known numbers of GNPs to determine the minimum amount required to prevent salt-induced flocculation of the particles as reported in chapter 2. Titration curves were obtained by plotting the colour change against the amount of DNP added. Overlaid titration curves for all of the synthesised DNP functionalised dextrans can be seen in Figure 6. When the mean number of DNP molecules per dextran is increased, there is an increase in the mean number of DNP molecules attached to the GNPs after conjugation. A graph showing this relationship can be seen in Figure 7.
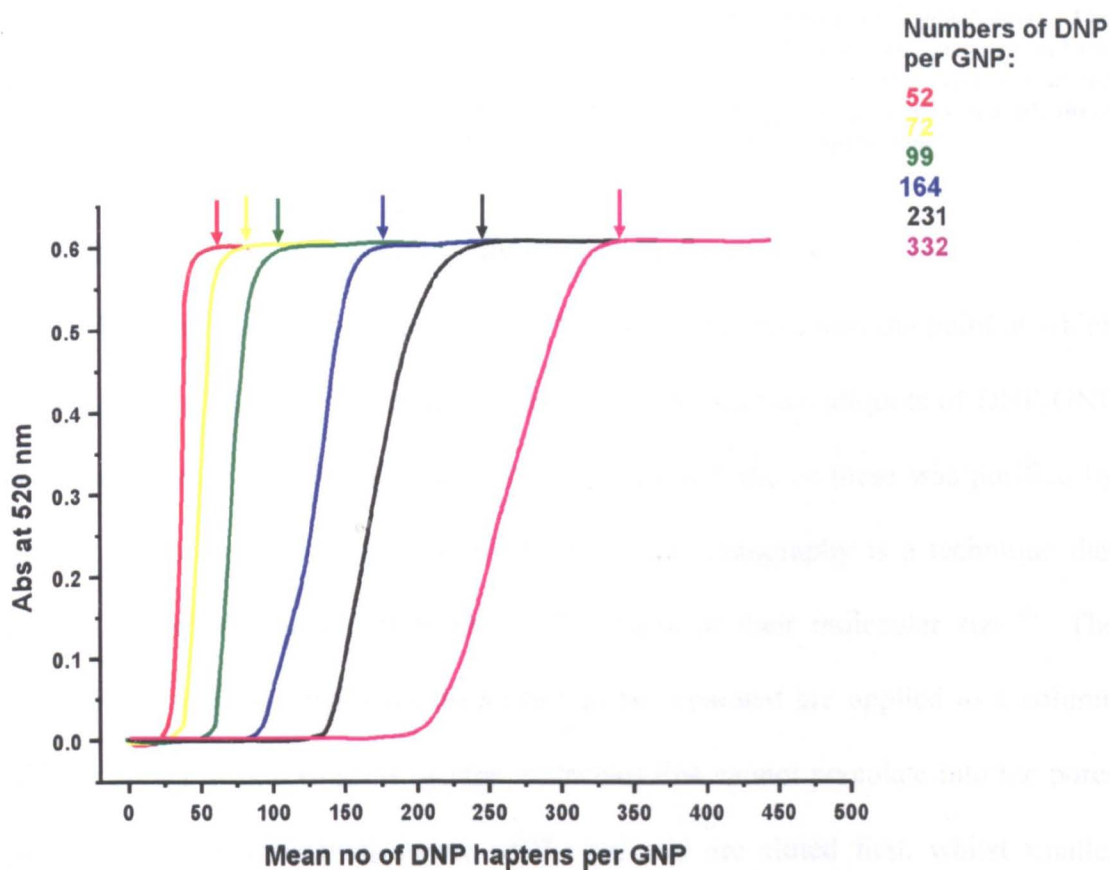
Figure 6: Overlaid titration curves for prepared DNP functionalised dextrans. Coloured arrows denote equivalence point for each dextran
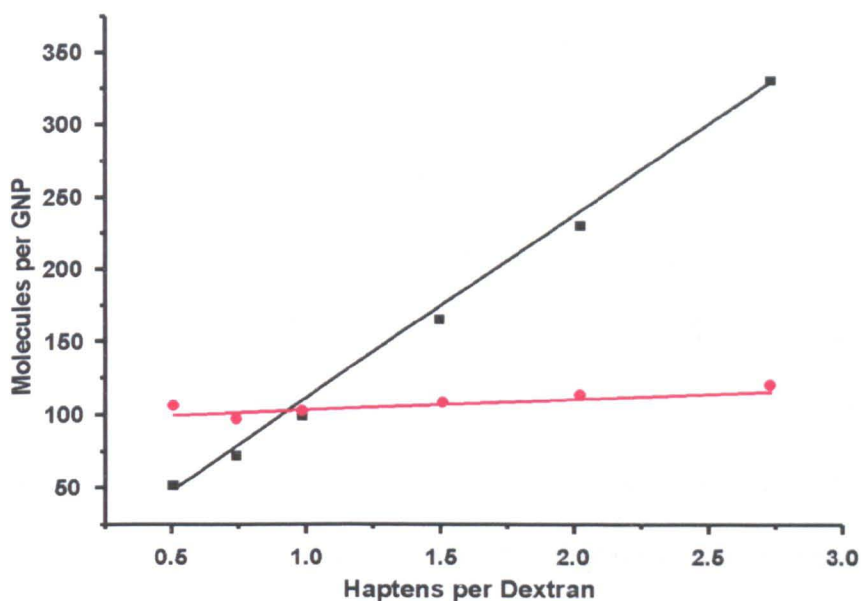
Figure 7: Graph showing the relationship between the mean number of DNP haptens per 70kDa dextran and the mean number of DNP molecules per GNP after conjugation (black line). The graph also shows the relationship between the mean number DNP haptens per dextran and the mean number of dextrans per GNP (red line). As the amount of dextran required to coat the GNPs remains constant, as the mean number of DNP molecules per dextran is increased, there is an increase in the mean number of DNP molecules per GNP after conjugation.

3.4.5- Gel exclusion chromatography and lateral flow assay

To confirm that the equivalence point on the titration curves was the point at which all of the added dextran was conjugated to the particles, two aliquots of DNP-GNP conjugate coated with this amount were prepared and one of these was purified by gel exclusion chromatography. Gel exclusion chromatography is a technique that enables the separation of molecules on the basis of their molecular size.[16] The general principle is simple; the molecules to be separated are applied to a column filled with gel or porous glass. Large molecules that cannot percolate into the pores pass through the interstitial spaces of the gel and are eluted first, whilst smaller molecules pass through the pores and are eluted later. A gel exclusion chromatograph detailing the separation of 40 nm GNPs from DNP functionalised dextran is shown in Figure 8. The elution fraction containing the DNP-GNP conjugate was collected and the un-purified aliquot of DNP-GNP conjugate was

diluted to contain the same number of GNP per ml. Lateral flow devices striped with anti-DNP were inserted into both purified and un-purified DNP-GNP conjugates and the colour developed on the test lines was determined. If there was free DNP functionalised dextran in solution at the equivalence point, there would be a reduction in the colour developed at the test line when the un-purified DNP-GNP was used in the lateral flow assay. This is because free DNP functionalised dextran would compete with the DNP conjugated to the particles for the antibody binding sites at the test line. Results showed that there was no significant difference in the colour of the test line when un-purified DNP-GNP conjugates were used (Figure 9). This further supports the results from the radiolabel experiments (section 3.4.2) and suggests that when the equivalence point of functionalised dextran is added, all of the dextran is conjugated to the particles and shows that the conjugate can be used in lateral flow assays without further purification.
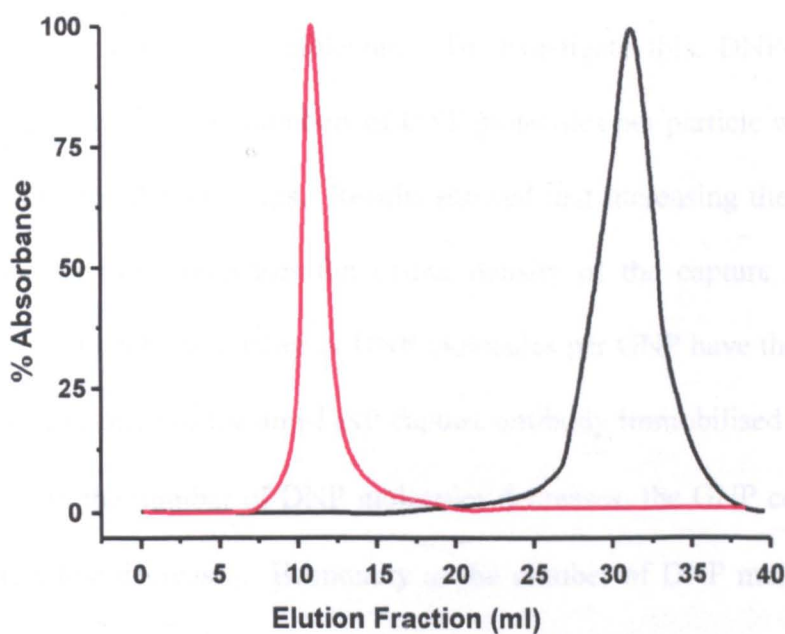
Figure 8: **Gel exclusion chromatograph showing the elution profiles of 40 nm DNP-GNPs (red line) and 70 kDa DNP functionalised dextran (black line). The chromatograph demonstrates that free functionalised dextran can be removed from DNP-GNPs by gel exclusion chromatography on Sepharose 2B.**

118
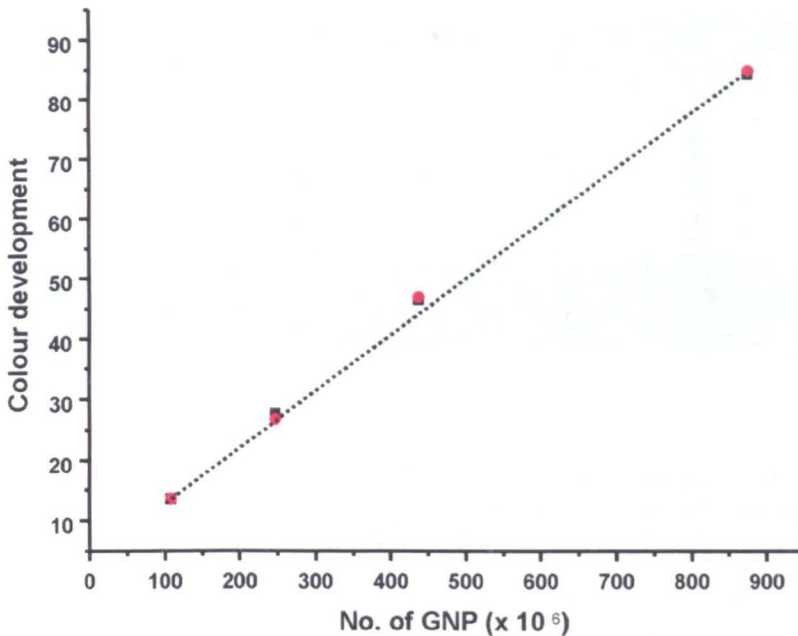
Figure 9: Graph showing colour development at the test lines on lateral flow strips with DNP-GNP conjugates that were un-purified (black) and purified by gel exclusion chromatography (red).

3.4.6- The effect of changing the mean number of DNP molecules per GNP analysed on lateral flow strips

GNPs with high mean numbers of probe molecules will have the greatest affinity for the complementary binding molecule. To investigate this, DNP-GNP conjugates containing different mean numbers of DNP molecules per particle were prepared and analysed on lateral flow strips. Results showed that increasing the number of DNP molecules per GNP increases the colour density of the capture line (Figure 10). Conjugates with a high number of DNP molecules per GNP have the greatest affinity for the binding sites of the anti-DNP capture antibody immobilised at the test line of the strip. As the number of DNP molecules decreases, the GNP conjugates affinity for the test line decreases. Eventually as the number of DNP molecules decreases, GNPs begin to pass through the test line without binding.
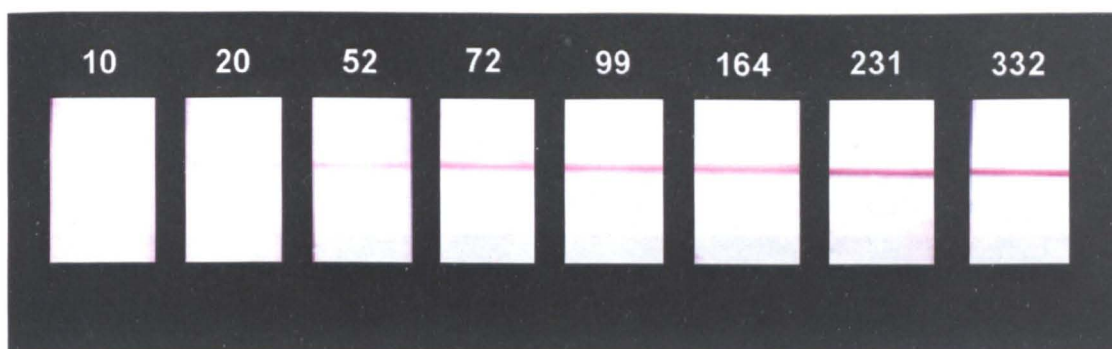
Figure 10: Images of lateral flow strips showing the effect of changing the number of DNP molecules per 40 nm particle. Numbers at top of images denote the mean number of DNP molecules per 40 nm GNP. As the number of molecules per particle is increased, the colour density of the test-line increases.

3.4.7- Non-traditional reagent-limited lateral flow immunoassays for DNP

In order to investigate the effects of changing the mean number of probe molecules per particle, GNPs coated with different mean numbers of DNP molecules were prepared and used in reagent-limited lateral flow immunoassays. In these immunoassays, free DNP in the sample competes with DNP molecules conjugated to the particles for the antibody binding sites at the test line. If the sample does not contain free DNP, all of the GNP labelled DNP binds to the anti-DNP capture antibody. If the sample contains free DNP, this competes with the labelled DNP and the colour of the test line decreases. As the amount of competing DNP is increased, the colour of the test line decreases so the colour of the test line is inversely proportional to the concentration of competing DNP in the sample. Changing the mean number of DNP probe molecules per GNP does affect the sensitivity of reagent-limited lateral flow immunoassays. Results showed that as the mean number of DNP molecules per particle was decreased, there was an increase in the sensitivity of the immunoassay. Images of the lateral flow strips from reagent-limited lateral flow immunoassays for DNP are presented in Figure 11. A graph showing the colour development at the test lines and a table detailing the sensitivities achieved in the

120

immunoassays with each DNP-GNP conjugate are presented in Figure 12 and Table 1 respectively.
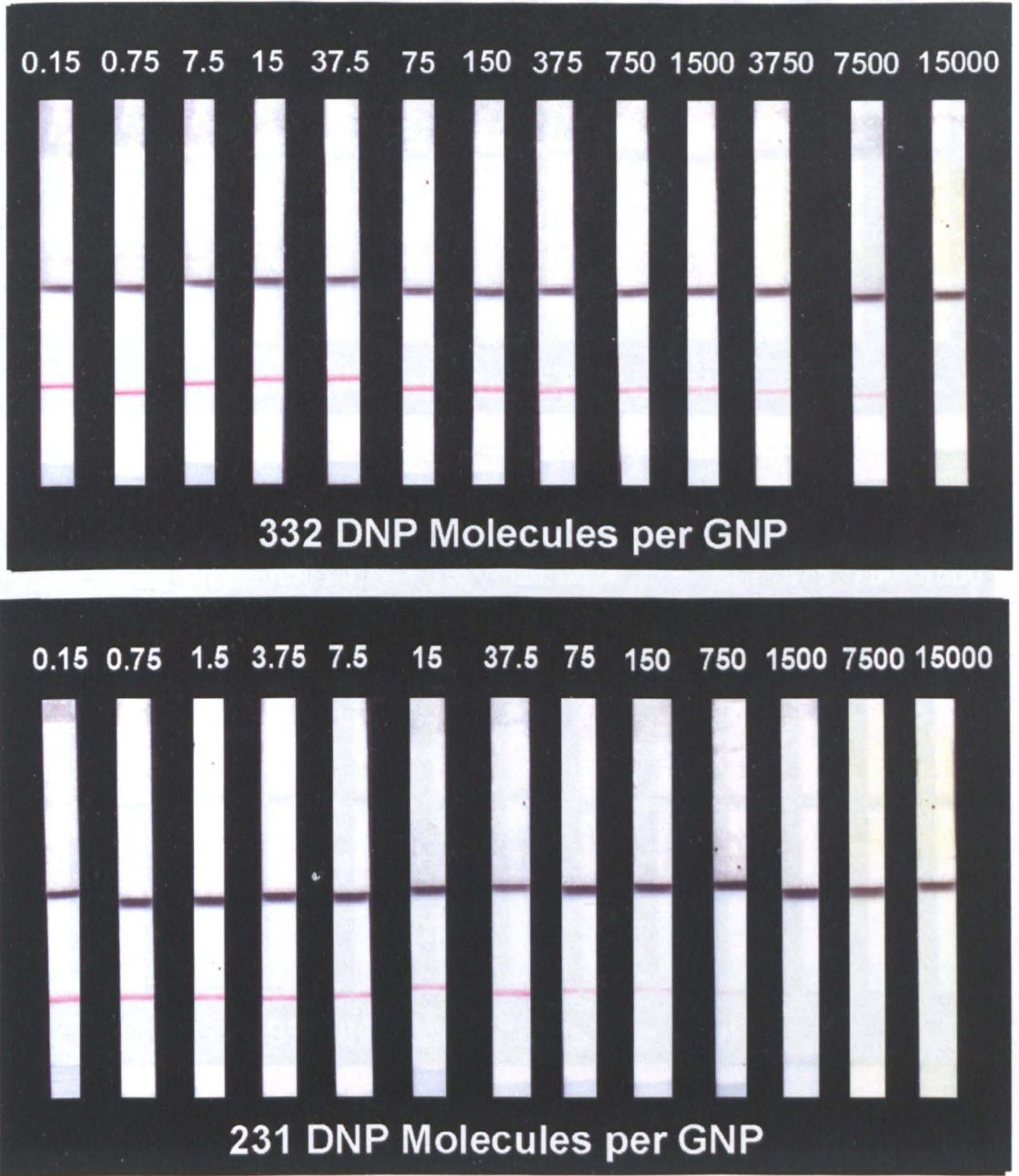
Figure 11: Images of lateral flow strips from the reagent-limited immunoassays for DNP. The numbers at the top of the diagrams denote the amount of competing DNP in nanograms (ng) and the numbers at the bottom denote the mean number of DNP molecules per GNP. As the amount of competing DNP in the sample is increased, there is a decrease in the colour density of the test line.

164 DNP Molecules per GNP

99 DNP Molecules per GNP

Figure 11 cont: Images of lateral flow strips from the reagent-limited immunoassays for DNP. The numbers at the top of the diagrams denote the amount of competing DNP and the numbers at the bottom denote the mean number of DNP molecules per GNP. As the amount of competing DNP in the sample is increased, there is a decrease in the colour density of the test line.

| 0.15 | 0.375 | 0.75 | 1.5 | 3.75 | 7.5 | 15 | 37.5 | 75 | 150 | 375 | 750 | 1500 |

72 DNP Molecules per GNP

| 0.15 | 0.375 | 0.75 | 1.5 | 3.75 | 7.5 | 15 | 37.5 | 75 | 150 | 375 | 750 | 1500 |

52 DNP Molecules per GNP
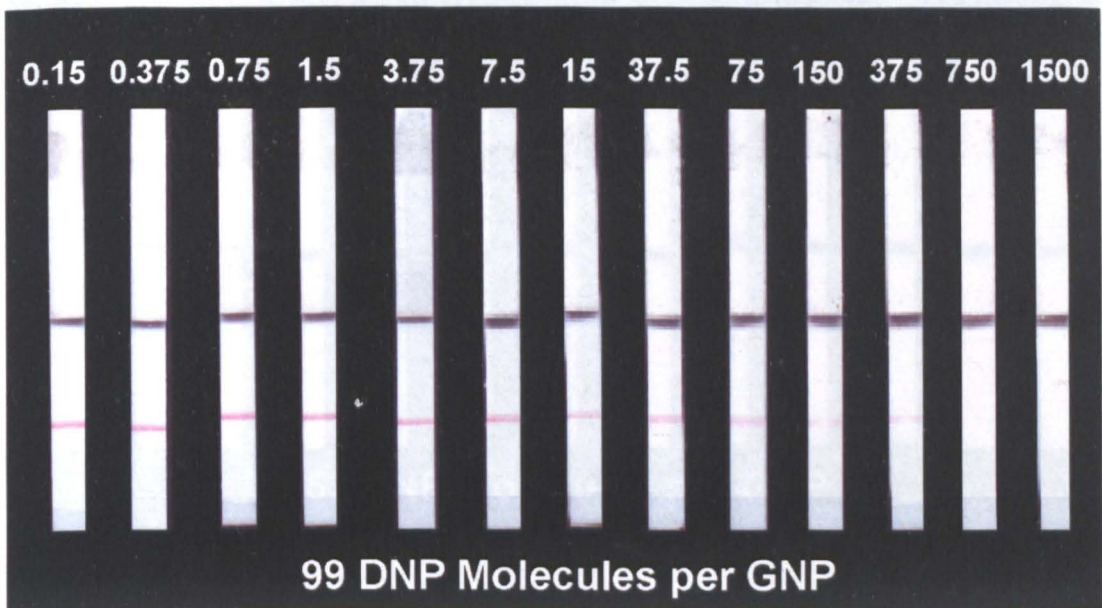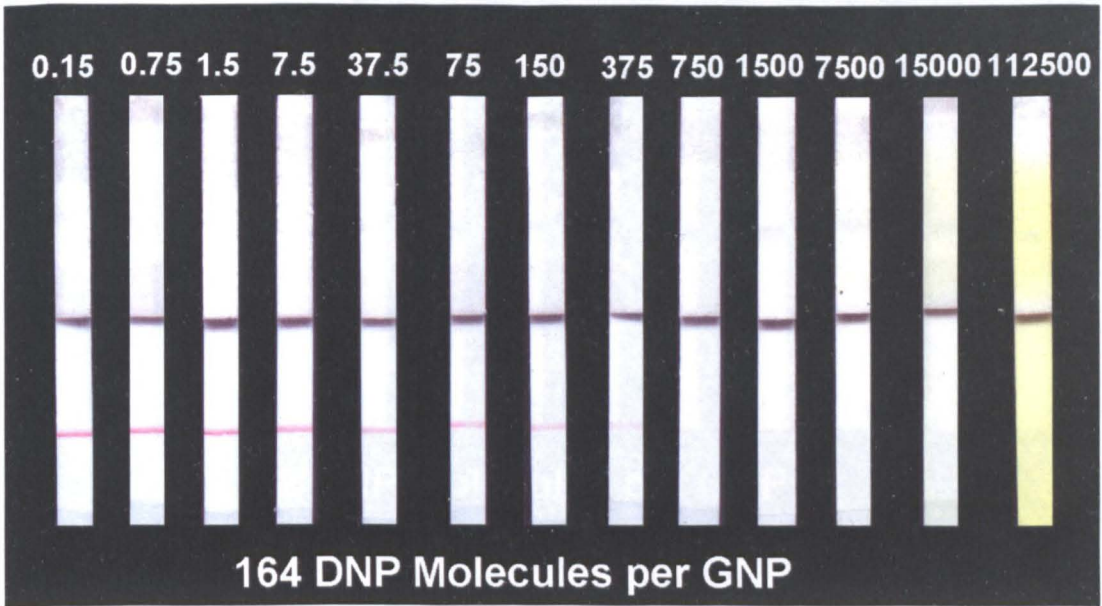
Figure 11 cont: Images of lateral flow strips from the reagent-limited immunoassays for DNP. The numbers at the top of the diagrams denote the amount of competing DNP and the numbers at the bottom denote the mean number of DNP molecules per GNP. As the amount of competing DNP in the sample is increased, there is a decrease in the colour density of the test line.
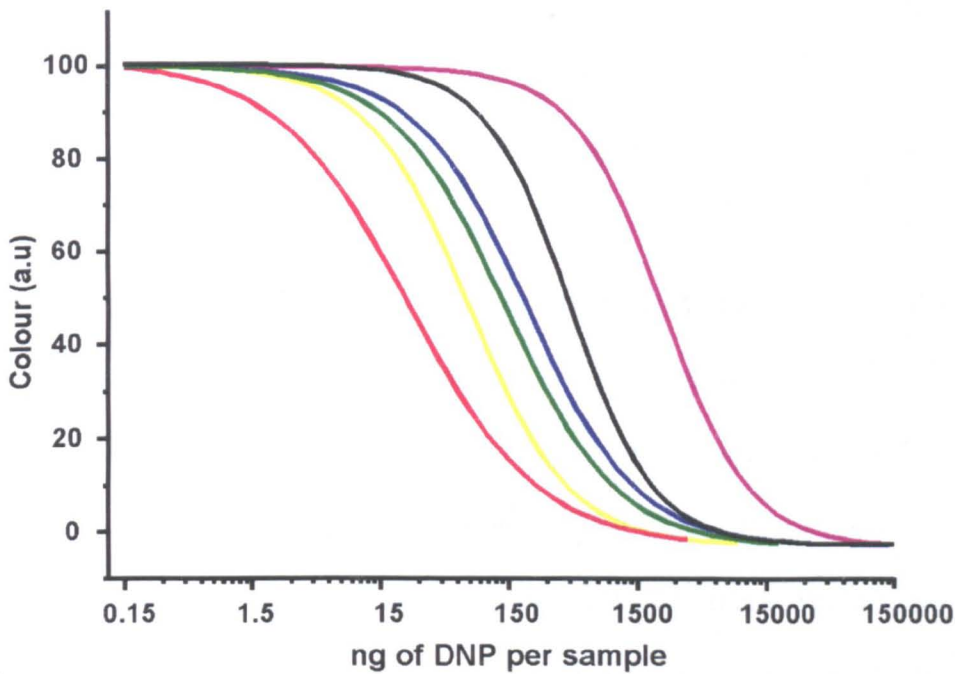
Figure 12: Overlaid graphs of colour development at the test line versus the amount of competing DNP in reagent-limited immunoassays with different DNP-GNP conjugates. Red = mean of 52 DNP haptens per GNP. Yellow = mean of 72 DNP haptens per GNP. Green = mean of 99 DNP haptens per GNP. Blue = mean of 164 DNP haptens per GNP. Black = mean of 231 DNP haptens per GNP. Purple = mean of 332 DNP haptens per GNP. The graphs show that as the mean number of DNP molecules per GNP is decreased, there is an increase in the sensitivity of the immunoassay.

Haptens / Dextran	Haptens / GNPs	Dextran / GNPs	Sensitivity (ng)
0.5	52	106	24
0.74	72	97	60
1.0	99	102	120
1.50	164	109	188
2.0	231	114	375
2.7	332	120	2250

Table 2: Table detailing the relationship between functionalised dextrans, mean number of DNP haptens and dextran molecules per GNP at the equivalence points and the sensitivities of reagent-limited immunoassays performed with these particles. The sensitivity is defined herein as the amount of competing DNP required to produce a 50% decrease in colour development at the test line.

3.4.8-Comparision of traditional and non-traditional lateral flow devices

As mentioned in the introduction to this chapter and depicted in Figure 2, the label in reagent-limited lateral flow devices is usually GNP conjugated to antibodies, and the capture reagent is usually the analogue of the analyte immobilised on the nitrocellulose strip. In this chapter, lateral flow device has been described that is the reverse of this design. When reagent-limited lateral flow immunoassays were performed with this device, results showed that the sensitivity of the device could be tuned by changing the number of molecules per GNP. Results also showed that as the number of molecules per GNP was decreased, there was an increase in the sensitivity of the device. In order to investigate whether the non-traditional device was more sensitive than the traditional format, reagent-limited immunoassays were performed with both designs under the same conditions. The results of these comparisons are shown in Figure 13. These results show that the prototype device was over 50 % more sensitive than the traditional device.
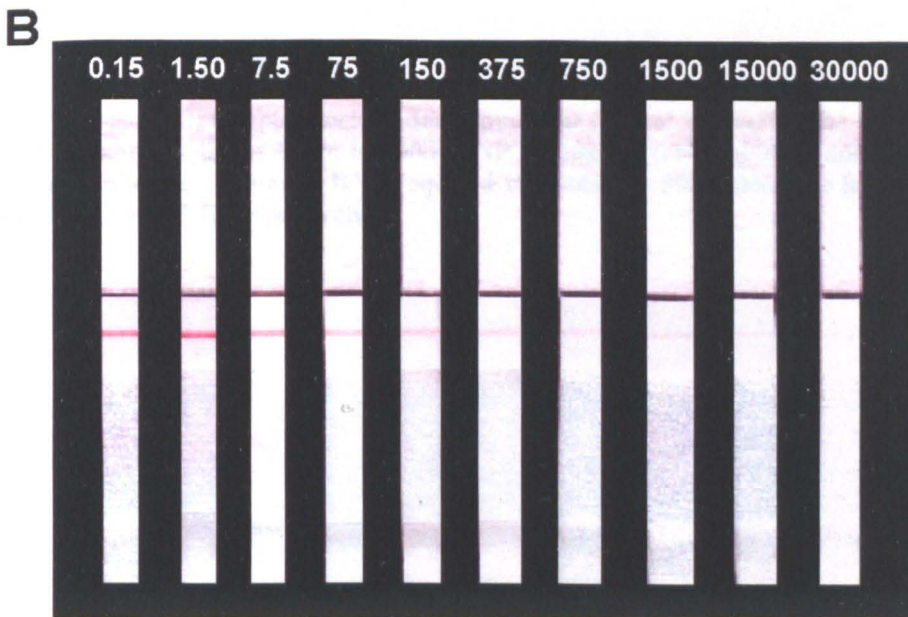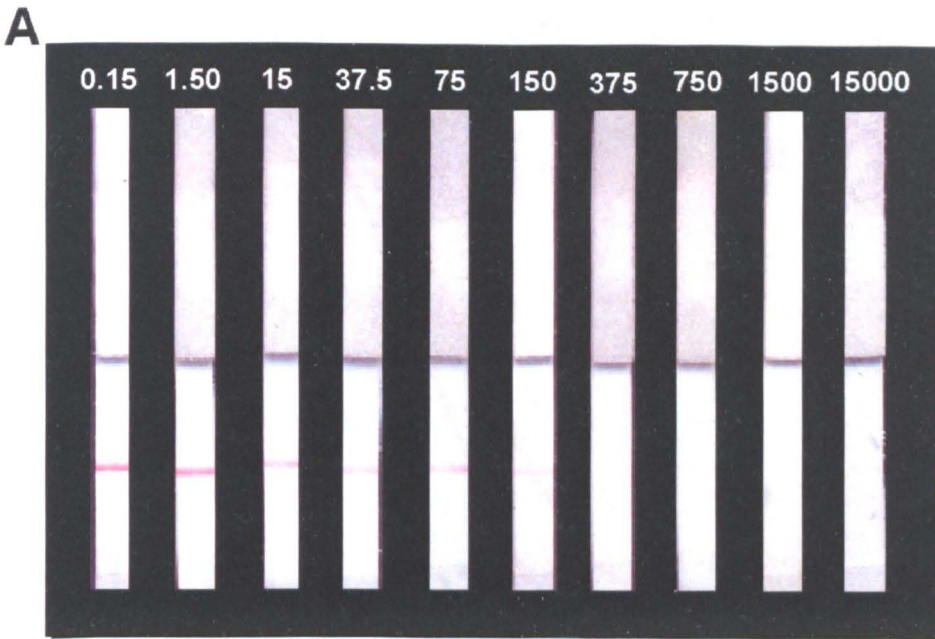
Figure 13: Reagent-limited lateral flow immunoassays for DNP based on: A) DNP-GNP conjugates, and B) antibody labelled GNPs; numbers denote the amount of competing DNP per sample in ng's.
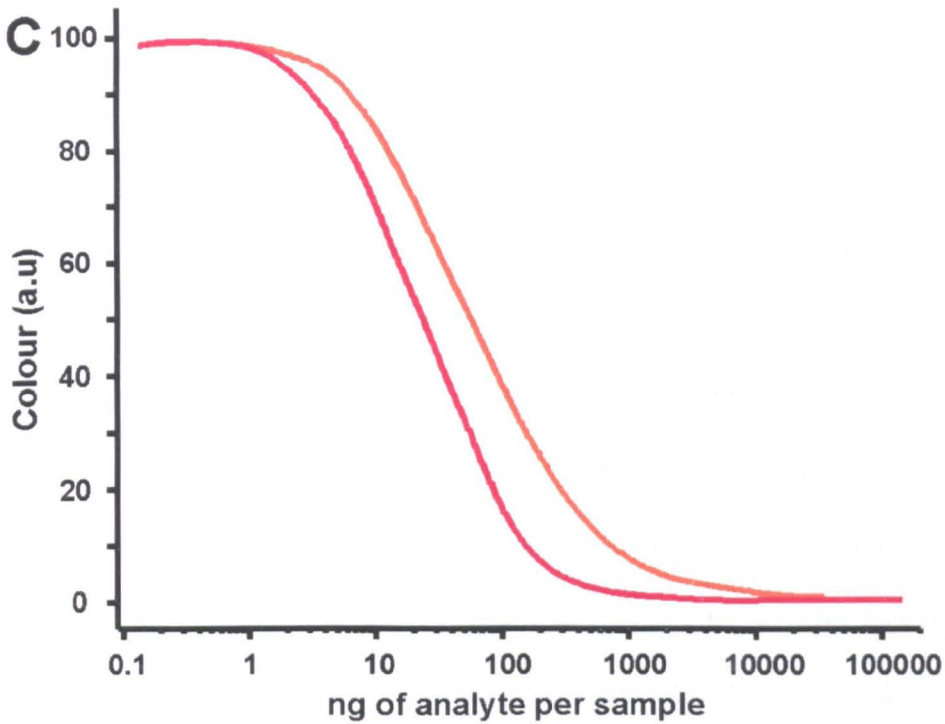
Figure 13 cont: C) Graph of colour development at the test line versus the amount of competing DNP for immunoassays based on DNP-GNP conjugates (red line) and antibody labelled GNPs (orange line); the amount of DNP required to produce a 50 % decrease in colour development was 24 ng and 55 ng respectively.

3.5-Discussion

3.5.1- Reagent-limited lateral flow devices- traditional and non- traditional formats

Since their development in the 1980's, lateral flow devices have become popular diagnostic tools because they allow specific, rapid and inexpensive detection of analytes in a user-friendly format. Reagent-limited lateral flow devices are porous membranes, commonly nitrocellulose, striped with a capture reagent, which is usually an analogue of the analyte (hapten). Fitted to the membrane is a glass fibre conjugate pad that contains dried detector reagent. This detector reagent is usually GNPs conjugated to antibodies specific for the analyte to be detected. In this chapter, a different type of reagent-limited lateral flow device was described. This device was the reverse of the traditional design and comprised of a nitrocellulose membrane striped with antibodies as the capture reagent, and the detector reagent was GNP conjugated to haptens. In traditional devices, the GNP labelled antibody detector reagent is prepared by a method that was first described by Faulk and Taylor in 1971.[17] In this method, excess antibodies are mixed with GNPs and become attached by a poorly understood process that is said to include a combination of: 1) initial charge attraction between the negative GNP and the positively charged amino acids within the protein (e.g., lysine); 2) hydrophobic adsorption of the protein to the particle surface, through certain amino acid residues including tryptophan; 3) dative binding between sulphur residues on the protein (from cysteine residues) and the GNP.[18] The antibody is attached to the GNP by the Fc region, leaving the Fab region protruding through the ionic layer surrounding the GNP. After attachment to the GNPs, un-bound antibody is then removed from the conjugate by several cycles of centrifugal precipitation and washing. This is an important step because if the

conjugate is used in a biological assay any excess unlabelled antibody would compete with the labelled antibody for the analyte which could result in false negative results. Although antibody-GNP conjugates prepared by this method are generally quite stable, there have been reports that antibodies can dissociate from the GNPs.[19,20] Kramarcy and Sealock tested commercially prepared antibody labelled GNPs and found that they all contained un-bound antibody, the amount of which increased after storage. They suggested that antibody dissociation could occur if the GNPs were labelled with an antibody that had a low affinity for the GNPs or could occur as a consequence of overloading the surface of the GNP. Attempting to coat the GNPs with a large excess of antibody or other protein molecule can reduce the number of contact points between each antibody / protein and the GNP surface leading to weakly bound antibody / protein that can readily dissociate from the GNPs.[21] The detector reagent used in the reagent-limited lateral flow device reported in this chapter is prepared in a different way to the traditional method. In this method, DNP molecules and protected disulphide (PDP) groups are first introduced into a high molecular weight aminodextran polymer using NHS ester chemistry. After purification and characterization, the functionalised dextran is then mixed with the GNPs. Upon contact with the GNPs, the PDP groups within the dextran rupture and the DNP functionalised dextran is anchored to the GNPs *via* a plurality of dative bonds. An advantage of preparing conjugates by this novel method is that the conjugate is very stable for long periods of time and there is no dissociation of the attached molecules from the GNPs. Previous work has shown that GNP conjugates prepared by this method can even withstand high temperatures and high concentrations of thiol (-SH) compounds such as dithiothreitol.[8,9] This enhanced stability is attributed to the many dative bonds that anchor the

functionalised dextran to the GNPs. For example, the aminodextran used in this work contains an average of 20 amine molecules per molecule of dextran. After functionalisation with DNP molecules, the remaining amines are functionalised with PDP groups. Results show (Figure 7, section 3.4.4. and Table 1, section 3.4.7) that there is a maximum of 3 DNP molecules per dextran (in the highest functionalised dextran), which suggests that there are a minimum of 17.3 PDP groups per molecule of dextran.

The capture reagent immobilised on the nitrocellulose membrane in traditional reagent-limited lateral flow devices is usually an analogue of the analyte (hapten). As these molecules are small, their size restricts them from direct attachment to the membrane and so in most cases they are first conjugated to a large protein that facilitates their attachment to the membrane. Proteins commonly used for this purpose include human serum albumin (HSA), ovalbumin (OVA) and bovine serum albumin (BSA). These proteins contain many functional groups that are suitable for hapten conjugation. For example, BSA contains 1 thiol group (-SH), a total of 59 lysine amine groups, 19 tyrosine phenolate residues and 17 histidine imidazolides.[18] Following conjugation with the hapten, the protein is then immobilised on the nitrocellulose membrane. Nitrocellulose was first used as a protein binding membrane in the 1980's and despite the considerable amount of research that has been conducted with this material the exact mechanism of protein binding is still unknown. It is thought that a number of forces are at work, specifically, hydrophobic interactions, hydrogen bonding, and electrostatic interactions, but a clear understanding of the exact effect of each force has remained elusive. Two models

have been proposed. The first model suggests that proteins are initially attracted to the membrane surface by electrostatic interaction, and long-term attachment is accomplished by a combination of hydrogen bonding and hydrophobic interactions. The second model suggests that the initial attachment of the protein is caused by hydrophobic interactions, and long-term binding is accomplished by electrostatic forces.[22] Due to the mechanisms involved in attachment to the membrane it is essential that the overall properties of the protein are retained after it has been functionalised with haptens. This can be difficult as even minor chemical modification can cause major structural changes within the protein.[23] For example, modification of the functional groups can change the net charge of the protein which can result in weak interactions between the functionalised protein and the membrane. This causes significant problems because the weakly bound protein can dissociate from the membrane and wash away upon application of the sample. It has also been reported that functionalising proteins such as BSA with hydrophobic haptens or over-functionalising with too many haptens can mask the hydrophilic surface of the protein resulting in precipitation. Although an increase in the hydrophobicity of the functionalised protein would facilitate strong attachment to the membrane, the presence of precipitated protein can lead to uneven test lines and blocked pores within the membrane leading to irreproducible results. In the non-traditional device described in this chapter, the capture reagent was antibodies immobilised on the nitrocellulose membrane. The use of antibodies as a capture reagent has two distinct advantages over hapten functionalised protein capture reagents. Firstly, due to the size of the antibodies they can be attached to the membrane directly without modification. This is simpler, faster and reproducible results can be obtained. Secondly, research has shown that antibodies bind to nitrocellulose more efficiently

than other proteins such as BSA. Studies carried out by Jones with a variety of nitrocellulose membranes from different manufacturers showed that in all membranes tested IgG antibody bound to the membrane with more strength than BSA.[22]

3.5.2-Improving the sensitivity of lateral flow immunoassays

Although lateral flow devices have many advantages, they are often not as sensitive as conventional immunoassays and improving the sensitivity without losing any of the attributes of the device is a major hurdle. Many researchers have increased the sensitivity of these devices by departing from the use of GNPs and choosing alternative labels that exhibit luminescent and phosphorescent properties. For example, Li and colleagues used colloidal semiconductor nanocrystals (quantum dots; QDs) as a label in their lateral flow device.[24] In recent years, QDs have attracted considerable attention as novel labels in biological assays due to their high luminescence quantum yields and unique spectral, chemical and physical properties. Li and colleagues conjugated antibodies to QD labels and immobilised a secondary antibody onto the nitrocellulose as a capture reagent. Bound QDs were then visualised using an ultraviolet lamp. Li and colleagues claim that the antibody labelled QDs did bind to the corresponding capture antibody, but they also observed a very high level of non-specific adsorption. They claimed that the majority of the non-specifically adsorbed QDs could be removed by multiple washing steps and that results could then be obtained by comparing the luminescence of the sample strip with the luminescence of the control. In another approach, Malamud and colleagues used up-converting phosphor (UP) particles as a label in their lateral flow device.[25] When they compared the results with those obtained using a GNP label they

observed a 100-fold increase in sensitivity when the UP label was used. Although these researchers increased the sensitivity of these devices by using these novel labels, a major disadvantage is that the results cannot be seen by eye. This means that the devices had to be interfaced with complicated and often expensive equipment in order to visualise the signal. This significantly increases the cost and complexity of the device and often limits its use to trained personnel. Detection using fluorescent labels can also be complicated by the sample itself as some common components of biological samples such as proteins or co-factors (NADH) exhibit fluorescence. These components can quench the fluorescent label and can also contribute significantly to the background fluorescence making detection of the analyte difficult.[26]

Many other research groups have sought to improve the sensitivity of lateral flow devices by incorporating enzymatic amplification steps. Zhang and colleagues developed a reagent-limited lateral flow device for the simultaneous detection of the insecticides carbaryl and endosulphan.[27] In this work, they used two different detection reagent labelling strategies and compared the sensitivity achieved with each. In the first device, carbaryl and endosulphan were conjugated to a protein anchor and immobilised onto a nitrocellulose membrane and GNP labelled antibodies were used as the detector reagent. In the second device, antibodies were immobilised onto the nitrocellulose membrane and the detector reagents were carbaryl and endosulphan conjugated to the enzyme horseradish peroxidase. In this case, sample was mixed with the enzyme conjugates and then applied to the membrane. After washing the membrane thoroughly, the substrate solution was then applied to the membrane to visualise the binding reaction. Zhang and colleagues

observed that the sensitivity increased 10-fold when the enzymatic label was used. Cho and colleagues observed similar increases in sensitivity when they incorporated an enzymatic step into their lateral flow device, but they also noted that the reaction time of the enzyme with the sample and the substrate had to be carefully controlled because high background colouration on the membrane could occur that made detection difficult.[28] Although the use of enzymatic labels can increase the sensitivity of lateral flow devices, this amplification strategy can also introduce problems and additional costs. Enzymatic labels are expensive and are also prone to deactivation, which in turn can lead to problems with reproducibility. In addition, devices incorporating enzymatic steps usually involve a complicated mix of substrate or developing solutions that must be mixed and incubated for a set time which increases the probability of operator error. Due to these problems, the use of enzymatic labelling strategies is usually limited to trained personnel. The use of novel fluorescent and enzymatic labels can increase the complexity of the lateral flow device, increase the possibility of operator error and in some cases necessitate the use of expensive detection equipment which in turn relinquishes the key advantages of lateral flow detection.

Whilst a great deal of work is still devoted to producing enzymatic and fluorescent labels, very few studies have been conducted on the effects of improving the sensitivity of existing GNP labels. One possibility is to vary the number of probe molecules attached to individual GNP labels. GNP labels that have a high number of probe molecules per particle will have a high affinity for the target molecule. This is because increasing the numbers of molecules increases the probability of a binding event with the target molecule. This is best explained by imagining two tennis balls,

one that is coated with many Velcro hooks and one that is coated with just one hook. If both tennis balls were rolled across a surface, the one with many hooks is more likely to stick to the surface than the ball with only one hook. The ball with one hook would have to be in the correct orientation with the surface in order for it to stick. Few research groups have investigated the effect of changing the number of probe molecules per particle but those that have did not use lateral flow devices in their investigations. Okano and colleagues investigated the effects of changing the number of antibodies per particle on the sensitivity of a microplate immunoassay.[29] In this investigation, Okano found that when the number of antibodies attached to each particle was increased, more particles bound to the surface of the microplate, but there was a decrease in the sensitivity of the assay. They attributed this decrease in sensitivity to an increase in non-specific adsorption of labelled antibodies to the microplate surface and found that the amount of adsorption was directly proportional to the amount of antibody attached to the particles. Okano and colleagues also investigated the effects of changing the concentration of the capture antibody immobilised on the microplate surface. They found that as the concentration of capture antibody was decreased, there was an increase in the sensitivity of the assay. They suggested that a lower density of capture antibodies decreased the amount of non-specific binding and thus increased the sensitivity. Okano and colleagues concluded that they were unable to increase the sensitivity of their immunoassay by increasing the numbers of antibodies per particle and that this could only be achieved if the amount of non-specific adsorption could be controlled. Spinke and colleagues also investigated the effects of changing the number of antibodies on the sensitivity of an immunoassay.[30] They found that as the number of antibodies per particle was increased, the sensitivity of the assay increased. However, they also discovered that

if the number of antibodies on the particles was too high, there was a significant decrease in assay sensitivity. They attributed this result to steric hindrance at high antibody loadings and lead to the conclusion that there was an optimum number of binding sites required to accomplish the greatest sensitivity. Hall and colleagues reported similar results but suggested that the number of antibodies per particle, the amount of capture antibody and the spatial orientation of both of these antibodies should be optimised for the best assay response.[31] Soukka and colleagues obtained different results. They found that increasing the number of antibodies increased the sensitivity of the assay.[32] However unlike the other researchers they did not observe a decrease in activity at high antibody loadings. They also suggested that if they increased the number further, even higher sensitivities could be achieved. It is not possible to derive any clear conclusions about the effects of changing the number of probe molecules per particle from the work of the authors mentioned above. This is because these studies were all conducted with relatively large latex particles, all of the results were obtained from reagent-excess immunoassays and most of these research groups obtained conflicting results.

The method for conjugating probe molecules to GNPs reported in this chapter is based on high molecular weight dextran polymers and it allows virtually any probe molecule to be attached to GNPs. The main advantage of this method is that it also allows the mean number of probe molecules per particle to be varied by simply changing the number of probe molecules attached to the dextran polymer. The concept is simple, and is shown in Figure 14; as there are more probe molecules to polymer A than to polymer B, there are more probe molecules attached to particle X than to particle Z after conjugation. The mean number of probe molecules per

polymer and GNP can also be determined without resorting to complicated and indirect methods to find out what this is. This is because after functionalisation, the dextran polymer is characterized to determine the mean number of probe molecules per polymer, then the precise amount of this functionalised polymer that is required to coat all of the GNPs is determined by titration against a known number of GNPs.
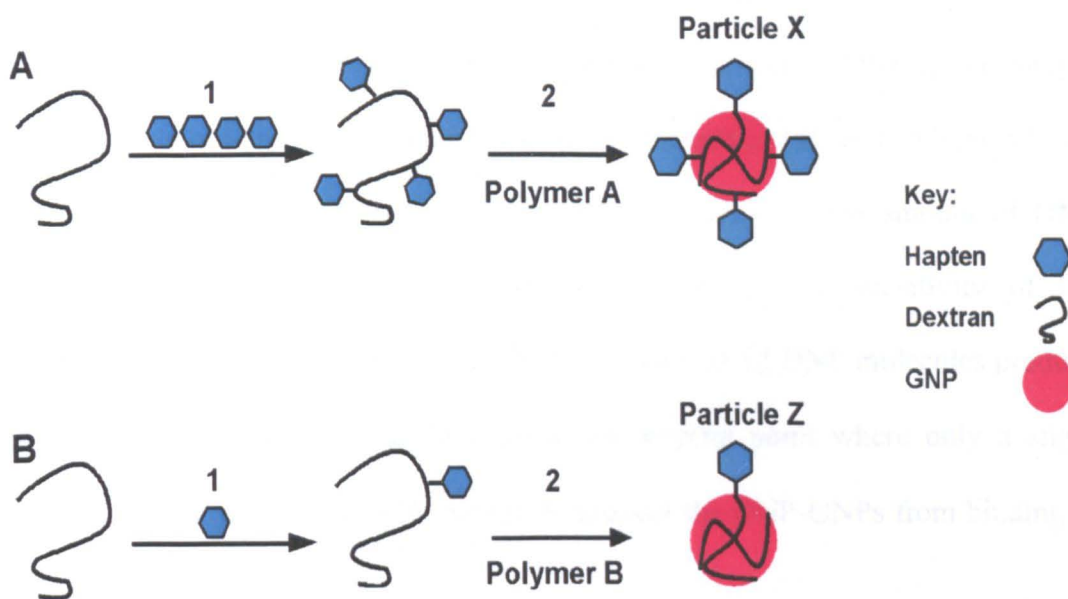
Figure 14: In step 1 the same amount of dextran is functionalised with different amounts of hapten, and in step 2 more haptens are attached to particle X than to particle Y because polymer A is functionalised with more haptens than polymer B.

This method was used to prepare a series of DNP-GNP conjugates, each containing a different mean number of DNP molecules per particle, and reagent-limited lateral flow immunoassays for DNP were carried out (section 3.4.7, Figure 11). In these immunoassays, DNP conjugated to the GNPs competes with DNP in the sample for antibodies immobilised on the test line of the membrane. As the amount of DNP in the sample increases, there is a decrease in colour development at the test line. Results in section 3.4.7, Figure 12, show that as the mean number of DNP molecules

per particle decreased, there was an increase in the sensitivity of the immunoassay. The sensitivity reached maximum when there was a mean of 52 DNP molecules per particle. In this type of reagent-limited immunoassay, when the lateral flow device is inserted into the sample, DNP-GNPs and DNP in the sample, migrate towards the test line at the same rate. They do not interact with each other until they reach the test line where they compete for antibody binding sites. Particles with high mean numbers of DNP per particle have a very high probability of binding to the antibodies and therefore very high concentrations of competing DNP in the sample are required to out-compete them and produce a decrease in colour development. As the mean number of DNP molecules per particle decreases, the amount of DNP required to out-compete them also decreases, and so the sensitivity of the immunoassay increases. GNPs conjugated to a mean of 52 DNP molecules produce the highest sensitivity because they are at the tipping point where only a slight increase of DNP in the sample is enough to prevent the DNP-GNPs from binding to the test line.

In this work, the developed device was also compared with a traditional device under the same conditions. Results in section 3.4.8, Figure 13 show that the non-traditional device was over 50 % more sensitive than the traditional format that is based on antibodies conjugated to GNPs. This is a surprising result because the sensitivity of traditional devices is promoted by an assay protocol in which the antibodies are allowed to react with the analyte first before being briefly exposed a high concentration of the analogue of the analyte at the test line. As the results showed that traditional devices were less sensitive than the non-traditional devices, this suggests that optimizing the number of probe molecules per particle is more

important than what the actual molecule is. The problem with this however is that traditional lateral flow devices are mostly based on antibodies that are conjugated to particles by a method that does not allow optimisation of the number of antibodies per particle. During this conjugation procedure, GNPs are loaded with high numbers of antibodies. This probably accounts for their inferior sensitivity in comparison to the prototype device. As the assay protocol used in traditional devices does promote sensitivity, the results from the comparison experiments suggest that if the number of antibodies per particle could be optimised, even higher sensitivities could be achieved with traditional devices.

3.6-Summary

In this chapter a versatile method that allows the number of probe molecules per particle to be controlled was reported. This method was used to prepare DNP-GNP conjugates that were then used in a different type of reagent-limited lateral flow device. Immunoassays were carried out and the results showed that as the mean number of molecules per particle decreased, there was an increase in the sensitivity of the assay. Although the traditional device was expected to be more sensitive because the antibody labelled GNPs are allowed to react with the analyte before being briefly exposed to the analogue of the analyte immobilised on the test line, results showed that the non-traditional device was over 50 % more sensitive than the traditional device. This suggests that optimizing the number of probe molecules per GNP is very important and suggests that this approach should yield improvements in sensitivity regardless of the particle type or the identity of the probe molecule attached to it. This is an important result because it suggests how improvements in the sensitivity of other rapid tests could be achieved without resorting to more sophisticated labels that require additional equipment for detection.

3.7- References

1. Yager, P., Edwards, T., Fu, E, Helton, K., Nelson, K., Tam, M.R & Weigl, B.H. *Nature*, (2006), **442**, 412-418.

2. Chandler, J., Gurmin, T., Robinson, N., *IVDTechnology magazine*, (2000), March issue.

3. Ekins, R.P. *The future development of immunoassay. In: Radioimmunoassay and related procedures in medicine.* (1977), 241-268, International Atomic Energy Agency, Vienna.

4. Price, C.P., Newman, D.J. *Principle and Practice of Immunoassay* (1997), Macmillan Publishers, London.

5. Qian, S., Bau, H.H. *Anal. Biochem.*, (2004), **326**, 211-224.

6. Qian, S., Bau, H.H. *Anal Biochem.*, (2003), **322**, 89-98.

7. Wilson, R. *Chem. Commun.*, (2003), 108-109.

8. Wilson, R., Chen, Y., Aveyard, J., Chem. Commun., (2004), 1156-1157.

9. Chen, Y., Aveyard, J., Wilson, R., *Chem. Commun.*, (2004), 2804-2805.

10. Mehrabi, M. & Wilson, R. *Small*, (2007), **9**, 1491-1495.

11. Keller, G.H., Cumming, C.U., Huang, DP., Manak, M.M., Ting, R. *Anal. Biochem.*, (1988), **170**, 441-450.

12. Wilson, R., Clavering, C., Hutchinson, A. *Analyst*, (2003), **128**, 480-485.

13. Carlsson, J., Drevin, H., Axen, R. *Biochem. J.*, (1978), **173**, 723-737.

14. Slater, R.J. *Radioisotopes in biology: a practical approach*, (1990), IRL, Oxford.

15. Williams, B.L., Wilson, K. *A biologist's guide to principles and techniques of practical biochemistry*, (1981), Edward Arnold, London.

16. Altgeit, G.H., Segal, L. *Gel permeation chromatography*, (1971), Dekker, New York.

17. Faulk, W.P & Taylor, G.M. *Immunohistochemistry,* (1971), **8**, 1081-1083.

18. Hermanson, G.T. *Bioconjugate Techniques*, (1996), Academic Press, San Diego.

19. Verkleij, A.J. & Leunissen, J.L.M. *Immuno-gold labelling in cell biology,* (1989) 44-60, CRC Press, Boca Raton, Fl.

20. Horisburger, M., Clerc, M.F. *Histochemistry*, (1985), **82**, 219-223.

21. Kramarcy, N.R. & Sealock, R. *J. Histochem. Cytochem.* (1989), **39**, 37-39.

22. Jones, K.D. *IVDTechnology magazine*, (1999), March-April issue.

23. Aslam, M., Dent, A., *Bioconjugation,* (1998), Macmillan Publishers, London.

24. Li, J., Zhao, K., Hong, X., Yuan, H., Ma, L., Li, J., Bai, Y., Li, T. *Colloid surface B*, (2005), **40**, 179-182.

25. Malamud, D., Bau, H., Niedbala, S., Corstjens, P. *Adv. Dent. Res.*, (2005), **18**, 12-16.

26. LaBorde, R.T., O'Farrell, B. *IVDTechnology Magazine*, (2002) April issue.

27. Zhang, C., Zhang, Y. & Wang, S. *J. Agri. Food Chem.*, (2006), **54**, 2502-2507.

28. Cho, JH., Paek, EH., Cho, IH., Paek, SH., *Anal. Chem.* (2005), **77**, 4091-4097.

29. Okano, K., Takahashi, S., Yasuda, K., Tokinaga, D., Imai, K., Koga, M. *Anal. Biochem.* (1992), **202**, 120-125.

30. Kubitschko, S., Spinke, J., Bruckner, T., Pohl, S., Oranth, N. *Anal. Biochem.* (1997), **253**, 112-122.

31. Hall, M., Kazakova, I., Yao, YM. *Anal. Biochem.* (1999), **272**, 165-170.

32. Soukka, T., Harma, H., Paukkunen, J., Lovgren, T. *Anal. Chem.*, (2001), **73**, 2254-2260.

CHAPTER 4

4.1-Introduction

Nucleic acids are organic substances found in the chromosomes of all living cells and viruses that play a central role in the storage and replication of hereditary information and in the expression of this information through protein synthesis. Nucleic acid molecules are complex chains of varying length and are composed of a sugar phosphate backbone to which nitrogenous heterocyclic bases are attached.[1] There are two main types of nucleic acids; deoxyribonucleic acid (DNA), which carries the hereditary information from generation to generation, and ribonucleic acid (RNA), which delivers the instructions coded in this information to the cell's protein manufacturing sites. Over the last few decades, advances in technology and the sequencing of the human genome, have enabled the development of tests that can detect specific nucleic acid sequences. These so-called nucleic acid tests (NATs) have had a major impact in areas including clinical diagnostics for infectious diseases, genetic testing for chromosomal disorders and cancer, pharmacogenetic testing, food testing, forensic science and environmental testing.[2]

NATs offer many advantages over traditional immunoassay based diagnostic assays such as enzyme-linked immunosorbent assays (ELISA),[3] for example ELISA's for viruses such as human immunodeficiency virus (HIV), hepatitis B and C (HBV and HCV) detect antibodies to the viruses produced by the body after infection. The problem with this is that it can take up to 60 days for the body to produce these antibodies. As NATs detect genetic material, diagnosis and treatment can be performed earlier and the risk of further transmission is lowered. In a recent study published in the New England Journal of Medicine, 37 million units of antibody non-

reactive blood from first time donors were re-tested for HBV, HCV and HIV using both antibody-based tests and a NAT. Two patients tested HIV positive from the antibody-based tests, whereas twelve tested HIV positive from the NAT.[4] As a result of this and many other studies, NATs are now a major requirement for blood screening in many countries. Along with faster detection, NATs can also be more sensitive. This is because they are often interfaced with an "amplification" technique which enables small amounts of nucleic acid extracted from a sample to be "amplified" into large quantities for detection. A commonly used amplification technique is the polymerase chain reaction (PCR).

Invented by Kary Mullis in the mid-1980s, PCR has revolutionized molecular biology as it allows small amounts of target DNA to be amplified in minutes.[5] The PCR protocol begins by mixing the genomic DNA from a sample, short oligonucleotide primers that are complementary to the target, a thermostable DNA polymerase, free nucleotides and buffer. A diagram depicting a typical PCR reaction can be seen in Figure 1. In step 1, the mixture is heated and all DNA melts into two single strands. In step 2, the temperature of the mixture is lowered and the primers anneal to the complementary sequence of the target strands. In step 3, DNA polymerase extends the primers, adding free nucleotides that are complementary to the original target strands. Once completed, this cycle is repeated many times, and the amount of target strand amplified increases exponentially. Detection of the amplified target can then be achieved by a number of techniques including gel electrophoresis; where target DNA is separated in a size dependent manner by applying an electric current to a gel and visualizing the fragments by staining the gel with intercalating dyes such as ethidium bromide or SYBR;[6] or southern blotting,

where the target DNA is identified by a combination of gel electrophoresis and specific hybridisation with a labelled oligonucleotide probe. In Southern blotting, target DNA is first separated by gel electrophoresis and then denatured by treatment with an alkaline solution to produce a single stranded target. This is then transferred by capillarity to a membrane, usually nitrocellulose or nylon, by blotting the gel. The target is then attached to the membrane by baking in an oven or exposing the membrane to UV light. The target is then identified by hybridisation with specific labelled oligonucleotide probes.[7] In addition to these techniques, the ability to incorporate hapten, fluorescent, chemiluminescent and radioactive labels into amplified target DNA during the PCR process also enables the detection of the amplified target DNA by a large variety of additional techniques including those based on antibodies, such as ELISA.[8]
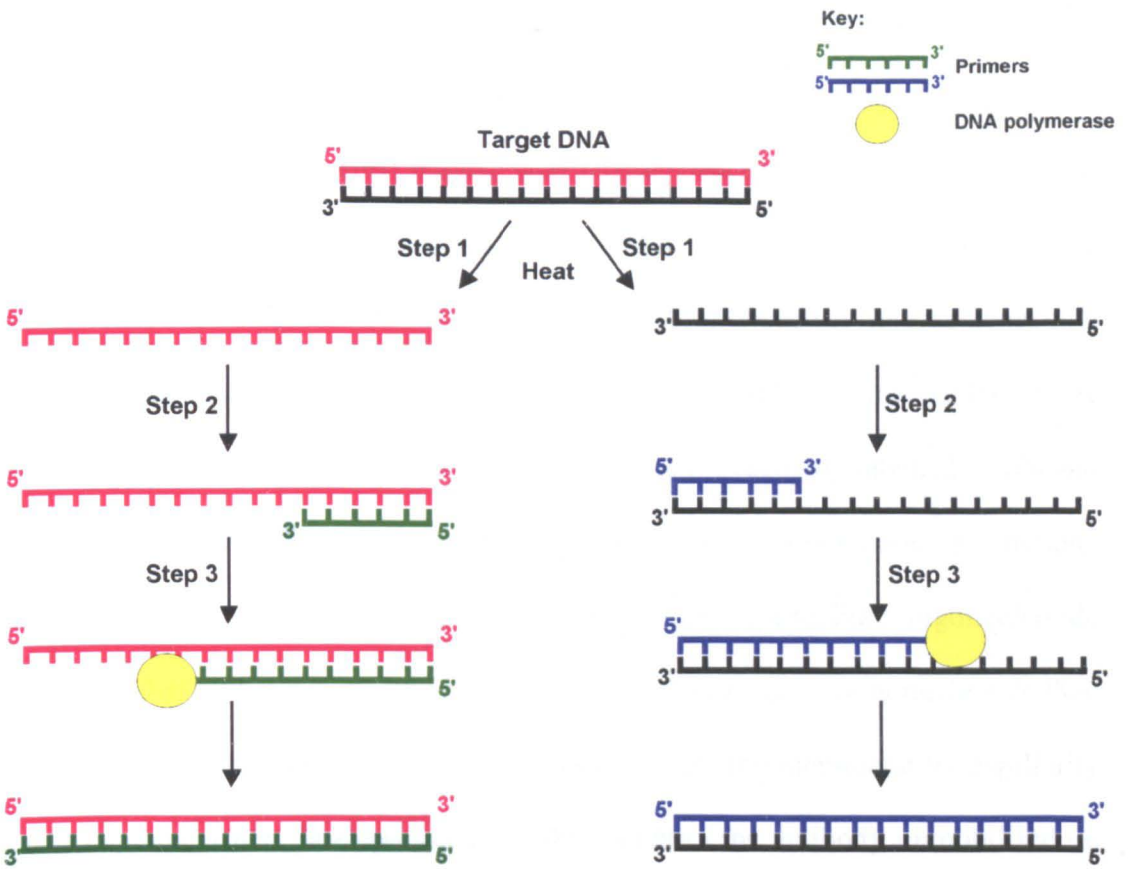
Figure 1: A diagram of a typical PCR reaction. In step 1 the target DNA is heated and the DNA melts into single strands. In step 2 the temperature is lowered and the primers anneal to the complementary bases of the target strands. In step 3, DNA polymerase binds extending the primers adding nucleotide bases that are complementary to the target strand.

Although NATs offer many advantages, they are also often expensive, complicated, time consuming and require specialized detection equipment. As a result, there is a strong desire to develop simple, affordable, rapid and reliable NAT devices. Lateral flow devices based on antibodies were first introduced in the 1980s and have subsequently become one of the most important products of the multibillion-dollar diagnostics industry. Their success is based on a combination of low cost and simplicity that allows untrained personnel to undertake immunoassays in extra-laboratory environments such as a physician's office or hospital bedside without

147

additional equipment. For these reasons many researchers have investigated the possibility of adapting simple, low-cost lateral flow devices for the detection of nucleic acids. These so-called nucleic acid lateral flow (NALF) devices have been developed for the detection amplified nucleic acids. In these devices, both capture and detection of nucleic acids is achieved in an antibody or hapten-dependent manner. A detailed diagram of an antibody / hapten-dependent NALF device can be seen in Figure 2. In this device, the detection reagent is antibody labelled GNPs and the capture reagent is antibodies immobilised on the nitrocellulose membrane. Target oligonucleotide labelled with a hapten hybridises to a specific oligonucleotide probe, labelled with a different hapten. The hapten on the target oligonucleotide then binds to the labelled antibody. This migrates through the membrane by capillarity and is captured when the haptenylated probe binds to the antibody immobilised on the test-line. When both haptenylated oligonucleotides are present, a red test line forms on the membrane. The main disadvantage of using antibody-dependent devices for the detection of amplified PCR products is the necessity for haptenylated primers and the corresponding antibody. Firstly, there are only four labelled primers that can be used in PCR protocols that also have a corresponding antibody that could be used for detection. These are digoxigenin (DIG), biotin, dinitrophenol (DNP) and fluorescein. Due to this problem, detecting many targets in one device (multiplexing) becomes difficult. Although this could be rectified by synthesizing alternative labels, raising the corresponding antibodies and checking for cross-reactivity, this would be both time consuming and expensive. Secondly, haptenylated oligonucleotides can be up to ten times more expensive than their unlabelled equivalents. This increases the cost of the device and makes multiplexed detection expensive. Another disadvantage of antibody-dependent devices is the

often large batch to batch variation of these devices that can occur due to the use of

different batches of antibodies,[9] making reproducibility a potential problem.

PCR with haptenylated primers
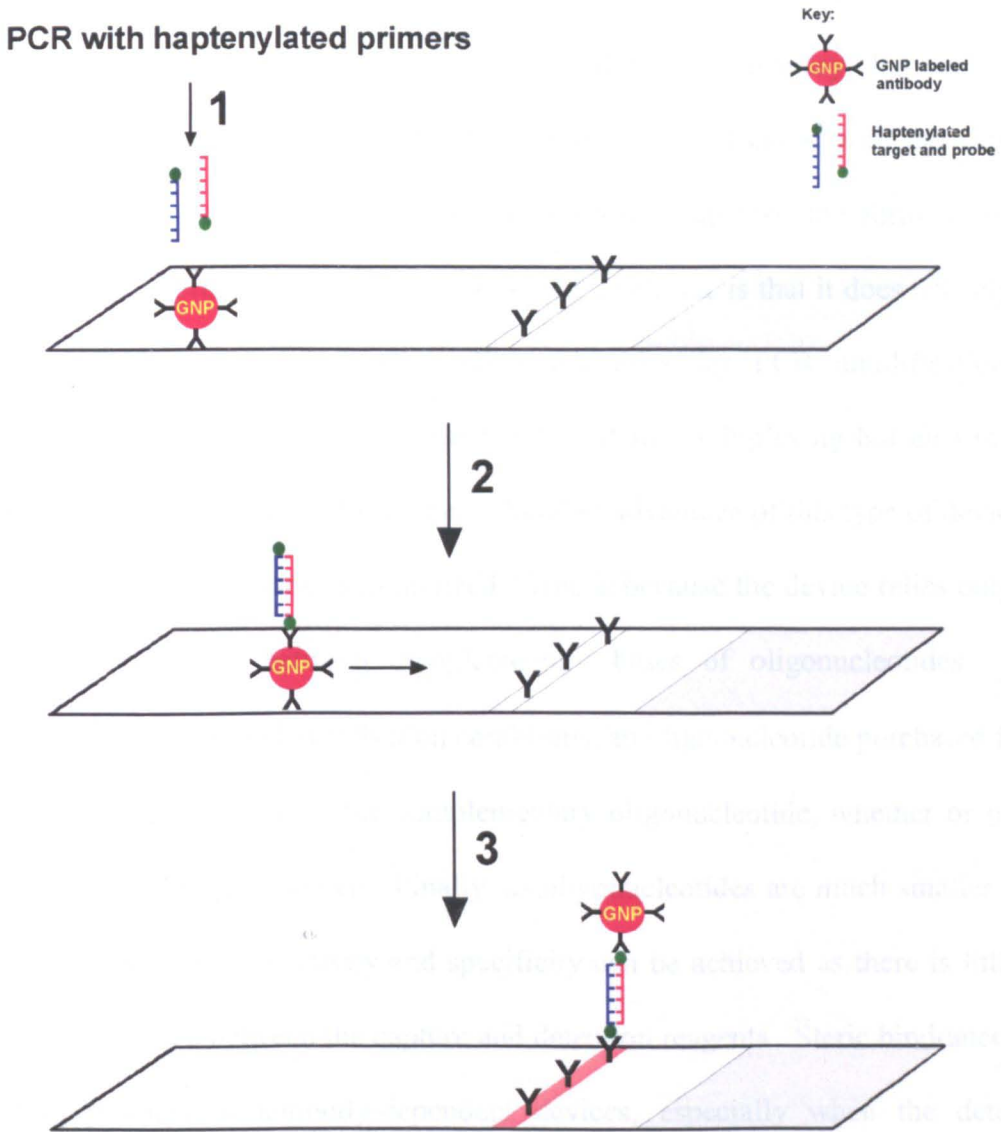
Figure 2: Diagram of an antibody-dependent NALF device. In step 1, sample is applied to the membrane and GNP labelled antibody (detector reagent) is solubilised. In step two, haptenylated target and probe oligonucleotides hybridize and bind to the antibodies on the GNPs and the oligonucleotide-GNP complex moves through the membrane by capillarity. In step 3, the GNP-oligonucleotide complex is captured by antibodies immobilised on the test line (capture reagent) of the membrane, producing a red line.

An alternative approach that would alleviate the problems associated with antibody-

dependent devices would be to capture and detect target nucleic acids in an antibody

/ hapten independent way. In this work, an antibody / hapten independent device was developed; a diagram of this can be seen in Figure 3.[10] In this approach, the detection reagent was oligonucleotide labelled GNPs and the capture reagent was oligonucleotides immobilised directly on the nitrocellulose membrane. When the target oligonucleotide is present, it hybridised to the complementary oligonucleotide on the GNP. This was then captured by specific hybridisation with the capture oligonucleotide immobilised on the membrane and a red test line formed on the membrane. The principal advantage of this type of device is that it does not rely on the use of haptenylated primers / oligonucleotides for PCR amplification or detection. This not only enables greater potential for multiplexing but also makes this type of device considerably cheaper. Another advantage of this type of device is that batch to batch variation is minimized. This is because the device relies only on specific hybridisation between complementary bases of oligonucleotides. For example, under the right hybridisation conditions, an oligonucleotide purchased from one source will hybridize to the complementary oligonucleotide, whether or not it was purchased the same source. Finally, as oligonucleotides are much smaller than antibodies, maximum sensitivity and specificity can be achieved as there is little or no steric hindrance between the capture and detection reagents. Steric hindrance is a common problem in antibody-dependent devices, especially when the detector reagent is antibody labelled GNPs. This is mainly due to the manner in which the antibodies are attached to the particle. As discussed in previous chapters, antibodies are usually attached to GNPs directly through electrostatic absorption, where the positively charged amino acid residues of the antibodies bind to the negatively charged GNPs; or by dative covalent bonds, where sulphur groups present in cysteine residues of the antibodies form strong sulphur bridge bonds with the GNP surface.

As both of these frequently used methods involve binding through amino acid residues, the reactivity of the attached antibody can be seriously affected and the GNP can mask the reactive epitopes of the antibody.[11]
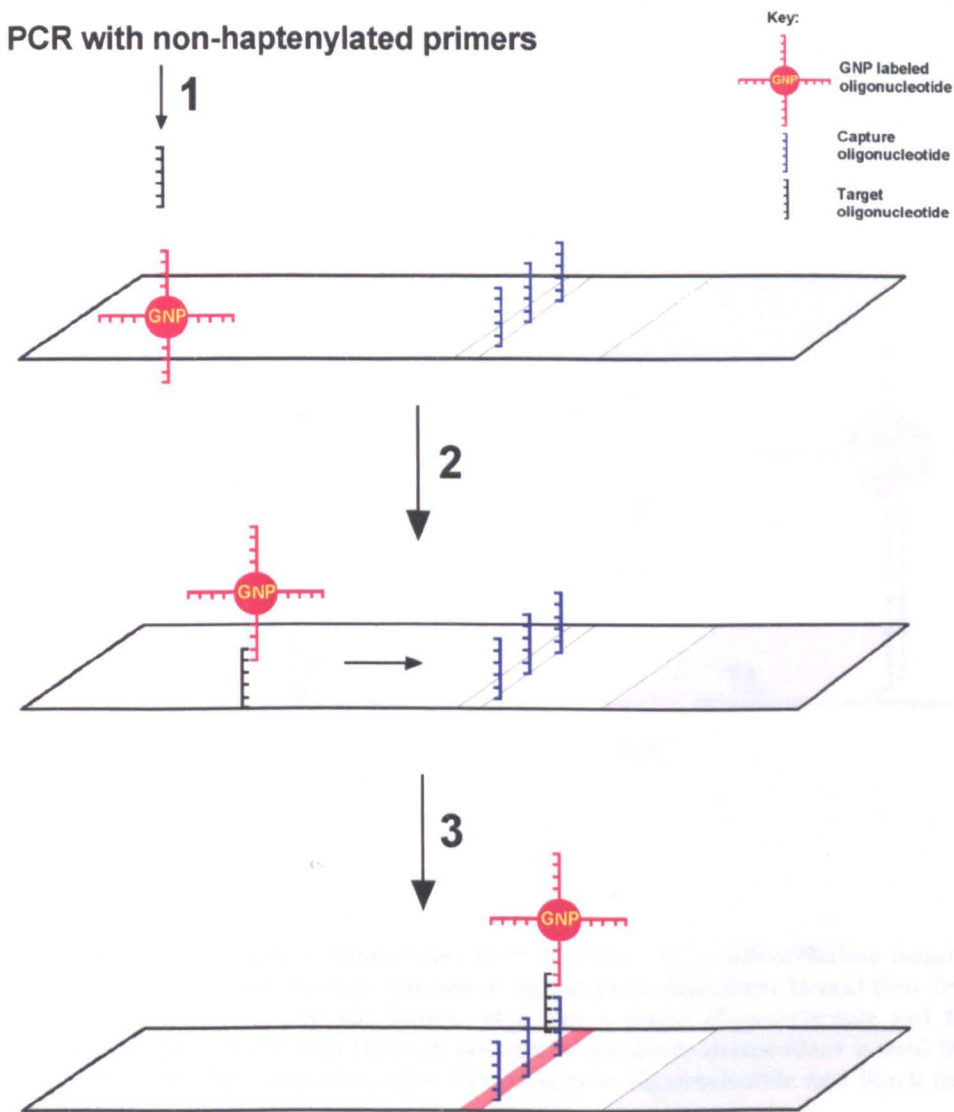
Figure 3: Diagram of antibody-independent NALF device. In step 1, sample is added and GNP labelled oligonucleotide (detector reagent) is solubilised. In step two, the target oligonucleotide in the sample hybridises to the GNP labelled oligonucleotide and travels through the membrane by capillarity. In step 3, the GNP-oligonucleotide complex is captured by oligonucleotides immobilised on the test line (capture reagent) of the membrane producing a red line.

To summarize, many NALF devices have been developed for the detection of target nucleic acids, but in all of these devices, both capture and detection of the nucleic acid target depend in someway on the use of antibodies or haptens. This can be both problematic and expensive. A simpler, more inexpensive approach would be to capture and detect nucleic acids in an antibody / hapten independent manner. A diagram showing antibody / hapten dependent and independent NALF devices can be seen in Figure 4.
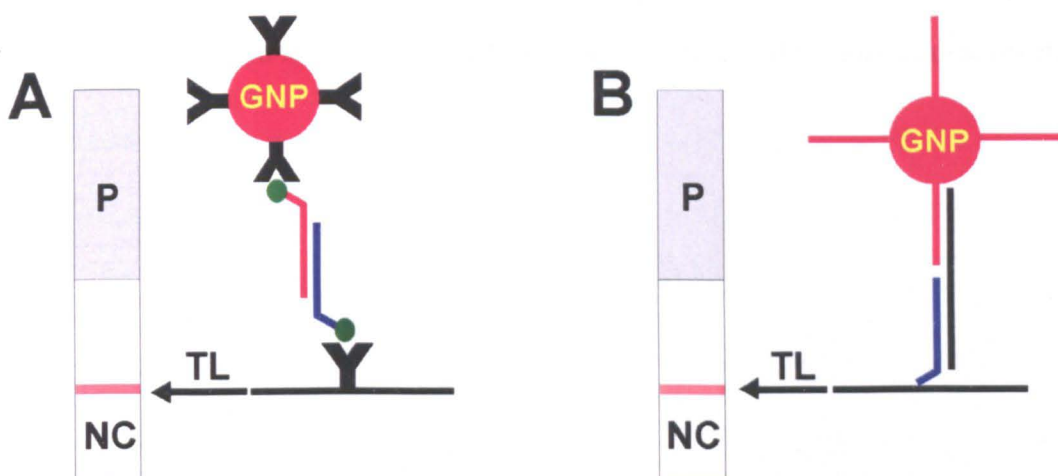
Figure 4: Key: GNP = gold nanoparticle; TL = test line; NC = nitrocellulose membrane; P = absorbent pad. A) Section through test line of an antibody-dependent lateral flow device based on haptens (green circles) and antibodies. Red line = target oligonucleotide and Blue line = oligonucleotide probe B) Section through test line of antibody-independent lateral flow device. Red line = detector oligonucleotide; Blue line = capture oligonucleotide and Black line = target oligonucleotide.

This chapter describes a simple, inexpensive, prototype antibody-independent NALF device for the detection of target nucleic acids (as shown in Figure 4B). The detection reagent was prepared without the use of antibodies or haptens, by

covalently attaching oligonucleotides to functionalised dextran polymers and then conjugating the polymer to GNPs. The capture reagent was oligonucleotides that had been striped directly onto a nitrocellulose membrane. Initially this device was used to detect single stranded target oligonucleotides, but, as it is frequently necessary to interface NALF devices with nucleic acid amplification techniques, the developed device was also used to detect un-purified PCR products. In this chapter the preparation and purification of oligonucleotide functionalised dextrans, the conjugation of these dextrans to GNPs and the use of these conjugates for the detection of nucleic acid targets will be discussed. In addition, a study on the effect that GNP size has on the sensitivity of the NALF device will be also be described.

4.2- Materials

Aminodextran (MW 70 kDa, 16 primary amines per molecule) was from Molecular Probes, Eugene, OR. Succinimidyl 4-hydrazinonicotinate acetone hydrazone (SANH; Solulink, San Diego, CA). 3-(2-pyridyldithio)propionic acid *N*-hydroxysuccinimide ester (SPDP), bovine serum albumin (BSA), sodium cyanoborohydride and dithiothreitol (DTT) were from Sigma. Thiopropyl Sepharose 4B and Cy5 monoreactive dye kit (Cy5-NHS ester) were from Amersham Biosciences. PCR master mix (BioMix) and agarose were from Bioline, London, UK. Ethidium bromide was from Continental Laboratory Products, San Diego, CA. Oligonucleotides with a 5' terminal aldehyde modification were from Trilink Biotechnologies, San Diego, CA. All other oligonucleotides were from Operon, Cologne, Germany. PBS: 15 mM sodium phosphate, 0.15 M NaCl, pH 7.4. Running buffer: PBS containing 1 mM ethylenediaminetetraacetic acid (EDTA). MES buffer: 0.2 M 2-(N-morpholino)ethanesulphonic acid, 0.3 M NaCl, pH 5. Bicarbonate solution: 0.1 M sodium hydrogen carbonate, pH 8.3. TBE: 45 mM Tris-borate, 1 mM EDTA, pH 8.3. GNPs (10, 20, 40, 60, 80, 100 and 150 nm) and chromatographic devices striped with oligonucleotides (5'-GGA TAT CAC CCG) were prepared and provided by BBInternational, Cardiff, UK. The diameters of the GNPs were determined using a ZetaPlus analyser (Brookhaven Instruments, Worcestershire, UK) and by transmission electron microscopy (TEM) using a Phillips 410 operating at 80 kV or a Phillips CM12 operating at 100 kV. TEM samples were prepared by placing a drop of GNP solution on a 200 mesh nickel grid (Agar Scientific) and allowing it to dry in air. PCR was carried out with an MJR thermal cycler from MJ Research Inc, MA.

4.3- Methods

4.3.1- Oligonucleotide concentrations

Oligonucleotides were supplied with a molar extinction coefficient at 260 nm. This value was used to determine the concentrations of stock solutions before dilution to the required concentration.

4.3.2- Functionalisation of aminodextran with Cy5

Cyanine 5 (Cy5) dye was introduced into aminodextran by adding 3 mg of aminodextran in 0.8 ml of PBS to Cy5-NHS ester and slow tilt rotating the solution in the dark at room temperature for 2 hours. At the end of this time, protected disulphide (3-(2-pyridyldithio)propionyl; PDP) groups were introduced into the Cy5 functionalised dextran by adding 100 μl of 30 mM SPDP in dry DMF dropwise with stirring over a period of 5 hours. After stirring overnight, un-reacted Cy5 and SPDP were removed by dialysing the solution against 4 x 1 litre of distilled water at 4 °C for a total of 48 hours.

4.3.3- Covalent chromatography of Cy5 functionalised dextrans

PDP groups in the dextran were reduced to unprotected thiol (-SH) groups by adding 100 μl of 100 mM DTT in 1 M sodium bicarbonate to 1 ml of Cy5 functionalised dextran and slow-tilt rotating the solution at room temperature for 1 hour. At the end of this time DTT was then removed by gel exclusion on a column containing Sephadex G-25 (diameter 1 cm; bed volume 11.78 ml) equilibrated with PBS containing 1 mM EDTA. Reduced Cy5 functionalised dextrans were immediately mixed with 25-fold excess (relative to the original protected disulphide content of the dextran) of washed Thiopropyl Sepharose 4B gel and slow-tilt rotated at room

temperature for 1 hour. Bound Cy5 functionalised dextrans were released from the gel with 10 ml of 10 mM DTT in 1 M bicarbonate solution, pH 8.3 and DTT was removed from the released dextrans by dialysing against 3 x 2 litres of distilled water for 48 hours.

4.3.4- Functionalisation of aminodextran with aromatic hydrazine and PDP and covalent attachment of aldehyde terminated oligonucleotide I

Aromatic hydrazine functionalities were introduced into aminodextran by adding 300 μl of 60 mM SANH in dry DMF, to 15 mg of aminodextran in 2.4 ml of PBS, dropwise with stirring over a period of 5 hours. After stirring for 2 hours, PDP groups were introduced into the functionalised dextran by adding 300 μl of 60 mM SPDP in dry DMF in the same way. After stirring overnight, un-reacted SANH and SPDP were removed by dialysing the solution against 4 x 1 litre of distilled water at 4 °C for a total of 48 hours. The concentration of protected disulphide groups in the dialysed solution was determined as reported in chapter 2. A 2-fold excess (relative to the amine content of the dextran) of aromatic aldehyde terminated oligonucleotide (5'CHO-TCT GCT GCC TGC TTG TCT GCG TTC T) in MES buffer, pH 5 was added to the functionalised dextran solution and slow-tilt rotated at 4 °C for 24 hours. PDP groups in the dextran were reduced to unprotected thiol (-SH) groups by adding 100 μl of 100 mM DTT in 1 M sodium bicarbonate to 1 ml of oligonucleotide-functionalised dextran and slow-tilt rotating the solution at room temperature for 1 hour. At the end of this time DTT was then removed by gel exclusion chromatography on a column containing Sephadex G-25 (diameter 1 cm; bed volume 11.78 ml) equilibrated with PBS containing 1 mM EDTA.

4.3.5- Functionalisation of aminodextran and covalent attachment of aldehyde terminated oligonucleotide II (cyanoborohydride method)

As above except that, PDP groups were reduced to unprotected thiol and Schiff bases were stabilized with 75 μl of 5 M sodium cyanoborohydride in 1 M NaOH. This was added to 1 ml of oligonucleotide functionalised dextran and allowed to react for 2 hours in a fume hood. At the end of this time, excess sodium cyanoborohydride was removed by gel exclusion chromatography on a column containing Sephadex G-25 (diameter 1 cm; bed volume 11.78 ml) equilibrated with PBS containing 1 mM EDTA.

4.3.6- Purification of oligonucleotide-functionalised dextrans

Un-reacted oligonucleotides were removed from functionalised dextrans by covalent chromatography on Thiopropyl Sepharose. Reduced oligonucleotide functionalised dextrans were immediately mixed with 25-fold excess (relative to the PDP content of the dextran) of washed Thiopropyl Sepharose 4B gel and slow-tilt rotated at room temperature for 1 hour. Un-reacted oligonucleotides were removed from the functionalised dextrans by washing the gel with running buffer. Bound oligonucleotide-functionalised dextrans were then released from the gel with 10 ml of 10 mM DTT in 1 M bicarbonate solution, pH 8.3 and DTT was removed from the released dextrans by dialysing the solution against 3 x 2 litres of distilled water for 48 hours.

4.3.7- Characterization of GNPs

The GNPs used in this work were obtained from a commercial source. Each batch is prepared from a known mass of gold (in gold (III) chloride) and characterized by

TEM. If the amount of gold used to prepare the particles and the mean diameter is known, the number of particles in a given volume of can be calculated using a value of 1.7×10^{-2} cubic nanometers for the volume occupied by one atom of gold. The particles used in this work were supplied with a data sheet that gave: 1) the mean diameter of the particles (CV% < 10) and, 2) the absorbance of these particles at a known number of particles per ml (for example, the supplied 10 nm particles contain 5.7×10^{12} particles per ml and have an absorbance of 0.8 at 520 nm). Upon receipt, the absorbance of the supplied particles was verified by UV/vis spectroscopy and the diameter was verified by dynamic light scattering using a ZetaPlus analyzer with particle size distribution software (PSDW). The concentration of GNPs was determined by multiplying the number of particles per ml by 1000 and then dividing by Avogadro's number (6.02×10^{23}).

4.3.8- Conjugation of oligonucleotide functionalised dextrans to GNPs

The minimum amount of oligonucleotide-functionalised dextran required to prevent salt-induced flocculation of GNPs in PBS was determined by titrating variable amounts of oligonucleotide functionalised dextran against 0.66 ml volumes of GNPs. Oligonucleotide-GNP conjugates were prepared by adding the minimum amount of oligonucleotide functionalised dextran to GNPs and 0.33 ml of PBS containing 3 mg ml^{-1} BSA and 1.5 % Tween 20. To concentrate the GNPs to the required OD, GNPs were centrifugally precipitated for 10 minutes and then re-suspended in the same buffer.

4.3.9- Comparison of GNPs coated with cyanoborohydride reduced and non-reduced oligonucleotide functionalised dextran on lateral flow strips

40 nm GNPs were coated with either cyanoborohydride-reduced or non-cyanoborohydride reduced oligonucleotide functionalised dextran. Lateral flow devices were inserted into 50 μl of a freshly prepared 1:1 mixture of the target sequence (5'-GGG ACT GAC GAT TCG GGT GAT ATC CAG AAC GCA GAC AAG CAG GCA) and 2 OD oligonucleotide functionalised GNPs (both in PBS), and developed for 20 minutes. Images of all lateral flow strips were acquired with an office document scanner and then imported into iGrafx Image 1.0 (Bournemouth, UK) and converted to greyscale. The depth of colour was determined on a scale of 0 – 255 by activating the "view → information" option and pointing the mouse cursor at the area to be interrogated.

4.3.10- Lateral flow detection of single stranded DNA

For detection of the 32 mer target sequence (5'-GGG ACT GAC GAT TCG GGT GAT ATC CAG AAC GCA GAC AAG CAG GCA) lateral flow devices were inserted into 50 μl of a freshly prepared 1:1 mixture of the target sequence and 2 OD oligonucleotide functionalised GNPs (both in PBS) then developed for 20 minutes. Images of all lateral flow strips were acquired and depth of colour at the test line was determined as in section 4.3.9.

4.3.11- Asymmetric PCR

The template sequence (5'-AGA GTT TGA TCC TGG CTC AGT CTG CTG CCT GCT TGT CTG CGT TCT GGA TAT CAC CCG ATT AGA TAC CCT GGT AGT CC), comprised a 32 mer sequence (underlined) nested between two 20 mer

159

sequences. The 32 mer sequence was the same as the reporter oligonucleotide linked to the capture oligonucleotide, the 20 mer sequence at the 5' end was the same as the forward primer (5'-AGA GTT TGA TCC TGG CTC AG) and the 20 mer sequence at the 3'end was the complementary to the reverse primer (5'-GGA CTA CCA GGG TAT CTA AT). The PCR mixture comprised 25 μl of master mix, 20 pmol of forward and different amounts of reverse primer. The ratios of reverse to forward primer were i) 1:1; ii) 2:1; iii) 3.5:1 and iv) 5:1; v) 6.25:1; vi) 7.5:1; vii) 10:1; viii) 25:1; ix) 50:1 and x) 100:1.The PCR protocol was an initial denaturation at 95 °C for 30 s, followed by 40 cycles of denaturation at 95 °C for 30 s, annealing at 55 °C for 45 s, and extension at 72 °C for 45 s, and completed with a final extension at 72 °C for 2 min. The product was analyzed by electrophoresis on 2.5% agarose with TBE containing 0.5 μg/ml ethidium bromide as the buffer.

4.3.12- Lateral flow detection of un-purified PCR products

PCR products were detected in the same way as in section 4.3.10; except that 2 OD oligonucleotide functionalised GNPs in PBS were diluted 1:1 with PCR products. Images of all lateral flow strips were acquired and depth of colour at the test line was determined as in section 4.3.9.

4.4- Results

4.4.1- Synthesis of Cy5 functionalised dextran and optimisation of covalent chromatography method

In order to investigate whether covalent chromatography was a viable method of purifying dextran conjugates in high yield, a model fluorescent dextran conjugate was synthesised. The reaction scheme showing the steps involved in the synthesis of this fluorescent dextran conjugate can be seen in Figure 5. In step 1, Cy5 molecules were attached to aminodextran using NHS ester chemistry. The NHS ester of the Cy5 reagent reacts with primary amines in the dextran to form stable amide bonds.[12] In step 2, protected disulphides (PDP) were introduced into the aminodextran using SPDP. As mentioned in previous chapters, SPDP is a heterobifunctional reagent that contains an NHS ester and a PDP functionality.[12, 13] After functionalisation the conjugate was dialysed to remove un-reacted SPDP and Cy5, then applied to a covalent chromatography column. A covalent chromatography gel (Sepharose 4B) functionalised with PDP groups was chosen as a suitable matrix as all the functionalised dextrans used in this work also contain PDP groups. A detailed diagram of the generic covalent chromatography procedure can be seen in Figure 6. In step 1, the PDP groups within the Cy 5 functionalised dextran were reduced to thiol (-SH) functionalities using a mild reducing agent (DTT). In step 2, the reduced dextran was applied to the column and became covalently attached via thiol-disulphide exchange reactions. In step 3, the gel was washed to remove any un-bound dextran or un-reacted reagents from the dextran synthesis. In step 4, the covalently linked Cy5 functionalised dextran was released by rupturing the disulphide bonds between the dextran and the column with DTT. Figure 7 is a covalent chromatography chromatograph showing the removal of un-bound Cy5

dextran from the column (red line). The chromatograph also shows the release of covalently bound Cy5 functionalised dextrans (blue line) from the gel after the addition of DTT.
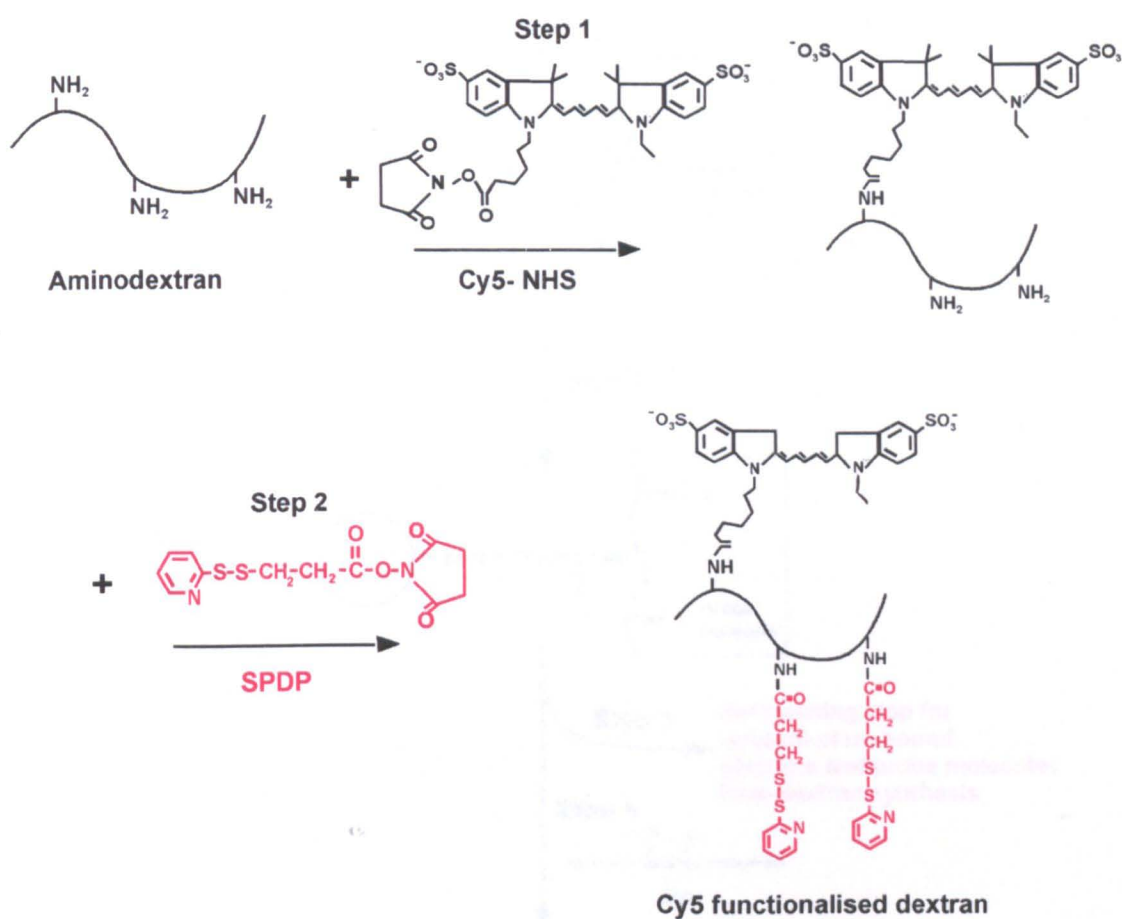
Figure 5: Reaction scheme showing the steps involved in the synthesis of Cy5 functionalised dextran. In step 1, Cy5-NHS ester is added to aminodextran. The NHS ester end of the reagent reacts with primary amines in the aminodextran to form stable amide bonds. In step 2, PDP groups are introduced into the dextran using SPDP. The NHS ester of the reagent reacts with amines to form stable amide bonds
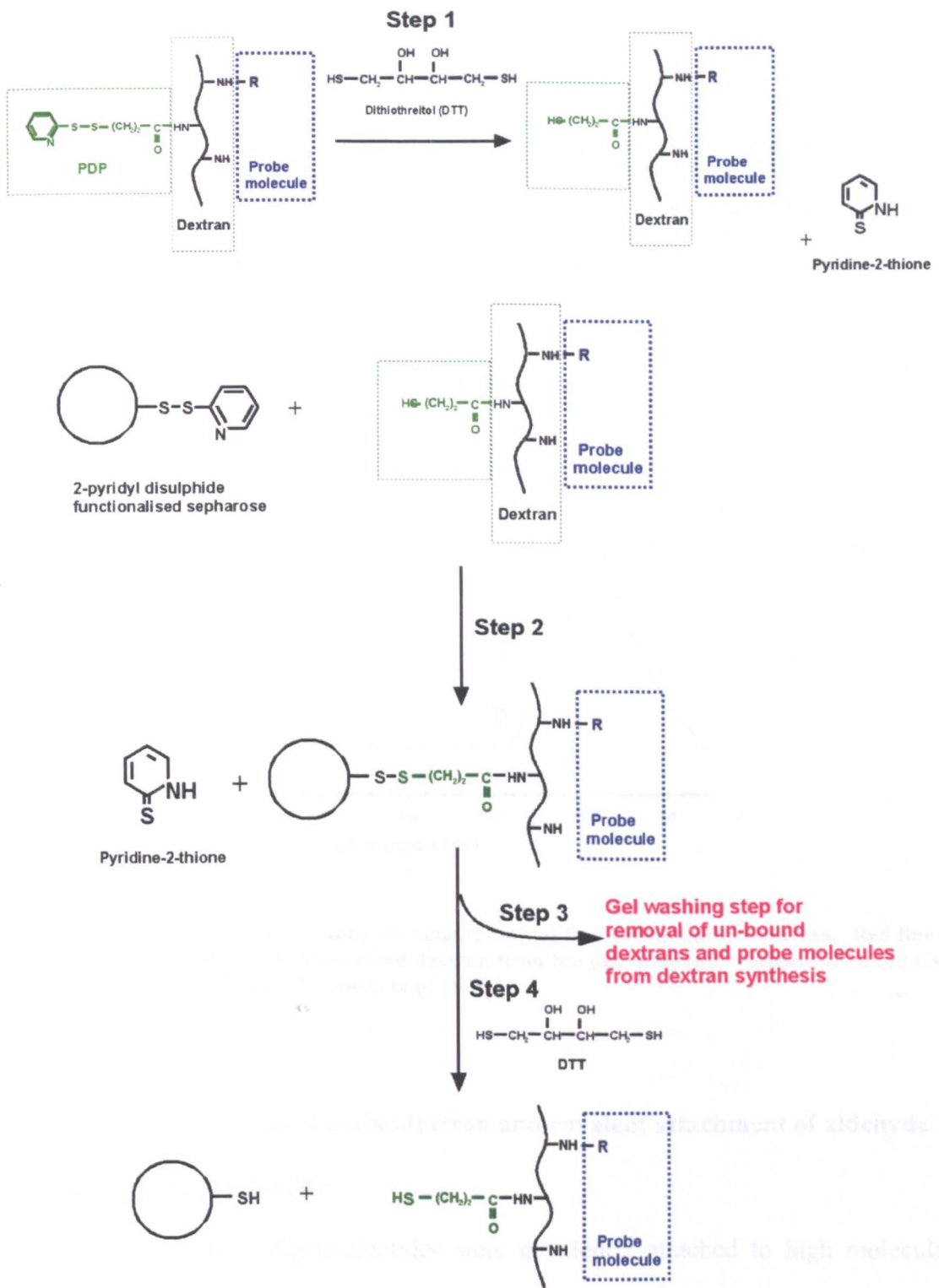
Figure 6: Diagram of generic covalent chromatography protocol. In step 1, PDP groups of dextran functionalised with probe molecules (e.gCy5 or oligonucleotide) are reduced to thiol (-SH) groups using a mild reducing agent (DTT). In step 2, reduced functionalised dextran is mixed with covalent chromatography gel that is functionalised with PDP groups. On contact, the PDP groups within the gel rupture and the functionalised dextran is attached via thiol-disulphide exchange reactions. In step 3, the gel is washed to remove any unbound dextrans or probe molecules remaining after the synthesis reaction. In step 4, the purified functionalised dextran is released from the column with DTT.
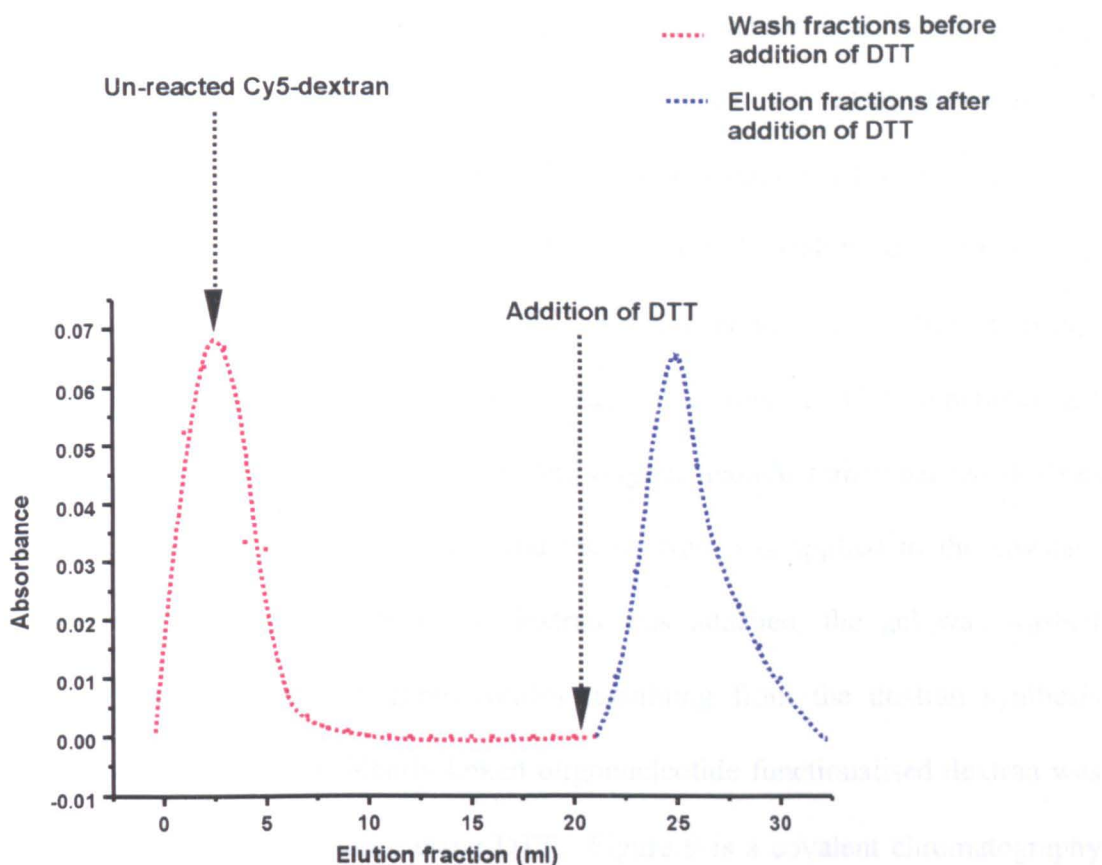
Figure 7: Covalent chromatography chromatograph of Cy5 functionalised dextran. Red line = elution of un-reacted Cy5 functionalised dextran from the gel. Blue line = release of bound Cy5 functionalised dextran after the addition of DTT

4.4.2- Functionalisation of aminodextran and covalent attachment of aldehyde terminated oligonucleotide

Aldehyde-terminated oligonucleotides were covalently attached to high molecular weight dextrans functionalised with aromatic hydrazines and PDP groups. The reaction scheme can be seen in Figure 8. In step 1 of the synthesis aminodextran was functionalised with aromatic hydrazines. The reagent used was SANH, a heterobifunctional reagent that contains an NHS ester and an aromatic hydrazine functionality. When added to aminodextran, the NHS ester in the reagent reacted

with the primary amines in the dextran to form stable amide bonds. In the step 2 of the synthesis, PDP groups were introduced into the aminodextran using SPDP. Finally, after purification by dialysis to remove un-reacted SPDP and SANH, in step 3, the dextran was then reacted with an excess of aldehyde-terminated oligonucleotide. The aldehyde groups of the oligonucleotide react with the aromatic hydrazines to form hydrazone bonds that do not need to be stabilized by a reduction step.[14] Following attachment of the oligonucleotide, the oligonucleotide functionalised dextrans were purified in the same way as Cy5 functionalised dextrans. First the PDP groups within the oligonucleotide functionalised dextran were reduced to thiol functionalities and the dextran was applied to the covalent chromatography column. Once the dextran was attached, the gel was washed thoroughly and any free oligonucleotides remaining from the dextran synthesis reaction were eluted. Covalently linked oligonucleotide functionalised dextran was then released from the column using DTT. Figure 9 is a covalent chromatography chromatograph showing the removal of un-reacted oligonucleotide from oligonucleotide functionalised dextrans (red line) and the release of covalently bound oligonucleotide functionalised dextrans (blue line) from the gel after addition of DTT.
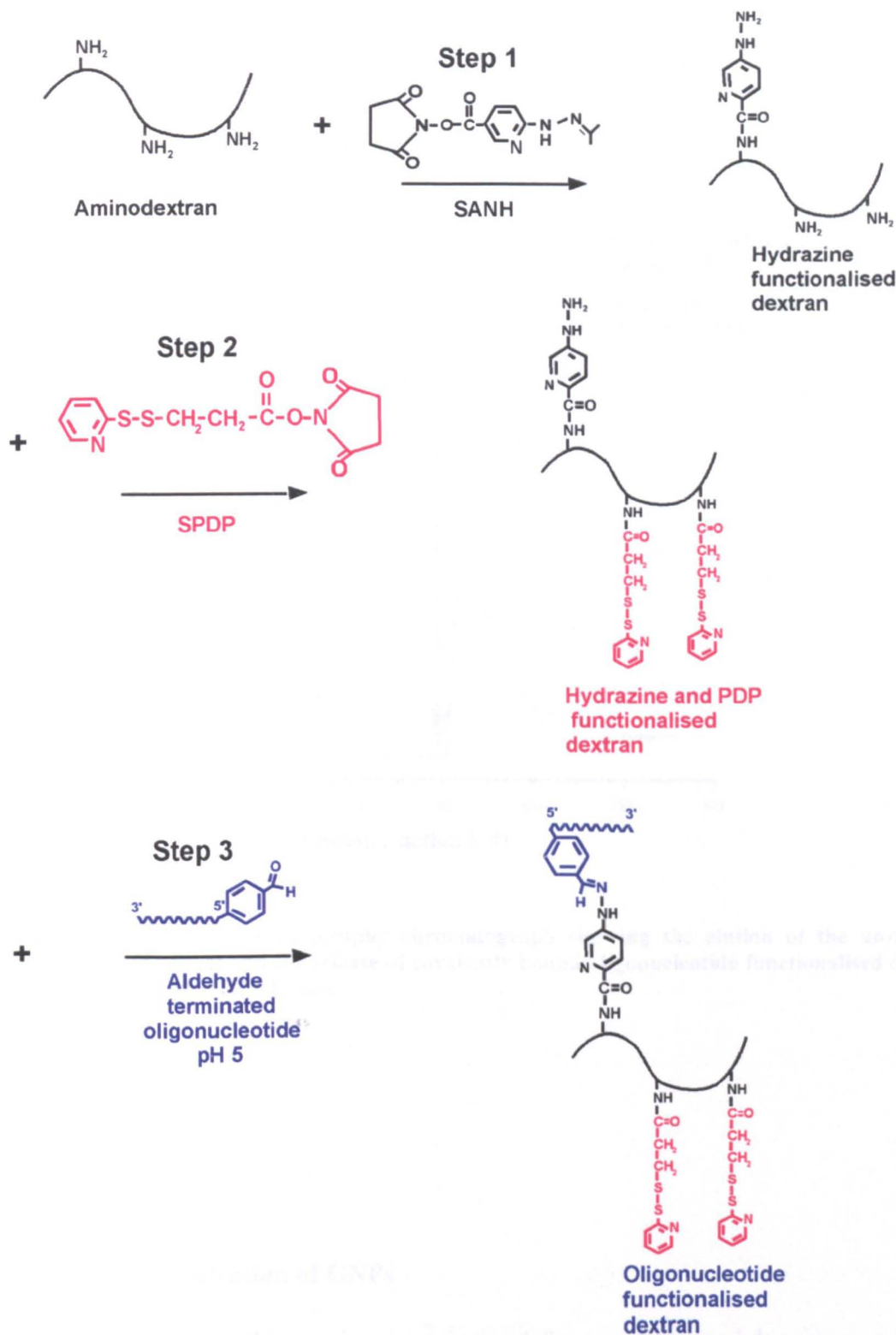
Figure 8: Reaction scheme showing the steps involved in the synthesis of oligonucleotide functionalised dextrans. In step 1, aromatic hydrazine groups are introduced into the dextran by reacting aminodextran with SANH. The NHS ester group of the reagent reacts with the amines within the aminodextran to form stable amide bonds. In step 2, PDP groups are introduced into the remaining amines in the dextran by reacting with SPDP. In step 3, aldehyde-terminated oligonucleotides are covalently linked to the functionalised dextran. The aldehydes react with the hydrazines within the dextran forming hydrazone bonds that do not need to be stabilized by a reduction step.
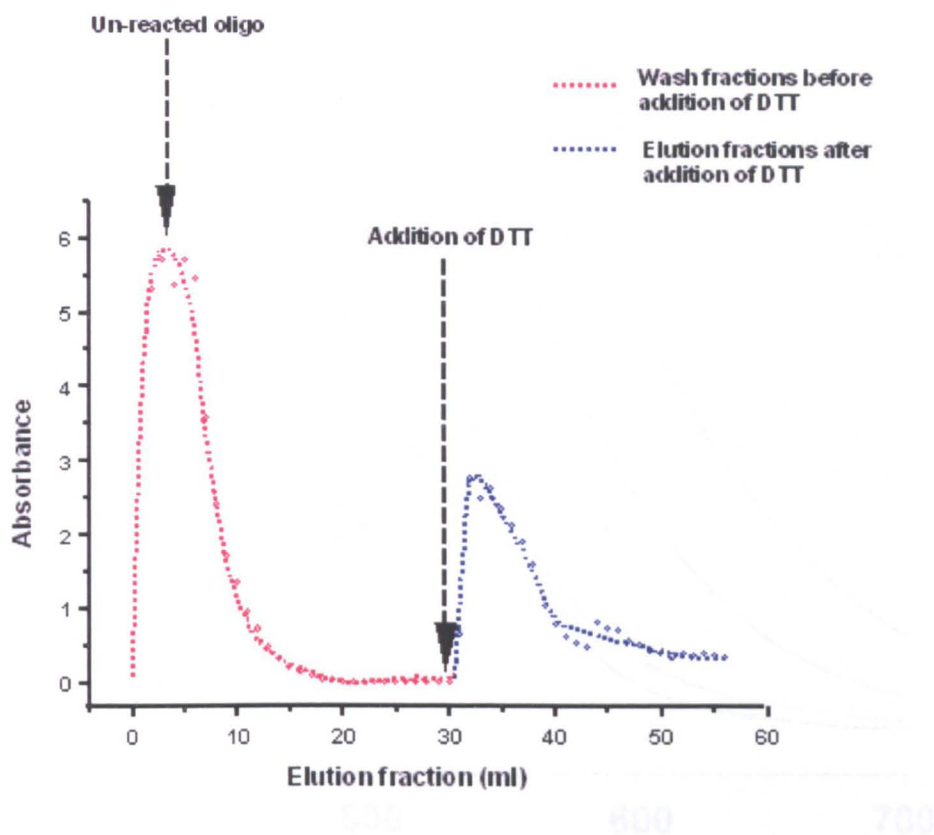
Figure 9: Covalent chromatography chromatograph showing the elution of the un-reacted oligonucleotide (Red) and the release of covalently bound oligonucleotide functionalised dextran after reduction with DTT (Blue).

4.4.3- Characterization of GNPs

The GNPs used in this work were obtained from a commercial source and were supplied with data sheets that gave: 1) the mean diameter of the particles (CV% < 10) and, 2) the absorbance of these particles at a known number of particles per ml. Before oligonucleotide functionalised dextrans were conjugated to GNPs, the diameters and UV/vis absorbances of GNPs supplied by a commercial source were

confirmed by dynamic light scattering and UV/vis spectroscopy respectively. Figure 10 is a graph showing the UV/vis absorbance spectra of all of the GNP solutions received from a commercial source, intersecting at 1 OD.
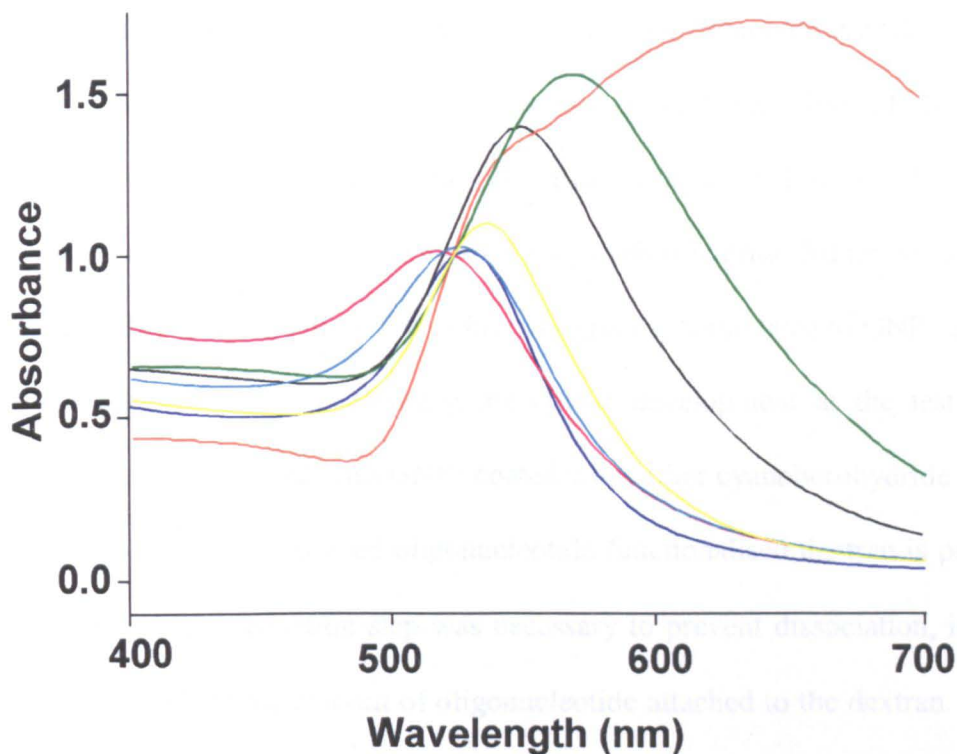
Figure 10: Overlaid absorbance spectra of all GNPs used in the sandwich assays. Key: Red = 10 nm; Light blue = 20 nm; Dark blue = 40 nm; Yellow = 60 nm; Black = 80 nm; Green = 100 nm; Orange = 150 nm.

4.4.4- Comparison of lateral flow assays carried out with GNPs coated with cyanoborohydride reduced and un-reduced oligonucleotide functionalised dextran

After functionalisation with aromatic hydrazines and PDP groups, it is possible that there are a small number of amine groups in the dextran that have not been functionalised. It was thought that the aldehyde terminated oligonucleotides could

168

react with these amines to form weak Schiff base intermediates that were in equilibrium with the free aldehyde oligonucleotides. If Schiff bases were forming, it would be essential to stabilize these intermediates as any weakly bound oligonucleotide could dissociate from the dextran either before or after conjugation to the GNPs and this would affect the sensitivity of the NALF device. Schiff bases can be chemically stabilised by reduction with sodium cyanoborohydride.[12] When the Schiff base is reduced a very stable secondary amide bond is formed. In order to investigate whether weak Schiff base intermediates were formed, the dextran synthesis protocol was modified to contain a cyanoborohydride reduction step. The dextran was then purified by covalent chromatography, conjugated to GNPs and used in NALF assays. A graph showing the colour development at the test line in sandwich assays performed with GNPs coated with either cyanoborohydride reduced or un-cyanoborohydride reduced oligonucleotide functionalised dextran is presented in Figure 11. If the reduction step was necessary to prevent dissociation, it should lead to an increase in the amount of oligonucleotide attached to the dextran. This in turn would lead to an increase in the colour density of the test line in the NALF assays. However, the results showed that there was no significant difference in the colour of the test line in assays performed with cyanoborohydride reduced oligonucleotide functionalised dextrans. This suggested that a reduction step was not necessary when preparing oligonucleotide functionalised dextrans.
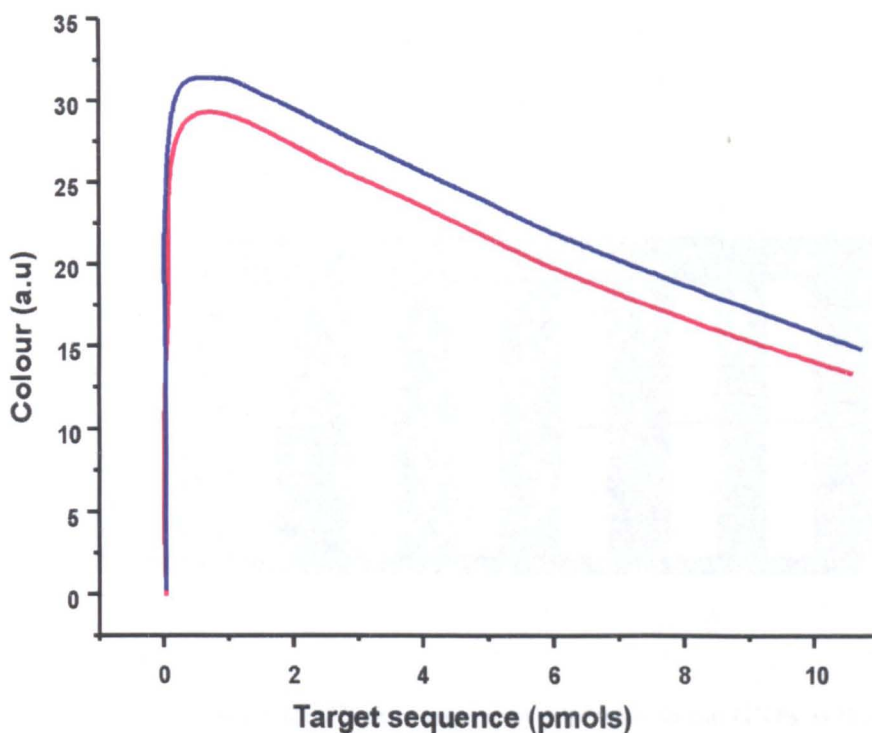
Figure 11: Graph showing colour development at the test line in assays for target oligonucleotide. GNPs were coated with either cyanoborohydride reduced (Red line) or non-cyanoborohydride reduced (Blue line) oligonucleotide functionalised dextran.

4.4.5- Lateral flow detection of single stranded DNA

Once it had been ascertained that a cyanoborohydride reduction step was not necessary, oligonucleotide functionalised dextran was conjugated to 80 nm GNPs and a series of assays for different amounts of target sequence in the range 0 – 10 picomoles were carried out. The 32-mer target sequence had a 20-mer 3'-terminal sequence complementary to the oligonucleotides conjugated to the GNPs, and a 12-mer 5'-terminal sequence that was complementary to capture oligonucleotides anchored to the test line of the nitrocellulose strip. Figure 12 shows images of test strips acquired from these experiments. There was no detectable colour development in the presence of 10 pmol of a non-complementary target sequence (Figure 13; 5'-GAC TCG GGG GAT ATC ACT GAT AAC GGT CAG GAC GCA AAG GCA CAG) and therefore the sensitivity (< 50 femtomoles) was determined by the amount

170

of GNPs that could be seen with the unaided eye. The images in Figure 12 show that as low as 50 femtomoles of target sequence can be detected.
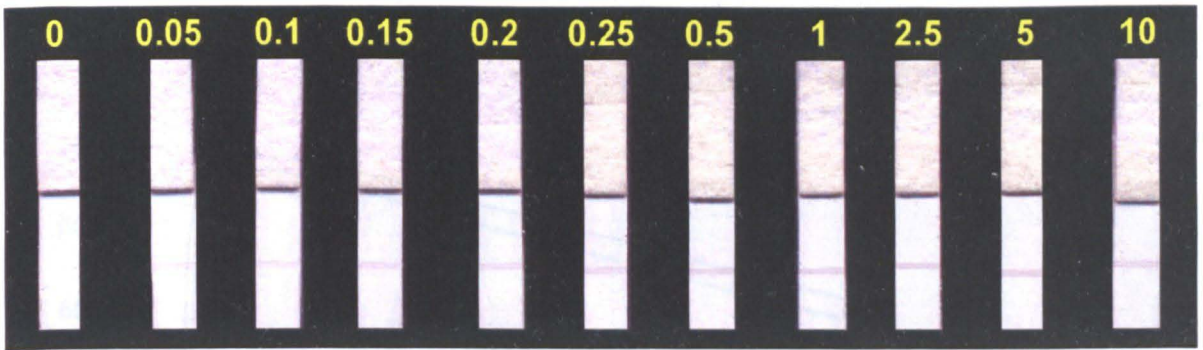
Figure 12: Results of NALF assays for 32 mer target sequence with 80 nm GNPs as the label. Numbers show the amounts of target sequence in pmol.
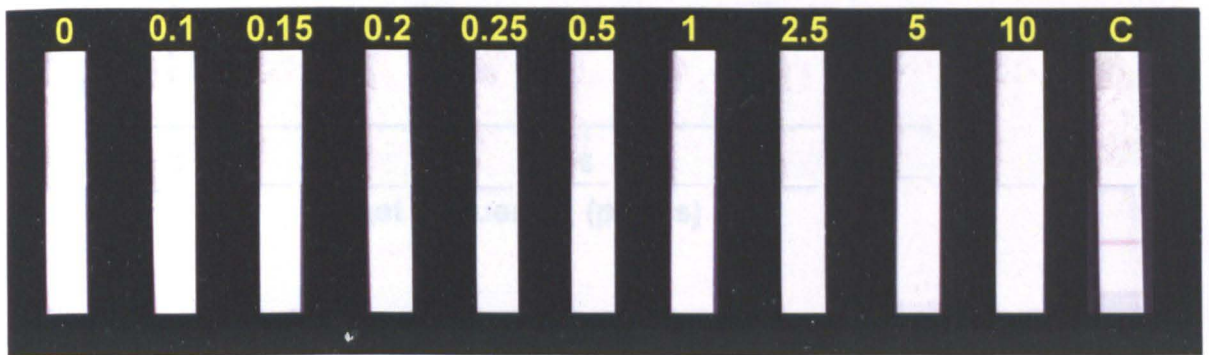
Figure 13: Images of test strips obtained from experiments with non-complementary sequence. Numbers denote amount of non- complementary sequence in pmol.

4.4.6- Investigating the effect of GNP size on NALF device sensitivity

Figure 14 is a graph showing the amount of colour development at the test line during NALF assays (0-10 pmol of target sequence) performed with oligonucleotide-coated GNP with diameters in the range 10 – 150 nm and Figure 15 shows images of these test strips. Both figures show that the amount of colour developed at the test

line increased as the diameter of the GNPs increased from 10 to 80 nm and then

decreased at larger diameters (100 and 150 nm).
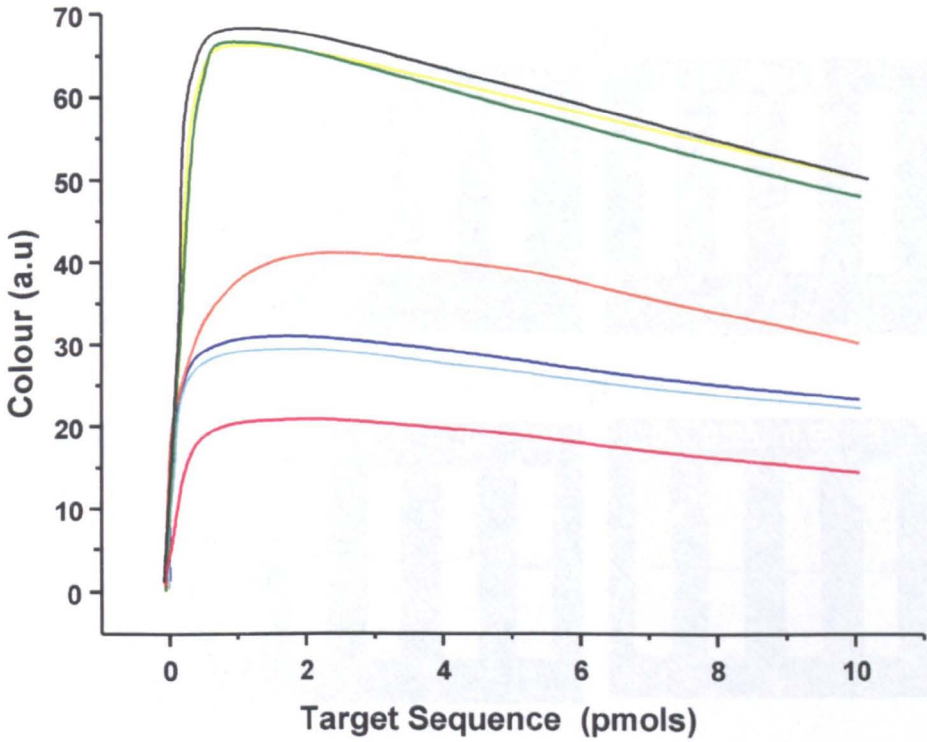
Figure 14: Graph showing the effect of GNP diameter on the amount of colour developed at the test-line of nucleic acid lateral flow devices. Key: Red= 10 nm; Light blue= 20 nm; Dark blue= 40 nm; Yellow= 60 nm; Black= 80 nm; Green= 100 nm; Orange= 150 nm.
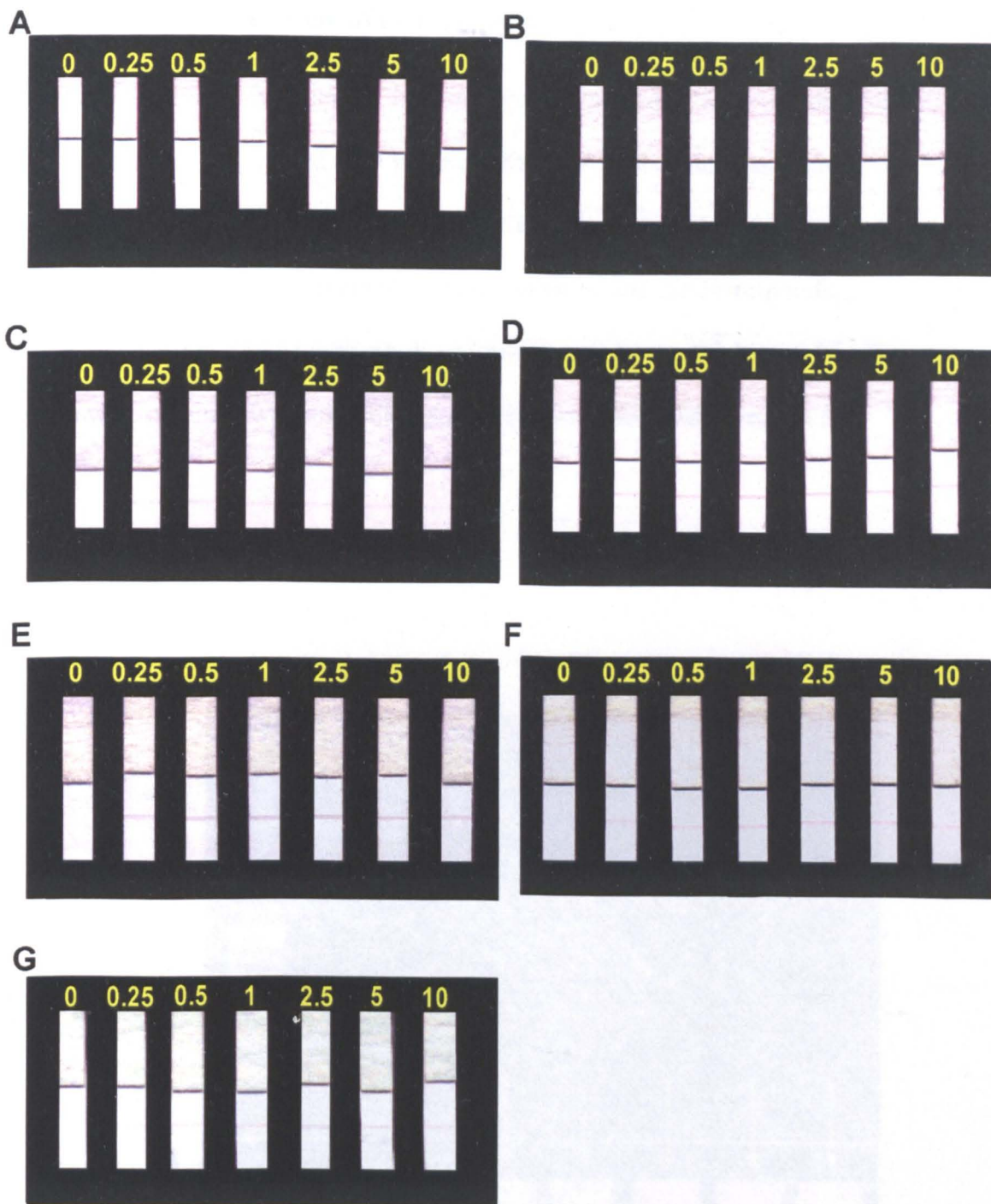
Figure 15: Comparison between NALF assays for 32 mer target sequence performed with different sized GNPs. Numbers denote the amount of target in pmol. A) 10 nm GNPs; B) 20 nm GNPs; C) 40 nm GNPs; D) 60 nm GNPs; E) 80 nm GNPs; F) 100 nm GNPs and G) 150 nm GNPs.

4.4.7- Lateral flow detection of PCR products

In order to determine whether the antibody / hapten independent NALF devices could also detect un-purified PCR products, the devices were inserted into a 1:1 mixture of oligonucleotide functionalised GNPs (80 nm) and the products of an asymmetric PCR protocol. Images of these test strips and the corresponding electrophoresis gel stained with ethidium bromide can be seen in Figure 16. The results were obtained with an initial ratio of reverse to forward primer of 5:1.
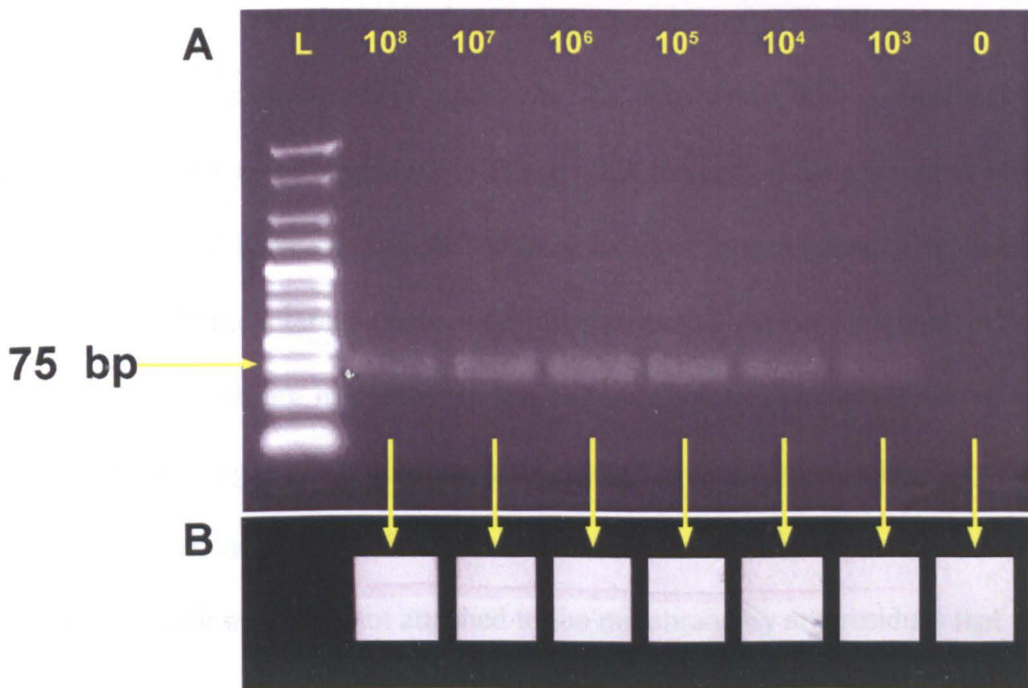
Figure 16: Results of PCR assays. A) Agarose gel stained with ethidium bromide. B) Test lines of lateral flow devices developed with 80 nm GNPs. Numbers denote the amount of template sequence at the start of PCR.

4.5-Discussion

4.5.1-Lateral flow detection of DNA

Many recent papers that describe chromatographic devices for nucleic acids detection are based at least in part on existing antibody-hapten technology.[15-17] As discussed in the introduction to this chapter, one of the principle disadvantages of this approach is the limited number of haptenylated primer / antibody combinations available for use with PCR. In addition, these haptenylated primers and labelled antibodies can be up to ten times more expensive than their unlabelled equivalents. In this work, an antibody-independent device was developed. In order to achieve this, the capture oligonucleotide was attached directly to the nitrocellulose membrane and non-haptenylated oligonucleotides were attached to GNPs. Oligonucleotides can be attached to nitrocellulose membranes by a number of different methods. In the simplest and most inexpensive approach, the oligonucleotide is attached by air drying or baking the membrane. Although this method of attachment is not fully understood, it is believed that the oligonucleotides are attached by a number of strong hydrophobic interactions between the membrane and the oligonucleotide.[18] In this approach, a strong link between the oligonucleotide and the membrane can be promoted by using capture oligonucleotides with a long hydrophobic poly-thymine (poly-T) tail at the 5' end. This also ensures that the oligonucleotides are in the correct orientation and are not attached to the membrane by any residues that may be essential for hybridisation.[18] A more complicated approach involves chemically functionalising the membrane and covalently attaching modified oligonucleotides. One of the most commonly used chemistries involves the attachment of thiol modified oligonucleotides to disulphide functionalised membrane via thiol-disulphide exchange reactions. Although chemical functionalisation is efficient, it

introduces additional costs and a limited number of attachment chemistries can be implemented as reactions must be carried out under mild conditions to prevent damage to the membrane. In addition, the reactive sites on the membrane must be stringently blocked before and after the attachment of oligonucleotide to avoid non-specific binding.[18] Oligonucleotides can also be introduced into membranes by covalently attaching them to large microparticles. Commonly known as the "boulders in the stream" approach, the particles are adsorbed onto the membrane and become trapped within the pores. The advantage of this approach is that the reaction between the oligonucleotide and the microparticle is carried out in the solution phase and as the membrane does not require chemical functionalisation, a wide range of attachment chemistries can be implemented.[18] In the antibody / hapten independent NALF device reported in this chapter, capture oligonucleotides with poly-T tails were striped directly onto nitrocellulose membranes and baked by BBInternational.

There are few strategies available that can be used to conjugate oligonucleotides to GNPs without the use of proteins or haptens. The most common approach is to attach oligonucleotides containing thiol groups to the GNP surface *via* the formation of dative covalent bonds. Mirkin and colleagues were the first research group to use this covalent interaction to conjugate oligonucleotides to GNPs and since this method was first reported in 1994,[19] the vast majority of oligonucleotide-GNP conjugates have been prepared in this way. Although relatively easy to perform, there are a number of drawbacks associated with this particular type of oligonucleotide conjugation. Firstly the yield of oligonucleotide-GNP conjugate obtained after purification is low, especially when larger sizes (>30 nm) of GNPs are coated, due to irreversible aggregation or adsorption of the coated nanoparticles to the reaction

vessel. This can make this particular conjugation method expensive. During this project, oligonucleotide-GNP conjugates were prepared by the method reported by Mirkin and colleagues. Due to yield of thiolated oligonucleotide received from the supplier and the irreversible aggregation and subsequent loss of GNPs during the functionalisation reaction, the cost of preparing 40 ml of 40 nm GNPs with a final OD of 1 was $634. Secondly, oligonucleotide-GNP conjugates prepared in this way can be rendered unstable when exposed to high temperatures and common thiol biological buffer additives, such as DTT and mercaptoethanol.[20] These conditions can cause the desorption of the thiolated oligonucleotides which subsequently leads to irreversible aggregation of the GNPs. More stable oligonucleotide-GNP conjugates can be prepared by conjugating oligonucleotides that contain multiple thiol groups to the GNP, but these more complex oligonucleotides are more expensive and are not as readily available as the mono-thiolated oligonucleotides. Thirdly, it has also been reported that under certain conditions, the individual bases of the attached oligonucleotide can electrostatically adsorb to the surface of the GNP which can inhibit hybridisation of this oligonucleotide with complementary oligonucleotides. Alivisatos and colleagues found that electrostatic adsorption of the bases was strongly influenced by the size and base composition of the oligonucleotide and the amount of oligonucleotide immobilised on the surface of the GNP.[21] They found that long oligonucleotide sequences or sequences containing a high number of guanine and cytosine bases were more likely to wrap around the GNP making them unavailable for hybridisation. Hamad-Schifferli and colleagues suggested that this electrostatic adsorption could be prevented by the addition of a low concentration of a competing thiol compound such as mercaptohexanol.[22] The main problem with this approach is that the reaction time has to be carefully

monitored and the mercaptohexanol solution has to be removed from the GNPs within the specified time to ensure that it did not completely displace the oligonucleotides from the GNPs. In addition, it is likely that the conditions required to displace different oligonucleotide sequences would differ and therefore the procedure would have to be optimised for each individual sequence.

In this work, to avoid the problems associated with the direct covalent attachment of oligonucleotides to GNPs and avoid the use of antibodies or haptens, oligonucleotides were covalently attached to aminodextran polymers that were also functionalised with multiple protected disulphide (PDP) groups. When mixed with GNPs, the disulphide groups rupture on contact and anchor the oligonucleotide functionalised dextran to the GNP *via* a plurality of dative covalent bonds. There are a number of advantages associated with this method of conjugation. Firstly, GNPs coated in this way exhibit increased stability in high temperatures and in the presence of competing thiol compounds such as DTT. This is because the functionalised dextrans are attached to the GNPs by multiple covalent bonds. In addition, as the oligonucleotides are attached to a polymer that coats the surface of the GNPs, electrostatic adsorption of the individual bases of the oligonucleotide to the GNP surface is avoided. Secondly, as the functionalised dextran is purified and characterized before it is attached to the GNPs conjugates can be prepared in minutes, in high yield and can be used without any further purification. This makes this particular method easy to perform and relatively inexpensive. For example, the cost of preparing 40 ml of 40 nm GNPs (1 OD) was $300.

In order to covalently attach oligonucleotides to aminodextran, it was first functionalised with aromatic hydrazines and PDP groups using NHS ester chemistry. Aldehyde terminated oligonucleotides were then reacted with the functionalised dextran as described in the methods section 4.3.4 and illustrated in Figure 8, section 4.4.2. Initially these oligonucleotide functionalised dextrans were purified by centrifugal filtration, but as the yields obtained from this method were low, covalent chromatography was investigated as an alternative method of purifying the dextran conjugates in high yield. Covalent chromatography is a technique that enables purification of molecules on the basis of their chemical structure.[23] During covalent chromatography the molecule to be purified is specifically but reversibly bound to a solid support. As the reagents used to synthesize oligonucleotide functionalised dextrans are expensive and it was necessary to optimize the covalent chromatography method in order to obtain the highest yields, a less expensive dye labelled dextran (Cy5 functionalised dextran) was synthesised (methods section 4.3.2 and illustrated in Figure 5, section 4.4.1). Following a series of optimisation experiments that determined the amount of covalent chromatography gel and correct conditions required to obtain the highest yields, oligonucleotide functionalised dextrans were purified using this method and then conjugated to GNPs. To demonstrate that the developed antibody-independent NALF device was able to detect nucleic acids a series of assays for a 32-mer target sequence that had a 20-mer 3'-terminal sequence complementary to oligonucleotides conjugated to the GNPs, and a 12-mer 5'-terminal sequence complementary to capture oligonucleotides anchored to the test line were performed. A diagram showing the key stages of nucleic acid detection in these assays is shown Figure 17. During the assays, the colour of the test line increased up to 2.5 pmol of target sequence and then decreased when this amount of

target was exceeded. The decrease in colour is attributed to the "hook effect". The term "hook effect" is commonly used to describe the decrease in signal that occurs in reagent excess binding assays when the amount of target exceeds the capacity of the reagent to bind it.[24] In this case, the amount of target sequence exceeded the number of capture oligonucleotides anchored to the nitrocellulose.
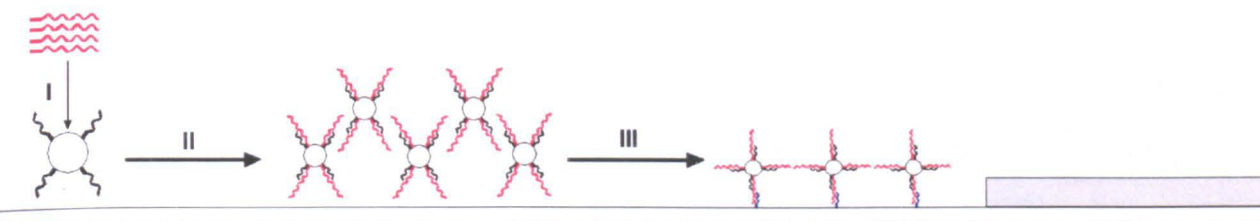
Figure 17: Diagram of antibody / hapten independent NALF device showing key stages in the assay for nucleic acids. I) Addition of sample; II) hybridisation of target sequences in sample to reporter oligonucleotides conjugated to GNPs; III) hybridisation of target sequences bound to GNPs with capture oligonucleotides anchored to the chromatographic strip.

4.5.2-Improving the sensitivity of NALF devices by changing GNP size

The widespread use of GNPs as labels in chromatographic devices is because these particles can be seen at very low concentrations with the unaided eye. For comparison the molar extinction coefficients of common dyes such as fluoresceins and rhodamines fall within the $10^4 - 10^6$ M^{-1} cm^{-1} range, but the extinction coefficients of GNPs are up to three orders of magnitude higher. As little as 1 x 10^9 40 nm diameter GNPs (the type most commonly used in chromatographic devices) can easily be seen with the unaided eye when they are bound to the test line of a typical lateral flow device. This allows femtomole amounts of analyte to be detected without any additional equipment, but, the theoretical sensitivities of immunoassays

and other nucleic acids assays are several orders of magnitude lower than this and therefore further increases in sensitivity are desirable.

Many different approaches have been applied to NALF devices to improve the sensitivity. For example, Lee and colleagues developed a signal amplification strategy for a multiplexed antibody-dependent NALF device in which oligonucleotides were labelled with multiple GNPs.[25] In this approach, target DNA in the sample hybridised to a target specific detector oligonucleotide that was labelled with multiple biotin haptens. Anti-biotin labelled GNPs then bound to the hybridised complex. As the detector oligonucleotides were labelled with multiple biotin haptens, multiple anti-biotin labelled GNPs could bind to the detector oligonucleotide forming a network that enhanced the signal. The GNP-oligonucleotide complex then migrated through the membrane by capillarity and was captured by the target specific capture oligonucleotide that was immobilised on the nitrocellulose membrane. A diagram of Lee and colleagues device detailing how they claim it works can be seen in Figure 18. Lee and colleagues used this format to detect 3 different target sequences. In order to achieve this they used 3 different target specific detector probes, all of which were labelled with multiple biotin haptens and the nitrocellulose strip was striped with 3 different target specific capture probes.
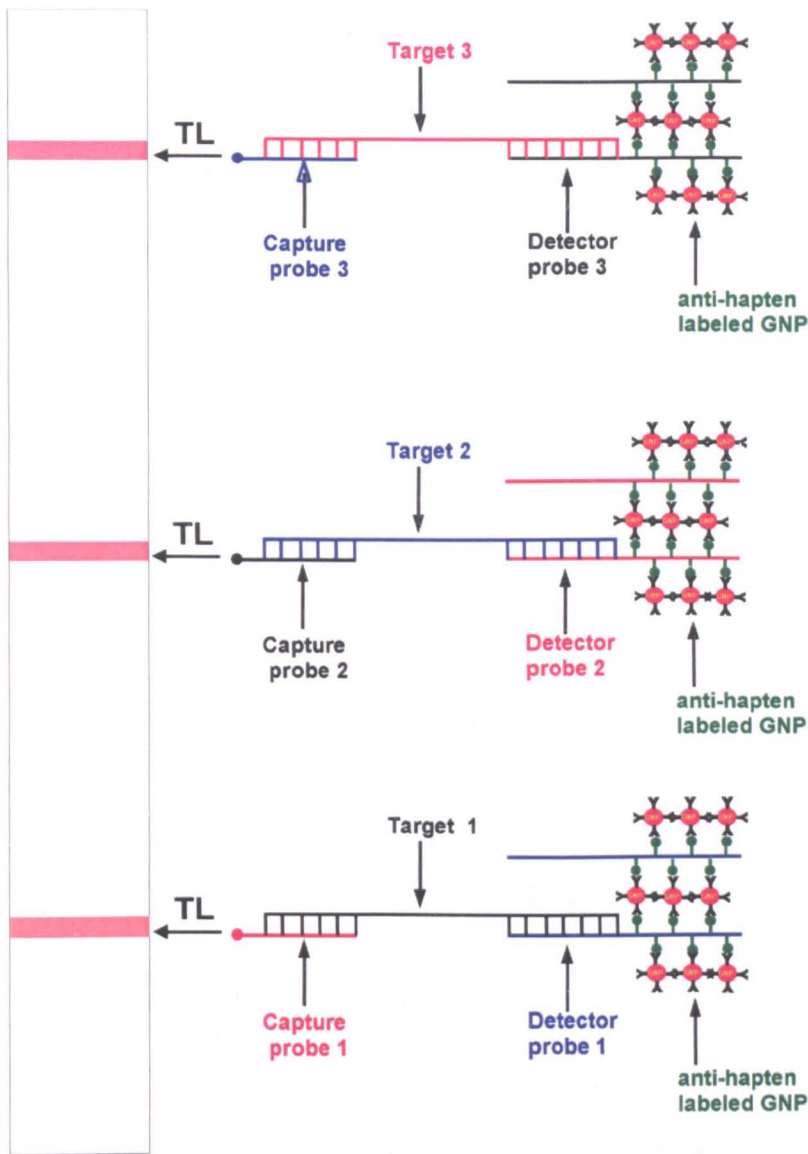
Figure 18: Diagram of the device developed by Lee and colleagues. Target DNA in the sample hybridises to a specific detector oligonucleotide labelled with multiple biotin haptens. Multiple anti-biotin labelled GNP bind to the hybridised complex and this migrates through the membrane by capillarity. The GNP-oligonucleotide complex hybridises to specific capture oligonucleotides immobilised on the nitrocellulose strip

There is a major problem associated with this approach which could lead to imprecise results; this is illustrated in Figure 19. The problem with this approach is that all of the specific detector probes are labelled with the same hapten. As Figure 19 shows, target 2 has hybridised to detector probe 2 and been captured, however, this is not visualised as all of the GNP labelled anti-biotin has bound to the network

of non-specific detector probes on target 1. For this same reason it is difficult to understand how Lee and colleagues can quantify the amount of target captured. If all three targets hybridised to the specific corresponding detector probe, to enable quantification, each signal would have to be amplified by the binding of a network of the same detector probe. The only way to combat this problem would be to use three detector probes, each labelled with a different hapten, and three corresponding antibody labelled GNPs.
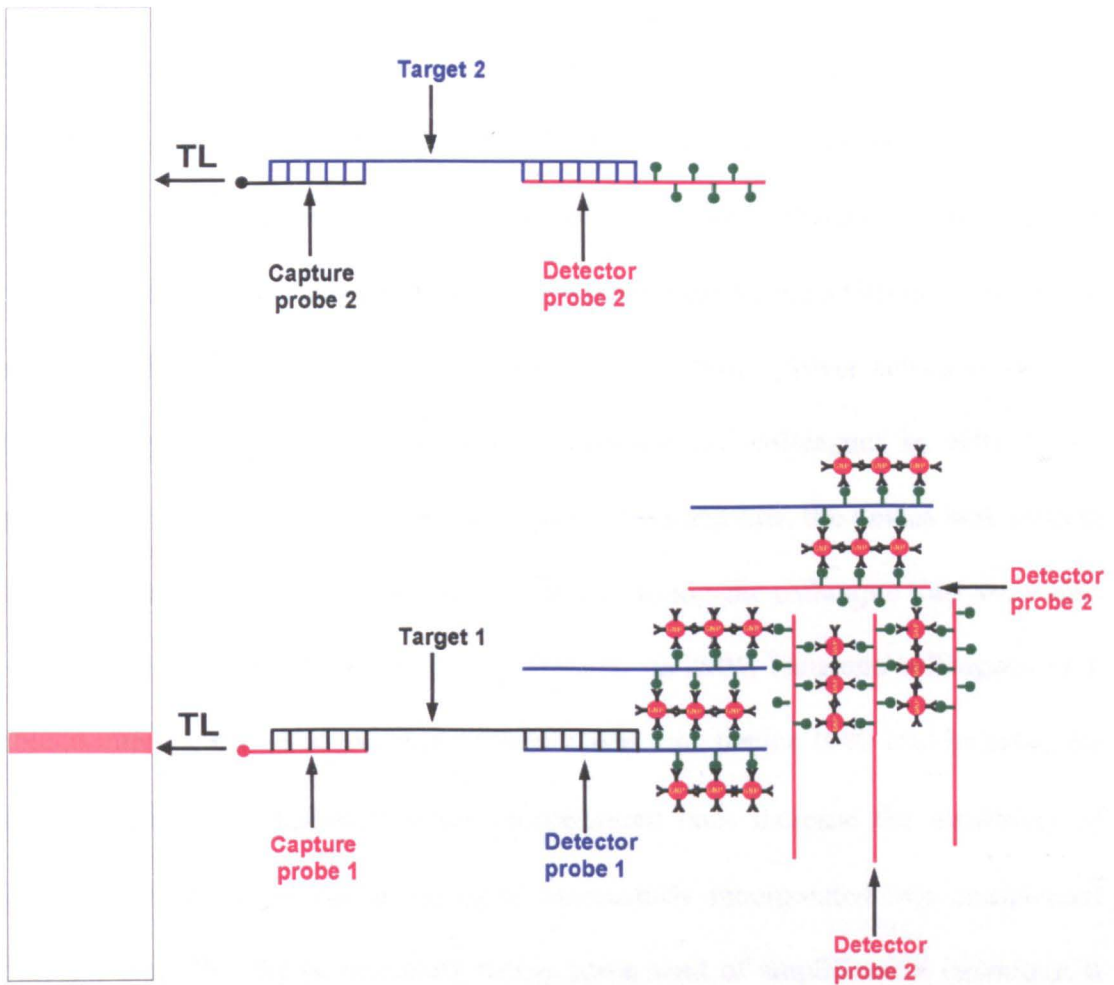
Figure 19: A diagram illustrating one of the problems associated with multiplexed detection on the NALF device developed by Lee and colleagues. Although specific hybridisation has occurred between target 2, detector probe 2 and capture probe 2, this is not visualised as all of the GNP labelled anti-biotin has bound to non-specifically bound detector probes on target 1.

The possibility of enhancing the signal from GNPs by using them as sites for the catalytic deposition of metallic silver has been widely used for many years. Metal particles can nucleate the highly specific deposition of silver from a silver salt solution in the presence of a suitable reducing agent. Once coated with silver, the GNP then catalyzes more silver deposition and the silver grains grow in size. In 1983 Holgate and colleagues were the first to use a silver enhancement step to enhance the signal generated by the binding of antibody labelled GNPs to antigens in tissue sections.[26] By enhancing the signal they were able to increase the sensitivity of antigen detection 200-fold which also enabled the visualization of this binding event by light microscopy. In 1984, this technique was applied by Moeremans and colleagues to improve the sensitivity of a membrane-based assay.[27] In this approach, a nitrocellulose strip with immobilised antigen was first soaked in a solution containing a primary antibody. The binding reaction between the antigen and primary antibody was then visualised on the membrane by the addition of secondary antibody labelled GNPs and silver enhancement solution. Silver enhancement was first employed in a lateral flow assay by Horton and colleagues in 1991.[28] To amplify the signal generated by GNPs bound to the test line, the device was washed then immersed in silver enhancement solution. Using the technique they were able to increase the sensitivity of the device 100-fold. In 2001, Tang and colleagues were able to improve the detection limit of their lateral flow device 1000-fold by using the same technique.[29] Although silver enhancement does increase the sensitivity of lateral flow detection, and it has been successfully incorporated into commercial devices, it would still be necessary to use some kind of amplification technique in order to detect low concentrations of nucleic acids.

In 2006, Tamiya and colleagues reported an alternative approach for improving the sensitivity of an immunochromatographic device, in which GNPs already bound to the test line were enhanced with a second wave of particles.[30] In this approach, primary antibody labelled GNP and unlabelled primary antibody were immobilised on the test line of a nitrocellulose strip. Antigen solution and secondary antibody labelled GNPs were mixed, applied to the strip and the bound antigen-secondary antibody labelled GNP complex migrated through the membrane by capillarity. The complex was then captured by the GNP labelled and unlabelled primary antibodies immobilised on the test line of the strip. Tamiya and colleagues also investigated the effect of changing the diameter of the GNP that was immobilised onto the membrane on the sensitivity of the immunochromatographic assay. They investigated GNP diameters in the range 5 – 100 nm and found that the sensitivity of the assay increased if they used primary antibody labelled particles with diameters in the range of 15 - 40 nm. Although Tamiya did not provide an explanation for this increase in sensitivity, it is likely that they did not observe increases in sensitivity with the particles larger than 40 nm due to steric hindrance effects between the GNP labelled and unlabelled primary antibodies immobilised on the test line and the GNP labelled secondary antibody.

Tamiya and colleagues conducted their investigations with an immunochromatographic device but until now the effect of GNP size on the sensitivity of NALF devices has never been investigated. In this work, GNP size was investigated to determine whether increasing the size of the GNPs would lead to an increase in sensitivity of the NALF assay. In all the NALF assays performed, the volume (50 μl) and O.D of the GNPs at 520 nm (1.0) was the same. In other words

185

the total absorbing power of GNPs on the NALF strip was the same for all diameters studied. Figure 20 shows the overlaid absorbance spectra of the GNPs intersecting at 1.0 O.D and how the sensitivity of normal human colour vision varies with wavelength. As the diameter of the GNPs is increased there is a red-shift in the absorbance spectrum into a region where the human eye was less sensitive. Figure 21 shows how the number of GNPs in 50 μl of a 1.0 O.D. solution decreased as the diameter on the NPs increased; there were, for example, approximately 8 times as many particles in the 40nm solution as there were in the 80 nm solution. The situation that obtains in NALF assays performed with GNPs having these diameters is shown in Figure 22. On addition of the sample, target sequences hybridize to oligonucleotides conjugated to the GNPs. Assuming the target sequences were evenly distributed each 80 nm particle is hybridised to 8 times as many target sequences as each 40 nm particle. The situation that obtains as the GNPs migrate through the test line can be understood by imagining what would happen if a ball covered with Velcro hooks was rolled across a narrow woolen strip orientated perpendicular to the direction its motion. A ball with 8 hooks would have a higher probability of binding to the strip than a ball with only one hook, and in the same way 80 nm particles hybridised to 8 times as many target sequences have a higher probability of binding to the test line than 40 nm particles. If the extinction coefficient of the GNPs was the only factor responsible for the increase in sensitivity, it would go on increasing as the diameter of the particles increased, but as explained above the increase in diameter is also associated with a red shift in the absorbance spectrum that eventually moves into a region where human vision is less sensitive. Therefore, instead of continuing to increase, the sensitivity levelled off at ~ 80 nm, and then decreased as the GNPs became less visible to the human eye.
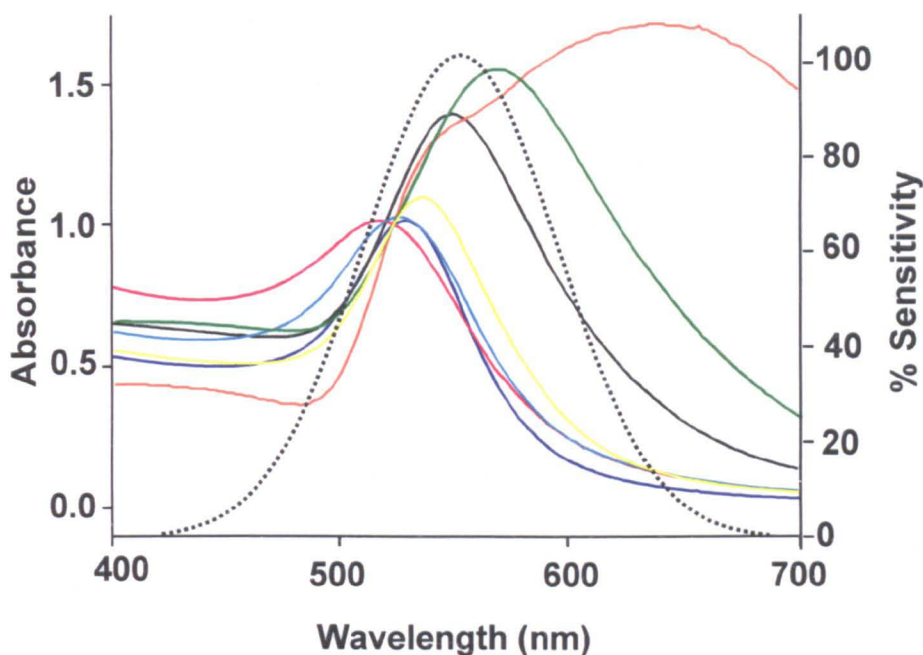
Figure 20: Overlaid absorbance spectra of all GNPs used in the sandwich assays. Key: Red = 10 nm; Light blue = 20 nm; Dark blue = 40 nm; Yellow = 60 nm; Black = 80 nm; Green = 100 nm; Orange = 150 nm. Dotted line= Sensitivity of normal colour vision plotted against wavelength.
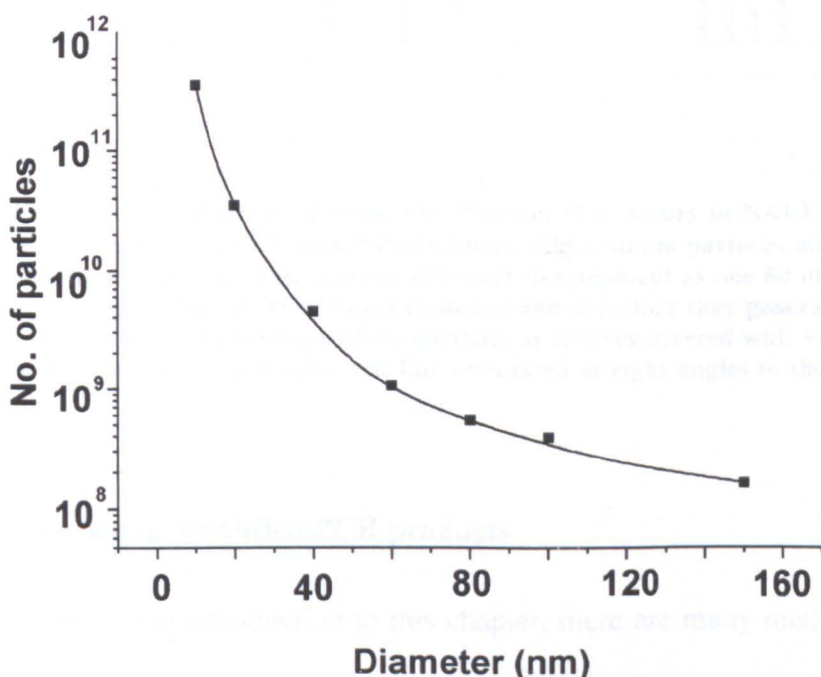
Figure 21: Graph of experimental data and line of best fit showing how the number of GNPs in 50 μl of 1 OD suspension (the amount used in all chromatographic assays) decreases as the diameter of the GNPs increases.
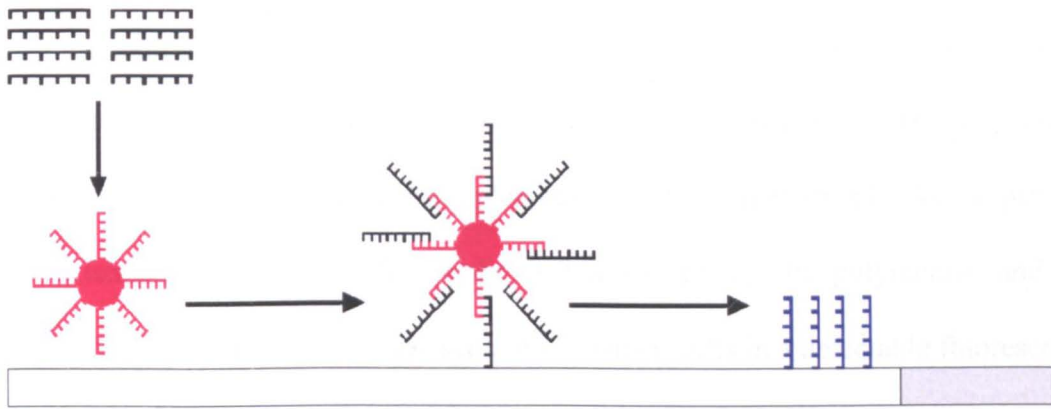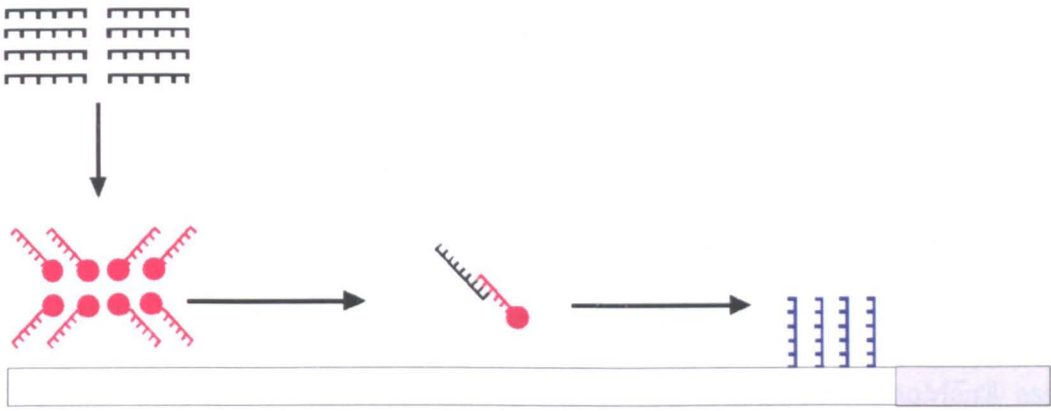
Figure 22: Schematic diagram showing the situation that occurs in NALF assays performed with 40 nm GNPs (top) and 80 nm GNPs (bottom). Eight 40 nm particles must be captured by the test line to produce the same amount of colour development as one 80 nm particle, but the latter have a higher probability of being captured and therefore they generate a higher signal. This can be understood by thinking of the particles as spheres covered with Velcro hooks rolling along the strip and across a woolen test line orientated at right angles to the direction of their motion.

4.5.3-Detection of amplified PCR products

As discussed in the introduction to this chapter, there are many methods available to detect amplified PCR products. The problem is that most of these methods are lengthy procedures that require skilled laboratory personnel and expensive equipment and reagents. In addition, some of these methods cannot identify the

specific target that has been generated (e.g. gel electrophoresis), and some are not amenable to multiplexed detection. In recent years, equipment has been developed that solves the latter of the problems listed above. Real-Time PCR (RT-PCR) is a technique that allows multiplexed amplification, identification and quantification of target DNA in real-time.[31] One commercially available RT-PCR system is based on TaqMan® probes developed by Applied Biosystems (Figure 23). TaqMan® assays utilise a dual-labelled oligonucleotide probe that is labelled with a fluorophore and a quencher dye. In the first stage, PCR primers and the TaqMan® probe hybridize to the complementary bases in the target strand. At this stage the fluorescence emitted by the fluorophore on the probe is quenched due to its close proximity to the quencher dye. In the second stage, DNA polymerase binds and extends the primers, adding free nucleotides that are complementary to the target strand. As the primers are extended, the dual-labelled probe is hydrolyzed by the polymerase and the fluorophore and quencher dye are separated. This results in a detectable fluorescence that is proportional to the amount of amplified product. Although RT-PCR enables amplification and detection in one step, the equipment and the reagents are expensive. In addition there are also issues with the multiplexing capability of these instruments. Currently, the most advanced RT-PCR machine is only capable of detecting four different targets and two controls at the same time. This is because detection relies on fluorescence and there are a limited number of suitable compatible fluorescent probes that do not have overlapping emission spectra.

Key:

5' ⊓⊓⊓⊓⊓ 3' Primer

DNA polymerase

5' F——————Q Taqman probe

Target

Step 1

Excitation

Step 2

Excitation **Emission**
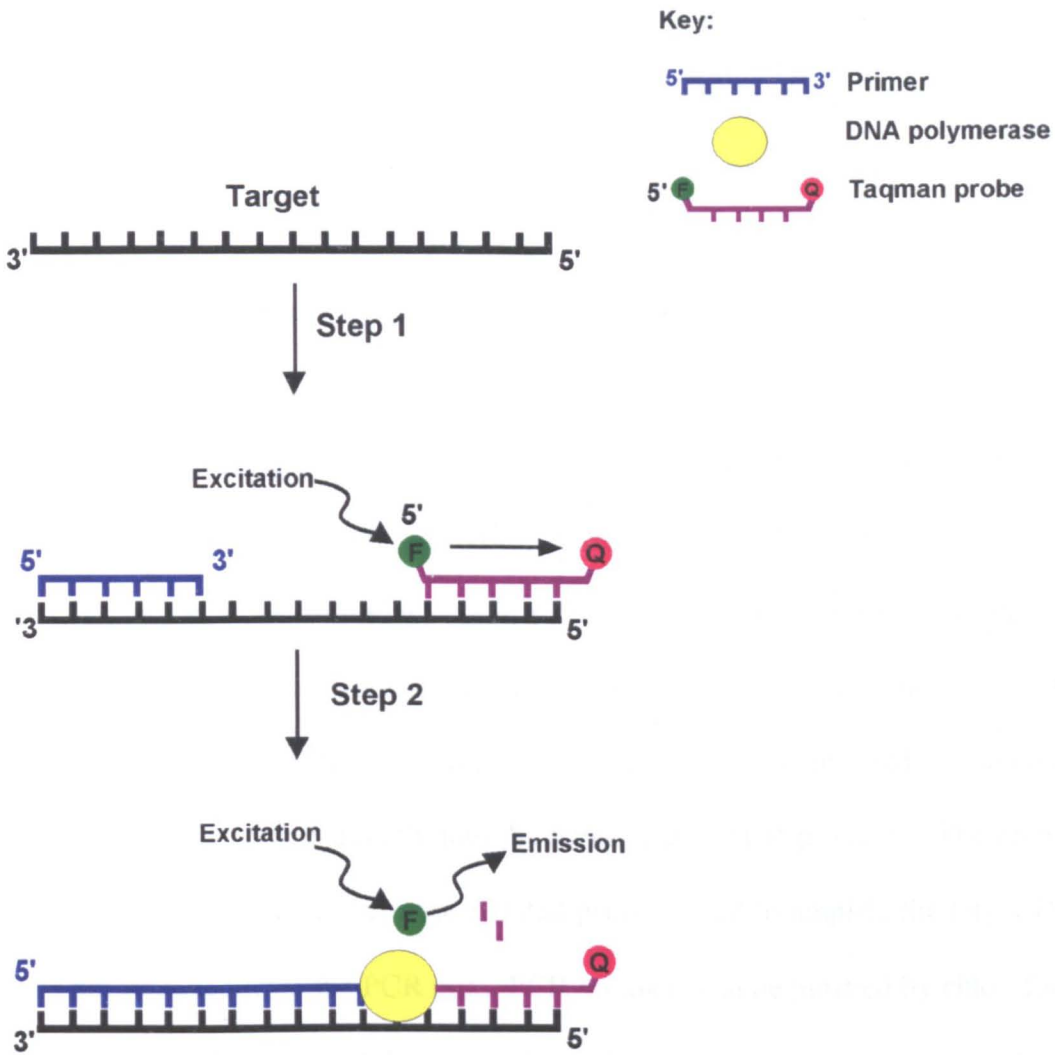
Figure 23: Diagram of the TaqMan RT-PCR system. In the first stage, PCR primer and the TaqMan dual labelled probe hybridize to complementary bases on the target strand. Fluorescence from the probe is quenched due to it's proximity to the quencher dye. In the second stage, the primer is extended by DNA polymerase. As the primer extends, nucleotide bases and the fluorophore label are displaced and fluorescence is emitted.

An alternative approach that could alleviate the multiplexing and cost issues associated with RT-PCR would be to develop an inexpensive, rapid and specific detection device that can detect multiple products and be interfaced with a PCR protocol. A great deal of work has been conducted in this area, however all of these devices are either based on antibodies and haptens, which as already discussed,

makes multiplexed detection difficult and expensive; require complicated PCR protocols to amplify the target sequences before detection; or require additional steps to enable detection of the target sequence between PCR and lateral flow. The additional steps are usually incorporated because PCR generates double stranded amplification products that must be rendered single stranded if they are to be detected by hybridisation with specific probes. Deborggraeve and colleagues added a reporter sequence to the PCR products, thermally denatured them and then re-annealed them before inserting a NALF device.[32] The problem with this approach is that the inclusion of additional steps increases the risk of user error and / or contamination. Hasagawa and colleagues did not include a denaturing or annealing step to detect PCR amplified products.[33] Instead they inserted an antibody-dependent NALF device directly into the haptenylated PCR products. The problem with this method was that the haptenylated primers used to amplify the target DNA were not removed from the PCR mix. PCR products can be purified by chloroform / phenol extraction followed by ethanol precipitation, however this procedure is technically demanding and requires safe handling of harmful reagents. There are a number of PCR purification kits that do not require phenol / chloroform available commercially. These purification kits are normally comprised of a silica membrane that selectively binds the PCR product and a selection of binding, washing and elution buffers of varying pH. The PCR product is applied and binds to the membrane then primers, enzymes and other PCR reagents are removed by washing the membrane with a wash buffer. Bound purified PCR product is then released from the membrane by the addition of an elution buffer. The problem with these kits is that they are often expensive and require the intervention of skilled personnel. As Hasagawa and colleagues did not purify the PCR mix, the haptenylated amplified

products would have been competing with the haptenylated primers for binding sites on the GNP labelled antibody and on the test strip. Although results were obtained using this particular format, sensitivity was inevitably limited and higher sensitivities could be achieved if a purification step to remove the haptenylated primers was included in the protocol.

Christopoulos and colleagues reported an even more complicated approach for the amplification and detection of nucleic acids. They used a two-step PCR protocol to boost the amount of amplification products that were generated, and then chemically denatured and annealed them in the presence of an added oligonucleotide probe before detecting them with a NALF device.[34] In this approach, one round of PCR was completed then the PCR product was subjected to a second round of PCR with different primers. After the second round of amplification, the oligonucleotide probe was added and the mixture was denatured with sodium hydroxide. Following a 10 minute incubation step, the mixture was neutralised by the addition of hydrochloric acid, subjected to another hybridisation step, then the target was detected with a NALF device. More recently the same group have used similar protocols to amplify target DNA enabling NALF detection of bacterial infections[35] and single nucleotide polymorphisms.[36] The problem with Christopoulos' approach is that it places a high technical demand on the user. The two step PCR protocol and subsequent denaturing, neutralising and hybridisation steps could increase the risk of user error and contamination. In addition, the necessity for multiple primers and probes for each target would make multiplexed detection expensive. As Christopolous' amplification strategy is so complicated the advantage of using a lateral flow device for detection instead of a standard laboratory technique is debatable.

The main objective of the work reported in this chapter was to reduce the complexity of nucleic acid detection with NALF devices to the bare minimum. To avoid complicated and expensive protocols the possibility of inserting the developed antibody / hapten-independent NALF device directly into un-purified PCR products at room temperature was investigated. Initially a standard PCR protocol was implemented to amplify target nucleic acids. However, when the NALF device was inserted into the products generated by this protocol, no colour developed at the test line of the strip. This was due to the presence of double stranded DNA products that could not be detected without first de-hybridizing the strands with a denaturing step. As a result, an asymmetric PCR protocol was used to amplify target DNA. Asymmetric PCR preferentially amplifies one strand of the original target DNA.[37] This is achieved by mixing an excess of the primer for the chosen strand. Amplification of the other strand slows as the limiting primer is used up during the exponential phase of the reaction resulting in the linear amplification of the chosen strand in successive cycles. Using the developed NALF device and an asymmetric amplification protocol it was possible to detect amplification products corresponding to ~1 attomole of template molecules with the unaided eye. Although similar amounts of PCR product can be detected by staining electrophoresis gels with a fluorescent dye, additional equipment and the intervention of a skilled technician is required. The NALF device also detects a specific target sequence, whereas electrophoresis only indicates that amplification products of a certain size have been generated and provides no other information about their identity. The results shown in Figure 16 (section 4.4.7) were obtained with an initial ratio of reverse to forward primer of 5:1 but a range of other ratios were also investigated. At ratios of 3.5:1 and 7.5:1 there was some colour development at the test line, but less than observed at a

ratio of 5:1, and at all other ratios no colour development was detected. The reduced

colour development at 3.5:1 was most likely because the ratio of reverse to forward

primers was not high enough. In this situation, although the desired strand would be

amplified, there would also a large amount of double stranded products present. In

this case, the ratio of reverse to forward primer was not sufficient to linearly amplify

the target strand. The reduced colour on the test line occurred because there was a

high concentration of double stranded products within the PCR mix that cannot be

detected on the strip. At the ratio of 7.5:1, the situation was reversed. As the

forward primer was limited, it did not produce enough template DNA for the reverse

primer. The maximum colour development at the test line was obtained when an

asymmetric PCR ratio of 5:1 was used, however, even at high template

concentrations the amount of colour developed at the test line was never as great as

when tests for single stranded target sequences in PBS were carried out. One

possibility was that hybridisation was inhibited by the presence of primers and / or

other components of the PCR mix, but when parallel tests with PCR mix spiked with

the 32-mer single stranded target sequence were carried out, the amount of colour

development was similar to the results shown in Figure 12 (section 4.4.5). In another

set of experiments, however, the amount of colour developed by the 32-mer target

sequence and the same sequence (underlined) nested between two 20 mer single

stranded extensions as would be generated in asymmetric PCR (5'-TCT CAA ACT

AGG ACC GAG TC <u>GGG ACT GAC GAT TCG GGT GAT ATC CAG AAC GCA</u>

<u>GAC AAG CAG GCA</u> GGA CTA CCA GGG TAT CTA AT) were compared.

There was a 50 % reduction in colour at the test line produced by the extended

sequence which suggested that steric hindrance was responsible for reduced colour

development in the PCR assays. In the future it might be advantageous to

incorporate spacers into the oligonucleotide attached to the GNP and / or capture sequences to accommodate this. The antibody / hapten independent device described in this chapter could be easily modified for detection of more than one target, but the PCR protocol would require optimisation for the amplification of multiple targets. Multiplexed asymmetric PCR is a complex procedure and successful amplification will require that the ratio between primers, the ratio of starting material to primers and the number of cycles for each individual target are optimised.[38]

Whilst PCR is still the principle amplification method of choice, a great deal of work has also been carried out on alternative amplification strategies. The main focus of this work has been to carry out the amplification of target DNA at a constant temperature (isothermal amplification), thus avoiding the need for thermal cyclers. The main advantage of this is that amplification and detection of target DNA can be carried out in resource limited settings as electricity would not be required. Many isothermal amplification techniques exist, such as cycling probe technology (CPT)[39] and nucleic acid sequence base amplification (NASBA)[40]. Like PCR, these techniques can also be easily interfaced with simple, inexpensive and user-friendly lateral flow devices. For example, Fong and colleagues used CPT (Figure 24) to amplify target sequences from methicillin-resistant *Staphylococcus aureus* and then detected the amplified products with a lateral flow device.[39] In step 1, an excess of a specific chimeric probe composed of DNA and RNA (DNA-RNA-DNA) labelled with fluorescein and biotin hybridises to the target strand. In step 2, the enzyme, RNase H, cleaves the RNA portion of the probe-target complex and the fragments of the probe are dissociated from the target strand. The target strand is then available for further hybridisation with other intact probe molecules and the cleaved molecules

accumulate. Fong and colleagues then used an antibody-dependent NALF device striped with streptavidin and anti-fluorescein labelled GNPs to detect the cleaved probe. In a different approach, Cary and colleagues used the NASBA technique (Figure 25) to amplify target sequences from *Bacillus anthracis*.[40] In this amplification technique, RNA is amplified using three enzymes. In the first step, Primer 1 with T7 RNA polymerase promoter binds to target single stranded RNA (ssRNA). In step 2, reverse transcriptase forms a cDNA copy of the RNA target (DNA / RNA hybrid). In step 3, RNaseH degrades the RNA component of the hybrid. In step 4, the second primer, which is complementary to an upstream portion of the RNA target anneals to the cDNA strand. This permits the DNA-dependent DNA polymerase activity of the reverse transcriptase to be engaged again, producing a double stranded cDNA copy of the original RNA analyte with a fully functional T7 RNA polymerase promoter at one end. This promoter is then recognised by the T7 RNA polymerase, which produces a large amount of single stranded RNA transcripts corresponding to the original RNA target. These RNA transcripts can then serve as templates for the amplification process, however the primers anneal in the reverse order. Following amplification, Cary and colleagues detected the products using a NALF device that had been adapted to increase multiplexing capability. Instead of striping the capture reagent onto the nitrocellulose, it was dispensed as small discrete spots like a microarray. This approach could lead to an increase in the number of target analytes that can be detected with a single strip, reduce the amount of sample required and reduce hybridisation time which ultimately leads to faster detection.

Key:

⌐⌐⌐⌐⌐⌐⌐⌐⌐⌐	Chimeric probe
● (red)	RNase H
● (green)	Fluorescein label
● (blue)	Biotin label
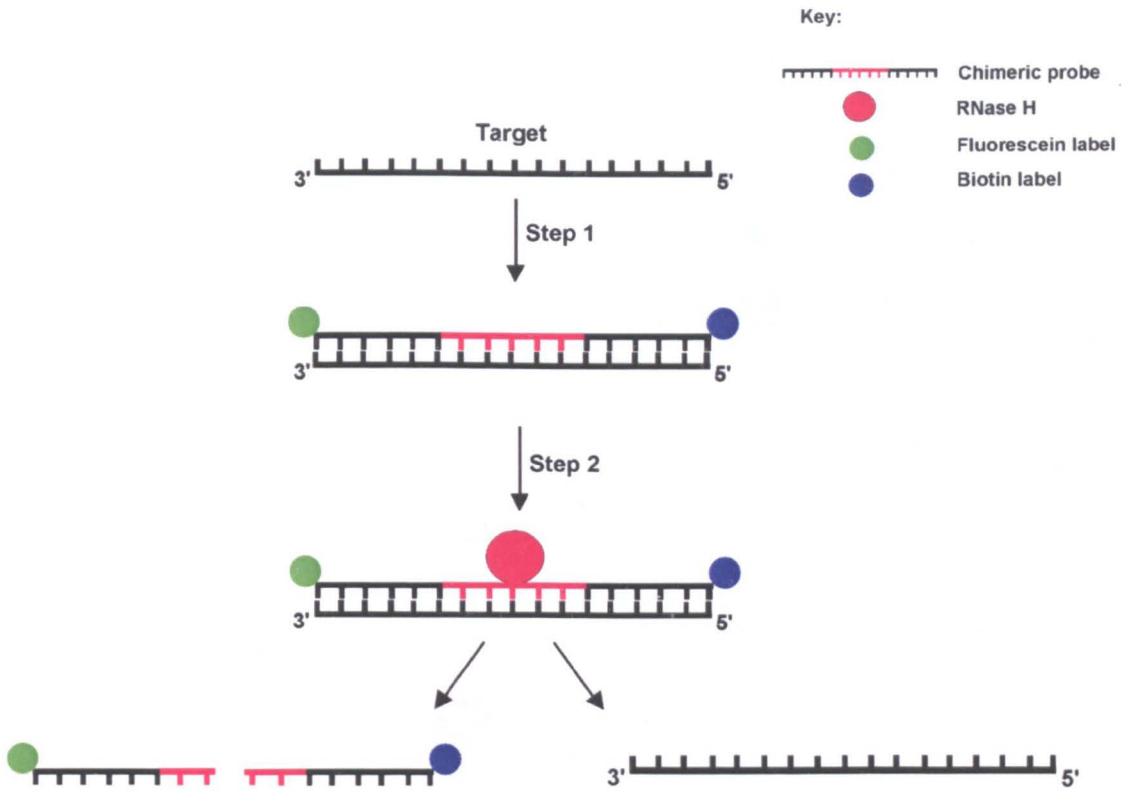
Figure 24: Diagram of cycling probe technology (CPT) used by Fong and colleagues to amplify target strands. In the first stage, an excess of specific chimeric labelled probe composed of DNA (black) and RNA (red) hybridises to complementary bases on the target strand. In the second stage, the enzyme RNase H cleaves the RNA portion of the probe and the probe dissociates from the target strand, leaving the target strand available for further hybridisation with other intact probe molecules.

Key:

ss-RNA

5' ———————————— 3'

Primer 1 with T7 RNA polymerase promotor

5' ——— 3' Primer 2

Reverse transcriptase

RNase H

Step 1

5' ———————————— 3'

5'

Step 2

RNA/DNA hybrid

5' 3'

3'

5'

Step 3

3'

3'

5'

Step 4

5'

3'

5'

ds cDNA copy

5'

3'

3'

5'

T7 RNA Polymerase

3' 5'
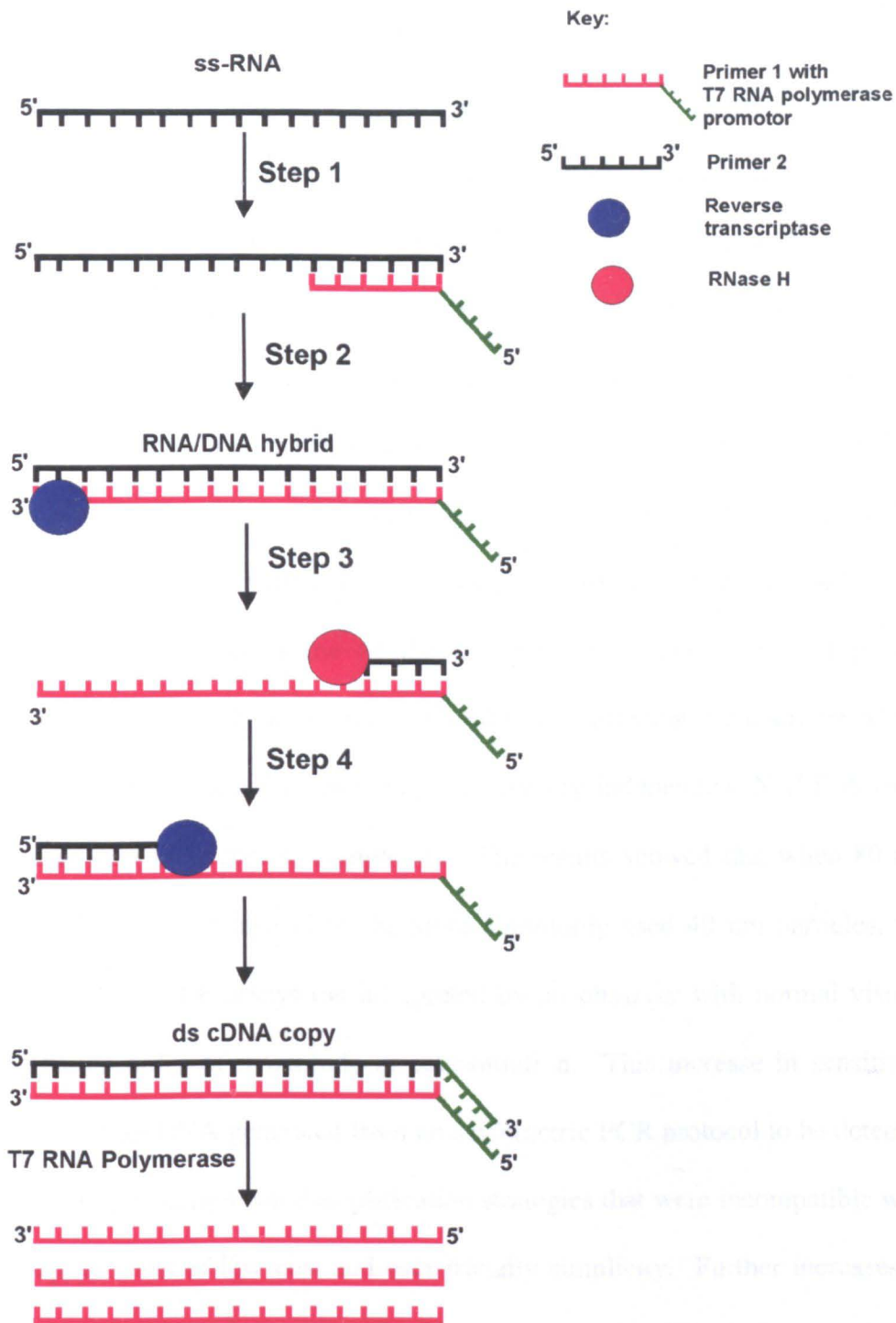
Figure 35: A diagram detailing the NASBA amplification technique. In the first step, Primer 1 binds to target single stranded RNA (ssRNA). In step 2, reverse transcriptase forms a RNA/DNA hybrid. In step 3, RNaseH degrades the RNA component of the hybrid. In step 4, the second primer anneals to the cDNA strand. This permits the DNA-dependent DNA polymerase activity of the reverse transcriptase to be engaged again, producing a double stranded cDNA copy of the original RNA analyte with a fully functional T7 RNA polymerase promoter at one end. This promoter is then recognised by the T7 RNA polymerase, which produces a large amount of single stranded RNA transcripts corresponding to the original RNA target.

4.6-Summary

In this chapter the development of a prototype NALF device that does not require antibodies or haptens was described. High molecular weight dextran polymers were functionalised with oligonucleotides, conjugated to GNPs and used as the detector reagent. Capture oligonucleotides with a poly-T tail were immobilised directly onto the test line of a nitrocellulose membrane and target oligonucleotide was detected using oligonucleotide functionalised GNPs. All other work in this area has been conducted with devices that were either based on antibodies and haptens, which make multiplexed detection difficult and expensive. By developing an antibody / hapten independent device, some of the problems associated with multiplexed detection are alleviated. Investigations showed that optimizing the diameter of the GNP labels could increase the sensitivity of antibody independent NALF devices without increasing their cost or complexity. The results showed that when 80 nm diameter GNPs are used instead of the more commonly used 40 nm particles, the sensitivity of the NALF assays (as interpreted by an observer with normal vision) increased by an order of magnitude in concentration. This increase in sensitivity helped allow target DNA generated from an asymmetric PCR protocol to be detected without resorting to complicated amplification strategies that were incompatible with the key requirements of low cost and user-friendly simplicity. Further increases in sensitivity, however, are desirable, and the results suggested how these could be obtained. Although other labels have been used in chromatographic devices, GNPs are the most popular choice because they are believed to offer the best combination of sensitivity, stability and ease of conjugation. Over a period of many years the diagnostics industry has identified 40 nm as the optimum diameter because larger particles are thought to hinder biomolecular reactions by steric hindrance and be

prone to aggregation.[41] However, it has been shown that the use of larger particles is not only possible but leads to an increase in sensitivity. The upper limit of this increase is imposed not by particle diameter *per se*, but by a red shift in the absorbance spectrum that accompanies the increase in size and which moves it into a region where the human eye is less sensitive. In order to obtain further increases in sensitivity, therefore, it would be necessary to use a label that retains the advantages of GNPs, but has a higher extinction coefficient in the region of the spectrum that is visible to the human eye. Silver NPs are known to have a higher extinction coefficient than GNPs of the same size and, as it has been shown elsewhere, they can be used for DNA detection.[42] Large silver NPs (~120 nm diameter) are reported to have absorbance maximum close to the wavelength at which the human eye is most sensitive[43] and their use as labels in chromatographic devices should lead to further increases in sensitivity. In addition, to the improvements in sensitivity, the simplicity and versatility of the developed NALF device suggests that it could also easily be interfaced with other amplification techniques such as CPT and NASBA.

4.7- References

1. Chargaff,E., Davidson, J.N. *The Nucleic Acids: Chemistry and Biology*, (1960), Academic Press, New York.

2. Fitch, J.P., Gardner, S.N., Kuczmarski, T.A., Kurtz, S., Myers, R., Ott, L.L., Slezak, T.R., Vitalis, E.A., Zemla, A.T., McCready, P.M. *P. IEEE*, (2002), **90**, 1708-1720.

3. Hill, C. *IVD Technology magazine*, (2000), Nov/Dec issue.

4. Stramer, S.L., Glynn, S.A., Kleinman, S.H., Strong, M., Caglioti, S., Wright, D.J., Dodd, R.Y., Busch, M.P. *N. Engl. J Med.*, (2004), **351**, 760-768.

5. Prescott, LM., Harley, J.P., Klein, D.A. *Microbiology*, (1996), Wm. C. Brown Publishers, London.

6. Rickwood, D., Hames, D.B. *Gel Electrophoresis of Nucleic Acids: A Practical Approach*, (1990), IRL Press, Oxford.

7. Southern, E.M., *J. Mol. Biol.*, (1975), **98**, 503-517.

8. Lockley, A.K., Jones, C.G., Bruce, J.S., Franklin, S.J., Bardsley, R.G. *Nucleic Acids Res.*, (1997), **25**, 1313-1314.

9. Seal, J., Braven, H., Wallace, P. *IVD Technology magazine*, (2006), Nov/Dec issue.

10. Aveyard, J., Mehrabi, M., Cossins, A., Braven, H., Wilson, R. *Chem. Commun.*, (2007), **41**, 4251-4253.

11. Robinson, N. *IVD Technology magazine*, (2002), March issue.

12. Hermanson, G.T. *Bioconjugate Techniques*, (1996), Academic Press, San Diego.

13. Carlsson, J., Drevin, H., Axen, R. *Biochem. J.*, (1978), **173**, 723-737.

14. Trilink Biotechnologies 2003 catalogue.

15. Fernandez-Sanchez, C., McNeil, C.J., Rawson, K., Nilsson, O., Leung, H.Y., Gnanapragasam, V. *J. Immunol. Methods.*, (2005), **307**, 1-12.

16. Chan, C.P.Y., Sum, K.W., Cheung, K.Y., Glatz, J.F.C., Sanderson, J.E., Hempel, A., Lehmann, M., Renneberg, I., Renneberg, R. *J. Immunol. Methods.*, (2003), **279**, 91-100.

17. Wang , S., Zhang, C., Wang, JP., Zhang, Y. *Anal. Chim. Acta.*, (2005), **546**, 161-166.

18. Jones, K.D. *IVD Technology Magazine*, (2001), July/Aug issue.

19. Mirkin, C.A., Letsinger, R.L., Mucic, R.C., Storhoff, J.J., *Nature*, (1996), **382**, 607-609.

20. Li, Z., Jin, R., Mirkin, C.A., Letsinger, R.L. *Nucleic Acids Res.*, (2002), **30**, 1558-1562.

21. Parak, W.J., Pellegrino, T., Micheel, C.M., Gerion, D., Williams, S.C., Alivisatos, A.P. *Nano Lett.*, (2003), **3**, 33-36.

22. Park, S., Brown, K.A., Hamad-Schifferli, K. *Nano Lett.*, (2004), **4**, 1925-1929.

23. Brocklehurst, K., Carlsson, J., Kierstan, M.P.J., Crook, E.M. *Biochem. J.*, (1973), **133**, 573-584.

24. Price, C.P., Newman, D.J. *Principle and Practice of Immunoassay* (1997), Macmillan Publishers, London.

25. Dineva, M.A., Candotti, D., Fletcher-Brown, F., Allain, J.P., Lee, H. *J. Clin. Microbiol.*, (2005), **43**, 4015-4021.

26. Holgate, C.S., Jackson, P., Cowen, P.N., Bird, C.C. *J. Histochem Cytochem.*, (1983), **31**, 938-944.

27. Moeremans, M., Daneels, G., Van Dijck, A., Langanger, G., De May, J. *J. Immunol. Methods*, (1984), **74**, 353-360.

28. Horton, J.K., Swinburne, S., O'Sullivan, M.J. *J. Immunol. Methods*, (1991), **140**, 131-134.

29. Tang, S, S., Shyu, R.H., Shyu, H. F., Liu, H.W. *Toxicon.* (2001), **40**, 255-258.

30. Tanaka, R., Yuhi, T., Nagatani, N., Endo, T., Kerman, K., Takamura, Y., Tamiya, T. *Anal. Bioanal. Chem.*, (2006), **385**, 1414-1420.

31. Molenkamp, R., van der Ham, A., Schinkel, J., Beld, M., *J. Virol. Methods.* (2007), **141**, 205-211.

32. Deborggraeve, S., Claes, F., Laurent, T., Mertens, P., Leclipteux, T., Dujardin, J.C., Herdewijn, P., Buscher P. *J. Clin. Microbiol.*, (2006), **44**, 2884-2889.

33. Suzuki, T., Tanaka, M., Otani, S., Matsuura, S., Sakaguchic, Y., Nishimura, T., Ishizaka, A., Hasegawa, N. *Diagn. Micr. Infec. Dis.*, (2006), **56**, 275-280.

34. Kalogianni, D.P., Bravou, V., Christopoulos, T.K., Ioannou, P.C., Zoumbos, N.C. *Nucleic Acids Res.*, (2007), **35**, e23.

35. Kalogianni, D.P., Goura, S., Aletras, A.J., Christopoulous, T.K, Chanos, M.G., Christofidou, M., Skoutelis, A., Ioannou, P.C., Panagiotopoulos, E. *Anal. Biochem.*, (2007), **361**, 169-175.

36. Litos, I.K., Ioannou, P.C., Christopoulous, T.K. *Anal. Chem.*, (2007), **79**, 395-402.

37. Poddar, S.K., *Mole. Cell. Probe.*, (2000), **14**, 25-32.

38. Aquiles Sanchez, J., Pierce, K.E., Rice, J.E., Wangh, L.J., *P. Natl. Acad. Sci USA*, (2004), **101**, 1933-1938.

39. Fong, W.K., Modrusan, Z., McNevin, J.P., Marostenmaki, J., Zin, B., Bekkaoui, F., *J. Clin. Microbiol.*, (2000), **38**, 2525-2529.

40. Carter, D.J., Cary, R.B., *Nucleic Acids. Res.*, (2007), **35**, e74.

41. Chandler, J., Gurmin, T., Robinson, N. *IVD Technology Magazine* (2000), March issue.

42. Chen, Y., Aveyard, J., Wilson, R., *Chem.Commun.*, (2004), 2804-2805.

43. Mock, J.J., Barbic, M., Smith, D.R., Schultz, D.A., Schultz, S., *J. Chem. Phys.*, (2002), **116**, 6755-6759.

One molecule per particle method for functionalising nanoparticles†

Robert Wilson,* Yang Chen and Jenny Aveyard

Department of Chemistry, Liverpool University, Liverpool, UK L69 7ZD. E-mail: R.Wilson@liv.ac.uk; Fax: 0151 794 3588

A mean of one biotinylated dextran molecule per particle is conjugated to 15 nm gold nanoparticles, by a process of self-assembly, which depends on the relationship between dextran molecular weight and particle size.

During the last few years the range of molecules that have been conjugated to gold and semiconductor nanoparticles has been extended by synthesizing thiolated derivatives, and conjugating them to the particles by dative covalent bonds.[1,2] Monothiolated oligonucleotides in particular have been conjugated to nanoparticles (NPs) and used in programmed self-assembly, hybridization assays, microarray analysis, enhanced surface plasmon resonance assays, dual labelled probes, and rapid test devices. Although monothiolated molecules are relatively easy to conjugate to nanoparticles they are also known to dissociate, especially at high temperature and in the presence of competing molecules such as mercaptoethanol.[3] Monothiolated oligonucleotides are readily available, but thiolated derivatives of most other probe molecules, such as haptens, are not. By contrast a wide range of molecules that can be covalently attached to primary amines have been synthesized and many of these are available commercially. In this paper we describe a method for conjugating an amine reactive derivative of biotin to a gold NP (GNP), by first linking it to a high molecular weight dextran polymer, and then conjugating the polymer to the particle by a plurality of dative covalent bonds. The number of polymers per particle is controlled by the relationship between the molecular size of the polymers and the surface area of the particles. This relationship allows a known number of biotin molecules to be conjugated to each particle. The specificity of the functionalized particles, and their ability to tolerate high temperature in the presence of competing thiols, is demonstrated in reactions with streptavidin-coated microbeads.

The method for functionalizing nanoparticles is shown schematically in Fig. 1. In the first step 2000 kDa aminodextran was functionalized with pyridyldithio propionate (PDP) and biotin by reacting it with the NHS (N-hydroxysuccinimide) esters of 3-(2-pyridyldithio) propionic acid (SPDP) and biotinamidocaproic acid (both from Sigma). The amounts of PDP and biotin in the purified product were determined with dithiothreitol (DTT)[4] and 4'-hydroxyazobenzene-2-carboxylic acid (HABA)[5] respectively. The final dextran concentration was calculated from the original concentration, and the volume of solution before and after purification. This allowed the mean numbers of PDP and biotin per dextran molecule to be calculated. The proposed structure of the biotinylated PDP dextran based on the results of these calculations is shown in Fig. 2.

Dextrans are long flexible polymers of D-glucose. Although there is some branching, molecules with MW of 2000 kDa have micrometer dimensions when extended. In the second step of the method the minimum amount of biotinylated PDP dextran required to prevent flocculation of 15 nm citrate-stabilized GNPs in the presence of PBS, (see ESI† for details), was conjugated to the particles. The dextran is bound to the particles by a plurality of dative covalent bonds that form when the disulfide bonds in PDP are broken on contact with the gold. Unlike certain other conjugation methods, which take more than two days,[1] this step is complete in a few seconds. The minimum amount of dextran required to stabilize the particles was found by adding different amounts of PDP dextran to a fixed amount of 15 nm citrate stabilized GNPs, followed by PBS. In the absence of sufficient dextran the solution changed color from red to purple due to flocculation of the GNPs. Flocculated particles were removed by passing the solution through a 0.2 µm PES filter. An image of the filtered particles and a plot of filtrate absorbance against the amount of dextran added is shown in Fig. 3. The minimum amount of dextran required to prevent flocculation corresponded to a mean of 1.05 dextran molecules per 15 nm particle. To our knowledge this is the first time that the similarity in size between biological molecules and nanoscale particles has been exploited in this way. Our results have also shown that for a given MW of PDP dextran there is a linear relationship between the minimum number of molecules required to prevent flocculation and the square of the particle diameter. This dependence on the square of the diameter suggests that the surface of a particle is enveloped by the dextran like a hand inside a glove. GNPs functionalized with this minimum

1) Functionalisation
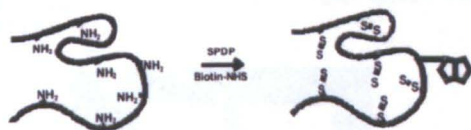
2) Self-Assembly

Fig. 1 The two-step conjugation method.
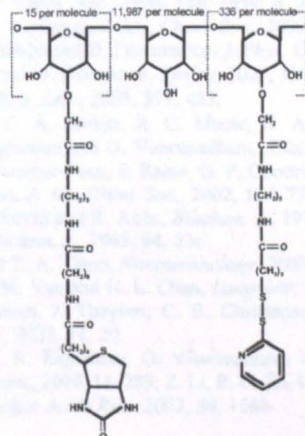
Fig. 2 Structure of 2000 kDa biotinylated PDP dextran.

"hand-in-glove" amount of dextran were used without further purification in the following experiments.

One aim of our work is to prepare nanoparticle conjugates that can be used in biomolecular assays. For this purpose it is important that probe molecules conjugated to the particles are able to react specifically with the corresponding binding molecule. The interaction of biotin (vitamin H) with avidin or streptavidin is one of strongest not-covalent affinities known. The strength of this interaction has led to its widespread use for specific targeting applications in biomolecular assays and self-assembly. To investigate the targeting properties of our particles we mixed different amounts with a fixed amount of white streptavidin-coated microbeads. Control experiments were carried out by incubating the beads with particles that were functionalized with PDP dextran, but not biotin. After 10 minutes the beads were washed, concentrated, and transferred to an in-house multiwell plate where they were imaged with a document scanner; the results are shown in Fig. 4. The pink color of the beads increased as the amount of biotin GNP conjugate increased, but the control beads remained white. This result shows that the functionalized particles bind specifically to streptavidin.

It is well known that monothiolated molecules conjugated to GNPs can dissociate, especially at high temperature in the presence of competing thiols such as mercaptoethanol and DTT.[3] These conditions are encountered during the polymerase chain reaction (PCR) and up until now there are no reported examples of functionalized GNPs that are stable under these conditions.[6] This has severely limited the range of applications for which GNPs are useful compared with otherwise inferior labels such as fluorescent dyes. The bond energy for molecules conjugated to GNPs by single bond between sulfur and gold is in the order of -30 to -40 kJ mol^{-1},[7] which corresponds to equilibrium constants (K_a values) of 0.2–10.4×10^6 M^{-1}. For comparison the K_a value for the biotin avidin interaction is 7.6×10^{14} M^{-1}. Clearly a situation in which a molecule is more tightly bound to the target molecule than to the particle is unsatisfactory. The stability of functionalized nanoparticle can be increased by conjugating probe molecules to the particles by more than one bond.[8] In the absence of intramolecular effects the K_a value for a molecule conjugated by n identical bonds is equal to $(K_a)^n$. The method described in this paper takes advantage of this effect by conjugating molecules to GNPs by a plurality of dative covalent bonds. To investigate their stability we exposed them to the conditions that are encountered during a typical PCR protocol. The buffer (30 mM tricine, pH 8.4, 2 mM MgCl) contained DTT up to a maximum concentration of 10 mM. The functionalized particles were heated to 94.5 °C for 1 minute, and then for 35 cycles of 94.5 °C (30 seconds), 37 °C (30 seconds) 72 °C (30 seconds), and finally for 10 minutes at 72 °C; the total time for the PCR protocol was 132 minutes. After allowing the solutions to cool, microbead assays were carried out as described above; a decrease in the number of biotins per particle would result in a decrease in the number of particles bound to the beads. Results showed that the particles were stable at DTT concentrations up to 1mM. At a DTT concentration of 10 mM the solution became slightly blue, indicating that some flocculation had occurred, but the particles still bound specifically to the beads. Biotinylated particles maintained at room temperature remained red and bound to the beads without loss of color at all the DTT concentrations that were studied. We expect that even more stable conjugates could be prepared by increasing the number of PDP groups per molecule of dextran.

In addition to biotin, we have used the method described here to conjugate a range of other molecules, including haptens, antibodies and oligonucleotides, to GNPs and semiconductor quantum dots. The method differs from other nanoparticle conjugation methods because the entire surface layer of the functionalized particle is synthesized prior to conjugation. This allows the surface layer to be purified and characterized at high concentration in the absence of interference from the particles themselves. The surface layer is then conjugated to the particles by a process of self-assembly, in which the number of polymer molecules per particle is determined by the relationship between polymer and particle size. Because the numbers of probe molecules per molecule of polymer and the number of polymer molecules per particle are both known, the number of probe molecules per particle is also known. Previous work has shown that the number of probe molecules per nanoparticle is important in optimizing the sensitivity of biomolecular assays, and at present we are using our method to optimize the sensitivity of several nanoparticle-based bioassays. We have also used it to prepare nanoparticles functionalized with known ratios of more than one different molecule per particle, which we expect to be useful in other areas of nanotechnology such as programmed self-assembly.
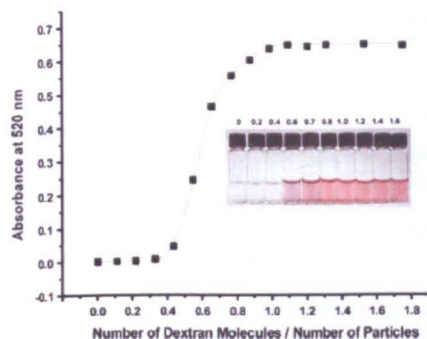
Fig. 3 Absorbance of filtrates at 520 nm showing how a minimum of 1.05 biotinylated PDP dextrans are required to prevent any decrease in absorbance. Inset: filtered GNPs; numerical values indicate number of dextrans per particle.
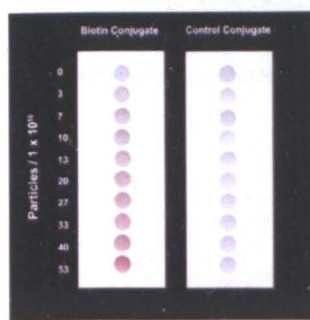
Fig. 4 Image of multiwell plate showing how colour of beads changed when they were incubated with increasing amounts of GNP conjugate.

Notes and references

1 J. J. Storhoff, R. Elghanian, R. C. Mucic, C. A. Mirkin and R. L. Letsinger, *J. Am. Chem. Soc.*, 1998, **120**, 1959; R. A. Reynolds, C. A. Mirkin and R. L. Letsinger, *J. Am. Chem. Soc.*, 2000, **122**, 3795.

2 S. Connolly, S. Cobbe and D. Fitzmaurice, *J. Phys. Chem. B*, 2001, **105**, 2222; M. Izumi and M. Shibakami, *Synlett*, 2003, 1395; D. Velic and G. Köhler, *Chem. Phys. Lett.*, 2003, **371**, 483.

3 L. M. Demers, C. A. Mirkin, R. C. Mucic, R. A. Reynolds, R. L. Letsinger, R. Elghanian and G. Viswanadham, *Anal. Chem.*, 2000, **72**, 5535; S. R. Nicewarner-Pena, S. Raina, G. P. Goodrich, N. V. Fedoroff and C. D. Keating, *J. Am. Chem. Soc.*, 2002, **124**, 7314.

4 J. Carlsson, H. Drevin and R. Axén, *Biochem. J.*, 1978, **173**, 723.

5 N. M. Green, *Biochem. J.*, 1965, **94**, 23c.

6 W. Fritzsche and T. A. Taton, *Nanotechnology*, 2003, **14**, R63.

7 M. Yang, H. C. M. Yau and H. L. Chan, *Langmuir*, 1998, **14**, 6121; R. Marie, H. Jensenius, J. Thaysen, C. B. Christensen and A. Boisen, *Ultramicroscopy*, 2002, **91**, 29.

8 R. L. Letsinger, R. Elghanian, G. Viswanadham and C. A. Mirkin, *Bioconjugate Chem.*, 2000, **11**, 289; Z. Li, R. C. Jin, C. A. Mirkin and R. L. Letsinger, *Nucleic Acids Res.*, 2002, **30**, 1558.

Supporting Information

Synthesis of biotinylated PDP dextrans

A 2.5 mg ml^{-1} solution of biotinamidocaproate N-hydroxysuccinimide ester (Sigma) in dry DMSO was used to prepare a 25 mg ml^{-1} solution of 3-(2-pyridyldithio) propionic acid N-hydroxysuccinimide ester (SPDP; Sigma). This solution (0.16 ml) was reacted with 4 ml of 2 mg ml^{-1} aminodextran (MW 2000 kDa; 351 primary amines per molecule; Helix Research, Springfield, OR) in 0.1 M sodium bicarbonate solution, for 2 hours at room temperature. At the end of this time the solution was dialyzed against water at 4°C. The final dextran concentration was calculated from the original dextran concentration and the increase in volume during dialysis. The corresponding PDP and biotin concentrations were determined with DTT and HABA respectively. Figure 1 shows the UV/vis spectrum of biotin substituted PDP dextran after dialysis. The peaks at 234 and 280 nm are due to PDP; biotin does not make a significant contribution to the spectrum and therefore it was determined by the displacement of HABA from avidin.
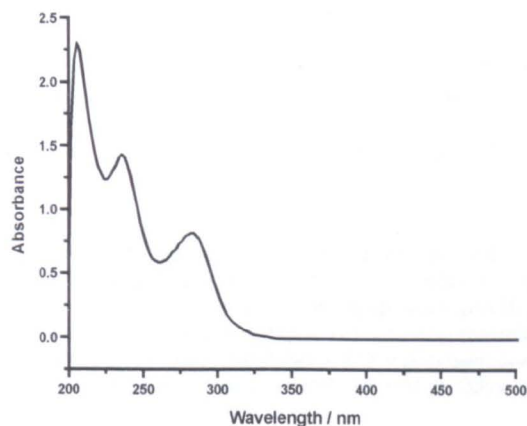
Figure 1 UV/vis spectrum of biotinylated PDP dextran.

Structure of PDP dextran

During dialysis, the dextran solution increased from a volume of 3.82 ml^{-1} to 5.53 ml^{-1}. Therefore the final dextran concentration was 1.38 mg ml^{-1}, or 0.69 µM assuming a MW of 2000 kDa. An aliquot of this solution was diluted 1:4 and assayed for PDP. The concentration of PDP corrected for dilution was 0.23 mM. A second aliquot of solution was assayed for biotin. The concentration of biotin was 10.4 µM. Therefore there were 336 PDP groups and 15 biotins per molecule of 2000 kDa dextran.

Conjugation of biotinylated PDP dextrans to 15 nm gold nanoparticles

Gold NPs of known diameter and number per ml were supplied by BBI International, Cardiff, UK; full details are available on their web site. The 15nm particles had a concentration of 1.4×10^{12} particles per ml. Different amounts of biotinylated PDP were added to a fixed number of GNPs. When high molecular weight PDP dextrans are conjugated to 15 nm GNPs intermediate dextran concentrations produce stable blue colloids; TEM images show that these blue colloids contain clusters of GNPs. Intermediate concentrations of low molecular weight dextrans do not produce stable blue colloids as shown in Figure 2. After diluting 1:3 with 3xPBS (45 mM sodium phosphate, 0.45 M NaCl, pH 7.5) the solutions were passed through a 0.2 µm polyethersulfone (PES) filter (Millipore) and the UV/vis absorbance spectra of the filtrates were recorded. The minimum number of PDP dextran required to prevent any flocculation is taken as the minimum amount that prevents any decrease in absorbance of the filtrate at 520 nm.
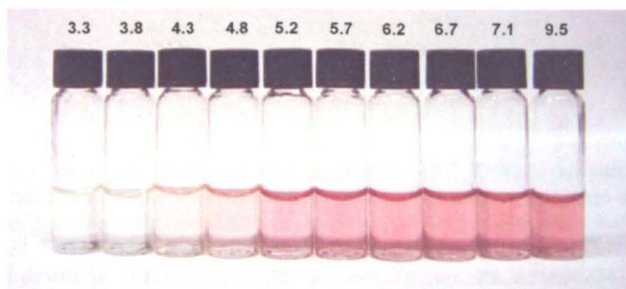
Figure 2 Filtered solutions of GNPs conjugated to 70kDa
PDP dextrans. Numerical values indicate the mean
number of dextran molecules per particle.

Microbead Assays

Different amounts of biotinylated gold nanoparticles were slow tilt rotated with 200 µg of streptavidin-coated
microbeads (0.56 µm diameter; Bangs Laboratories, Fishers, IN) in PBS (containing 1 mg ml^{-1}BSA and 0.5 % Tween-
20) for 10 minutes at room temperature. At the end of this time the beads were spun down at 300 g for 15 minutes in
PBS containing 0.5 % Tween-20 (twice) and at 9000 g in water (once). The final precipitate was evaporated to dryness
in a vacuum centrifuge, resuspended in 25µl of water, and imaged with a document scanner in an in-house multiwell
plate. Control experiments were carried out with the same numbers of gold particles conjugated to PDP dextran that
was not biotinylated.

PCR protocol

Figure 3 shows the results of microbead assays carried out on GNP conjugates that had been subjected to the PCR
protocol. Control experiments were carried out with the same number of gold particles conjugated to PDP dextran that
was not biotinylated.
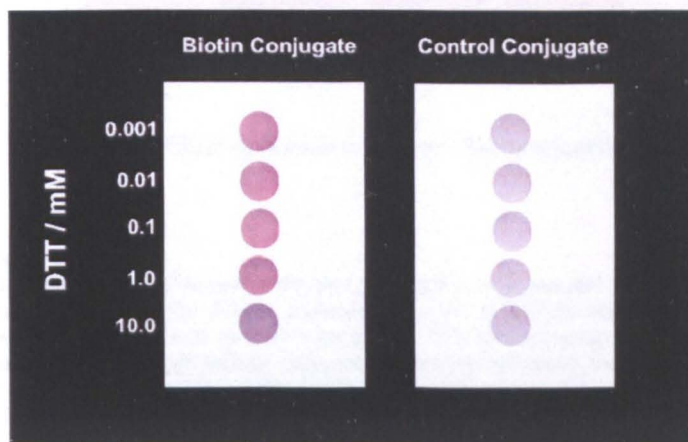
Figure 3 Effect of PCR protocol on affinity of GNP conjugates
for streptavidin-coated microbeads.

Hand-In-Glove

The effect of adding increasing amounts of 2000 KDa PDP dextran to a fixed amount of GNPs is shown in Figure 4. In the absence of PDP dextran, or at low ratios of dextran to particles (0.2 dextrans per particle), a black precipitate is formed, which can be removed by passing the solution through a 0.2 μm filter; the filtrates do not contain any particles. As the ratio of dextrans to particles is increased (0.6 dextrans per particle) stable blue solutions that do pass through a 0.2 μm filter are produced. TEM images show that these solutions contain clusters of GNPs. The size of the clusters decreases as the ratio of dextran to particles increases (0.7 and 0.8 dextrans per particle). At the minimum ratio of dextran to particles that prevents any decrease in absorbance (~1 dextran per particle) the solution is monodisperse. The minimum ratio required to prevent any decrease in absorbance depends on the MW of the dextran and square of the particle diameter; the latter is proportional to the surface are of the particles. These observations are consistent with the idea that the minimum ratio of dextran does not produce clusters because it is the lowest amount of dextran required to completely coat the surface of all the particles.

Number of Biotinylated PDP Dextrans per Nanoparticle

0   0.2   0.4   0.6   0.7   0.8   1.0   1.2   1.4   1.6

Number of Biotinylated PDP Dextrans per Nanoparticle

0.6   0.7   0.8   1.0
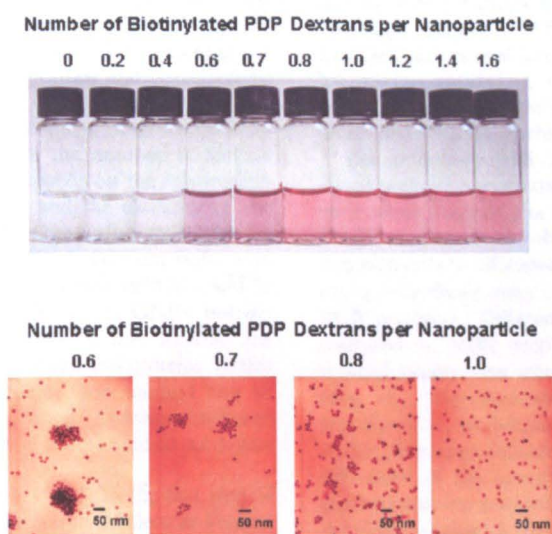
Figure 4 Effect of dextran to particle ratio on dispersity.

One Molecule Per Particle

How do we know that there is only one dextran molecule conjugated to each particle? What the paper actually says is that the minimum number of 2000 kDa dextran molecules required to prevent any flocculation of 15 nm gold nanoparticles corresponds to a mean of 1.05 molecules per particle. This does not mean that one molecule of dextran is conjugated to each particle because not all dextrans molecules or particles are exactly the same size. The values of 2000 kDa and 15 nm refer to the peak molecular weight of the dextran and the mean diameter of the particles respectively. This is why we refer to mean rather than absolute numbers of dextran molecules per particle. When we conjugate PDP dextrans to gold nanoparticles we add a known amount of dextran to a known number of particles, and therefore there is certainly a known ratio of dextran molecules to particles in the solution, but how do we know that all these dextrans are actually conjugated to the particles? If there was unconjugated dextran in the solution then the biotin molecules linked to it would decrease the sensitivity of our microbead assays. To investigate this we carried out microbead assays with biotinylated gold nanoparticles that had been washed by centrifugal precipitation and resuspension. This did not lead to any increase in sensitivity and therefore we conclude that all the dextrans are conjugated to the particles.

Gold and silver nanoparticles functionalized with known numbers of oligonucleotides per particle for DNA detection†

Yang Chen, Jenny Aveyard and Robert Wilson*

Department of Chemistry and Centre for Bioarray Innovation, Liverpool University, Liverpool, UK L69 7ZD. E-mail: R.Wilson@liv.ac.uk

The biospecificity of gold and silver nanoparticles, functionalized with known numbers of oligonucleotides, is demonstrated in colorimetric microbead assays for complementary and mismatch sequences.

The convergence of nanotechnology and biology is expected to produce major advances in diagnostics, therapeutics and materials science,[1] but the range of molecules that have been conjugated to nanoparticles is still limited. Recently we have reported a new type of conjugation method in which the entire surface of the NP conjugate is synthesized prior to conjugation.[2] The advantage of this approach is that the surface can be purified and characterized at high concentration in the absence of interference from the particles themselves. The surface is then conjugated to the particles by a process of self-assembly, in which the number of surface molecules conjugated to each particle depends on the relationship between MW of the surface molecules and the diameter of the particles. High stability is possible because the surface molecules are conjugated to the particles by multiple bonds between sulfur and gold.[2] In the previous report we showed how this method could be used to conjugate low MW organic molecules to GNPs, but the NHS ester chemistry used in this work is less suitable for hydrophilic molecules such as oligonucleotides and proteins. In this communication we show how this conjugation method can be extended to hydrophilic molecules using hydrazine/carbonyl chemistry. We also show that the method can be used to conjugate molecules to silver NPs.

The conjugation method is shown in Fig. 1. In the first step of the method molecules of 70 kDa aminodextran (Molecular Probes, Eugene, OR) were functionalized with hydrazone and disulfide groups by reacting them with C6-succinimidyl 4-hydrazinonicotinate acetone hydrazone (C6-SANH; Solulink, San Diego, CA) and 3-(2-pyridyldithio)propionic acid *N*-hydroxysuccinimide ester (Sigma) respectively, followed by purification on a gel-exclusion column. In the second step of the method the hydrazone functionalized PDP (pyridyldithiopropionyl) dextran was reacted with an excess of oligonucleotide terminating in an aromatic aldehyde group (Solulink). Unreacted oligonucleotide was removed with a centrifugal concentrator. In the third step of the method the oligonucleotides were conjugated to 9.3 nm citrate-stabilized GNPs of known concentration (5.7×10^{12} particles per ml; BBInternational, Cardiff, UK) by mixing them with the minimum amount of PDP-dextran-oligo required to prevent flocculation in the presence of PBS. The PDP-dextran-oligo is bound to the particles by bonds between sulfur and gold that form when the disulfide bonds in PDP are ruptured on contact with gold.[3] In the absence of enough
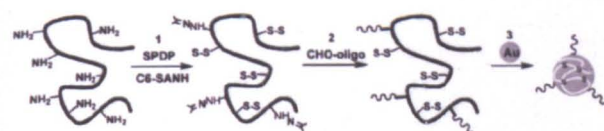
PDP-dextran-oligo the solutions changed colour from red to purple when PBS (15 mM sodium phosphate, 0.15 M NaCl, pH 7.5) was added, due to flocculation of the particles. Flocculated particles were selectively removed by passing the solution through a 0.2 μm filter. A plot of filtrate absorbance at 520 nm against the amount of oligonucleotide in PDP-dextran-oligo added is shown in Fig. 2. The minimum amount of oligonucleotide in the PDP-dextran-oligo required to prevent any decrease in absorbance due to flocculation corresponds to a mean of 29 oligonucleotides per particle. Once the minimum amount of PDP dextran required to prevent flocculation has been determined larger volumes of conjugate can be prepared by mixing equivalent ratios of dextran and particles. GNPs functionalized with this minimum amount of PDP-dextran-oligo were used without further purification in the following assays.

The immediate goal of our work is to prepare oligonucleotide functionalized nanoparticles that can be used for microbead and microarray analysis. For this purpose it is important that the oligo-GNP conjugate is able to hybridize specifically with the complementary oligonucleotide. To investigate this we carried out a microbead assay of the kind used to capture and quantify PCR products.[4] Different amounts of target oligonucleotide were captured on white streptavidin-coated microbeads, and then the washed beads were incubated with excess oligo-GNP conjugate (Fig. 3A). After one hour the beads were washed, concentrated and transferred to an in-house multiwell plate where they were imaged with a document scanner. The results (Fig. 3B) show that less than 500 fmol of the complementary oligonucleotide can be distinguished with the unaided eye. We also investigated the specificity of the GNP conjugate for base mismatch sequences. Although two-base mismatch sequences could be distinguished without difficulty, we were unable to distinguish single base mismatch-sequences even under stringent hybridisation conditions (Fig. 3B).

Recently there has been considerable interest in the use of silver nanoparticles as enhancers for surface enhanced Raman scattering (SERS).[5] This enhancement arises from the intense localized fields

Fig. 1 The three-step conjugation method.
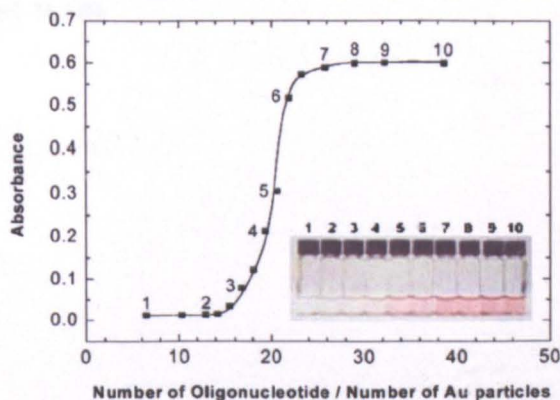
Fig. 2 Absorbance at 520 nm of filtered oligo-GNP solutions showing how the minimum amount of PDP-dextran-oligo required to prevent any decrease in absorbance corresponds to 29 oligonucleotides per nanoparticle. Inset: image of filtered solutions; numbers correspond to numbered points on the graph.
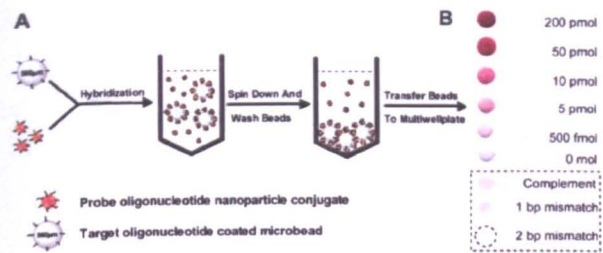
Fig. 3 (A) Schematic diagram of microbead assays. (B) Image of washed and filtered microbeads showing the effect of target oligonucleotide loading and sequence on colour. The oligonucleotide sequences were 5′ → 3′: GNP conjugate: CHO-GCGGCAGGTGCGACGCGGT; complement: biotin-ACCGCGTCGCACCTGCCGC; one base-mismatch: biotin-ACCGCGTCG*G*ACCTGCCGC; two base-mismatch: biotin–ACCG*GG*TCG*G*ACCTGCCGC.

that are associated with surface plasmon resonance in these particles. It allows low numbers of biological binding events to be detected when these result in an accumulation of Raman active molecules at the surface of the particles. Most of the work on silver nanoparticles has been carried out with non-specifically adsorbed molecules, which limits the range of materials that can be studied. To investigate whether our method could be used to conjugate molecules to silver we mixed different amounts of PDP-dextran-oligo with a fixed volume of 20 nm silver nanoparticles of known concentration (7×10^{10} particles per ml; BBInternational, Cardiff, UK). In the absence of enough PDP-dextran-oligo the solutions became colourless when PBS was added as shown in Fig. 4A. A plot of absorbance at 408 nm against the amount of PDP-dextran-oligo added showed that the minimum amount of PDP-dextran-oligo required to prevent any decrease in absorbance corresponded to a mean of 126 oligonucleotides per particle. Microbead assays with particles conjugated to this amount of dextran showed that as little as 500 fmol of complementary oligonucleotide could be detected with the unaided eye, as shown in Fig. 4B. These results demonstrate that oligonucleotides conjugated to silver nanoparticles with PDP-dextrans are suitable for use in biomolecular assays.

In summary we have shown how PDP-dextrans can be used to conjugate oligonucleotides to gold and silver nanoparticles for biomolecular assays. The oligonucleotides were first linked to PDP-dextrans using hydrazine/carbonyl chemistry. The advantages of this chemistry are that both functional groups are stable in aqueous solution for many weeks and the reaction between them can be performed under a variety of conditions that are compatible with biological molecules. We have also used this chemistry to conjugate proteins (antibodies) to gold nanoparticles after activating them with succinimidyl 4-formylbenzoate (Solulink). This suggests that our method can be used to conjugate a broad range of molecules to metal nanoparticles. A particular advantage of the method is that it allows a known number of one or more molecules to be conjugated
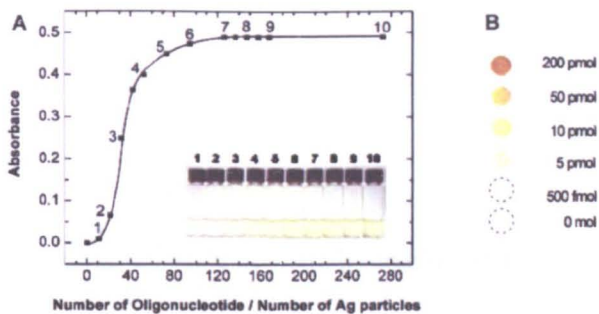
Fig. 4 (A) Absorbance at 408 nm of oligonucleotide silver nanoparticle solutions showing how the minimum amount of PDP-dextran-oligo required to prevent any decrease in absorbance corresponds to oligonucleotides per nanoparticle. Inset: image of unfiltered solutions; numbers correspond to numbered points on the graph. (B) Image of filtered microbeads showing the effect of oligonucleotide loading on colour.

to the same particle. In the examples described here we have demonstrated how known numbers of oligonucleotides can be conjugated to gold and silver nanoparticles. Previous work has shown that an ability to modulate the number of molecules conjugated to nanoparticles is important when optimising the sensitivity of biomolecular binding assays.[6] We expect that this advantage, along with the ability to conjugate well-defined ratios of two or more molecules (such as an oligonucleotide and a Raman active dye) to the same particle, will have important applications in the new generation of surface enhanced resonance Raman scattering (SERRS) based assays.

Notes and references

1 C. M. Niemeyer, *Angew. Chem., Int. Ed.*, 2001, **40**, 4128.
2 R. Wilson, Y. Chen and J. Aveyard, *Chem. Commun.*, 2004, 1156.
3 H. B. Lu, C. T. Campbell and D. G. Castner, *Langmuir*, 2000, **16**, 1711.
4 (a) C. S. Martin, L. Butler and I. Bronstein, *BioTechniques*, 1995, **18**, 908; (b) A. C. Syvanen, M. Bengstrom, J. Tenhunen and H. Soderlund, *Nucleic Acids Res.*, 1990, **16**, 11327.
5 (a) K. Faulds, W. E. Smith and D. Graham, *Anal. Chem.*, 2004, **76**, 412; (b) D. Graham, W. E. Smith, A. M. T. Linacre, C. H. Munro, N. D. Watson and P. C. White, *Anal. Chem.*, 1997, **69**, 4703.
6 (a) K. Okano, S. Takahashi, K. Yasuda, D. Tokinaga, K. Imai and M. Koga, *Anal. Biochem.*, 1992, **202**, 120; (b) S. Kubitschko, J. Spinke, T. Bruckner, S. Pohl and N. Oranth, *Anal. Biochem.*, 1997, **253**, 112; (c) M. Hall, I. Kazakova and Y. M. Yao, *Anal. Biochem.*, 1999, **272**, 165; (d) T. Soukka, H. Harma, J. Paukkunen and T. Lovgren, *Anal. Chem.*, 2001, **73**, 2254.

Supporting Information

Synthesis of PDP-dextran-oligo

A 25 mg ml^{-1} solution of C6-succinimidyl 4-hydrazinonicotinate acetone hydrazone (C6-SANH; Solulink, San Diego, CA) in dry DMSO was used to prepare a 25 mg ml^{-1} solution of 3-(2-pyridyldithio) propionic acid N-hydroxysuccinimide ester (SPDP; Sigma). This solution (0.16 ml) was reacted with 4 ml of 2 mg ml^{-1} 70 kDa aminodextran[1] (22 primary amines per molecule of dextran; Molecular Probes, Eugene, Or) in PBS, for 2 hours at room temperature. The dextran was purified on Sephadex G-25 with 0.1 M sodium acetate buffer (pH 4.5) as the eluent. For other reports describing the synthesis of PDP dextrans functionalized with bio-specific probes see references 2 and 3. An excess of oligonucleotide with a 5'-terminal aldehyde group (Solulink) was reacted with hydrazone functionalized PDP-dextran in acetate buffer, overnight at 4°C. Then unreacted oligonucleotide was removed with a 30 kDa MWCO centrifugal concentrator (Millipore); the washing solution was ice-cold HPLC grade water. The UV/vis spectrum of the oligonucleotide functionalized PDP dextran (PDP-dextran-oligo) is shown in Figure 1A. The peak at 360 nm corresponds to hydrazone bonds between the oligonucleotide and the dextran (ε_{360} = 1.8 × 10^{4}). Most of the absorbance at 280 nm is due to oligonucleotides (ε_{260} = 1.63 × 10^{5}), but separate determination with dithiothreitol (DTT)[4] showed that the remainder (13%) was due to PDP. The structure of the PDP-dextran-oligo is shown in Figure 1B.

Gold NP titration

Variable amounts of PDP-dextran-oligo were mixed with 0.75 ml of 9.3 nm GNPs (7 x 10^{12} particles per ml; BBInternational, Cardiff, UK) and then the solution was diluted 1:3 with pH 7.4 buffer solution to give final concentrations of 15 mM phosphate and 0.15 M
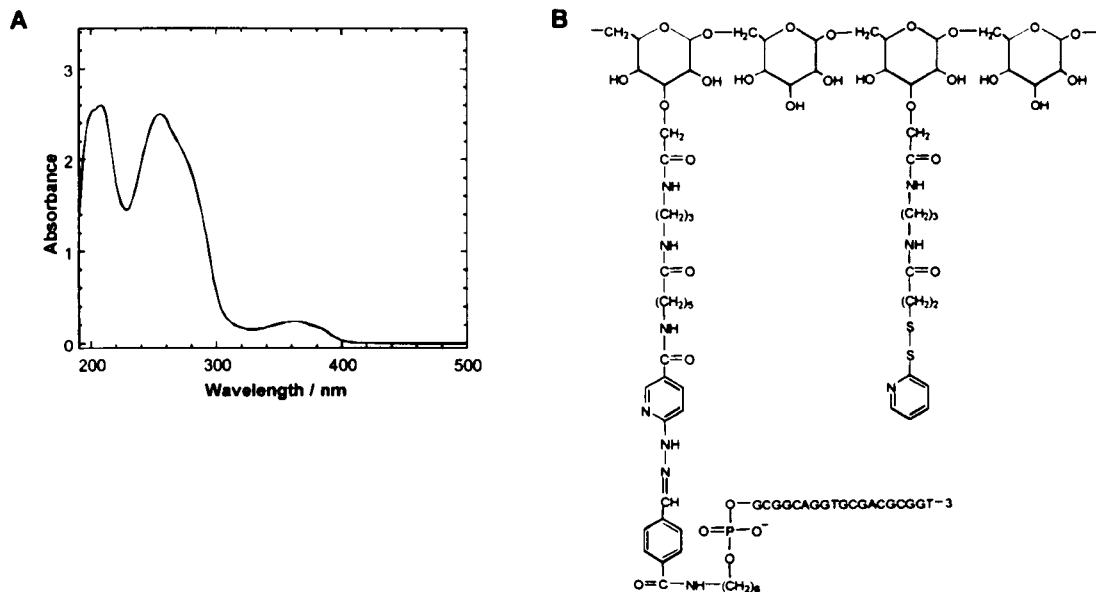
Figure 1 A) UV/vis spectrum of PDP-dextran-oligo; B) Structure of PDP-dextran-oligo. One 70 kDa dextran molecule is a mainly linear polymer (there is some branching) of 431 anhydroglucose monomers, of which a mean of 17 were derivatized with PDP and with 4 with oligonucleotides.

NaCl. The solutions were passed through a 0.2 μm PES filter (Millipore) and the UV/vis absorbance spectra of the filtrates were recorded. The absorbance at 520 nm was plotted against the ratio of oligonucleotides per particle in the solution prior to filtration. The minimum amount of PDP-dextran-oligo required to prevent flocculation was taken as the minimum amount that did not result in a decrease in absorbance at 520 nm. This corresponded to a mean of 29 oligonucleotides per particle.

Silver NP titration

Variable amounts of PDP-dextran-oligo were mixed with 0.75 ml of 20 nm Silver NPs (7 x 10^{10} particles per ml; BBInternational) and then the solution was diluted 1:3 with pH

3

7.4 buffer solution to give final concentrations of 15 mM phosphate, 0.15 M NaCl. The particles were not filtered because (unlike gold) there was no spectral interference between dextran-coated and flocculated particles.

DNA detection with gold nanoparticles

The target oligonucleotide was captured on microbeads by incubating (slow-tilt rotating) 200 µg aliquots of streptavidin-coated beads (560 nm diameter, Bangs Laboratories, Fishers, IN) with different amounts of 5'-terminal biotinylated oligonucleotide. Based on the manufacturers data sheet each aliquot of beads could bind a maximum of 218 pmols of biotinylated oligonucleotide. The amount of oligonucleotide incubated with the beads was always less than the maximum binding capacity of the beads. This incubation step is identical to the procedure used to isolate target sequences from polymerase chain reaction products prior to quantification.[5,6] The sequence of the target oligonucleotide was complementary to the sequence conjugated to the gold nanoparticles. Any unbound oligonucleotide was removed from the beads by centrifugal precipitation at 9000 g in PBS, containing 0.05% Tween-20, four times. The beads were then slow-tilt rotated with excess oligo-GNP conjugate in hybridization solution (10 mM sodium citrate, pH 7.0, containing 0.5 M NaCl, 1 mg ml^{-1} BSA, 1 mg ml^{-1} glucose and 0.5% Tween-20) for 1 hour at room temperature. Then the beads were washed for 15 minutes at 300 g in PBS (three times) and at 9000 g in water (once). The final precipitates were evaporated to dryness in a vacuum centrifuge, resuspended by sonicating in 21 µl of water, and then imaged in an in-house multiwell plate with a document scanner. Numerical values given in Figures 3B and 4B of the paper are based on the assumption that the amount of

4

biotinylated oligonucleotide captured by the beads was the same as the amount of oligonucleotide that was incubated with the beads. This assumption is based on the high association constant of the biotin streptavidin binding reaction, but is should be understood that that the numerical values given in these figures refer to the maximum amount of target oligonucleotide bound to the beads. Figure 2 shows TEM images of oligo-GNP conjugate hybridized to beads loaded with 200 pmol of the complementary oligonucleotide. Less than 10 % of the bead surface is covered with GNP conjugates, which suggests that the dynamic range of the microbead assay could be extended for at least one more order of magnitude.
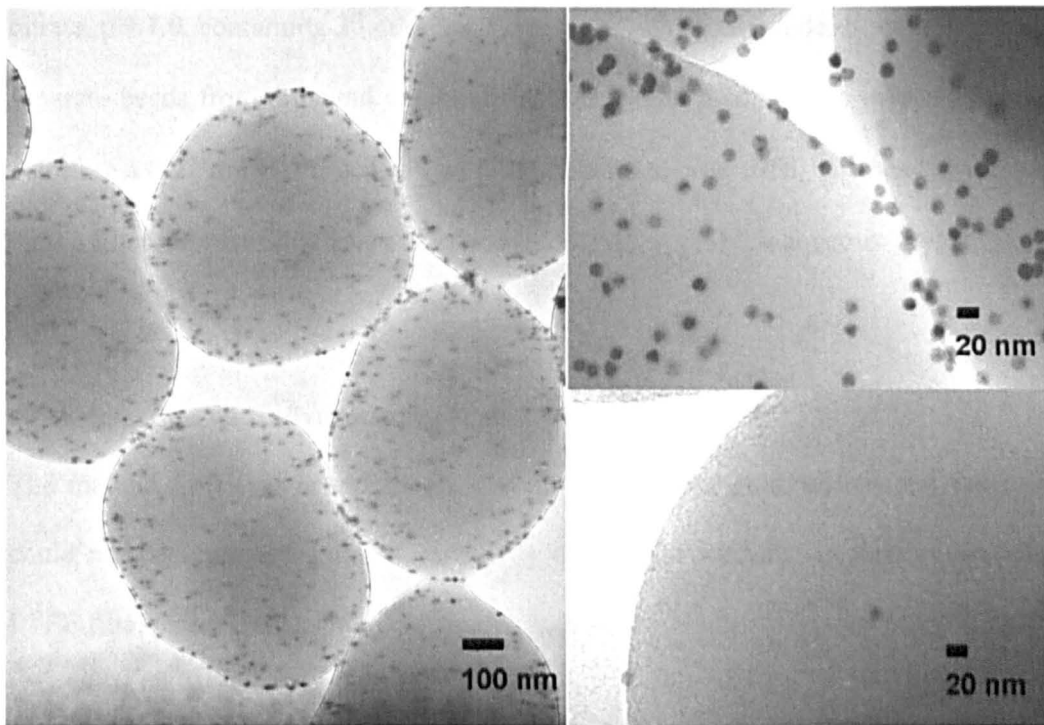
Figure 2 TEM images of oligo-GNP conjugate hybridized to beads loaded with 200 pmol of target oligonucleotide (left and upper right) and no target control bead (lower right).

Mismatch assays

DNA hybridization is not an all-or-nothing process. Under the right conditions sequences with less than 100% homology can form duplexes. In order to distinguish between complementary and mismatch sequences it is necessary to hybridize under high stringency conditions. In this work we increased the stringency of the hybridization buffer by adding formamide and decreasing the ionic strength of the hybridization buffer. Microbeads were coated with the target by slow-tilt rotating the beads with an excess of the biotinylated target (mismatch) oligonucleotide. The beads were then washed to remove unbound target oligonucleotide as described above and slow-tilt rotated with an excess of oligo-nanoparticle conjugate. The hybridization solution was 10 mM sodium citrate, pH 7.0, containing 30 mM NaCl and 70 % (v/v) formamide. It was not possible to separate beads from unbound conjugate by centrifugal precipitation in this solution and therefore a 0.22 µm PTFE centrifugal filter (Millipore) was used. The beads were imaged on the filter after washing away unhybridized GNPs with 0.5% aqueous Tween-20.

DNA detection with silver nanoparticles

The method for silver nanoparticles was the same as for gold, except that the particles could not be separated from the beads by centrifugal washing, and therefore 0.22 µm PTFE filters were used as in the mismatch assays.

A Known Number Of Oligonucleotides Per Particle

We use gold and silver nanoparticles of known size and concentration supplied by BBl. The mean diameter of these nanoparticles has been determined by dynamic light scattering and the number of particles per ml is based on the OD at 520 nm. The concentration of oligonucleotides in the PDP-dextran-oligo solution is known from calculations based on the UV/vis spectra shown in Figure 1. A known volume of particles is mixed with the minimum volume of PDP-dextran-oligo that prevents flocculation in PBS. After mixing the particle concentration and the oligonucleotide concentration are both known, and therefore the mean number of oligonucleotides per particle in the solution can easily be calculated, but are all the oligonucleotides conjugated to the particles? We use this solution for microbead assay without further purification. If there were unconjugated oligonucleotides in the solution they would decrease the sensitivity of these assays. To investigate this we carried out microbead assays with oligonucleotide-functionalized nanoparticles that had been washed by centrifugal precipitation. Purification by this method would remove any unconjugated oligonucleotides, but it does not lead to an increase in sensitivity, and therefore we conclude that all the oligonucleotides are conjugated to the particles.

References

1. R. Wilson, C. Clavering, A. Hutchinson, *J. Electroanal. Chem,* 2003, **557**, 109.

2. R. Wilson, C. Clavering, A. Hutchinson, *Analyst*, 2003, **128**, 480.

3. R. Wilson, Y. Chen, J.Aveyard, *Chem. Commun.* 2004, 1156.

4. J. Carlsson, H. Drevin, R. Axen, *Biochem. J.*, 1978, **173**, 723.

5. C. S. Martin, L. Butler, I. Bronstein, *BioTechniques*, 1995, **18**, 910.

6. A.C. Syvanen, M. Bengtstrom, J. Tenhunen, H. Soderlund, *Nucleic Acids Res.*, 1988, **16**, 11327.

One step visual detection of PCR products with gold nanoparticles and a nucleic acid lateral flow (NALF) device†

Jenny Aveyard,[a] Maryam Mehrabi,[a] Andrew Cossins,[b] Helen Braven[c] and Robert Wilson*[a]

Specific PCR products are detected with an antibody-free lateral-flow device by sandwiching them between reporter oligonucleotides covalently attached to gold nanoparticles (GNPs) and capture oligonucleotides covalently attached to a nitrocellulose chromatographic strip.

Lateral flow devices based on antibodies were first introduced in the 1980s and have subsequently become one of the most important products of the multibillion-dollar diagnostics industry. Their success has been based on a combination of low cost and simplicity that allows untrained personnel to undertake immunoassays in extra-laboratory environments such as a physician's office or hospital bedside without additional equipment. In their most simple embodiment these devices consist of a porous strip striped with a test line of antibodies or antigens, and fitted with a reagent pad impregnated with antibodies conjugated to a label that can be seen at low concentrations with the unaided eye.[1–3] Most often the porous strip is made of nitrocellulose and the label consists of GNPs. On insertion of this device into a sample, the liquid migrates along the chromatographic strip and solubilizes the labeled antibodies. Analyte antigens in the sample bind to the antibodies and their presence or absence is then indicated by the extent of colour development at the test line as the labeled antibodies bind to it. During the last few years these lateral flow devices have been adapted for nucleic acid detection,[4–6] but because they are still based on haptens and antibodies they are unnecessarily complicated and expensive. In a typical example, nucleic acids are amplified with haptenylated primers and detected by sandwiching them between antibodies conjugated to GNPs and a nitrocellulose membrane striped with adsorbed antibodies (Fig. 1A). In this communication we describe a nucleic acids lateral-flow (NALF) device that does not depend in any way on antibodies or haptens (Fig. 1B) and show how it can be used to detect unpurified PCR products with the unaided eye.

In order to avoid using GNPs conjugated to antibodies or an equivalent protein such as streptavidin, we conjugated reporter oligonucleotides directly to GNPs (for a full description of the methods see ESI†). Briefly high molecular weight mercaptodextrans were covalently attached to oligonucleotides and purified by covalent chromatography.[7] The purified dextrans were then

[a] Department of Chemistry, Liverpool University, Liverpool, L69 7ZD, UK
[b] Department of Biological Sciences, Liverpool University, Liverpool, L69 7ZB, UK
[c] BBInternational, Golden Gate, Ty Glas Avenue, Llanishen, Cardiff, CF14 5DX, UK. E-mail: R.Wilson@liv.ac.uk

† Electronic supplementary information (ESI) available: materials and methods. See DOI: 10.1039/b708859k
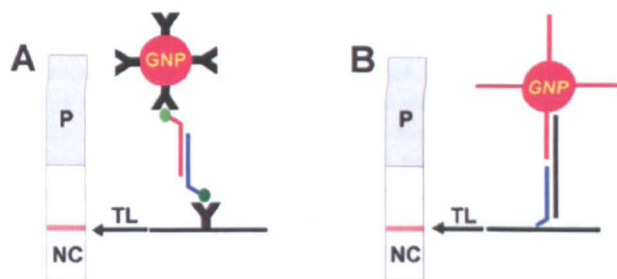
Fig. 1 Simple lateral flow devices consist of a strip of nitrocellulose (NC) striped with a test line (TL) of capture probes. When the device is inserted into a liquid sample, GNPs conjugated to reporter probes migrate along the nitrocellulose and through the test line in the direction of an absorbent pad (P). A) Section through test line of lateral flow device based on haptens (green circles) and antibodies. B) Section through test line of antibody-free lateral flow device.

conjugated to GNPs as described previously.[8] Simple lateral flow devices were constructed by striping (spraying) a sheet of plastic backed nitrocellulose with narrow lines of 5'-tailed oligonucleotides. Oligonucleotides tailed with poly-dT$_{20}$ can be covalently attached to dried nitrocellulose by irradiating it with UV light. After covalent attachment of the capture oligonucleotides, the nitrocellulose was cut into strips and fitted with an absorbent pad. To demonstrate that these devices could detect nucleic acids we performed a series of sandwich assays for a 32 base target sequence (5'-GGGACTGACGATTCGGGTGATATCCAGAACGCAG-ACAAGCAGGCA) that had a 20 base 3'-terminal sequence complementary to the reporter oligonucleotides, and a 12 base 5'-terminal sequence complementary to the capture oligonucleotides. Fig. 2 shows images of strips acquired after performing a series of sandwich assays for different amounts of the target sequence in the range 0–10 pmol. The colour of the test line increased up to 2.5 pmol of target sequence and then levelled off and decreased due to the hook effect that occurred when the amount of target sequence exceeded the number of capture oligonucleotides anchored to the nitrocellulose; this is shown

Fig. 2 Results of antibody-free nucleic acid lateral flow tests for a 32 base target sequence. Numbers show amounts of target sequence in pmol.

Fig. 3 Comparison between lateral flow tests developed with different sized GNPs. **A)** 40 nm; **B)** 80 nm; **C)** 150 nm. Numbers show amounts of 32 base target sequence in pmol.

graphically in the ESI†. There was no detectable colour development in the presence of 10 pmol of a non-complementary target sequence (5′-GACTCGGGGGATATCACTGATAACG-GTCAGGACGCAAAGGCACAG) and therefore the sensitivity (<50 femtomoles) was determined primarily by the amount of GNPs that could be seen with the unaided eye. The images in Fig. 2 show devices that were developed with 80 nm diameter GNPs, but we also performed assays with other diameters in the range 10–150 nm. Fig. 3 shows selected examples of how the amount of colour developed at the test line increased as the diameter of the GNPs increased from 10 to 80 nm (Figs. 3A and 3B) and then decreased as the diameter increased to 150 nm (Fig. 3C). A full set of images for all diameters studied is shown in the ESI†.

In all of these lateral flow tests the volume (50 μl) and O.D of the GNPs at 520 nm (1.0) was the same. In other words the total absorbing power of GNPs used to develop the devices was the same at all diameters studied. Fig. 4A shows the overlaid spectra of all the GNPs that were studied intersecting at 1.0 O.D. and Fig. 4B shows how the sensitivity of normal human colour vision varies with wavelength. As the diameter of the GNPs is increased there is a red-shift shift in the spectrum that eventually moves it into a region where the human eye is less sensitive. Fig. 4C shows how the number of GNPs in 50 μl of a 1.0 O.D. solution decreased as the diameter of the NPs increased; there were, for example, approximately 8 times as many particles in the 40 nm solution as there were in the 80 nm solution. In other words the extinction coefficient of the 80 nm GNPs (due to absorbance and scattering) is 8 times higher than the extinction coefficient of the 40 nm particles. The situation that obtains in chromatographic tests performed with GNPs having these diameters is shown in Fig. 5.

On addition of the sample, target sequences hybridize to reporter oligonucleotides conjugated to the GNPs. Assuming the target sequences are evenly distributed each 80 nm particle is hybridized to 8 times as many target sequences as each 40 nm particle, and therefore the 80 nm particles have a higher probability of binding to capture oligonucleotides in the test line than 40 nm particles. If the extinction coefficient of the GNPs was the only factor responsible for the increase in sensitivity, it would go on increasing as the extinction of the particles increased, but as explained above the increase in diameter is also associated with a red shift in the absorbance spectrum that eventually moves it into a region where human vision is less sensitive. Therefore, instead of continuing to increase, the sensitivity levelled off at 80 nm, and then decreased as the GNPs became less visible to the human eye.

The results shown in Fig. 2 show that less than 50 fmol of single stranded target DNA can be detected with 80 nm GNPs, but the amount present in real samples is generally much less than this. The yield of DNA from a biopsy sample, for example, would typically be in the order of 3×10^5 copies (0.5 amol) of target sequence, which is well below the detection limit of our devices and of most other detection techniques. For this reason, an important requirement of devices like ours is that they can be interfaced with some form of amplification technique such as PCR. The results in Fig. 6 show the test lines of lateral flow devices that have been inserted into unpurified PCR mixtures (see ESI† for methods) at room temperature and the corresponding electrophoresis gel stained with ethidium bromide. It was possible to detect amplification products corresponding to 1000 template molecules (~0.002 amol) with the unaided eye. Although similar amounts of PCR product can be detected by staining electrophoresis gels with fluorescent dyes, this approach requires additional equipment and
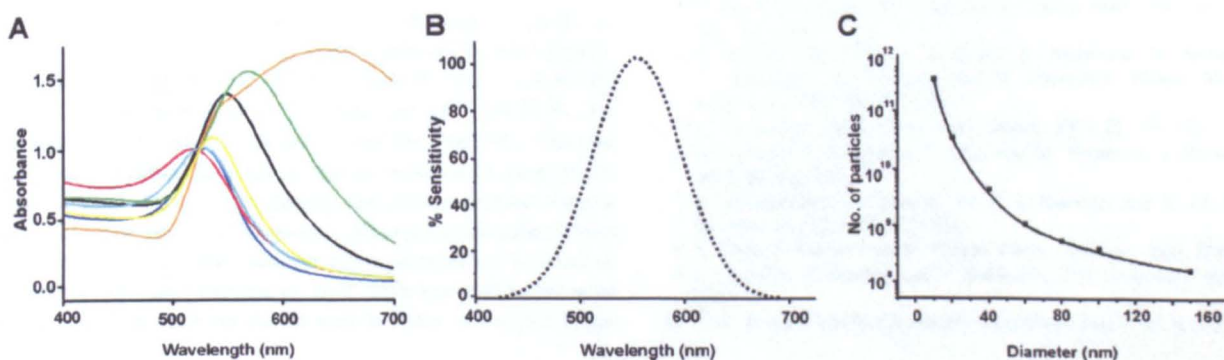
Fig. 4 **A)** Overlaid absorbance spectra of all GNPs used in the sandwich assays. Key: Red = 10 nm; Light blue = 20 nm; Dark blue = 40 nm; Yellow = 60 nm; Black = 80 nm; Green = 100 nm; Orange = 150 nm. **B)** Sensitivity of normal colour vision plotted against wavelength. **C)** Graph of experimental data and line of best fit showing how the number of GNPs in 50 μl of 1 O.D. suspension (the amount used in all chromatographic assays) decreases as the diameter of the GNPs increases.
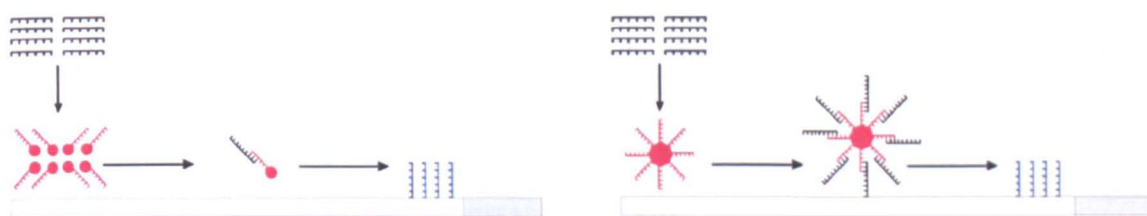
Fig. 5 Comparison between nucleic acids lateral flow tests performed with 40 nm GNPs (**left**) and 80 nm GNPs (**right**). Eight 40 nm particles must be captured by the test line to produce the same amount of colour development as one 80 nm particle, but the latter have a higher probability of being captured and therefore they generate a higher signal. This can be understood by thinking of the particles as spheres covered with Velcro hooks rolling along the strip and across a woollen test line orientated at right angles to the direction of their motion.
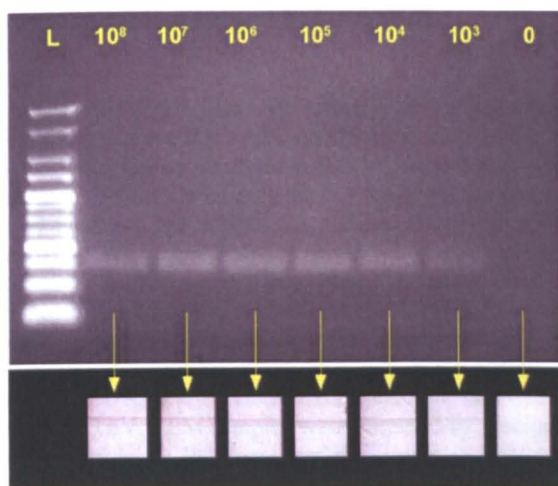
Fig. 6 Results of PCR assays. **A)** Agarose gel stained with ethidium bromide. **B)** Test lines of lateral flow devices developed with 80 nm GNPs. Numbers denote the amount of template sequence at the start of PCR.

the intervention of a skilled technician. The lateral flow devices also detect specific target sequences, whereas the stained gel only indicates that amplification products of a certain size have been generated and provides no other information about their identity.

In conclusion we have shown how unpurified PCR products can be detected with a lateral flow device that does not depend in any way on existing antibody hapten technology. To our knowledge this is the first time that such a device has been reported. A particular advantage of this approach is that it opens the way to detecting many nucleic acid sequences on the same test strip, an option that is not possible when immunochromatographic methods are used because of the limited number of antibody hapten combinations that are available for use with PCR. An unexpected outcome of this work was the discovery that the sensitivities of lateral flow devices can be increased by using 80 nm GNPs instead of the more commonly used 40 nm particles. Over a period of many years, the diagnostics industry has identified 40 nm as the optimum diameter because larger particles are believed to hinder biomolecular reactions by steric hindrance and be prone to aggregation.[9] As we have shown here, however, the use of larger

particles is not only possible, but leads to an increase in sensitivity. Although we have used larger particles to increase the sensitivity of NALF devices, the same strategy should also enhance the sensitivity of lateral flow immunoassays. When GNPs are used the upper limit of the increase in sensitivity is imposed not by particle diameter *per se*, but by a red shift in the absorbance spectrum that accompanies the increase in size and moves it into a region where the human eye is less sensitive. In order to obtain further increases in sensitivity, therefore, it is necessary to use a label that retains the advantages of GNPs, but has a higher extinction coefficient in the region of the spectrum that is visible to the human eye. Silver NPs interact with light more efficiently than a particle of the same dimensions composed of any other known organic or inorganic chromophore, and have a plasmon resonance that can be tuned to any wavelength in the visible spectrum. Large silver NPs ($\sim$100 nm diameter) have absorbance maxima close to the wavelength at which the human eye is most sensitive,[10] and therefore their use as labels in lateral flow devices should lead to further increases in sensitivity.

Notes and references

1 C. Fernandez-Sanchez, C. J. McNeil, K. Rawson, O. Nilsson, H. Y. Leung and V. Gnanapragasam, *J. Immunol. Methods*, 2005, **307**, 1–12.
2 C. P. Y. Chan, K. W. Sum, K. Y. Cheung, J. F. C. Glatz, J. E. Sanderson, A. Hempel, M. Lehmann, I. Renneberg and R. Renneberg, *J. Immunol. Methods*, 2003, **279**, 91–100.
3 S. Wang, C. Zhang, J. P. Wang and Y. Zhang, *Anal. Chim. Acta*, 2005, **546**, 161–166.
4 T. Suzuki, M. Tanaka, S. Otani, S. Matsuura, Y. Sakaguchie, T. Nishimura, A. Ishizaka and N. Hasegawa, *Diagn. Microbiol. Infect. Dis.*, 2006, **56**, 275–280.
5 Y. Matsubara and S. Kure, *Hum. Mutat.*, 2003, **22**, 166–172.
6 K. Takada, Y. Sakaguchi, C. Oka and M. Hirasawa, *J. Periodontol.*, 2005, **76**, 508–512.
7 K. Brocklehurst, J. Carlsson, M. P. J. Kierstan and E. M. Crook, *Biochem. J.*, 1973, **133**, 573–584.
8 Y. Chen, J. Aveyard and R. Wilson, *Chem. Commun.*, 2004, 2804–2805.
9 J. Chandler, T. Gurmin and N. Robinson, *IVD Technology Magazine*, 2000, 37.
10 D. D. Evanoff and G. Chumanov, *ChemPhysChem*, 2005, **6**, 1221–1231.

One Step Visual Detection Of PCR Products With Gold Nanoparticles And A Nucleic Acid Lateral Flow (NALF) Device

Jenny Aveyard,[1] Maryam Mehrabi,[1] Andrew Cossins,[2] Helen Braven,[3] and Robert Wilson.[1]*

1. Department of Chemistry, Liverpool University, Liverpool L69 7ZD, UK.
2. Department of Biological Sciences, Liverpool University, Liverpool, UK.
3. BBInternational, Golden Gate, Ty Glas Avenue, Llanishen, Cardiff CF14 5DX, UK.
E-Mail R.Wilson@liv.ac.uk

Electronic Supplementary Information

Materials
Aminodextran (MW 70 kDa, 16 primary amines per molecule) was from Molecular Probes, Eugene, OR. Succinimidyl 4-hydrazinonicotinate acetone hydrazone (SANH; Solulink, San Diego, CA). 3-(2-pyridyldithio)propionic acid N-hydroxysuccinimide ester (SPDP), bovine serum albumin (BSA), dithiothreitol (DTT) were from Sigma. Thiopropyl Sepharose 4B was from Amersham Biosciences. PCR master mix (BioMix) and agarose were from Bioline, London, UK. Ethidium bromide was from Continental Laboratory Products, San Diego, CA. Oligonucleotides with a 5' terminal aldehyde modification were from Trilink Biotechnologies, San Diego, CA. All other oligonucleotides were from Operon, Cologne, Germany. PBS: 15 mM sodium phosphate, 0.15 M NaCl, pH 7.4. Running buffer: PBS containing 1 mM ethylenediaminetetraacetic acid (EDTA). MES buffer: 0.2 M 2-(N-morpholino)ethanesulphonic acid, 0.3 M NaCl, pH 5. Bicarbonate solution: 0.1 M sodium hydrogen carbonate, pH 8.3. TBE: 45 mM Tris-borate, 1 mM EDTA, pH 8.3. Gold nanoparticles (GNPs) (10, 20, 40, 60, 80, 100 and 150 nm) were prepared by BBInternational, Cardiff, UK. The diameters of the particles were determined using a ZetaPlus analyser (Brookhaven Instruments, Worcestershire, UK) and by transmission electron microscopy (TEM) using a Phillips 410 operating at 80 kV or a Phillips CM12 operating at 100 kV. TEM samples were prepared by placing a drop of GNP solution on a 200 mesh nickel grid (Agar Scientific) and allowing it to dry in air. PCR was carried out with an MJR thermal cycler from MJ Research Inc, MA.

Methods
Characterization of GNPs
The GNPs used in this work were obtained from a commercial source. Each batch is prepared from a known mass of gold (in gold (III) chloride) and characterized by TEM. If the amount of gold used to prepare the particles and the mean diameter are known, the number of particles in a given volume of can be calculated using a value of 1.7×10^{-2} cubic nanometers for the volume occupied by one atom of gold. The particles used in our work were supplied with a data sheet that gave: 1) the mean diameter of the particles (CV% < 10) and, 2) the absorbance of these particles at a known number of particles per ml (for example, the 10 nm particles had 5.7×10^{12} particles per ml and an absorbance of 0.8 at 520 nm). The concentration of GNPs was determined by multiplying the number of particles per ml by 1000 and then dividing by Avogadro's number (6.02×10^{23}).

Oligonucleotide concentrations
Oligonucleotides were supplied with a molar extinction coefficient at 260 nm. This value was used to determine the concentrations of stock solutions before dilution to the required concentration.

Functionalization of aminodextran and covalent attachment of aldehyde terminated oligonucleotide
Aromatic hydrazide functionalities were introduced into aminodextran by adding 300 μl of 60 mM SANH in dry DMF, dropwise with stirring to 15 mg of aminodextran in 2.4 ml of PBS (Figure S1A). After stirring for 2 hours, protected disulfide groups (3-(2-pyridyldithio)propionyl; PDP) were introduced by adding 300 μl of 60 mM SPDP in dry DMF in the same way. After stirring overnight, unreacted SANH and SPDP were removed by dialyzing the solution against 4 x 1 litre of distilled water at 4 °C for a total of 48 hours. The concentration of protected disulfide groups in the dialyzed solution was determined according to the method of Carlsson et al.[1] A 2-fold excess (relative to the original amine content of the dextran) of aromatic aldehyde terminated oligonucleotide (5'CHO-TCT GCT GCC TGC TTG TCT GCG TTC T) in MES was added to the functionalized dextran solution and slow-tilt rotated at 4 °C for 24 hours.

Purification of oligonucleotide-functionalized dextrans
Unreacted oligonucleotides were removed from functionalized dextrans by covalent chromatography [2] on Thiopropyl Sepharose (Figure S1B). Protected disulfide groups in the dextran were reduced to unprotected thiol (-SH) groups by adding 100 μl of DTT in 1 M sodium bicarbonate to 1 ml of oligonucleotide-functionalized dextran and slow-tilt rotating the solution at room temperature for 1 hour. At the end of this time DTT was then removed by gel exclusion on Sephadex G-25. The eluted dextrans were immediately

1

mixed with 25-fold excess (relative to the original protected disulfide content of the dextran) of washed Thiopropyl Sepharose 4B gel and slow-tilt rotated at room temperature for 1 hour. Unreacted oligonucleotides were removed from the functionalized dextrans by washing the gel with running buffer. Bound oligonucleotide-functionalized dextrans were released from the gel with 10 mM DTT in bicarbonate solution and DTT was removed from the released dextrans by dialyzing against 3 x 2 litres of distilled water for 48 hours. For conjugation to GNPs (Figure S1C), the minimum amount of oligonucleotide-functionalized dextran required to prevent salt-induced flocculation of GNPs was determined as described in previous methods.[2,3] To purify and concentrate the GNPs to the required OD, GNPs were centrifugally precipitated for 10 minutes and then resuspended in PBS containing 1 mg ml^{-1} BSA and 0.5 % Tween 20.
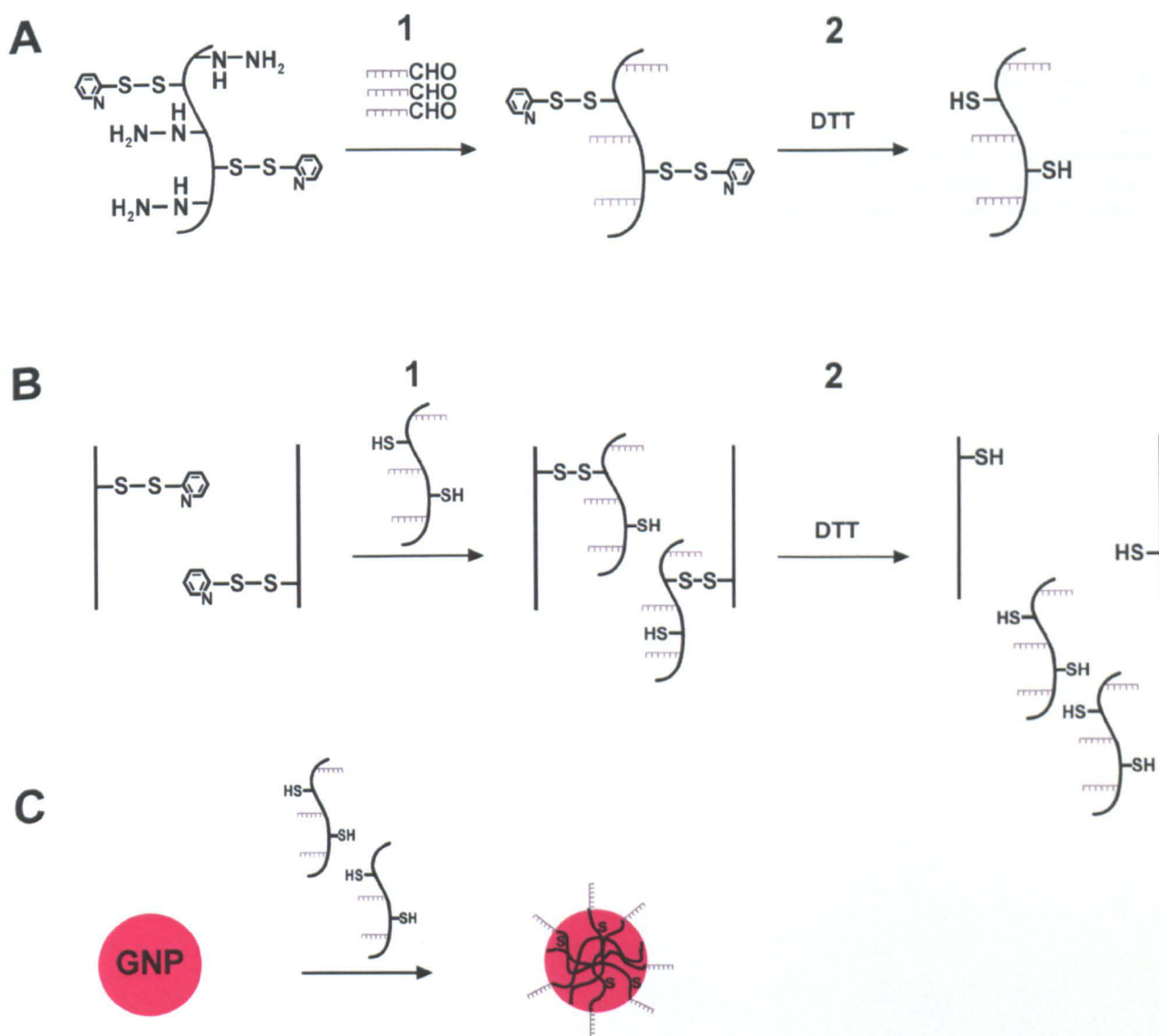
Figure S1: Preparation of reporter oligonucleotide-GNP conjugates. **A)** In step **1** aldehyde-terminated oligonucleotides are covalently attached to dextrans functionalised with aromatic hydrazides and protected disulphide bonds, and in step **2** disulphide

bonds in dextran are reduced to thiols (-SH) with DTT. **B)** In step **1** reduced dextrans are extracted by covalent attachment to Sepharose functionalised with disulphide bonds, and in step **2** purified dextrans are eluted with DTT. **C)** Purified dextrans are conjugated to GNPs via a plurality of dative covalent bonds as previously reported.

Lateral flow detection of DNA

Lateral flow devices were prepared by striping tailed capture oligonucleotides onto pre-assembled, pre-blocked Hi-Flow plus nitrocellulose membrane (Millipore, UK) using a Kinematic Matrix 1600 (Kinematic Automation, CA) and cut into 40 mm x 3 mm strips using a Kinematic Matrix 2360 automatic cutter. For detection of the 32 base target sequence (5'-GGGACTGACGATTCGGGTGATATCCAGAACGCAGACAAGCAGGCA) chromatographic devices were inserted into 50 µl of a freshly prepared 1:1 mixture of the target sequence and 2 OD oligonucleotide functionalized GNPs (both in PBS) and developed for 15 minutes. PCR products were detected in the same way except that PCR products were diluted 1:1 with GNPs in PBS. Images of all lateral flow strips were acquired with an office document scanner and then imported into iGrafx Image 1.0 (Bournemouth, UK) and converted to greyscale. The depth of colour was determined on a scale of 0 – 255 by activating the "view → information" option and pointing the mouse cursor at the area to be interrogated.

PCR

The template sequence (5'-AGAGTTTGATCCTGGCTCAG<u>TCTGCTGCCTGCTTGT CTGCGTTCTGGATATCACCCG</u>ATTAGA TACCCTGGTAGTCC), comprised a 32 mer sequence (underlined) nested between two 20 mer sequences. The 32 mer sequence was the same as the reporter oligonucleotide linked to the capture oligonucleotide, the 20 mer sequence at the 5' end was the same as the forward primer (5'-AGAGTTTGATCCTGGCTCAG) and the 20 mer sequence at the 3'end was the complementary to the reverse primer (5'-GGACTACCAGGGTATCTAAT). The PCR mixture comprised 25 µl of master mix, 20 pmol of reverse and 100 pmol of forward primer. The PCR protocol was an initial denaturation at 95 °C for 30 s, followed by 40 cycles of denaturation at 95 °C for 30 s, annealing at 55 °C for 45 s, and extension at 72 °C for 45 s, and completed with a final extension at 72 °C for 2 min. The product was analyzed by electrophoresis on 2.5% agarose with TBE containing 0.5 µg/ml ethidium bromide as the buffer.

Supplementary Information Results
Figure S2 shows images of nucleic acid lateral flow devices that have been developed with different diameter GNPs in the range 10 –
150 nm and Figure S3 shows how the amount of colour developed by these devices depends on the amount of nucleic acid target
sequence.

Figure S2 : Comparison between sandwich assays for 32 mer target sequence performed with
different sized GNPs. Numbers denote the amount of target in pmols. **A)** 10 nm GNPs;
B) 20 nm GNPs; **C)** 40 nm GNPs; **D)** 60 nm GNPs; **E)** 80 nm GNPs; **F)** 100 nm GNPs
and **G)** 150 nm GNPs.

4
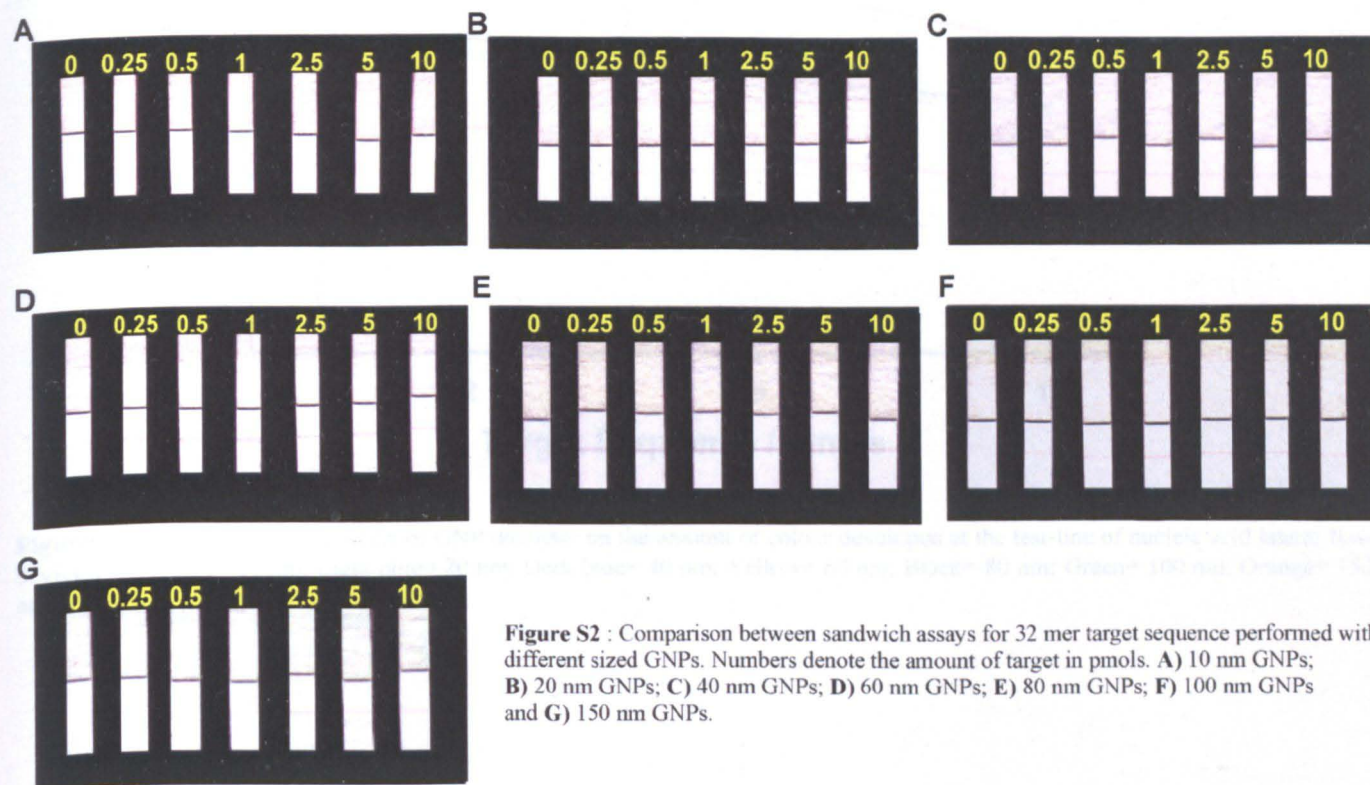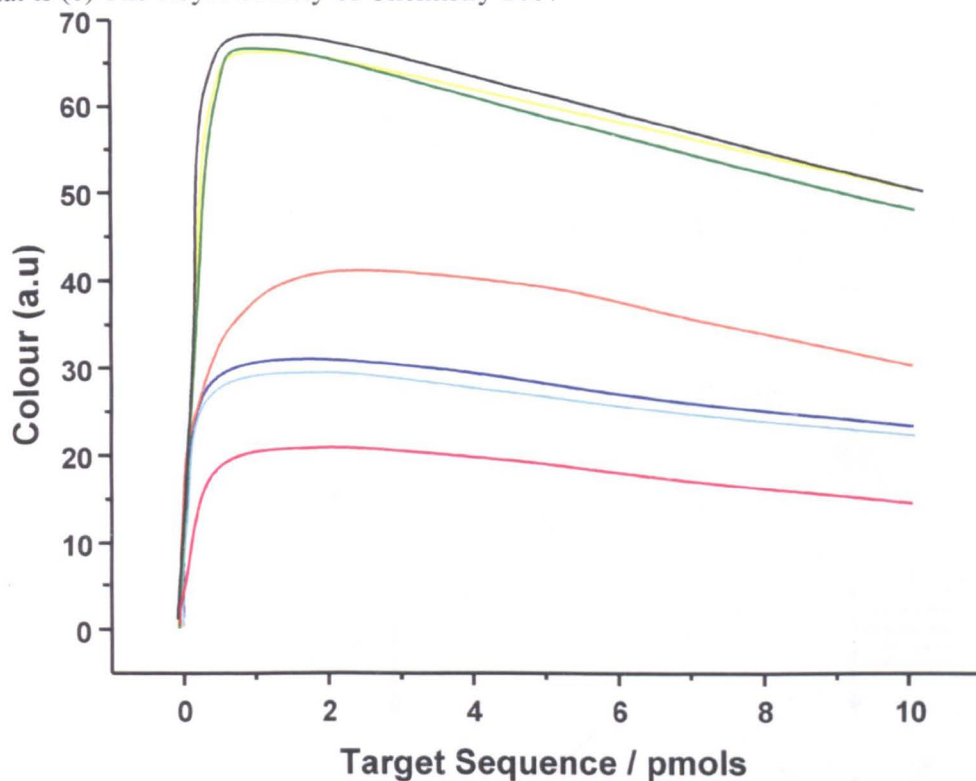
Figure S3: Graph showing the effect of GNP diameter on the amount of colour developed at the test-line of nucleic acid lateral flow devices. Key: Red= 10 nm; Light blue= 20 nm; Dark blue= 40 nm; Yellow= 60 nm; Black= 80 nm; Green= 100 nm; Orange= 150 nm.

Supplementary Discussion On The Effect Of Gold Nanoparticle Diameter On Sensitivity

Our results show that the sensitivity of lateral flow devices can be enhanced by using 80 nm diameter GNPs instead of the more commonly used 40 nm particles. The reason for this is not obvious, because the total absorbing power of GNPs (at 520 nm) on every lateral flow device was the same. This means that if all the 10 nm GNPs on a device were bound to the test line then the amount of colour developed would be the same when if all the 80 nm particles on a device were bound. The explanation for why more colour is developed by 80 nm GNPs depends on the number of particles on the device rather than their total absorbing power. Figure 4C in the paper shows that there are eight times as many 40 nm GNPs as there are 80 nm GNPs in the same volume of suspension, even though the absorbance at 520 nm is the same.
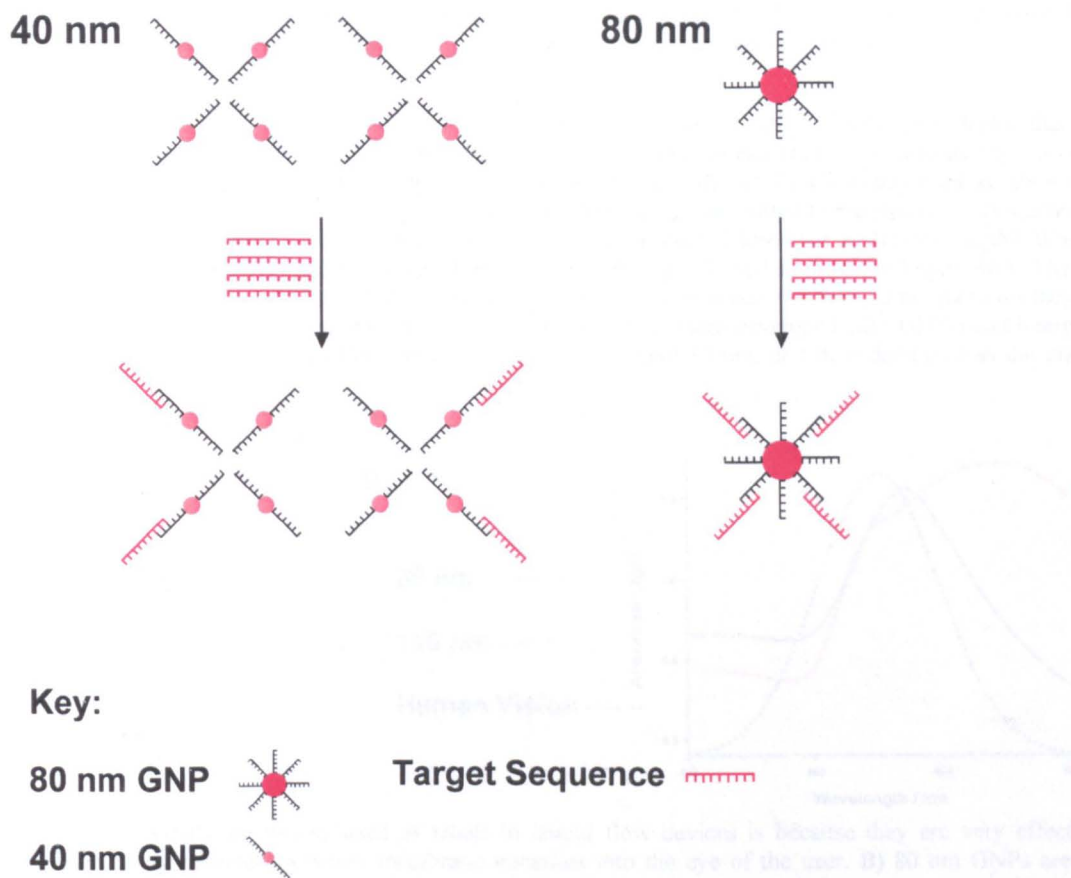
Figure S4: There are eight times as many 40 nm GNPs as 80 nm particles in a suspension that has the same volume and the same absorbance. Therefore, when they are mixed with the same number of target sequences, each 80 nm particle is hybridized to a mean of 8 times as many target sequences as each 40 nm particle.

Figure S4 shows schematically what happens when the same numbers of target oligonucleotides are mixed with suspensions of 40 and 80 nm GNPs that have the same volume and the same absorbance. Under well-mixed conditions the target sequences are evenly distributed among the reporter probes conjugated to the particles. Each 80 nm particle is hybridised to a mean of eight times as many target sequences as each 40 nm particle. Figure S5 shows what happens when these particles migrate through the test line of a lateral flow device. Even if it is assumed that any particle hybridised to a target sequence will also hybridise to a capture probe some 40 nm particles migrate through the test line without binding. In practice, the probability that a given particle will bind is related to the number of target sequences hybridised to its surface. This can be understood by thinking of each particle as a ball coated with Velcro hooks rolling across a test line composed of some adhesive material such as wool: a ball with only one hook has a low probability of binding, but a ball coated with many hooks has a high probability of binding. This additional effect explains why the amount of colour developed by 40 nm particles is less than half of the colour developed by 80 nm particles as shown in Figure S3.

40 nm

80 nm

Key: Target Sequence   ⟋⟋⟋⟋⟋   Capture Probe   ᴜᴜᴜ
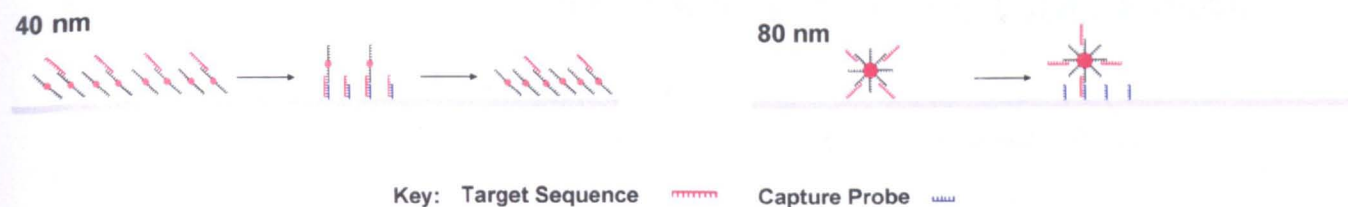
Figure S5: All 40 nm particles, even those hybridized to target sequences, have a lower probability of binding to capture probes than 80 nm particles. Therefore the latter have a higher probability of contributing to colour development at the test line.

If the increase in absorbance and scattering that accompanies the increase in diameter of GNPs was the only factor that affected colour development then it would go on increasing beyond 80 nm, but the increase in diameter is also accompanied by movement of the spectrum to longer wavelengths that are not visible to the human eye. The reason why GNPs are widely used as labels in lateral flow devices is because they are very efficient at preventing reflected light from being transmitted to the observer. Nitrocellulose and other materials used in lateral flow devices are white in colour, and therefore they reflect visible light at all wavelengths. When GNPs bind to the test line of a lateral flow device they prevent some of this light from being reflected as shown in Figure S6A. The overlaid spectra in Figure S6B show that even though 150 nm particles have a higher extinction maximum than 80 nm particles they are less efficient at absorbing visible light. The result is that the sensitivity of lateral flow devices developed with GNPs, and interpreted by the unaided eye, reaches a maximum when the particles have a diameter of around 80 nm, and then decreases as the diameter is further increased.

A Incident Light

Reflected Light

White Nitrocellulose Background

B

80 nm

150 nm

Human Vision ------

Absorbed Light

Wavelength / nm
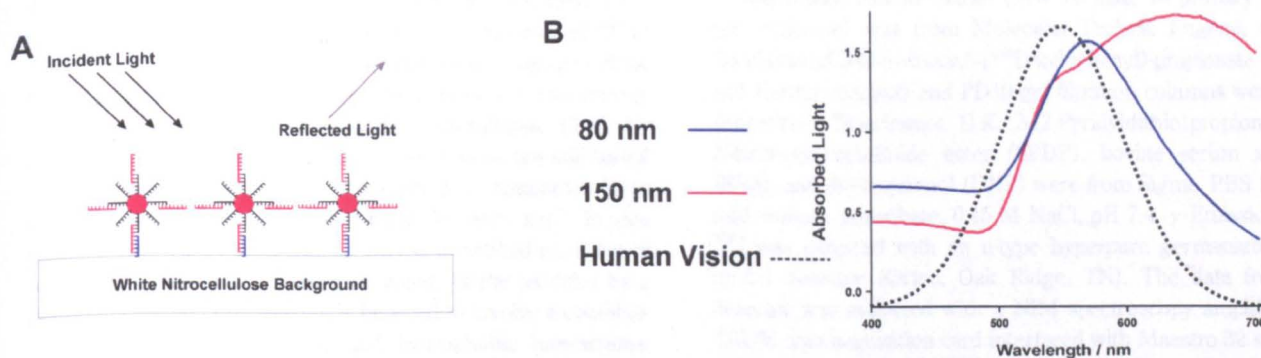
Figure S6: A) One reason why GNPs are widely used as labels in lateral flow devices is because they are very effective at preventing visible light from being reflected by white membrane materials into the eye of the user. **B)** 80 nm GNPs are more effective than 150 nm particles at preventing visible light being reflected from a white background because their spectrum coincides more closely with the wavelengths that are seen by the human eye.

Supplementary Information References

1. Carlsson, J., Drevin, H., Axen, R. *Biochem. J.,* (1978), **173**, 723-737.
2. Brocklehurst, K., Carlsson, J., Kierstan, M.P.J., Crook, E.M. *Biochem. J.,* (1973), **133**, 573-584.
3. Wilson, R., Chen, Y., Aveyard, J., *Chem. Commun.* (2004), 1156-1157.
4. Chen, Y., Aveyard, J., Wilson, R., *Chem. Commun.,* (2004), 2804-2805.

Improving the Sensitivity of Immunoassays by Tuning Gold Nanoparticles to the Tipping Point

Jenny Aveyard,[†] Paul Nolan,[‡] and Robert Wilson*,[†]

Department of Chemistry, Liverpool University, Liverpool L69 7ZD, U.K., and Department of Physics, Liverpool University, Liverpool L69 7ZE, U.K.

Conventional lateral flow immunoassays are based on labeled antibodies. In this paper we describe an alternative design based on gold nanoparticles labeled with haptens. The haptens are conjugated to gold nanoparticles by a method that allows the number per particle to be tuned to the point of maximum sensitivity. This leads to improvements compared with conventional lateral flow devices without relinquishing any of their advantages. In parallel assays for the environmental pollutant 2,4-dinitrophenol the alternative devices were 50% more sensitive.

Lateral flow immunochromatographic devices are one of the most important products of the diagnostics industry. They are inexpensive to develop and once developed can be manufactured in large batches at low cost. Their popularity with users derives from their simplicity, which allows complicated tests to be performed at the point of need without additional equipment. Since their introduction in the 1980s, the basic components of these devices have changed very little, primarily because any alterations to the basic design have always led to increases in cost and/or complexity that have outweighed their advantages. Thus, for example, the vast majority of lateral flow devices are still based on gold nanoparticles (GNPs) conjugated to antibodies by a method that was first reported nearly 30 years ago.[1] In this method, GNPs are mixed with an excess of antibodies, some of which then become attached (conjugated) to the particles by a poorly understood process that is believed to involve a combination of electrostatic, covalent, and hydrophobic interactions. Excess antibodies are then removed by centrifugal washing and discarded. GNP conjugates produced in this way are usually quite stable, but there are reports describing subsequent desorption of the antibodies,[2,3] and it is well-known in industry that some types of monoclonal antibody cannot be adsorbed in the first place. In the intervening period since lateral flow devices were first introduced, GNPs have been at the heart of some of most exciting and innovative research in nanotechnology,[4–8] but surprisingly

given their enormous economic importance very little of this research has had any impact on the design of lateral flow devices. There are a few reports describing lateral flow devices based on GNPs conjugated to oligonucleotides by one of the newer methods,[9–11] but to our knowledge the more established area of lateral flow immunoassays has been entirely unaffected by recent advances. This is unfortunate because some of these advances have the potential to improve the performance of lateral flow devices and decrease their cost without compromising any of the advantages that have made them so successful. In this report we describe a lateral flow immunoassay based on GNPs conjugated to haptens rather than antibodies and show how advances in nanotechnology can lead to improvements in sensitivity without any increase in either cost or complexity.

EXPERIMENTAL SECTION

Materials. Aminodextran (MW 70 kDa, 16 primary amines per molecule) was from Molecular Probes, Eugene, OR. *N*-Succinimidyl 3-(4-hydroxy,5-[^{125}I] iodophenyl)-propionate (Bolton and Hunter reagent) and PD10 gel filtration columns were from Amersham Biosciences U.K. 3-(2-Pyridyldithio)propionic acid *N*-hydroxysuccinimide ester (SPDP), bovine serum albumin (BSA), and dinitrophenol (DNP) were from Sigma. PBS (3×): 45 mM sodium phosphate, 0.45 M NaCl, pH 7.4. γ Emission from ^{125}I was detected with an n-type hyperpure germanium GMX model detector (Ortec, Oak Ridge, TN). The data from the detector was collected with a NIM spectroscopy amplifier and TRUM data acquisition card interfaced with Maestro 32 software (all from Ortec). DNP-NHS was synthesized as reported previously.[20] GNPs and DNP lateral flow devices were supplied by BBInternational, Cardiff, U.K.

Characterization of GNPs. GNPs prepared from a known mass of gold (in gold(III) chloride) were characterized by TEM using a Phillips CM12 microscope operating at 100 kV and dynamic light scattering with a ZetaPlus analyzer from Brookhaven Instruments, Worcestershire, U.K. The number of particles in a given volume was calculated from the diameter (39 nm; CV % < 8) using a value of 1.7×10^{-2} nm^3 for the volume occupied by

---

* To whom correspondence should be addressed. E-mail: R.Wilson@liv.ac.uk.
† Department of Chemistry.
‡ Department of Physics.

(1) Faulk, P.; Taylor, G. M. *Immunohistochemistry* **1971**, *8*, 1081–1083.
(2) Verkleij, A. J.; Leunissen, J. L. M. *Immuno-Gold Labelling in Cell Biology*; CRC Press: Boca Raton, FL, 1989.
(3) Kramarcy, N. R.; Sealock, R. *J. Histochem. Cytochem.* **1989**, *39*, 37.
(4) Daniel, M. C.; Astruc, D. *Chem. Rev.* **2004**, *104*, 293–346.
(5) Rossi, N. L.; Mirkin, C. A. *Chem. Rev.* **2005**, *105*, 1547–1562.
(6) Pellegrino, T.; Kudera, S.; Liedl, T.; Munoz-Javier, A.; Manna, L.; Parak, W. J. *Small* **2005**, 48–63.

(7) Han, G.; Ghosh, P.; Rotello, V. *Nanomedicine* **2007**, *2*, 113–123.
(8) Wilson, R. *Chem. Soc. Rev.* **2008**, accepted.
(9) Aveyard, J.; Mehrabi, M.; Cossins, A.; Braven, H.; Wilson, R. *Chem. Commun.* **4251**–4253.
(10) Glynou, K.; Ioannou, P. C.; Christopoulous, T. K.; Syriopoulou, V. *Anal. Chem.* **2003**, *75*, 4155–4160.
(11) Deborggraeve, S.; Claes, F.; Laurent, T.; Mertens, P.; Leclipteux, T.; Dujardin, J. C.; Herdewijn, P.; Buscher, P. *J. Clin. Microbiol.* **2006**, *44*, 2884–2889.
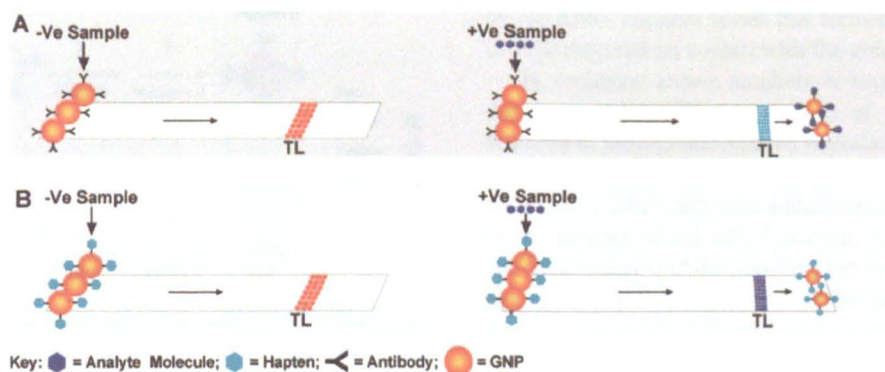
Figure 1. Design and operation of competitive lateral flow devices based on (A) labeled antibodies (conventional design) and (B) labeled haptens (alternative design used in this work). Both designs result in a decrease in color development at the test line (TL) as the amount of analyte molecule in the sample increases.

one atom of gold. This calculation indicated that suspension of the GNPs with an absorbance of 1.0 at 520 nm had a concentration of 9×10^{10} particles/mL.

Functionalized Dextrans. Six dextrans functionalized with different amounts of DNP haptens were synthesized as follows: 100 μL of DNP-NHS in dry DMF was added dropwise with stirring over a period of 5 h to 1 mL aliquots of PBS containing 5 mg of aminodextran; the concentrations of DNP-NHS in the DMF solutions were (1) 0.5, (2) 0.85, (3) 2, (4) 3, (5) 7, or (6) 28 mM. At the end of this time, 100 μL of 60 mM SPDP in dry DMF was added to the dextran solution in the same way. After stirring for a further 5 h, unreacted DNP and SPDP were removed by dialysis against 4×1 L of deionized water for a total of 48 h. The concentration of dextran in the dialyzed solutions was calculated by correcting for the increase in volume of the solution, and the concentration of DNP haptens was determined by UV–vis spectrophotometry ($\epsilon_{360} = 1.7 \times 10^4$ M^{-1} cm^{-1}). Dextran functionalized with radioactive labels was synthesized as follows: 100 μL of Bolton and Hunter reagent (18.5 MBq) in dry DMF was added dropwise with stirring to 5 mg of aminodextran in 1 mL of PBS over a period of 2 h. At the end of this time, 100 μL of 60 mM SPDP in dry DMF was added in the same way. After the recation mixture was stirred for a further 5 h, unreacted Bolton and Hunter reagent and SPDP were removed by gel exclusion chromatography on a PD10 column.

GNP Conjugates. The minimum amount of functionalized dextran required to stabilize the particles was determined by adding different amounts of dextran to a fixed amount of GNPs (5.94×10^{10} particles in 0.66 mL) followed by 0.33 mL of PBS (45 mM sodium phosphate, 0.45 M NaCl, pH 7.4). Particles that flocculated on addition of PBS eventually precipitated, but to facilitate the acquisition of absorbance measurements at 520 nm they were removed by passing the solutions through a 0.2 μm microbiological filter. Once the minimum amount of dextran required to stabilize a fixed amount of particles was known, larger volumes of conjugate were prepared by mixing the same ratio of dextran to GNPs. These conjugates were then used in lateral flow immunoassays without further purification. For comparison with particles purified by methods designed to remove free dextran, the conjugates were centrifugally washed three times at 700g or purified by gel exclusion chromatography on Sepharose 2B (column dimensions, 1×60 cm; void volume, 10 mL).

Lateral Flow Immunoassays. Devices were immersed 150 μL of DNP in PBS that also contained 1 mg mL^{-1} BSA and 0.05% (v/v) Tween-20; the number of GNPs (4.5×10^9) per device was the same in all assays. After the color was allowed to develop for 10 min, images of the devices were acquired with an office document scanner and imported into iGrafx Image 1.0 software (Bournemouth, U.K.) where they were converted to grayscale, before determining the color of the test lines on a scale of 0–255 by activating the "view → information" option and pointing the mouse cursor at the area to be interrogated.

RESULTS AND DISCUSION

Although competitive immunoassays are sometimes used to screen for high molecular weight molecules, they are most often employed to detect small molecules that can only accommodate one antibody binding site; examples are hormones, drugs, pesticides, and explosives. Competitive immunoassays have been applied to these molecules in various ways, but because many of them routinely require detection outside the laboratory, lateral flow devices have often figured prominently.[12-15] The basic format of a competitive immunoassay on a conventional lateral flow device (Figure 1A) is very simple: when a device is inserted into a sample, labeled antibodies are rehydrated and released into the migrating liquid. In the absence of any analyte molecules (negative sample), all of the labeled antibodies bind to the test line (TL), but when analyte molecules are present (positive sample), antibody binding sites are occupied and the probability that the labels will bind decreases. This leads to a decrease in the amount of color developed at the test line in proportion to the amount of analyte in the sample.

The reason why conventional lateral flow devices have the design shown in Figure 1A is because at the time of their introduction there was no reliable method for conjugating a wide range of low molecular weight molecules to particulate labels. Such methods have subsequently become available, however,[16-18]

(12) Liu, L.; Peng, C.; Jin, Z.; Xu, C. *Biomed. Chromatogr.* **2007**, *21*, 861–866.
(13) Zhang, C.; Zhang, Y.; Wang, S. *J. Agric. Food Chem.* **2006**, *54*, 2502–2507.
(14) Zhang, G. P.; Wang, X. N.; Yang, J. F.; Yang, Y.Y.; Xing, G. X.; Li, Q. M.; Zhao, D.; Chai, S. J.; Guo, J. Q. *J. Immunol. Methods* **2006**, *312*, 27–33.
(15) Delmulle, B. S.; De Saeger, S. M. D. G.; Sibanda, L.; Barna-Vetro, I.; Van Peteghem, C. H. *J. Agric. Food Chem.* **2005**, *53*, 3364–3368.
(16) Levy, R.; Thanh, N. K. T.; Dot, R. C.; Hussain, I.; Nichols, R. J.; Schiffrin, D. J.; Brust, M.; Fernig, D. G. *J. Am. Chem. Soc.* **2004**, *126*, 10076–10084.
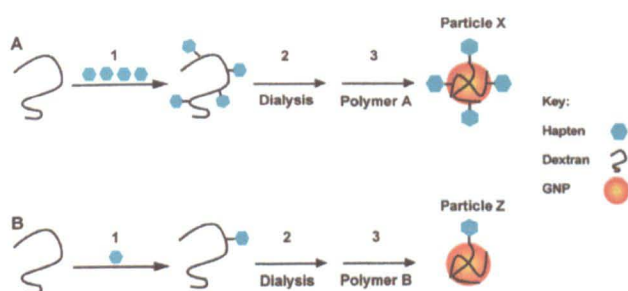
Figure 2. In step 1, the same amount of dextran is functionalized with different amounts of DNP hapten, and in step 2, the functionalized dextran is purified and characterized. In step 3, more haptens are conjugated to particle X than to particle Y because polymer A is functionalized with more haptens than polymer B.

Table 1. Relationship between Functionalized Dextran, Mean Numbers of Haptens and Dextran Molecules per GNP at the Equivalence Points, and the Sensitivities of Lateral Flow Immunoassays Based on These Particles[a]

haptens/dextran	haptens/GNPs	dextran/GNPs	sensitivity (ng)
0.5	52	106	24
0.74	72	97	60
1.0	99	102	120
1.50	164	109	188
2.0	231	114	375
2.7	332	120	2250

[a] Sensitivity is defined here as the amount of DNP required to produce a 50% decrease in color development at the test line.

including one developed by us in which low molecular weight molecules are attached to GNPs via high molecular weight dextran polymers.[19–22] This method allows the mean number of molecules attached to the particles to be known and varied without resorting to indirect methods of determination in order to find out what this number is. The concept is very simple: because there are more molecules attached to polymer A than to polymer B before conjugation (Figure 2) there are more molecules attached to particle X than to particle Z after conjugation. In order to investigate the effect of this on competitive immunoassays, we attached different amounts of 2,4-dintrophenol (DNP) haptens to high-molecular weight dextran polymers and then conjugated these functionalized dextrans to GNPs. The process by which these dextrans were functionalized and conjugated is shown schematically in Figure 2. In step 1, DNP haptens were covalently attached to a known amount of aminodextran that was also functionalized with 3-(2-pyridyldithio)propionyl (PDP) groups; the amount of DNP hapten was varied by reacting stoichiometric amounts of the corresponding N-hydroxysuccinimide ester with a fixed amount of dextran. In step 2, the products were dialyzed to remove haptens that were not covalently attached to dextran and then the DNP hapten concentration of each dialyzed solution was determined by UV–vis spectroscopy (see Table 1). In step 3, the dextrans were conjugated to 40 nm citrate-stabilized GNPs

(17) Lee, S.; Perez-Luna, V. H. *Anal. Chem.* **2005**, *77*, 7204–7211.
(18) Latham, A. H.; Williams, M. E. *Langmuir* **2006**, *22*, 4319–4326.
(19) Wilson, R. *Chem. Commun.* **2003**, 108–109.
(20) Wilson, R.; Chen, Y.; Aveyard, J. *Chem. Commun.* **2004**, 1156–1157.
(21) Chen, Y.; Aveyard, J.; Wilson, R. *Chem. Commun.* **2004**, 2804–2805.
(22) Mehrabi, M.; Wilson, R. *Small* **2007**, *9*, 1491–1495.

by the dative covalent bonds that formed when disulfide bonds in PDP ruptured on contact with the gold.

To conjugate known numbers of haptens to GNPs, we first determined the minimum amount of functionalized dextran required to prevent salt-induced flocculation of the particles. To do this, we added different amounts of dextran solution to known numbers of GNPs and then added concentrated NaCl solution. In the absence of any added dextran, the solution turned blue due to flocculation of the particles, but as the amount of dextran increased, an increasing fraction of the particles remained red as shown in Figure 3B. When this color change was plotted against the amount of hapten added, titration curves of the type shown in Figure 3C were obtained; the arrow on this plot indicates the equivalence point at which just enough dextran has been added to prevent any flocculation of the particles. There was a linear relationship between the hapten concentration at this point and the molar ratio of haptens to dextran, but the mean number of dextran molecules per particle was almost constant as shown in Figure 3D. When particles mixed with this amount of dextran are centrifugally washed or purified by gel exclusion chromatography, their performance in biological assays is identical to that of particles that have not been treated in these ways. This suggests that at the equivalence point, all of the added dextran is conjugated to the particles because the removal of free dextran in solution would lead to increases in sensitivity. To investigate this we also functionalized dextrans with radioactive (N-succinimidyl 3-(4-hydroxy,5-[^{125}I]iodophenyl)-propionate (Bolton and Hunter reagent) instead of DNP. When GNPs mixed with the minimum amount of this dextran required to prevent salt-induced flocculation were centrifugally washed, all radioactivity precipitated with the particles and no residue remained in the supernatant. Because all of the added dextran is conjugated to the particles at the equivalence point, the mean number of haptens (or radioactive labels) per particle is equal to their ratio in solution at this point on the titration curve. No subsequent purification step is necessary, and because the performance of the conjugates in biological assays is independent of the way in which the dextrans and the particles are mixed (dropwise addition and rapid mixing produce the same results), larger volumes can be prepared simply by scaling up the amounts of reagents mixed at the equivalence point.

In order to investigate the performance of GNPs conjugated to different numbers of haptens in competitive immunoassays, we used lateral flow devices with the design shown in Figure 1B; notice that this design is the reverse of the conventional design shown in Figure 1A because the antibodies are immobilized at the test line instead of conjugated to the particles. In these alternative devices, DNP molecules in the sample and haptenylated GNPs migrate toward the test line at the same rate. They do not interact with each other until they reach the test line where they compete for antibody binding sites. Particles conjugated to high numbers of haptens have high affinities and therefore very high concentrations of DNP are required to out-compete them and produce a decrease in color development. As the number of haptens per particle is decreased, the amount of DNP required to out-compete them also decreases, and the sensitivity (defined here as the amount of DNP required to produce a 50% decrease in color development at the test line) increases. Some of the results obtained with these devices in immunoassays for DNP are shown

Figure 3. (A) As the ratio of functionalized dextran to GNPs increases, the fraction of particles that flocculate (turn blue) when NaCl is added decreases. (B) The decrease in flocculation results in a visible color change from blue to red. (C) When the increase in red color is plotted against the amount of functionalized dextran added, a sigmoid curve is obtained; the arrow marks the point on this curve at which the minimum amount of dextran required to prevent any flocculation has been added. In the example shown, the ratio of haptens to GNPs at this point is 231. Numbered points correspond to numbered samples in part B. (D) Graph showing the relationship between the number of haptens per 70 kDa dextran molecule and number of haptens (black line) and dextrans (red line) per GNP.
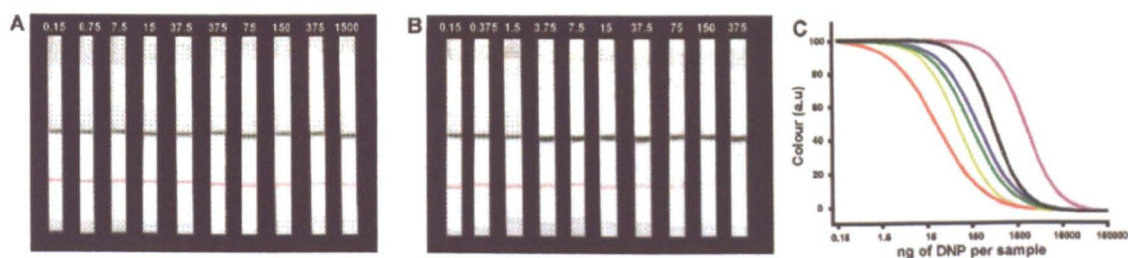
Figure 4. Lateral flow immunoassays performed with GNPs conjugated to a mean of (A) 332 and (B) 72 haptens per GNP showing how less DNP is required to produce a decrease in color development at the test line as the number of haptens per GNP decreases; numerals indicate the amount of DNP per sample in nanograms. (C) Overlaid plots showing how color development depends on the number of haptens per particle. Key to numbers of haptens per particle: red = 52; yellow = 72; green = 99; blue = 164; black = 231; mauve = 332.
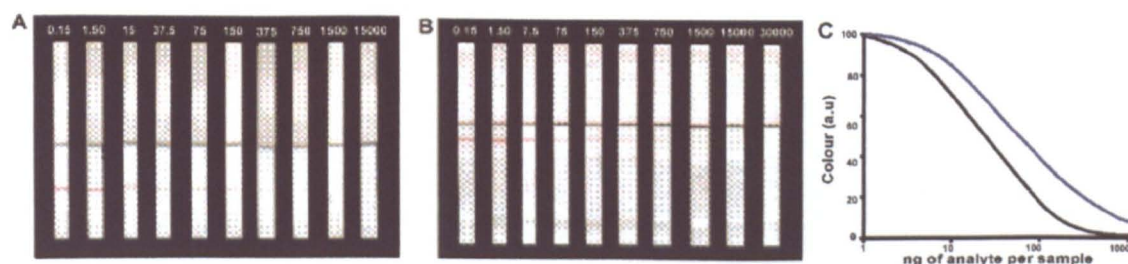
Figure 5. Lateral flow immunoassays for DNP based on (A) GNPs conjugated to an optimum number of haptens and (B) GNPs conjugated to antibodies; numbers indicate the amount of DNP per sample in nanograms. (C) Graph of color development at the test line versus amount of DNP for immunoassays based on GNPs conjugated to haptens (black line) and antibodies (blue line); the amount of DNP required to produce a 50% decrease in color development was 24 ng and 55 ng, respectively.

in Figure 4. The sensitivity reached a maximum when there was a mean of 52 haptens per particle. When the number of haptens was decreased below this, the sensitivity decreased again as an increasing number of particles migrated through the test line without binding to it even when there was no DNP in the sample. Particles conjugated to a mean of ~50 haptens produce the highest sensitivity because they are at the tipping point where only a slight increase in the amount of DNP is enough to prevent them from binding to the test line. We also compared our devices (Figure

1B) with traditional lateral flow devices (Figure 1A) based on antibodies conjugated to GNPs. The results of these comparisons shown in Figure 5 indicated that our devices were more than 50% more sensitive (24 ng compared to 55 ng at half-maximum color development) than the conventional devices. This shows that optimizing the number of binding molecules per nanoparticle can lead to improvements in well established technologies.

In summary, we have shown how the performance of competitive lateral flow immunoassays can be improved by using GNPs

conjugated to an optimum number of haptens. Apart from an increase in sensitivity, our approach has several other advantages over existing methods. The GNP labels are prepared by a method that does not require a subsequent purification step, and therefore there is no loss of expensive reagents. The absence of a purification step is also advantageous when the GNPs are very small because these can only be centrifugally precipitated at high speeds, which may damage the molecules that have been conjugated to them. Our results also have shown that once the equivalence point has been determined by titration, larger volumes of conjugate can be prepared simply by mixing the same ratio of functionalized dextrans and GNPs. We have prepared volumes of up to 10 mL in this way, but we suspect that it would be possible to prepare much larger volumes. At present, most nanoparticle conjugation methods seek to load the particles with high and/or indeterminate numbers of recognition sites, but our results indicate that the performance of such conjugates in biological assays may not reflect their true potential. One reason why the effect of adjusting the number of recognition sites per nanoparticle has not been more widely investigated is that the preparation of particles engineered in this way is perceived to be difficult and at best only possible in low yield, but as we have shown here this need not be the case. Although our results were obtained with GNPs conjugated to haptens, the same approach should yield improvements in sensitivity regardless of the particle type or the identity of the recognition sites attached to it. Because this approach is inexpensive and easy to perform, we anticipate that it will not only be useful as a means of improving sensitivity in analytical applications but also for exploring the relationship between nanoparticles and the number of molecules attached to them in other areas of nanotechnology.